

Research School of Chemistry
Institute of Advanced Studies



**Australian
National
University**

REGULATION OF PEPTIDE HORMONES

A thesis submitted for the admission to the degree of

Doctor of Philosophy

By

Chen Gu

Canberra, Australia

May 2019

Declaration

This is to declare that the research presented in this thesis represents original work that I have undertaken during my PhD candidature under the supervision of Prof. Chris Easton, at the Research School of Chemistry, College of Physical & Mathematical Sciences, the Australian National University, Canberra, Australia.

The work about the identification of hydroxyglycine-extended calcitonin (HO-CTG) produced by DMS53 cells, described in Chapter 6, has been published in the paper “Detection of Biosynthetic Precursors, Discovery of Glycosylated Forms, and Homeostasis of Calcitonin in Human Cancer Cells”, F. Cao, A. B. Gamble, H. Onagi, J. Howes, J. E. Hennessy, C. Gu, J. A. Morgan and C. J. Easton, *Anal. Chem.*, **2017**, DOI: 10.1021/acs.analchem.7b00457.

I give permission for this copy of my thesis when deposited at the library of the ANU to be made available for loan and photocopying.

Chen Gu

01/05/2019

Acknowledgements

I want to give my deepest thanks to my supervisor Prof. Chris Easton who gave me the precious opportunity to study in his group, and thank for all his help, guidance, encouragement, patience and support given throughout my PhD program. I will never forget the day when I got his email that I would be given a chance to study for a PhD degree with him. It is him who offered me with his fabulous wisdom and knowledge during my PhD period. He is a great supervisor but also a great friend and somehow changed my way of thinking and even my course of life during these six years. I will be forever grateful.

I would also like to give my thanks to my parents for their continuous and patient support for my PhD studying.

I am especially thankful to Dr. Feihua Cao for helping me with every part of my project, answering my questions with enthusiasm, kindness and patience. Besides, many thanks to Dr. Daniel Fankhauser for his guidance with the knowledge of organic chemistry and synthesis experiment; and thanks to Dr. Hideki Onagi as well for his support and direction with all the HPLC and MS methods and relevant problems. Thanks to all the members in the PAM group, you are all here by my side when I am in need of the help in the cell culture, HPLC fixing and language support.

I would like to thank the past and present members of the Easton research group, especially Mantas Liutkus and Thomas Loan for their suggestions on my PhD project and thesis writing. Thank you for all your support, encouragement, stimulating chemistry discussions and joy over the six years. I would also like to thank all the staff in the Research School of Chemistry for their generous help. A special thank to Mr. Chris Blake for his help with nuclear magnetic resonance spectroscopy and Ms Anitha Jeyasingham for her help with mass spectrometry.

Finally, a thank you to Australia, an amazing country that I love.

Table of Contents

Declaration	i
Acknowledgements	i
Table of Contents	iii
Abbreviations	vi
Abstract	xi
Chapter One	1
<i>Introduction</i>	1
1.1 C-Terminal Amidated Peptide Hormones.....	1
1.2 General Introduction to PAM Enzyme	7
1.2.1 Mechanistic Insight of PHM	8
1.2.2 Mechanistic Insight of PAL	10
1.2.3 PAM Cofactors.....	11
1.2.4 Substrate Specificity of PAM.....	12
1.3 PAM Inhibition	15
1.3.1 PHM Inhibitors.....	16
1.3.2 PAL Inhibitors.....	34
1.4 Summary	36
Chapter Two.....	37
<i>Study of Peptide Sequence Recognition by Peptidylglycine α-Amidating Monooxygenase</i>	37
2.1 Introduction	37
2.2 Synthesis of Peptide Substrates.....	44
2.3 Measurements of Binding Affinities of Peptide Substrates with PAM	52
Chapter Three.....	64
<i>Synthesis and Evaluation of Interactions of Glycine Derivatives of Medicinal Agents with Peptidylglycine α-Amidating Monooxygenase</i>	64
3.1 Introduction	64
3.2 Synthesis of Bex-glycine (3-4).....	68
3.3 Interaction of Bex-glycine (3-4) with Medium PAM	69
3.4 Cytotoxicity Profile of Bex (3-1) and Bex-glycine (3-4).....	72
3.5 Synthesis of <i>N</i> -Ac-(<i>S</i>)-His-Gly-COOH (3-6) and <i>N</i> -Ac-(<i>S</i>)-His-NH ₂ (3-7)	74

3.6 Interaction of <i>N</i> -Ac-(<i>S</i>)-His-Gly-COOH (3-6) with Medium PAM	77
3.7 Discussion	79
Chapter Four.....	81
<i>Investigation of the Subunit Activity of Peptidylglycine α-Amidating Monooxygenase</i>	81
4.1 Introduction	81
4.2 Investigation of PHM and PAL Activities Using HPLC-MS	83
4.3 Conclusion.....	93
Chapter Five	94
<i>Structure-Activity Relationship Study for Peptidyl-α-Hydroxyglycine α-Amidating Lyase Inhibition</i>	94
5.1 Introduction	94
5.2 Synthesis of Candidate Molecules for PAM Inhibition Assay	95
5.3 Measurements of PAM Inhibition Potencies of Molecules	102
5.4 pH-Dependent PAM Inhibition Assays with <i>N</i> -Ac-Phe-Pyruvate.....	116
5.5 Conclusion.....	121
Chapter Six.....	122
<i>Detection of an α-Hydroxyglycine-extended Peptide Hormone Produced by Human Small Cell Lung Cancer Cells</i>	122
6.1 Introduction	122
Chapter Seven	146
<i>Conclusions and Future Directions</i>	146
Chapter Eight	148
<i>Experimental</i>	148
8.1 General	148
8.2 Experimental for Chapter 2: Study of Sequence Recognition by PAM.....	150
8.2.1 Synthesis Work Described in Chapter 2	150
8.2.2 Cell Culture Maintenance and PAM Enzyme Preparation	181
8.2.3 Procedure for Determination of IC ₅₀ Values of Peptide Prohormones with PAM	182
8.2.4 HPLC Method for Detection and Quantification of (<i>R</i>)-Tyr-(<i>S</i>)-Val-Gly- COOH and (<i>R</i>)-Tyr-(<i>S</i>)-Val-NH ₂ in IC ₅₀ Assays.....	183
8.3 Experimental for Chapter 3: Synthesis and Evaluation of Interactions of Glycine Derivatives of Medicinal Agents with Peptidylglycine α -Amidating Monooxygenase	195

8.3.1 Synthesis Work Described in Chapter 3	195
8.3.2 Procedure for Determination of IC ₅₀ of Prodrug Candidates with PAM 207	
8.3.3 Procedure for Cytotoxicity Evaluation of Bexarotene (3-1) and Bex- glycine (3-4)	210
8.3.4 Procedure for Standard PAM Assay with <i>N</i> -Ac-(<i>S</i>)-His-Gly-COOH (3-6)	210
8.4 Experimental for Chapter 4: Investigation of the Subunit Activity of Peptidylglycine α -Amidating Monooxygenase.....	212
8.4.1 Synthesis Work Described in Chapter 4	212
8.4.2 General Procedure for PAM assay using HPLC-MS.....	221
8.4.3 Procedure for pH-Dependent PAM Assay	222
8.5 Experimental for Chapter 5: Structure-Activity Relationship Study for Peptidyl- α -Hydroxyglycine α -Amidating Lyase Inhibition.....	223
8.5.1 Synthesis Work Described in Chapter 5	223
8.5.2 Procedure for PAM Inhibition Assay.....	258
8.5.3 Procedure for pH-Dependent PAL Inhibition Assay Using <i>N</i> -Ac-Phe- pyruvate (1-143).....	264
Appendix	269
Bibliography.....	273

Abbreviations

A/Ala	Alanine
ACTH	Adrenocorticotropic hormone
ATCC	American Type Culture Collection
Bex	Bexarotene
BOP	Benzotriazole-1-yl-oxy-tris-(dimethylamino)- phosphonium hexafluorophosphate
br	Broad
CGRP	Calcitonin gene-related peptide
CT	Calcitonin
CTG	Calcitonin-glycine
CTGK	Calcitonin-glycine-lysine
CTGKK	Calcitonin-glycine-lysine-lysine
δ	Chemical shift in parts per million
d	Doublet
dd	Doublet doublet
D/Asp	Aspartic acid
DCM	Dichloromethane
DIC	<i>N,N</i> -Diisopropylcarbodiimide
DIPEA	Diisopropylethylamine
DMAP	4-Dimethylaminopyridine

DMMP	Dimethyl methylphosphonate
DMF	Dimethylformamide
DMSO	Dimethyl sulfoxide
DPBS	Dulbecco's phosphate-buffered saline
EDC	<i>N</i> -(3-Dimethylaminopropyl)- <i>N'</i> -ethylcarbodiimide
ESI	Electrospray ionisation
Ex.	Excitation
Fmoc	Fluorenylmethyloxycarbonyl
F/Phe	Phenylalanine
G/Gly	Glycine
HBTU	2-(1 <i>H</i> -Benzotriazole-1-yl)-1,1,3,3-Tetramethyluronium hexafluorophosphate
H/His	Histidine
HOBt	Hydroxybenzotriazole
HPLC	High performance liquid chromatography
Hz	Hertz
<i>i.e.</i>	<i>Id est</i> (that is)
IC ₅₀	Concentration required to observe 50 % inhibition of activity
<i>J</i>	Coupling constants (Hz)
K/Lys	Lysine
L	Litre (s)
L/Leu	Leucine

LC	Liquid chromatography
LD ₅₀	Concentration required to observe 50 % decrease in viable cell number
M	Molarity (mol L ⁻¹)
MALDI	Matrix assisted laser desorption/ionization
MES	2-(<i>N</i> -morpholino) ethanesulfonic acid
MHz	MegaHertz
M/Met	Methionine
m.p.	Melting point
MS	Mass spectrometry
MSH	Melanocyte-stimulating hormone
<i>N</i> -terminus	Amino-terminus
NMM	<i>N</i> -Methylmorpholine
NMO	<i>N</i> -Methylmorpholine <i>N</i> -oxide
NMR	Nuclear magnetic resonance
OsO ₄	Osmium tetroxide
OT	Oxytocin
R/Arg	Arginine
PAL	Peptidylamidoglycolate lyase
PAM	Peptidylglycine α -amidating monooxygenase
PBA	<i>E</i> -4-Phenyl-3-butenoic acid
PCs	Prohormone convertases
Pd/C	Palladium on carbon

PHM	Peptidylglycine α -hydroxylating monooxygenase
P/Pro	Proline
q	Quartet
Q/Gln	Glutamine
r.t	Room temperature (approximately 18 °C)
R/Arg	Arginine
s	Singlet
SAR	Structure-activity relationship
SCLC	Small cell lung cancer
t	Triplet
TFA	Trifluoroacetic acid
TIPS	Triisopropylsilane
THF	Tetrahydrofuran
TLC	Thin layer chromatography
Tmz	Temozolomide
TRH	Thyrotropin-releasing hormone
UV-Vis	Ultraviolet-visible spectroscopy
V/Val	Valine
w/w	Unit weight per weight (ratio)
vs.	Versus
v/v	Unit volume per volume (ratio)
Y/Try	Tyrosine

> Greater than

< Less than

Abstract

C-Terminal amidated peptide hormones regulate numerous physiological process and are associated with many pathological conditions. Their C-terminal amidation is exclusively catalysed by the enzyme peptidylglycine α -amidating monooxygenase (PAM), which has two subunits: peptidylglycine α -hydroxylating monooxygenase (PHM; EC 1.14.17.3) and peptidyl- α -hydroxyglycine α -amidating lyase (PAL; EC 4.3.2.5). In the present study, the substrate specificity and inhibition of the PAM sourced from DMS53 human small cell lung cancer cells were investigated. A peptide consensus sequence *N*-Ac-Gly-(*S*)-Pro-Gln-(*S*)-Arg-(*S*)-Phe-Gly-COOH was constructed from the human amidated peptide hormone database, and a library of peptide substrates was designed by varying the amino acids located at the penultimate and antepenultimate positions from the C-terminus. These peptides were synthesised by solid phase peptide synthesis and studied in a competitive PHM binding assay. The results indicated that human glycine-extended hormone precursors having -Arg-Phe-Gly-COOH are likely to bind to PHM effectively in living bodies with IC₅₀ values around 20 μ M and those having -Asp-Phe-Gly-COOH and -Ala-Phe-Gly-COOH are likely to bind with IC₅₀ values around 70 μ M. The results also show that antepenultimate amino acids affect binding to PHM but to a lesser degree than the effect of penultimate amino acids.

In a prodrug study, the anti-cancer drug bexarotene was synthetically extended with a glycine to obtain a derivative that was expected to be cleaved by PAM and then deliver a cytotoxic drug. However, the derivative compound showed poor binding to PHM at

the millimolar level, but had a similar cytotoxic activity against DMS53 cells to its parent agent. Unlike bexarotene, a previous study showed that the glycine derivative of temozolomide (another anti-cancer drug) has strong binding to PHM at micromolar concentration, but somehow does not convert to temozolomide by PAM. One possible reason is that the glycine derivative possessing an imidazole moiety could inhibit PHM by metal chelation. To investigate this, a structurally-similar molecule *N*-Ac-(*S*)-His-Gly-COOH was tested and found to be processed by PAM and not undergo copper coordination. This implies that the glycine derivative of temozolomide is unlikely to chelate the copper of the PHM active site.

To investigate PHM and PAL activity simultaneously, a new PAM assay with a direct, rapid and sensitive HPLC-MS system was established. With this new assay the PAL inhibitor *N*-Ac-Phe-pyruvate and analogues were evaluated in terms of PAM inhibition through isolated enzyme competitive assays. This demonstrated that *N*-Ac-Phe-pyruvate is a PAL inhibitor at the nanomolar level against the medium PAM from DMS53 cells and deprotonation of its enol form results in a decrease of PAL inhibition.

By using the established HPLC-MS detection system, the intermediate of the C-terminal amidation of calcitonin-Gly (CTG), α -hydroxyglycine-extended calcitonin (HO-CTG), was detected in the culture medium of DMS53 cells. This is the first time HO-CTG produced by cells has been detected. With and without a PAL inhibitor, the concentration of the HO-CTG in the medium sample was found to be more than two orders of magnitude lower than those of the corresponding substrate and amidated

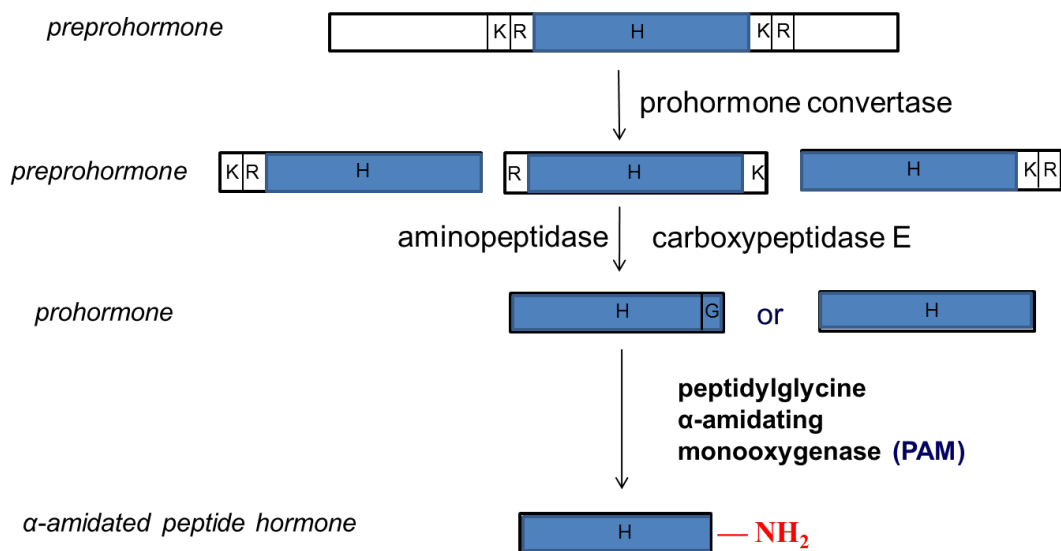
product, suggesting the PAL catalysis is much faster than PHM catalysis, and PHM catalysis is the rate-limiting step of amidation of calcitonin in human cells.

Chapter One

Introduction

1.1 C-Terminal Amidated Peptide Hormones

Peptide hormones play many important roles in biological activities in living bodies. Their roles include but are not limited to digestion,^[1] body temperature control,^[2] growth,^[3] uterine contractions,^[4] cardiovascular function,^[5] and antidiuretic regulation.^[6] Through regulated secretory pathways, peptide hormones are synthesised from larger, inactive precursors by a set of co- and post-translational modifications to become biologically active. As illustrated in **Figure 1.1** below, some prohormones have paired basic sites containing arginine (R) or lysine (K) which can undergo endoproteolysis by prohormone convertases (PCs). The cleaved residue extensions are then recognised and removed by carboxypeptidase E (CPE) and aminopeptidase to produce active hormones.^[7] However, some hormones will not be biologically active unless they are treated with an additional modification including glycosylation, acetylation, sulfation, phosphorylation, or C-terminal amidation. Among them, C-terminal amidation is the most important because around 50% of mammalian peptide hormones and more than 80% of insect hormones require amidation at the C-terminus for biological activity.^[8] This process is accomplished through a sequential reaction of two enzymes encoded by a single bifunctional enzyme - peptidylglycine α -amidating monooxygenase (PAM, EC 1.14.17.3).^[7]



Lucy

Figure 1.1 Biosynthesis of C-terminal amidated peptide hormones.^[7]

The sequences of all known human α -amidated peptide hormones are listed in **Table 1.1**. These peptides have a vast range of functions. For instance, kisspeptin stimulates the secretion of aldosterone and the release of insulin;^[9] vasopressin serves as an antidiuretic regulator^[6] and helps to alleviate pulmonary inflammation^[10] as well as influence pair-bonding in voles for its various neurological effect on brains;^[11] Cholecystokinin plays a key role in a number of physiological processes including digestion,^[12] satiety,^[13] and anxiety;^[14-15] and calcitonin participates in regulation of calcium and phosphorus metabolism,^[16] which may induce cancer growth.^[17-18] Therefore, from the above mentioned it is inferred that some correlation may exist between peptide hormone amidations and pathological conditions (*e.g.* chronic pain, inflammation, asthma or cancer).

Table 1.1 Human α -amidated peptide hormones.

No.	Name	Sequence
1	Adrenomedullin ^[19]	YRQSMNNFQGLRSFGCRFGTCTVQKLAHQIQFTDKDKDNVAPRSKISPQ GY-NH ₂
2	Adrenomedullin-2 ^[20]	TQAQLLRVGCVLGTCQVQNLSHRLWQLMGPAGRQDSAPVDPSSPHSY- NH ₂
3	Arg-vasopressin ^[6]	CYFQNCPRG-NH ₂
4	Big gastrin ^[21]	QLGPQGPPHLVADPSKKQGPWLEEEEEAYGWMDF-NH ₂
5	Calcitonin ^[22]	CGNLSTCMLGTYTQDFNKFHTFPQTAIGVGAP-NH ₂
6	Calcitonin gene-related peptide ^[23]	ACDTATCVTHRLAGLLSRSGGVVKNNFVPTNVGSKAF-NH ₂
7	Calcitonin gene-related peptide 2 ^[24]	ACNTATCVTHRLAGLLSRSGGMVKS NFVPTNVGSKAF-NH ₂
8	Cholecystokinin-5 ^[25]	GWMDF-NH ₂
9	Cholecystokinin-7 ^[26]	YMGWMDF-NH ₂
10	Cholecystokinin-8 ^[27]	DYMGWMDF-NH ₂
11	Cholecystokinin-12 ^[28]	ISDRDYMGWMDF-NH ₂
12	Cholecystokinin-18 ^[29]	LDPSHRISDRDYMGWMDF-NH ₂
13	Cholecystokinin-25 ^[29]	YIQQARKAPSGRMSIVKNLQNLDP SHRISDRDYMGWMDF-NH ₂
14	Cholecystokinin-58 ^[27]	VSQRTDGESRAHLGALLARYIQQARKAPSGRMSIVKNLQNLDP SHRISDRD YMGWMDF-NH ₂
15	Corticoliberin ^[30]	SEPPISLDLTFHLLREVLEMARAEQLAQQAH SNRKLMEII-NH ₂
16	Endokinin-A ^[31]	DGGEEQTLSTEAE TWVIVALEEGAGPSIQLQLQEVKTGKASQFFGLM-NH ₂

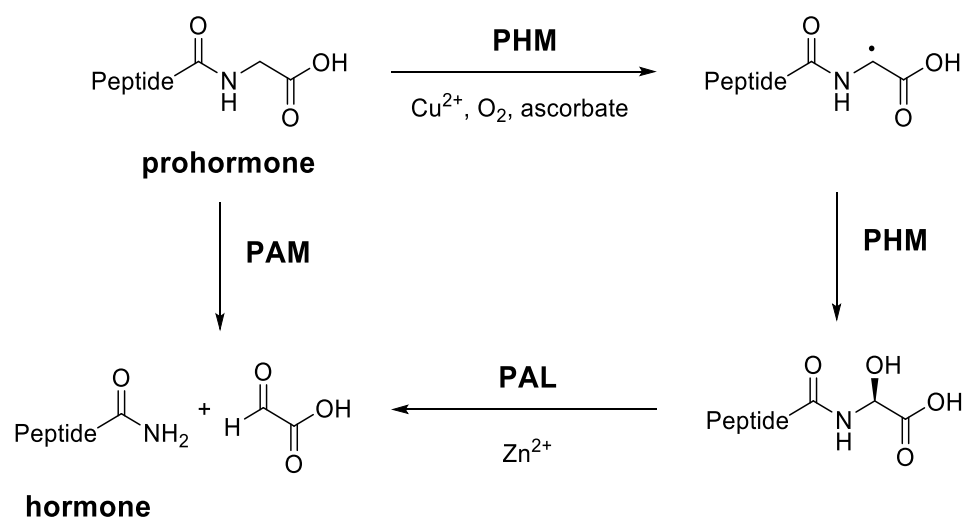
17	Endokinin-A/B ^[31]	GKASQFFGLM-NH ₂
18	Endokinin-C ^[31]	KKAYQLEHTFQGLL-NH ₂
19	ER-37 ^[32]	EEEGSANRRPEDQELESLSAIEAELEKVAHQQLQALRR-NH ₂
20	Gastrin ^[33]	QGPWLEEEEEAYGWMDf-NH ₂
21	Gastrin-6 ^[34]	YGWMDf-NH ₂
22	Gastrin-14 ^[33]	WLEEEEEAYGWMDf-NH ₂
23	Gastrin-52 ^[35]	DLELPWLEQQGPASHHRRQLGPQGPPHLVADPSKKQGPWLEEEEEAYGWMDf-NH ₂
24	Gastrin-71 ^[36]	SWKPRSQQPDAPLGTGANRDLELPWLEQQGPASHHRRQLGPQGPPHLVADPSKKQGPWLE-NH ₂
25	Gastrin-releasing peptide ^[37]	VPLPAGGGTVLTKMYPRGNHWAVGHLM-NH ₂
26	Glucagon-like peptide 1(7-36) ^[38]	HAEGTFTSDVSSYLEGQAAKEFIAWLVKGR-NH ₂
27	Gonadoliberin-1 ^[39]	QHWSYGLRPG-NH ₂
28	Gonadoliberin-2 ^[40]	QHWSHGWYPG-NH ₂
29	GR-44 ^[32]	GYPEEKKEEEGSANRRPEDQELESLSAIEAELEKVAHQQLQALRR-NH ₂
30	Intermedin-short ^[41]	VGCVLGTCQVQNLSHRLWQLMGPAGRQDSAPVDPSSPHSY-NH ₂
31	Intestinal peptide PHM-27 ^[42]	HADGVFTSDFSKLLGQLSAKKYLESLM-NH ₂
32	Islet amyloid polypeptide ^[43]	KCNTATCATQRLANFLVHSSNNFGAILSSTNVGSNTY-NH ₂
33	Kisspeptin ^[44]	GTSLSPPPSSGSPQQPGLSAPHSRQIPAPQGAVLVQREKDLPNYNWNSFGLRF-NH ₂
34	Kisspeptin-10 ^[45]	YNWNSFGLRF-NH ₂
35	Kisspeptin-13 ^[45]	LPNYNWNSFGLRF-NH ₂
36	Kisspeptin-14 ^[45]	DLPNYNWNSFGLRF-NH ₂
37	Melanotropin alpha ^[46]	SYSMEHFRWGKPV-NH ₂
38	Melanotropin gamma ^[47]	YVMGHFRWDRF-NH ₂
39	Neurokinin A ^[48]	HKTDSFVGLM-NH ₂
40	Neurokinin-B ^[49]	DMHDFVGLM-NH ₂

41	Neuromedin-B ^[50]	GNLWATGHFM-NH ₂
42	Neuromedin-B-32 ^[51]	APLSWDLPEPRSRASKIRVHSRGNLWATGHFM-NH ₂
43	Neuromedin-C ^[37]	GNHWAVGHLM-NH ₂
44	Neuromedin-S ^[52]	ILQRGSGTAAVDFTKKDHTATWGRPFLLFRPRN-NH ₂
45	Neuromedin-U-25 ^[53]	FRVDEEFQSPFASQSRGYFLFRPRN-NH ₂
46	Neuropeptide gamma, 2nd part ^[54]	GHGQISHKRHKTDSEFVGLM-NH ₂
47	Neuropeptide-glutamic acid-isoleucine ^[55]	EIGDEENSAKFPI-NH ₂
48	Neuropeptide AF ^[56]	AGEGLNSQFWSLAAPQRF-NH ₂
49	Neuropeptide FF ^[57]	FLFQPQRF-NH ₂
50	Neuropeptide K ^[54]	DADSSIEKQVALLKALYGHGQISHKRHKTDSEFVGLM-NH ₂
51	Neuropeptide NPSF ^[58]	SLNFEELKDWGPKNVIKMSTPAVNKMPHSFANLPLRF-NH ₂
52	Neuropeptide NPVF ^[57]	VPNLPQRF-NH ₂
53	Neuropeptide RFRP-1 ^[57]	MPHSFANLPLRF-NH ₂
54	Neuropeptide SF ^[59]	SQAFLFQPQRF-NH ₂
55	Neuropeptide Y ^[60-61]	YPSKPDNPGEDAPAEDMARYYSALRHYINLITRQRY-NH ₂
56	Obestatin ^[62]	FNAPFDVGIKLSGVQYQQHSQAL-NH ₂
57	Orexin-A ^[63]	QPLPDCCRQKTCSCRLYELLHGAGNHAAGILTL-NH ₂
58	Orexin-B ^[64]	RSGPPGLQGRLLQASGNHAAGILTM-NH ₂
59	Osteocrin ^[65]	SFSGFGSPLDRLSAGSVDHKGKQRKVVDHPKRRFGIPMDRIGRNRLSNSR-NH ₂
60	Oxytocin ^[4]	CYIQNCPLG-NH ₂
61	Pancreastatin ^[66]	GESRSEALAVDGAGKPGAEAAQDPEGKGEQEHSSQKEEEEEMA VVPQGLFRG-NH ₂
62	Pancreatic hormone ^[67]	APLEPVYPGDNATPEQMAQYAADLRRYINMLTRPRY-NH ₂
63	Peptide YY ^[68]	YPIKPEAPREDASPEELNRYASLRHYLNLVTRQRY-NH ₂
64	Peptide YY(3-36) ^[69]	IKPEAPREDASPEELNRYASLRHYLNLVTRQRY-NH ₂

65	Pituitary adenylate cyclase-activating polypeptide 27 ^[70]	HSDGIFTDSYSRYRKQMAVKKYLA AVL-NH ₂
66	Pituitary adenylate cyclase-activating polypeptide 38 ^[70]	HSDGIFTDSYSRYRKQMAVKKYLA AVLGKRYKQRVKNK-NH ₂
67	Pneumadin ^[71]	AGEPKLDAGV-NH ₂
68	Potential peptide ^[72]	EDVSAGEDCGPLPEGGPEPRSDGAKPGPRE-NH ₂
69	Proadrenomedullin N-20 terminal peptide ^[73]	ARLDVASEFRKKWNKWALSR-NH ₂
70	Prolactin-releasing peptide PrRP31 ^[74]	SRTHRHSMEIRTPDINPAWYASRGIRPVGRF-NH ₂
71	Prolactin-releasing peptide PrRP20 ^[75]	TPDINPAWYASRGIRPVGRF-NH ₂
72	QRF-amide ^[76]	QDEGSEATGFLPAAGEKTSGPLGNLAEELNGYSRKKGGFSFRF-NH ₂
73	Salusin-alpha ^[77]	SGALPPAPAAPRALRAQRAGPAGPGAK-NH ₂
74	Secretin ^[78]	HSDGTFTSELSRLREGARLQRLQGLV-NH ₂
75	Somatoliberin ^[79]	YADAIFTNSYRKVLGQLSARKLLQDIMSRQQGESNQERGARARL-NH ₂
76	Spexin ^[80]	NWTPQAMLYLKGAQ-NH ₂
77	Substance P ^[5]	RPKPQQFFGLM-NH ₂
78	Thyroliberin ^[81]	QHP-NH ₂
79	Urocortin ^[82]	DNPSLSIDLTFHLLRTLLELARTQSQRERAEQNRIIFDSV-NH ₂
80	Urocortin-3 ^[83]	FTLSLDVPTNIMNLLFNIAKAKNLRAQAAANAHLMAQI-NH ₂
81	Vasoactive intestinal peptide ^[84]	HSDAVFTDNYTRLRKQMAVKKYLN SILN-NH ₂

1.2 General Introduction to PAM Enzyme

PAM is the only known enzyme that catalyses *C*-terminal amidation both in mammals and insects.^[85] It exists not only in neuroendocrine tissues, but also in endothelial cells, smooth muscle cells, airway, brain ependymal cells, and astrocytes.^[8, 86-88] In an adult human body, high levels of PAM activity have been found in the central nervous system,^[89] endocrine cells of the pituitary,^[85] and at atrium cordis.^[90] PAM consists of two subunits: peptidylglycine α -hydroxylating monooxygenase (PHM; EC 1.14.17.3) and peptidyl- α -hydroxyglycine α -amidating lyase (PAL; EC 4.3.2.5). PHM catalyses stereospecific hydroxylation of the glycine α -carbon of all the peptidylglycine substrates; then PAL catalyses *N*-dealkylation of the α -hydroxyglycine intermediates to produce amidated hormones and glyoxylate (**Scheme 1.1**).^[85] Since some pathological conditions can be attributed to dysfunction of α -amidated peptides, there has been a constant interest in developing PAM inhibitors that could moderate α -amidated peptide hormone levels.



Scheme 1.1 Mechanism of PAM Catalysis.

1.2.1 Mechanistic Insight of PHM

The first subunit of PAM enzyme, PHM, is copper-, molecular oxygen- and ascorbate-dependent. **Figure 1.2** shows the X-ray crystal structure of the active pocket of PHM with encapsulated substrate. PHM catalytic core consists of two β -sandwich domains, of which one binds to an active site cupric ion (CuA) with three histidine residues (H107, H108, and H172); and another binds to the second cupric ion (CuB) with H242, H244, and M314.^[91] The distance between these two coppers is 11 Å and is not affected by the binding of the peptide. The CuA site has been identified as an electron transfer site,^[91] while the CuB site is close to the substrate binding site.^[91] This structural analysis is consistent with the results attained in several kinetic and structural studies.^[92-95] It is worth noting that the key structural change for peptide binding is hydrogen bond formation between the glycy NH of the peptide substrate and the carbonyl group of N316 through rotation of N316 side chain, which leads to the breaking of a hydrogen bond between N316 and Y318. Further, the carboxylate of the substrate forms not only an ion-ion interaction with the guanidinium group of

R240 but also a hydrogen bond with the hydroxyl group of Y318. Additionally, some hydrophobic residues like the CuB ligand M314 have good contact with the hydrophobic side chain of the substrate, anchoring it in the PHM active site^[91].

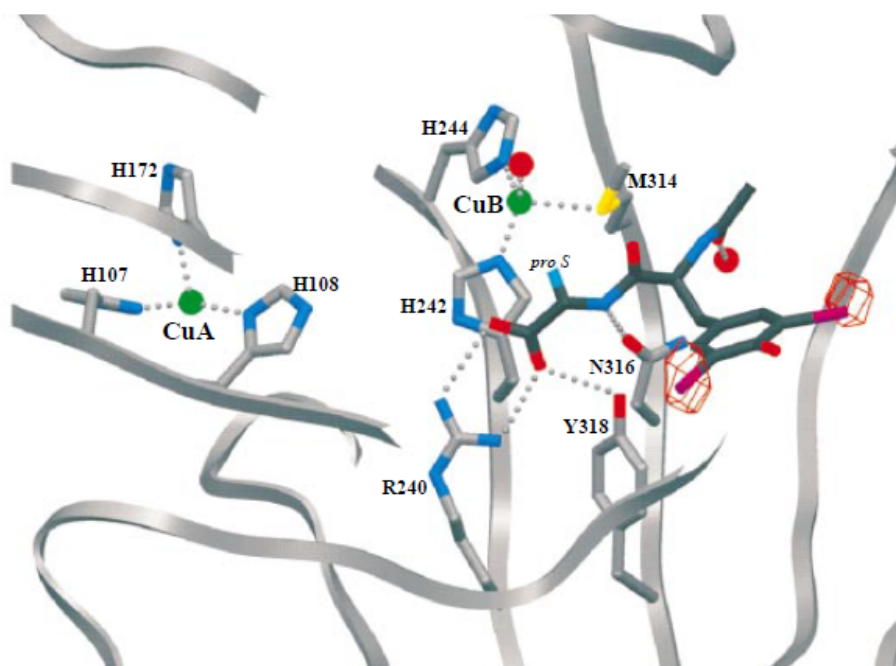


Figure 1.2 Crystal structure of an oxidised PHM-substrate complex.^[91] The substrate is *N*-Ac-l-3,5-diiodotyrosylglycine. (From Prigge *et al.*, *Science* **1997**, 278, 1300. Reprinted with permission from American Association for the Advancement of Science.)

The two PHM copper ions cycle between Cu(I) and Cu(II) during the hydroxylation of the *C*-terminal glycine residue of a peptide substrate.^[96-98] This redox reaction as part of PHM activity requires the participation of ascorbic acid.^[8] Ascorbate reduces the two PHM copper atoms from Cu(II) to Cu(I) through two single-electron transfers and itself is oxidised to semidehydroascorbate at the same time.^[99] The reduced Cu(I)

binds to molecular oxygen as the glycine-extended substrate binds to the enzyme,^[100] followed by abstraction of H \cdot and formation of C-OH bond in the substrate.^[92, 101-102] However, to date, it has not been confirmed what the abstracting species are^[92-93, 95, 103] and how formation of C-OH bond is performed.^[92-93]

1.2.2 Mechanistic Insight of PAL

PAL, a zinc-dependent enzyme, catalyses the cleavage of the α -hydroxyglycine extended intermediate produced by PHM to the corresponding amidated product and glyoxylate at physiological pH.^[104] The PAL enzyme active site consists a Zn(II) coordinated by H585, H690 and H786.^[105-106] Based on the analysis of the X-ray crystal structure of a PAL-substrate complex, as shown in **Figure 1.3**, several interactions between the substrate and the enzyme are considered important.^[105] For example, an important tyrosine residue, Y654, conserved in all known PAL enzymes, and is proposed to be first deprotonated as the catalytic base through the interaction with R706 and Zn(II).^[106-107] Afterwards, Y654 deprotonates the α -hydroxyl group of the PAL substrate already bound to the active site through coordination of the α -OH to the Zn(II). Finally, it transfers the proton to the leaving $-NH$ group which triggers the formation of the amidated peptide and glyoxylate (**Scheme 1.2**).^[105] In addition, R533 anchors the terminal carboxylate of the substrate by ion-ion interactions, while M784 anchors the carbonyl of the substrate *via* sigma-hole bond and determines the stereo specificity of the PAL reaction.^[105]

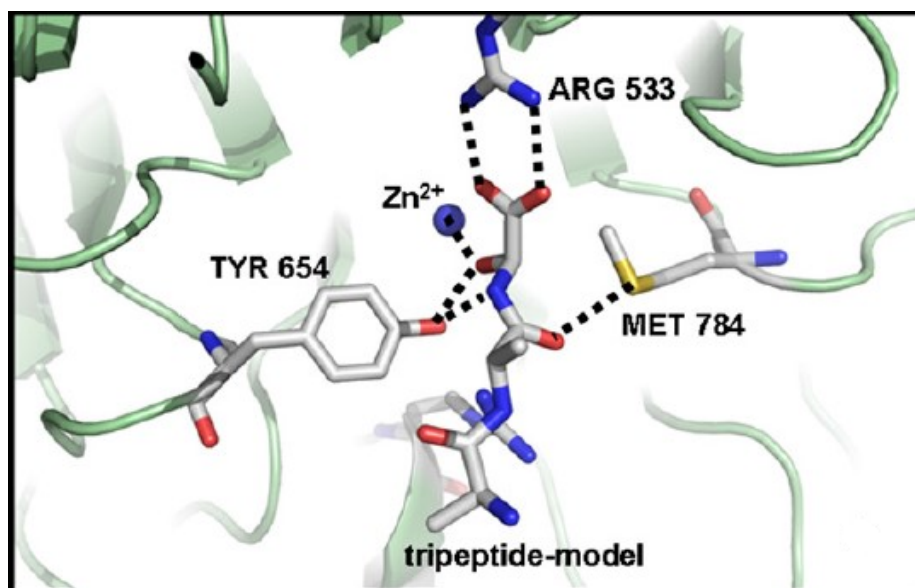
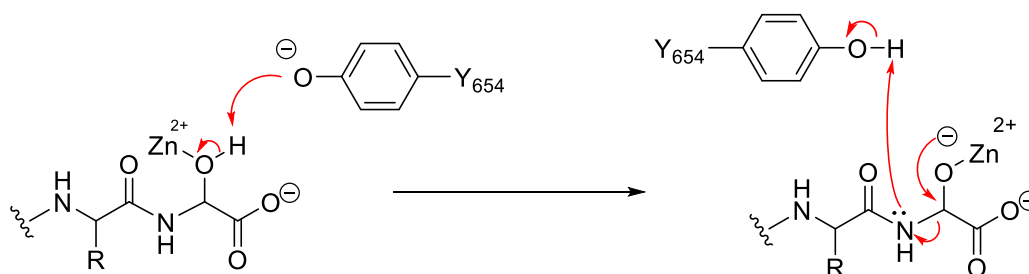


Figure 1.3 Crystal structure of a PAL-substrate complex.^[105] The substrate is HO-Ala-Ala-(S)-Gly-COOH. (From Chufan et al., *Structure* **2009**, *17*, 965. Reprinted with permission from Cell Press.)



Scheme 1.2 PAL catalytic reaction mechanism.^[105]

1.2.3 PAM Cofactors

The PAM reaction mainly depends on PHM cofactors, which are oxygen, copper and ascorbate, lacking one of them can lead to inactivation of PAM activity.^[8, 104, 108] For example, loss of oxygen in tissue-related experiments can completely inhibit amidation,^[108] and acute hypoxia in cell assay can significantly restrain production of

amidated peptides.^[109] Copper ion is the only metal ion present in the PHM structure and crucial for monooxygenase activity.^[110] PAM-catalysed amidation can be inhibited by copper chelation. For instance, copper chelator, *N,N*-diethyldithiocarbamate, reduces the production of adrenocorticotrophic hormone (ACTH) and α -melanocyte-stimulating hormone (α -MSH);^[108] bathocuproinedisulfonic acid, a cell impermeant copper chelator specific for Cu(I), inhibits the formation of peptide YY and neuromedin U in Chinese hamster ovary cell medium.^[111] Activity can only be restored by addition of copper ion.^[110, 112] Its oxidizing agent, ascorbate, is another important factor for PAM activity. In cultured pituitary cells, the lack of ascorbate can lead to the loss of amidated peptide α -MSH while the addition of ascorbate can re-establish α -amidation.^[113] Pre-incubating AtT-20 cells (a type of pituitary corticotrope tumor from mouse) with medium containing ascorbate for 24 h can increase intracellular concentration of ascorbate as well as levels of amidated joining peptide.^[114] A similar scenario can also be seen with thyrotropin-releasing hormone (TRH) in the cultures of hypothalamic cells.^[113]

1.2.4 Substrate Specificity of PAM

PAM has a high substrate specificity for *C*-terminal glycine-extended peptide prohormones,^[115-117] and especially has a preference for those with a hydrophobic amino acid with (*S*)- α -configuration in the penultimate position at the *C*-terminus, adjacent to the glycine.^[115, 118-119] In the binding affinity study by Tamburini *et al.*,^[118] all twenty natural amino acids were one by one put at the position X of *N*-dansyl-(Gly)₄-X-Gly-COOH for binding affinity test and a 130-fold variation in apparent K_m

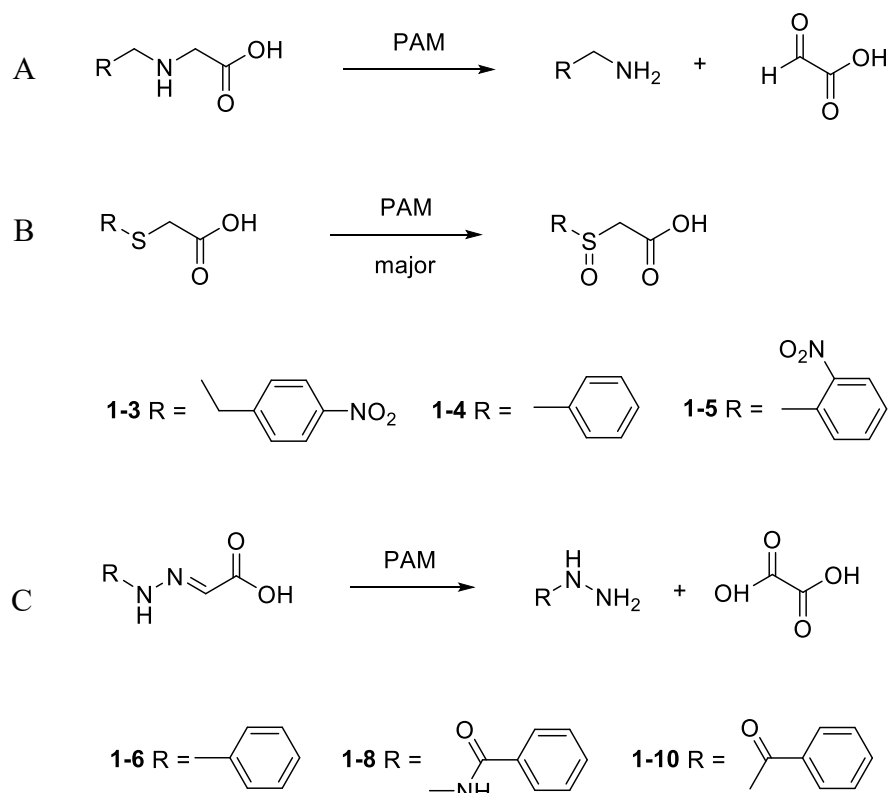
values were observed. The broad range in K_m values indicates that the interaction of a side chain at the penultimate position from the C-terminus with the enzyme active site can play an important role to the stabilization of the enzyme-substrate complex. Its positive effect on binding to PAM decreases sequentially through four groups which are sulphur containing or planar aromatic, neutral aliphatic, polar and basic, and cyclic aliphatic or acidic.^[118] More specifically, **Table 1.2** illustrates the effect of each of the twenty amino acids at the penultimate position of the hexapeptide substrate on the binding affinity with PAM.^[118]

Table 1.2 Kinetic parameters for enzymatic α -amidation of peptides of the form N -dansyl-(Gly)₄-X-Gly-OH.^[118]

Group	X	K_m (μ M)	V_{max} (nmol min ⁻¹ mg ⁻¹)
Planar aromatic or sulphur containing	Phe	4	50
	Tyr	5	40
	Met	7	23
	Cys	11	10
Neutral aliphatic	Ile	20	55
	His	41	10
	Ala	46	6
	Val	49	48
	Leu	54	22
	Trp	58	58
Polar and basic	Asn	83	7
	Ser	196	9
	Arg	200	15
	Lys	206	4
	Gln	308	17
	Thr	334	50
Cyclic aliphatic or acidic	Glu	449	5
	Pro	618	22
	Gly	-	(< 1 at 240 μ M)
	Asp	-	No detectable activity

In addition, the length of peptide substrate sequence is another factor that affects binding affinity. Recognition of peptide substrate extends to about five amino acids from the *C*-terminus, as displayed by the study of Morris *et al.*^[120] showing that K_m values for tri-, tetra-, and pentapeptide analogues of procalcitonin, and of mono-, di-, tri-, and tetrapeptide analogues of prooxytocin decrease accordingly and are all higher than the K_m values of the corresponding natural prohormones. It is worth noting that peptides with *C*-terminal (*R*)-Ser or (*R*)-Ala can also be processed by PAM but the enzyme binding affinities are less than one percent of those with *C*-terminal Gly.^[117]

Apart from peptides, several types of non-peptide compounds can also be competitive substrates for PAM. As shown in **Scheme 1.3A**, PAM can catalyse amine *N*-dealkylation, for example, converting *N*-(4-nitrobenzyl)glycine (**1-1**) to 4-nitrobenzylamine.^[102] However, their PAM binding affinities are relatively low with millimolar K_m values.^[102] Sulphide (4-nitrobenzyl)thioacetic acid (**1-3**) is also oxidatively cleaved by bovine PAM, with the K_m value of 340 μM , yielding mainly sulfoxide through formation of sulphur cation radical and thus sulfoxidation (**Scheme 1.3B**).^[104] In addition, some hydrazones and semicarbazones of glyoxylic acid **1-6 - 1-16** are well recognised and oxidised by porcine PAM (**Scheme 1.3C**).^[121]



Scheme 1.3 Variety of non-peptide substrates accommodated by PAM. (A): *N*-dealkylation of amine compounds;^[102] (B): Sulfoxidation of sulphide;^[104] (C) PAM-catalysed reaction of hydrazones and semicarbazones of glyoxylic acid.^[121]

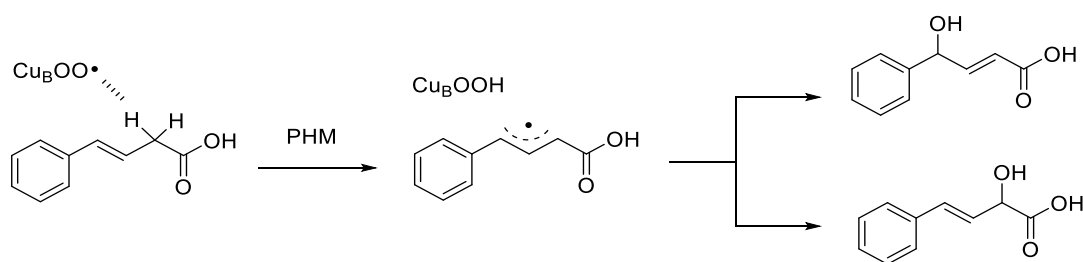
1.3 PAM Inhibition

As mentioned before, overexpression of α -amidated peptide hormones may contribute to inflammation, disease recurrence, cancer cell proliferation, or tumour growth *etc.*^[17, 87, 122-123] For instance, calcitonin secreted by prostate carcinoma cell lines can stimulate cell growth in the tumour;^[17] substance P and calcitonin gene-related peptide (CGRP) give rise to acute inflammation including rheumatoid arthritis.^[87] The disease-promoting role of some amidated peptides makes PAM a promising target for therapeutic strategies.^[87] Furthermore, the fact that PAM activity is the rate-limiting

and final step in the production of α -amidated peptide hormones *in vivo*,^[110] makes the regulation of amidated peptide hormones possible through the regulation of PAM. Hence, many studies focus on drug development through the production of inhibitors that regulate PAM both *in vivo* and *in vitro*.^[87, 104, 124-127]

1.3.1 PHM Inhibitors

Considerable effort has been made on studying compounds, which can be processed by PHM and that result in inactivation of the enzyme. *E*-4-phenyl-3-butenoic acid (PBA) (**1-17**), is an irreversible mechanism-based PHM inhibitor. Michael addition/Cu(I) chelation is thought to be the main chemistry for PHM inhibition by PBA, which occurs *via* formation of a delocalised radical prior to hydroxylation, producing an inactivated copper-oxygen species (**Scheme 1.4**).^[128] PBA shows anti-inflammatory and analgesic effects in animal models of acute and chronic inflammation, probably by reducing the level of the amidated peptide substance P, which is linked to inflammation.^[87] In addition, PBA (**1-17**) exhibits anti-tumorigenic potential in that PBA (**1-17**) reduces lung cancer cell proliferation by inhibiting amidated growth factors: gastrin-releasing peptide (GRP).^[129-130] Apart from PBA, the PBA derivatives **1-18 - 1-21** containing methyl, methoxy and benzyloxy substituents on their phenyl rings also show similar PHM inhibitory potency.^[128]



Scheme 1.4 Radical formation and hydroxylation of PBA by PHM.^[128]

α,β -Unsaturated acids such as cinnamate and its analogues **1-25** - **1-34** have different chemistry for the inactivation of PHM *via* a reversible Michael addition of an active site nucleophile at the α,β -unsaturated carbonyl of cinnamate and corresponding analogues (**Figure 1.4**).^[124] Among them, *trans*-benzoylacrylic acid (**1-37**) shows approximately eight times better PHM inactivation than that of monoethyl fumarate (**1-36**), indicating that aromatic ring enhances the binding affinity with PHM.^[102] Further, compounds more closely resembling PHM substrates such as enantiomeric compounds (*R*)- and (*S*)-5-acetamido-4-oxo-6-phenyl-2-hexenoic acid (**1-38**) - (**1-39**) have similar PHM inhibitory effects, illustrating that the binding mode of α,β -unsaturated γ keto acids is different to those of peptide substrates and peptidyl competitive inhibitors, for which PHM exhibits subsite stereospecificity.^[131-132]

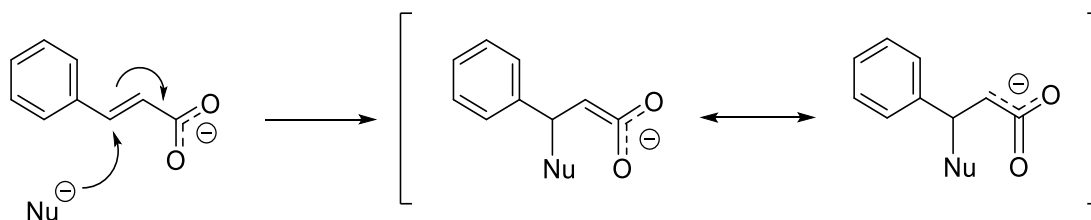
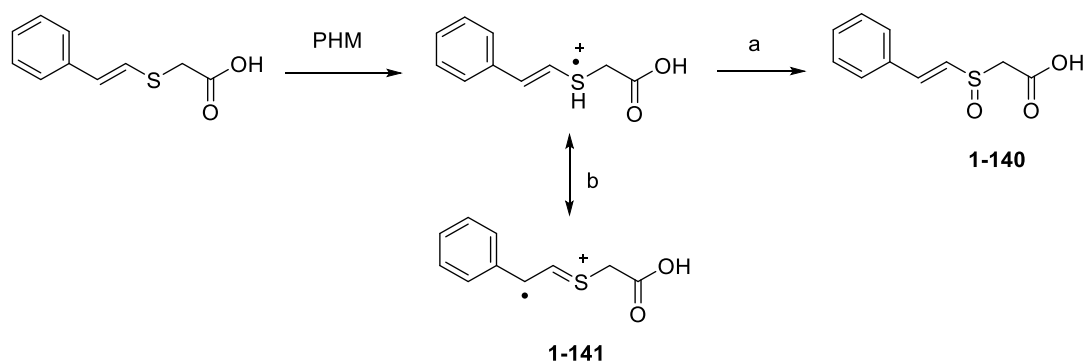


Figure 1.4 Proposed mechanism for cinnamate-mediated inactivation of PHM.^[124]

Glycolates such as compounds **1-45 - 1-58** are a type of reversible and competitive PHM inhibitor.^[102, 119, 127, 133-134] In terms of structure, glycolates and PHM substrates are alike and the only difference is that the NH of glycine in substrates is replaced with O in glycolates. This change blocks enzyme catalysis because of the inability to perform an α -hydroxylation.^[135] A study by Cao *et al.*^[133] shows that fatty acid derivatives of glycolates **1-45 - 1-49** are efficient inhibitors against enzyme extracted from frog and human small cell lung carcinoma (H889 and DMS53). Compared with the corresponding glycine substrate with $K_{m,app}$ values of 30 μ M, the decanoate **1-47** has an IC_{50} of only 40 nM against PAM extracted from DMS53 Cells.^[133] Similar to glycine-extended substrates of PAM, glycolate analogues also show high enzyme affinity when an α -(*S*)-amino acid is present at the penultimate position. For example, (*S*)-phenylalanine and leucine derivatives **1-57** and **1-58** have K_I values of 45 and 60 μ M, respectively, while the corresponding enantiomers **1-59** and **1-60** have much higher K_I values of 2250 and 2100 μ M, respectively.^[119]

The unsaturated thioacetic acid, *trans*-styrylthioacetic acid (**1-109**), behaves as an irreversible mechanism-based PHM inhibitor.^[136] Two possible pathways of PHM-catalysed reaction of compound **1-109** were proposed as shown in **Scheme 1.6**. Since synthesised compound **1-140** was tested (used up to 3 mM) and shows no inhibitory effect,^[136] it is thus more likely that, after delocalization, benzylic radical in compound **1-141** is formed according to pathway **b** (**Scheme 1.5**), followed by reaction with a radical residue of PHM, leading to inactivation. The corresponding *cis* isomer **1-110** shows no inhibition, indicating that the configurational isomerism affects PHM inactivation significantly and only *trans*-form is active.^[136]

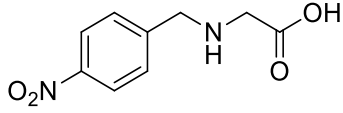
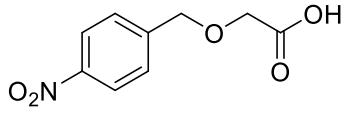
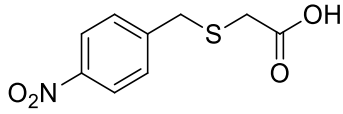
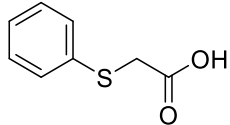
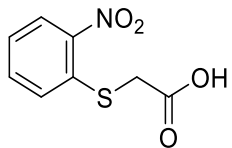
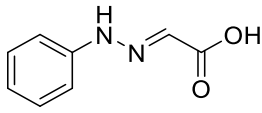
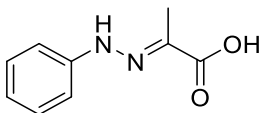
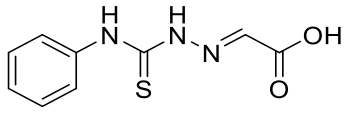
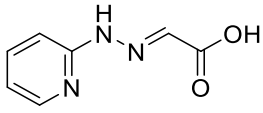
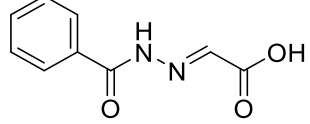


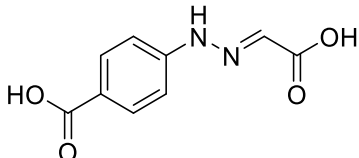
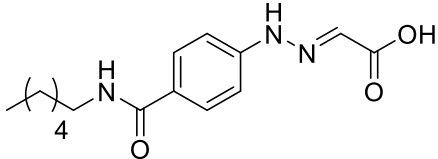
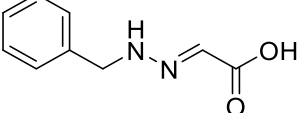
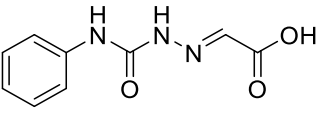
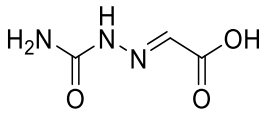
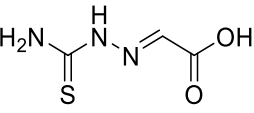
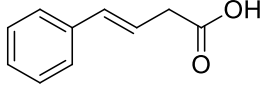
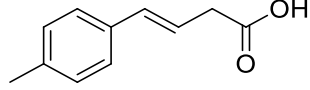
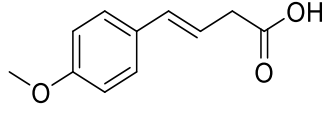
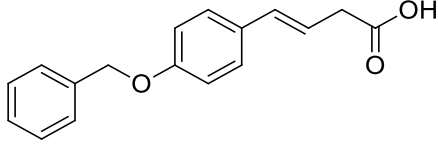
Scheme 1.5 Two possible pathways of PHM oxidation of *trans*-styrylthioacetic acid.^[136]

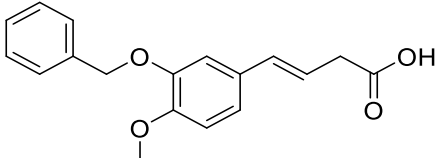
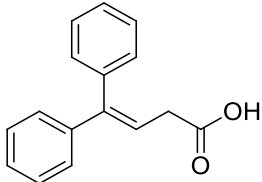
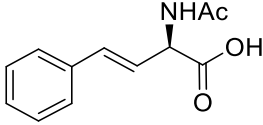
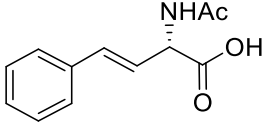
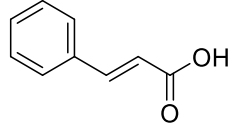
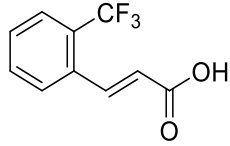
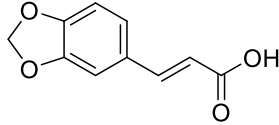
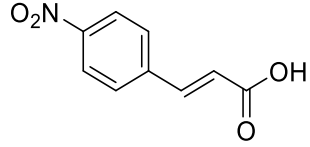
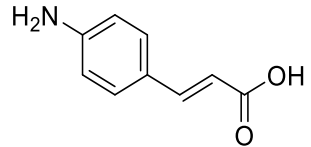
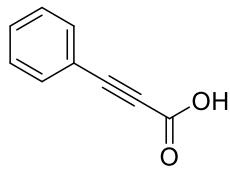
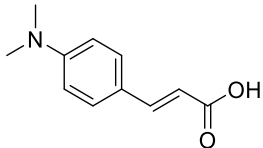
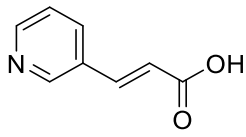
Some non-peptide *N*-formyl amides **1-131** - **1-137** are recognised as moderate mechanism-based irreversible inactivators of PHM.^[137] *N*-formyl amides **1-133** - **1-137** with phenyl groups show better PHM inhibition than those with aliphatic ones, among which compound **1-137** that mimics phenylalanine is the most potent one.

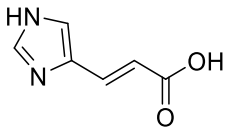
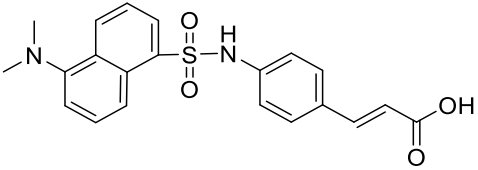
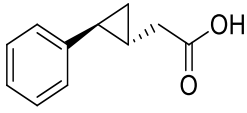
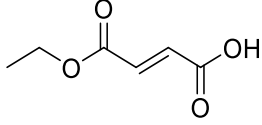
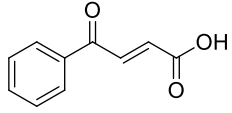
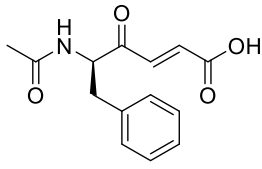
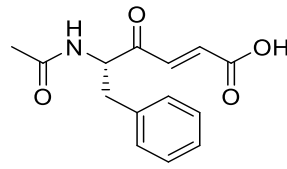
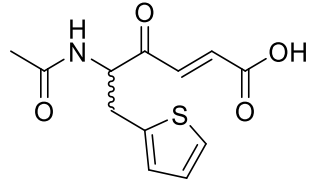
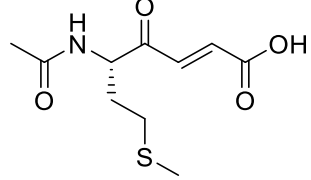
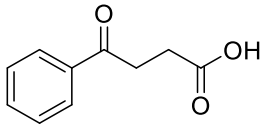
Table 1.3 summarises all reported PHM substrates and inhibitors.

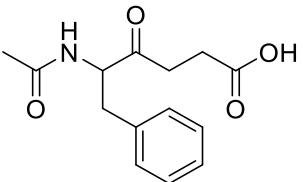
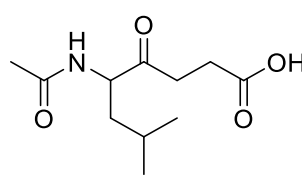
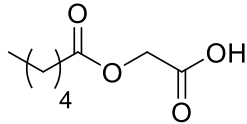
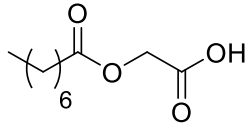
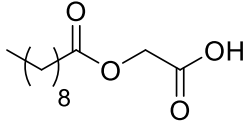
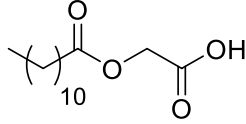
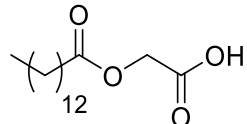
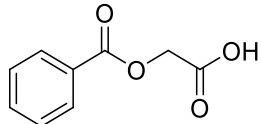
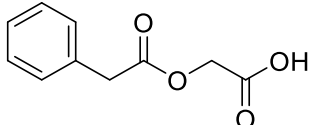
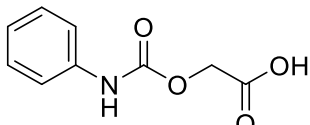
Table 1.3 PHM substrates and inhibitors.

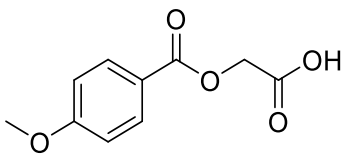
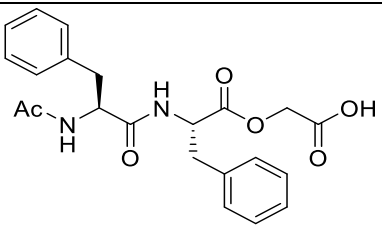
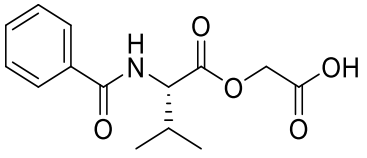
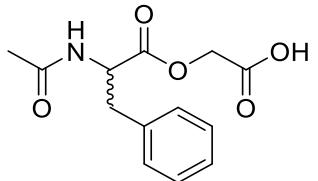
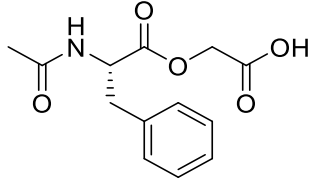
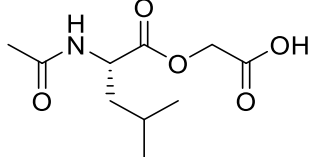
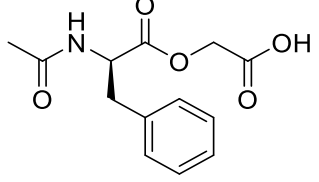
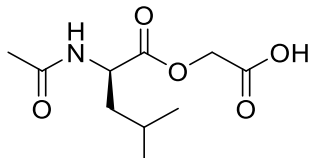
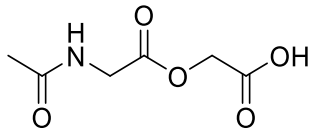
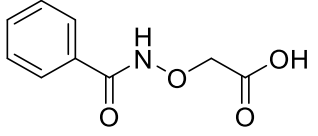
Structure and Binding Data	Structure and Binding Data
 <p style="text-align: center;">1-1</p> <p style="text-align: center;">$K_m = 1800 \mu\text{M}(\text{bovine})^{[102]}$</p>	 <p style="text-align: center;">1-2</p> <p style="text-align: center;">$K_m = 160 \mu\text{M}(\text{bovine})^{[102]}$</p>
 <p style="text-align: center;">1-3</p> <p style="text-align: center;">$K_m = 340 \mu\text{M}(\text{bovine})^{[102]}$</p>	 <p style="text-align: center;">1-4</p> <p style="text-align: center;">$K_I = 380 \pm 40 \mu\text{M}(\text{rat})^{[127]}$</p>
 <p style="text-align: center;">1-5</p> <p style="text-align: center;">$K_I = 29 \mu\text{M}(\text{rat})^{[127]}$</p>	 <p style="text-align: center;">1-6</p> <p style="text-align: center;">$K_I = 15 \mu\text{M}$ (96% inhibition with 100 μM; porcine)^[121]</p>
 <p style="text-align: center;">1-7</p> <p style="text-align: center;">0% inhibition with 100 μM (porcine)^[121]</p>	 <p style="text-align: center;">1-8</p> <p style="text-align: center;">93% inhibition with 100 μM (porcine)^[121]</p>
 <p style="text-align: center;">1-9</p> <p style="text-align: center;">45% inhibition with 100 μM (porcine)^[121]</p>	 <p style="text-align: center;">1-10</p> <p style="text-align: center;">8% inhibition with 100 μM (porcine)^[121]</p>

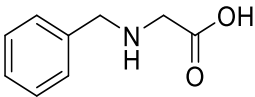
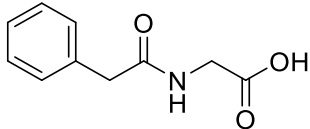
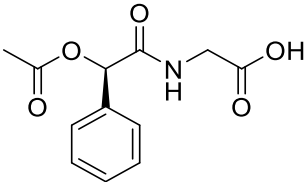
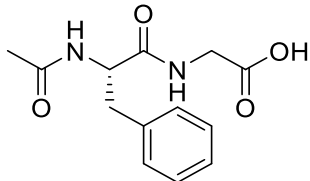
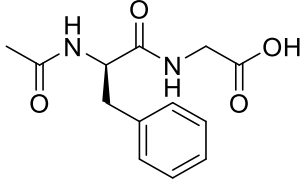
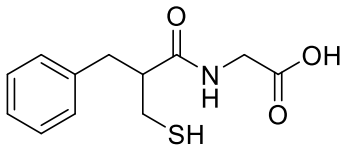
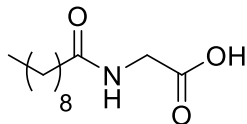
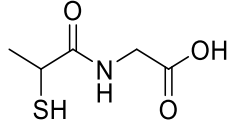
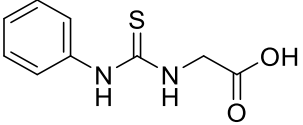
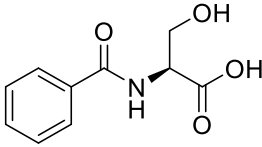
 <p style="text-align: center;">1-11</p> <p style="text-align: center;">46% inhibition with 100 μM (porcine)^[121]</p>	 <p style="text-align: center;">1-12</p> <p style="text-align: center;">94% inhibition with 100 μM^[121]</p>
 <p style="text-align: center;">1-13</p> <p style="text-align: center;">52% inhibition with 100 μM (porcine)^[121]</p>	 <p style="text-align: center;">1-14</p> <p style="text-align: center;">50% inhibition with 100 μM (porcine)^[121]</p>
 <p style="text-align: center;">1-15</p> <p style="text-align: center;">33% inhibition with 100 μM (porcine)^[121]</p>	 <p style="text-align: center;">1-16</p> <p style="text-align: center;">$K_I = 110 \mu\text{M}$ (83% inhibition with 100 μM; porcine)^[121]</p>
 <p style="text-align: center;">1-17</p> <p style="text-align: center;">$K_I = 1 \mu\text{M}$ (bovine)^[102] $K_I = 19 \pm 2 \mu\text{M}$ (porcine)^[128] $K_I = 0.096 \pm 0.028 \mu\text{M}$ (human)^[138]</p>	 <p style="text-align: center;">1-18</p> <p style="text-align: center;">$K_I = 5.7 \pm 0.9 \mu\text{M}$ (porcine)^[128]</p>
 <p style="text-align: center;">1-19</p> <p style="text-align: center;">$K_I = 15 \pm 2 \mu\text{M}$ (porcine)^[128]</p>	 <p style="text-align: center;">1-20</p> <p style="text-align: center;">$K_I = 19 \pm 2 \mu\text{M}$ (porcine)^[128]</p>

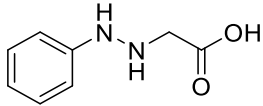
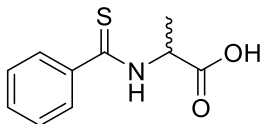
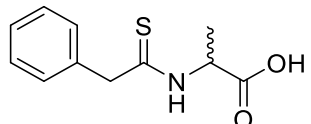
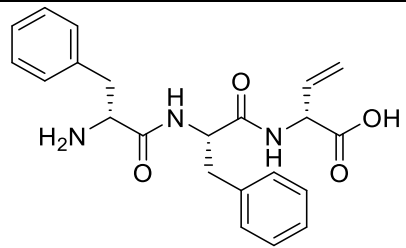
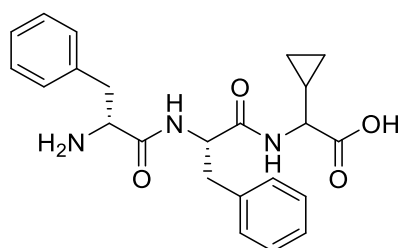
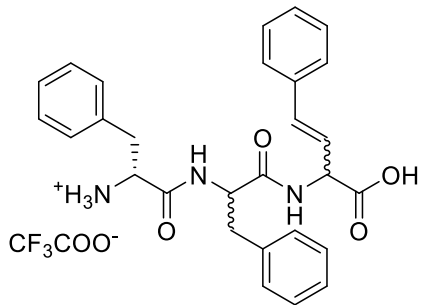
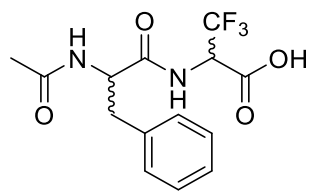
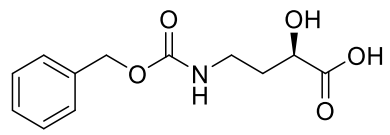
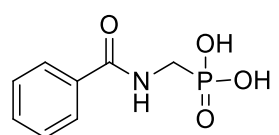
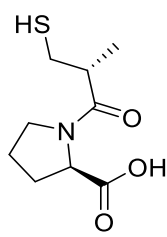
 <p style="text-align: center;">1-21 $K_I = 3.9 \pm 0.7 \mu\text{M}$ (porcine)^[128]</p>	 <p style="text-align: center;">1-22 $K_I > 700 \mu\text{M}$ (porcine)^[128]</p>
 <p style="text-align: center;">1-23 $IC_{50} = 1000 \mu\text{M}$ (rat)^[139]</p>	 <p style="text-align: center;">1-24 $IC_{50} = 1500 \mu\text{M}$ (rat)^[139]</p>
 <p style="text-align: center;">1-25 $K_I = 4000 \pm 200 \mu\text{M}$ (rat)^[124]</p>	 <p style="text-align: center;">1-26 $K_I = 200 \pm 20 \mu\text{M}$ (rat)^[124]</p>
 <p style="text-align: center;">1-27 $K_I = 300 \pm 40 \mu\text{M}$ (rat)^[124]</p>	 <p style="text-align: center;">1-28 $K_I = 600 \pm 40 \mu\text{M}$ (rat)^[124]</p>
 <p style="text-align: center;">1-29 $K_I = 500 \pm 60 \mu\text{M}$ (rat)^[124]</p>	 <p style="text-align: center;">1-30 $K_I = 2000 \pm 300 \mu\text{M}$ (rat)^[124]</p>
 <p style="text-align: center;">1-31 $K_I = 3000 \pm 500 \mu\text{M}$ (rat)^[124]</p>	 <p style="text-align: center;">1-32 $K_I = 6000 \pm 600 \mu\text{M}$ (rat)^[124]</p>

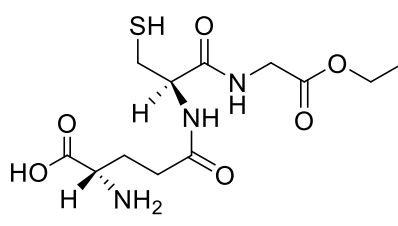
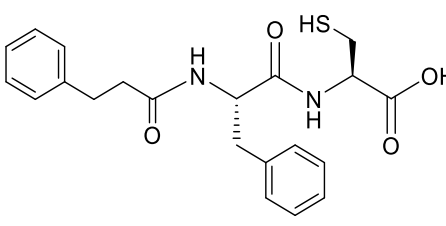
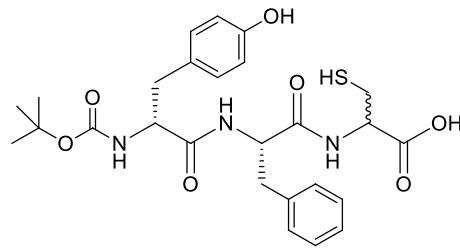
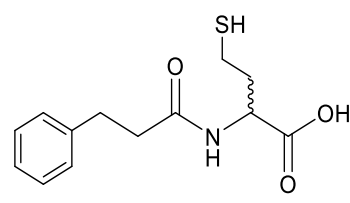
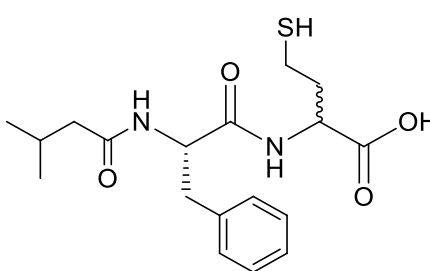
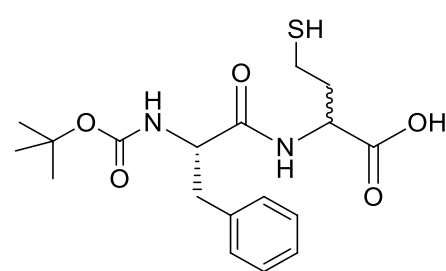
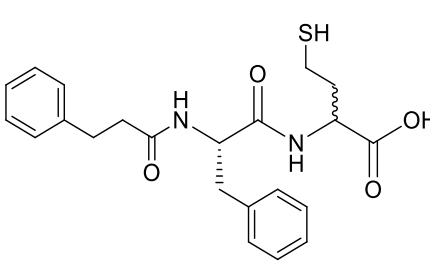
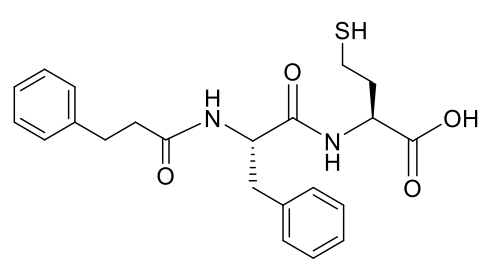
 <p>1-33 $K_I = 10000 \pm 2000 \mu\text{M}$ (rat)^[124]</p>	 <p>1-34 $K_I = 10 \pm 1 \mu\text{M}$ (rat)^[124]</p>
 <p>1-35 $K_I = 131 \pm 26 \mu\text{M}$ (porcine)^[128]</p>	 <p>1-36 $K_I = 1300 \mu\text{M}$ (bovine)^[102]</p>
 <p>1-37 $K_I = 160 \mu\text{M}$ (bovine)^[102] $K_I = 440 \pm 50 \mu\text{M}$ (porcine)^[128]</p>	 <p>1-38 $K_I = 60 \mu\text{M}$ (frog)^[131]</p>
 <p>1-39 $K_I = 54 \mu\text{M}$ (frog)^[131]</p>	 <p>1-40 $K_I = 26 \pm 2 \mu\text{M}$ (L) (frog)^[140] $K_I = 60 \pm 3 \mu\text{M}$ (racemate) (frog)^[140]</p>
 <p>1-41 $K_I = 57 \mu\text{M}$ (frog)^[131]</p>	 <p>1-42 $K_I = 2900 \pm 480 \mu\text{M}$ (rat)^[127]</p>

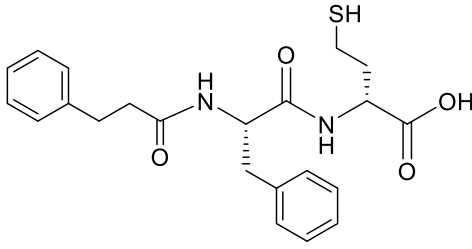
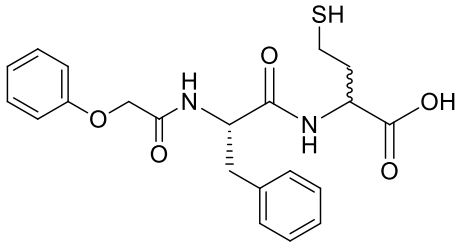
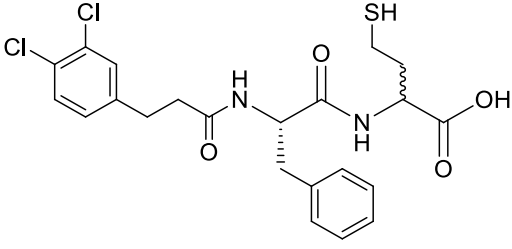
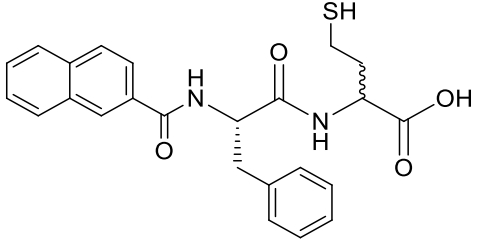
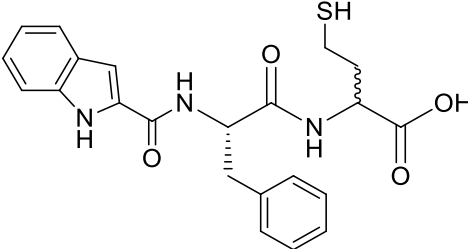
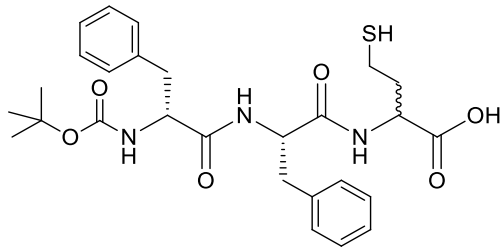
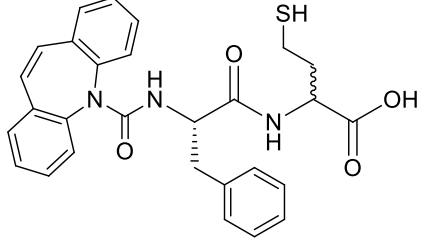
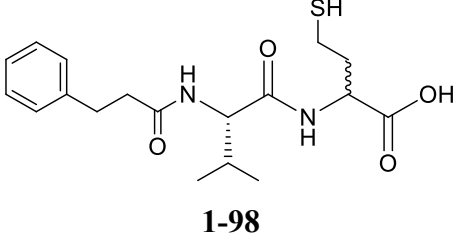
 <p>1-43 $IC_{50} = 3000 \mu M$ (frog)^[135]</p>	 <p>1-44 $IC_{50} = 6000 \mu M$ (frog)^[135]</p>
 <p>1-45 $IC_{50} = 780 \mu M$ (frog)^[133]</p>	 <p>1-46 $IC_{50} = 250 \mu M$ (frog)^[133]</p>
 <p>1-47 $IC_{50} = 40 \mu M$ (frog)^[133] $IC_{50} = 0.04 \mu M$ (human)^[133]</p>	 <p>1-48 $IC_{50} = 35 \mu M$ (frog)^[133] $IC_{50} = 0.06 \mu M$ (human)^[133]</p>
 <p>1-49 $IC_{50} = 30 \mu M$ (frog)^[133]</p>	 <p>1-50 $IC_{50} = 250 \mu M$ (frog)^[134]</p>
 <p>1-51 $IC_{50} = 510 \mu M$ (frog)^[133] $IC_{50} = 2.0 \mu M$ (human)^[133]</p>	 <p>1-52 $K_I = 54 \pm 4 \mu M$ (rat)^[127]</p>

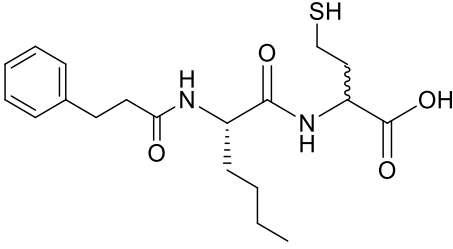
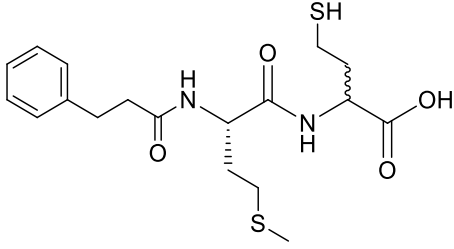
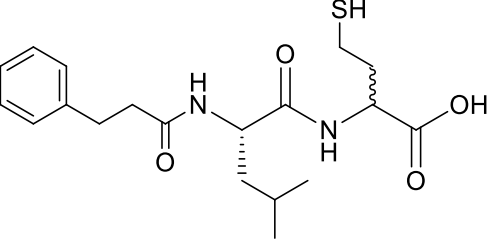
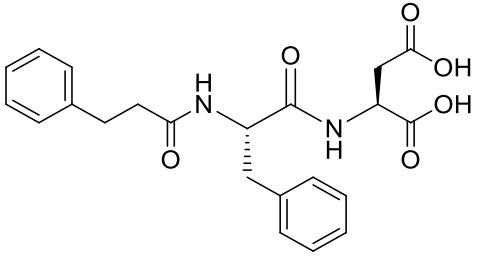
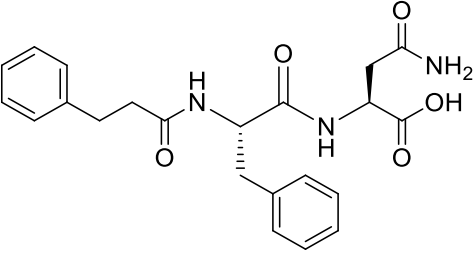
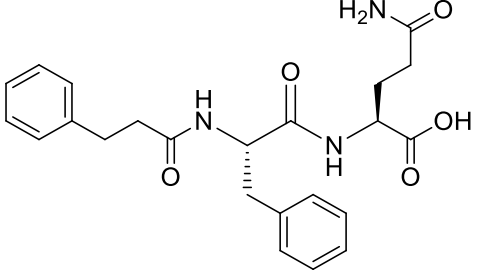
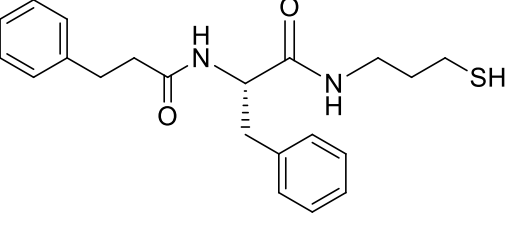
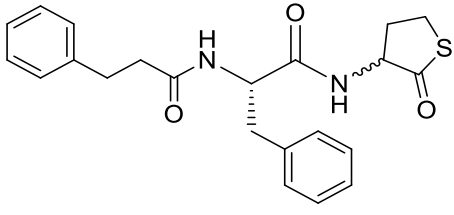
 <p>1-53 $K_I = 480 \mu\text{M}$ (bovine)^[102]</p>	 <p>1-54 $IC_{50} = 50 \mu\text{M}$ (frog)^[134]</p>
 <p>1-55 $IC_{50} = 500 \mu\text{M}$ (frog)^[134]</p>	 <p>1-56 $K_I = 52 \mu\text{M}$ (bovine)^[119]</p>
 <p>1-57 $K_I = 45 \mu\text{M}$ (bovine)^[119] $IC_{50} > 2000 \mu\text{M}$ (frog)^[133] $IC_{50} = 6 \mu\text{M}$ (human)^[133]</p>	 <p>1-58 $K_I = 60 \mu\text{M}$ (bovine)^[119]</p>
 <p>1-59 $K_I = 2250 \mu\text{M}$ (bovine)^[119]</p>	 <p>1-60 $K_I = 2100 \mu\text{M}$ (bovine)^[119]</p>
 <p>1-61 $K_I = 1250 \mu\text{M}$ (bovine)^[119]</p>	 <p>1-62 $K_I = 1000 \pm 60 \mu\text{M}$ (rat)^[127]</p>

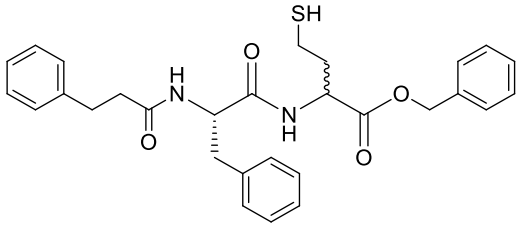
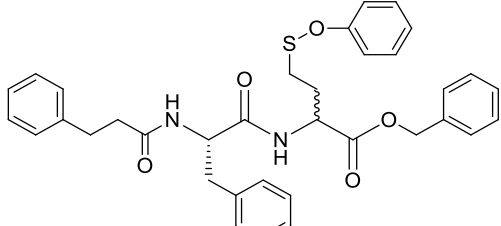
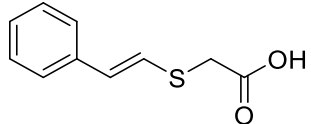
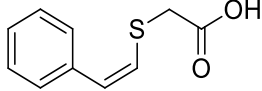
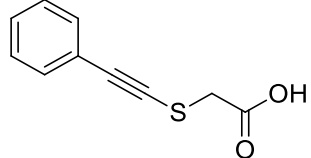
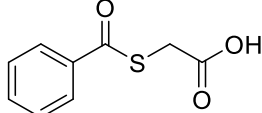
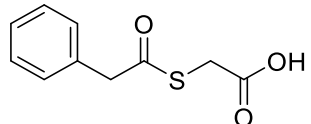
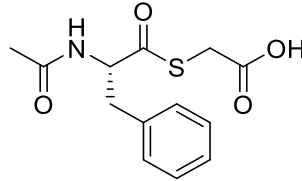
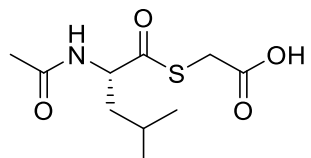
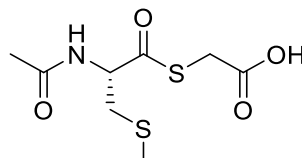
 <p>1-63 $K_I = 18000 \pm 5100 \mu\text{M}$ (rat)^[127]</p>	 <p>1-64 $IC_{50} = 440 \mu\text{M}$ (frog)^[133] $IC_{50} = 330 \mu\text{M}$ (human)^[133]</p>
 <p>1-65 $K_I = 8100 \mu\text{M}$ (bovine)^[119]</p>	 <p>1-66 $K_I = 2.0 \mu\text{M}$ (bovine)^[119] $IC_{50} = 170 \mu\text{M}$ (frog)^[133] $IC_{50} = 15 \mu\text{M}$ (human)^[133]</p>
 <p>1-67 $K_I = 1300 \mu\text{M}$ (bovine)^[119]</p>	 <p>1-68 $K_m = 82 \pm 11 \mu\text{M}$ (rat)^[141]</p>
 <p>1-69 $IC_{50} = 440 \mu\text{M}$ (frog)^[133] $IC_{50} = 200 \mu\text{M}$ (human)^[133]</p>	 <p>1-70 $K_m = 33 \pm 5 \mu\text{M}$ (rat)^[141]</p>
 <p>1-71 $K_I = 110 \pm 20 \mu\text{M}$ (rat)^[127]</p>	 <p>1-72 $K_I = 1500 \pm 150 \mu\text{M}$ (rat)^[127]</p>

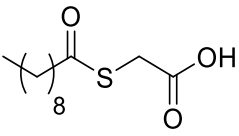
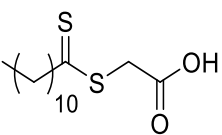
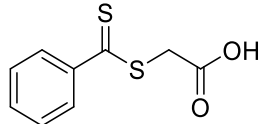
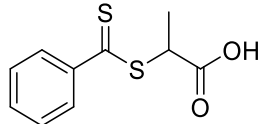
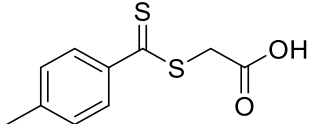
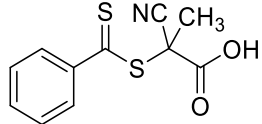
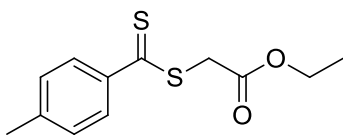
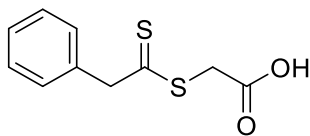
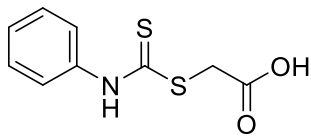
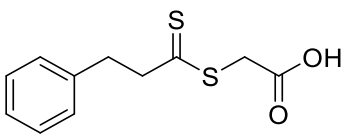
 <p>1-73 17% inhibition with 100 μM (porcine)^[121]</p>	 <p>1-74 $K_I = 7.2 \pm 0.9 \mu\text{M}$ (rat)^[127]</p>
 <p>1-75 $K_I = 3.6 \pm 0.4 \mu\text{M}$ (rat)^[127]</p>	 <p>1-76 $K_I = 20 \mu\text{M}$ (porcine)^[142]</p>
 <p>1-77 $K_I > 5000 \mu\text{M}$ (porcine)^[142]</p>	 <p>1-78 $\text{IC}_{50} = 300 \mu\text{M}$ (rat)^[139]</p>
 <p>1-79 $\text{IC}_{50} = 5000 \mu\text{M}$ (frog)^[135]</p>	 <p>1-80 $K_I = 1400 \pm 110 \mu\text{M}$ (rat)^[127]</p>
 <p>1-81 $K_I = 7900 \pm 980 \mu\text{M}$ (rat)^[127]</p>	 <p>1-82 $K_I = 100 \mu\text{M}$ (rat)^[143]</p>

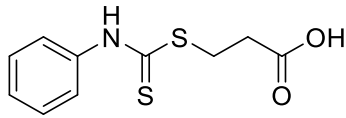
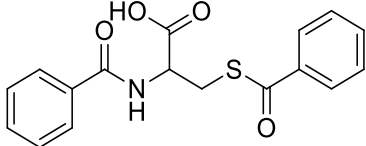
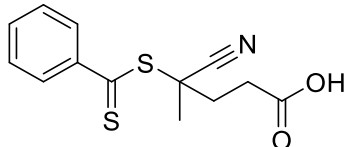
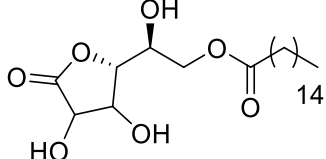
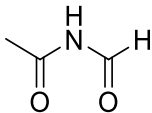
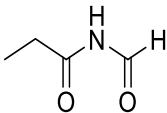
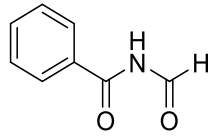
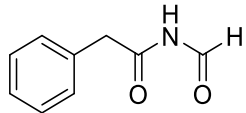
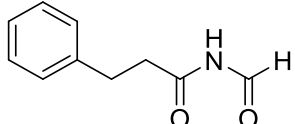
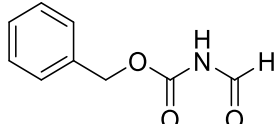
 <p style="text-align: center;">1-83 $K_I = 66 \pm 8 \mu\text{M}$ (rat)^[127]</p>	 <p style="text-align: center;">1-84 $K_I = 330 \text{ nM}$ (rat)^[16]</p>
 <p style="text-align: center;">1-85 $K_I = 340 \text{ nM}$ (rat)^[16]</p>	 <p style="text-align: center;">1-86 $K_I = 7500 \text{ nM}$ (rat)^[16]</p>
 <p style="text-align: center;">1-87 $K_I = 29 \pm 4 \text{ nM}$ (rat)^[16]</p>	 <p style="text-align: center;">1-88 $K_I = 53 \pm 12 \text{ nM}$ (rat)^[16]</p>
 <p style="text-align: center;">1-89 $K_I = 15 \pm 3 \text{ nM}$ (rat)^[16]</p>	 <p style="text-align: center;">1-90 $K_I = 10 \pm 1 \mu\text{M}$ (rat)^[16]</p>

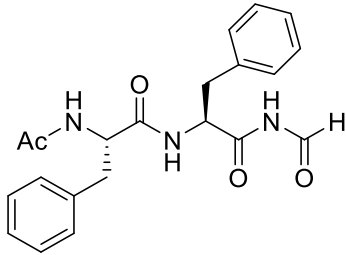
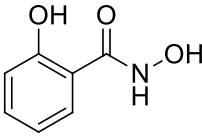
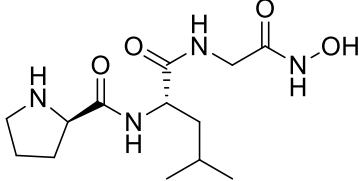
 <p style="text-align: center;">1-91 $K_I = 610 \pm 80 \text{ nM (rat)}^{[16]}$</p>	 <p style="text-align: center;">1-92 $K_I = 14 \pm 3 \text{ nM (rat)}^{[16]}$</p>
 <p style="text-align: center;">1-93 $K_I = 55 \pm 5 \text{ nM (rat)}^{[16]}$</p>	 <p style="text-align: center;">1-94 $K_I = 10 \pm 3 \mu\text{M (rat)}^{[16]}$</p>
 <p style="text-align: center;">1-95 $K_I = 8 \pm 1 \text{ nM (rat)}^{[16]}$</p>	 <p style="text-align: center;">1-96 $K_I = 39 \pm 8 \text{ nM (rat)}^{[16]}$</p>
 <p style="text-align: center;">1-97 $K_I = 18 \pm 3 \text{ nM (rat)}^{[16]}$</p>	 <p style="text-align: center;">1-98 $K_I = 160 \pm 30 \text{ nM (rat)}^{[16]}$</p>

 <p>1-99 $K_I = 23 \pm 2 \text{ nM (rat)}^{[16]}$</p>	 <p>1-100 $K_I = 18 \pm 2 \text{ nM (rat)}^{[16]}$</p>
 <p>1-101 $K_I = 300 \pm 17 \text{ nM (rat)}^{[16]}$</p>	 <p>1-102 $K_I > 10000 \text{ nM (rat)}^{[16]}$</p>
 <p>1-103 $K_I > 10000 \text{ nM (rat)}^{[16]}$</p>	 <p>1-104 $K_I > 10000 \text{ nM (rat)}^{[16]}$</p>
 <p>1-105 $K_I = 1600 \text{ nM (rat)}^{[16]}$</p>	 <p>1-106 $K_I > 10000 \text{ nM (rat)}^{[16]}$</p>

 <p>1-107 $K_I > 10000 \text{ nM (rat)}^{[16]}$</p>	 <p>1-108 $K_I = 2 \text{ }\mu\text{M (whole cell inhibition)}^{[144]}$</p>
 <p>1-109 $K_I = 100 \text{ }\mu\text{M (horse)}^{[136]}$</p>	 <p>1-110 No Inhibition (horse)^[136]</p>
 <p>1-111 $K_I = 190 \text{ }\mu\text{M (horse)}^{[136]}$</p>	 <p>1-112 $IC_{50} = 150 \text{ }\mu\text{M (frog)}^{[133]}$</p>
 <p>1-113 $IC_{50} = 20 \text{ }\mu\text{M (frog)}^{[133]}$ $IC_{50} = 45 \text{ }\mu\text{M (human)}^{[133]}$</p>	 <p>1-114 $IC_{50} = 25 \text{ }\mu\text{M (frog)}^{[133]}$ $IC_{50} = 45 \text{ }\mu\text{M (human)}^{[133]}$</p>
 <p>1-115 $IC_{50} = 260 \text{ }\mu\text{M (frog)}^{[133]}$</p>	 <p>1-116 $IC_{50} = 50 \text{ }\mu\text{M (frog)}^{[133]}$</p>

 <p>1-117 $IC_{50} = 9 \mu\text{M}$ (frog)^[133] $IC_{50} = 7 \mu\text{M}$ (human)^[133]</p>	 <p>1-118 $K_I = 0.54 \pm 0.05 \mu\text{M}$ (rat)^[127]</p>
 <p>1-119 $K_I = 39 \pm 5 \mu\text{M}$ (rat)^[127]</p>	 <p>1-120 $K_I = 58 \pm 9 \mu\text{M}$ (rat)^[127]</p>
 <p>1-121 $K_I = 3.5 \pm 0.4 \mu\text{M}$ (rat)^[127]</p>	 <p>1-122 $K_I = 5.7 \pm 0.4 \mu\text{M}$ (rat)^[127]</p>
 <p>1-123 $K_I = 110 \pm 10 \mu\text{M}$ (rat)^[127]</p>	 <p>1-124 $K_I = 7.9 \pm 1.8 \mu\text{M}$ (rat)^[127]</p>
 <p>1-125 $K_I = 8.6 \pm 1.4 \mu\text{M}$ (rat)^[127]</p>	 <p>1-126 $K_I = 9.4 \pm 0.8 \mu\text{M}$ (rat)^[127]</p>

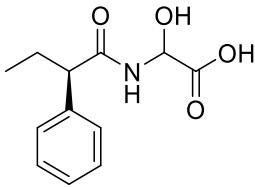
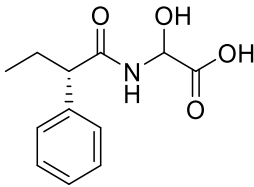
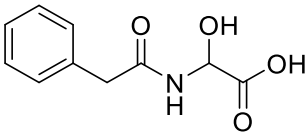
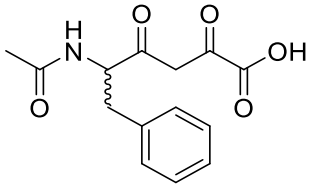
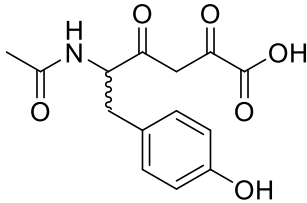
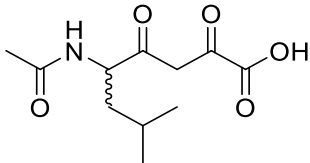
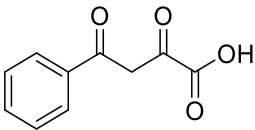
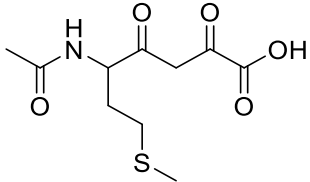
 <p>1-127 $K_I = 2.6 \pm 0.7 \mu\text{M}$ (rat)^[127]</p>	 <p>1-128 $K_I = 66 \pm 8 \mu\text{M}$ (rat)^[127]</p>
 <p>1-129 $K_I = 20 \mu\text{M}$ (rat)^[127]</p>	 <p>1-130 $K_I = 35 \pm 4 \mu\text{M}$ (rat)^[127]</p>
 <p>1-131 $IC_{50} > 2500 \mu\text{M}$ (honeybee)^[137]</p>	 <p>1-132 $IC_{50} > 2500 \mu\text{M}$ (honeybee)^[137]</p>
 <p>1-133 $IC_{50} = 890 \mu\text{M}$ (honeybee)^[137]</p>	 <p>1-134 $IC_{50} = 820 \mu\text{M}$ (honeybee)^[137]</p>
 <p>1-135 $IC_{50} = 570 \mu\text{M}$ (honeybee)^[137]</p>	 <p>1-136 $IC_{50} = 800 \mu\text{M}$ (honeybee)^[137]</p>

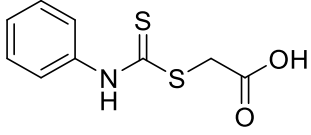
 <p style="text-align: center;">1-137</p> <p style="text-align: center;">$IC_{50} = 400 \mu\text{M}$ (porcine)^[137]</p>	 <p style="text-align: center;">1-138</p> <p style="text-align: center;">$K_I = 300 \mu\text{M}$ (rat)^[127]</p>
 <p style="text-align: center;">1-139</p> <p style="text-align: center;">$K_I = 1000 \mu\text{M}$ (rat)^[127]</p>	

1.3.2 PAL Inhibitors

Compared with the wide range of PHM inhibitors investigated, fewer studies focus on inhibitors specific for PAL. The first relevant publication was reported by Mounier *et al.* finding that PAL substrate analogues, 2-hydroxy-2-((*R*)-2-phenylbutanamido)acetic acid (**1-140**) and 2-hydroxy-2-((*S*)-2-phenylbutanamido)acetic acid (**1-141**), are both competitive PAL inhibitors with K_I values of 280 μM and 310 μM , respectively.^[119] Afterwards, they reported that pyruvate-extended *N*-acylamino acid derivatives are potent PAL inhibitors that resemble transient substrate species along the catalytic pathway of PAL.^[126] Among them, *N*-Ac-Phe-pyruvate (**1-143**), with a K_I value of 0.24 μM , is the most potent PAL inhibitor known so far.^[126] **Table 1.4** summarises all reported PAL inhibitors.

Table 1.4 PAL substrates and inhibitors.

Structure and Binding Data	Structure and Binding Data
 <p>1-140 $K_I = 280 \mu\text{M}$ (bovine)^[119]</p>	 <p>1-141 $K_I = 310 \mu\text{M}$ (bovine)^[119]</p>
 <p>1-142 $K_I = 770 \mu\text{M}$ (bovine)^[119]</p>	 <p>1-143 $K_I = 0.24 \pm 0.03 \mu\text{M}$ (bovine)^[126]</p>
 <p>1-144 $K_I = 0.52 \pm 0.06 \mu\text{M}$ (bovine)^[126]</p>	 <p>1-145 $K_I = 1.0 \pm 0.1 \mu\text{M}$ (bovine)^[126]</p>
 <p>1-146 $K_I = 10 \pm 1 \mu\text{M}$ (bovine)^[126]</p>	 <p>1-147 $K_I = 15 \pm 2 \mu\text{M}$ (bovine)^[126]</p>

 <p>1-119</p> <p>40% inhibition with 750 μM (rat)^[127]</p>	
--	--

1.4 Summary

Regulation of amidated peptide hormone production is of great interest due to their crucial role in intercellular communication as well as the link between a variety of pathological conditions and imbalances in the expression of peptide hormones. PAM as the only enzyme that catalyses amidation of peptide hormones is therefore an important target for hormone regulation. Hence, the aim of thesis is to investigate features that govern the binding of substrates and inhibitors to PHM and PAL. The first part in this thesis is to study PHM binding. In Chapter 2, the recognition of a peptide substrate consensus sequence by PHM is investigated, while Chapter 3 describes the evaluation of glycolate and glycine derivatives as medicinal agents. The rest of the work, shown in Chapters 4 - 6, focuses on PAL activity. In Chapter 4, a new PAM assay was developed using HPLC-MS allowing simultaneous observation of PHM and PAL activities. The new assay was then employed in Chapter 5 for the assessment of compounds as PHM and PAL inhibitors. In Chapter 6, natural α -hydroxyglycine peptide from human cancer cell line was attempted to be detected and quantified to explore the importance of PAL activity of PAM activity in cells.

Chapter Two

Study of Peptide Sequence Recognition by Peptidylglycine α -Amidating Monooxygenase

2.1 Introduction

In this Chapter, the focus was the amidation of human peptide hormone precursors that are the substrates of the amidating enzyme PAM. Peptide hormone levels are very low in tissues and cells, normally at picomolar or nanomolar levels.^[145] However, the peptide binding affinities are usually micromolar, and different prohormones have quite different values with the processing enzyme. For example, the K_i values of prohormones such as adrenomedullin-Gly and Peptide-YY-Gly are about 20 μ M with the medium PAM from the DMS53 cell line, while the K_i value of Thyroliberin (TRH)-Gly is 1235 μ M under identical test conditions.^[146] Therefore amidation of peptide prohormones is significantly dependent on the binding affinity with PAM, where a prohormone with better binding affinity is likely to be amidated in preference to one with lower binding affinity. It follows that factors which affect the binding affinity of peptide hormones are of considerable importance.

As mentioned in Chapter 1, Tamburini *et al.*^[118] investigated the effect of the C-terminal penultimate amino acid on the peptide substrate binding affinity with PAM by using a synthetic hexapeptide model, and found that penultimate amino acids with a planar aromatic group had highest binding affinity while cyclic aliphatic or acidic

ones gave rise to lower binding affinities. Further to this, Easton *et al.*,^[120] studied substrate recognition by PAM by utilizing natural prohormones such as prooxytocin (oxytocin-Gly) and its analogues. They found that the binding affinities of *N*-acetylated di-, tri-, and tetra-peptide prooxytocin analogues, along with prooxytocin, with the PAM enzyme from the DMS53 cell line, increase in order. The phenomenon that increasing the length of the prohormone sequence increases the binding affinity again highlights the importance of the peptide sequence on recognition by the amidating enzyme. However, when they substituted Gly at the penultimate position of analogues of the peptide with Phe, the binding affinities of all tested peptides increased significantly, but no further increase was then observed with increased peptide sequence length. Comparison between the above results demonstrates that Phe changes the binding mode from one where recognition depends on the peptide sequence to another where recognition by the amidating enzyme is predominantly dependent on the penultimate Phe.^[120] However, prooxytocin does not naturally have Phe at the *C*-terminus. These observations attracted us to investigate in more details the binding affinities of natural prohormones having Phe at the penultimate position from the *C*-terminus and see whether there is sequence recognition of these natural prohormones with PAM

With this aim, a statistical analysis was performed of the human amidated peptide hormone database. From **Table 1.1** in Chapter 1, among all eighty one peptide hormones, there are twenty eight having Phe at the amidated end, which corresponds to the *C*-terminal penultimate position (P1) in their respective Gly-extended prohormones. Since investigating the binding affinities of all twenty eight full-length peptide prohormones would be impractical, instead consensus sequence models that

cover all the possibilities of amino acids at the antepenultimate position (P2) were studied. As shown in **Table 2.1** and **Table 2.2**, there are three possibilities of –X-Phe-Gly-COOH in natural human Gly-extended peptide prohormones, of which X can only be one of Arg (R), Asp (D) or Ala (A). Specifically, fourteen out of twenty eight peptide prohormones containing Phe at P1, including those of kisspeptin, prolactin-releasing peptide, QRF-amide, and some neuropeptides, have the fragment –Arg-Phe-Gly-COOH. Another twelve prohormones, cholecystokinin and gastrin related-hormones, have the fragment –Asp-Phe-Gly-COOH. The remaining two prohormones with –Ala-Phe-Gly-COOH at the C-terminus, are calcitonin gene-related peptide and calcitonin gene-related peptide 2.

Table 2.1 Human Gly-extended prohormones having penultimate Phe at the C-terminus, divided into three groups in terms of the amino acids at P2.

Group	Name	Sequence
RFG	Neuropeptide NPVF-Gly	VPNLPQ <u>RFG</u>
	Neuropeptide FF-Gly	FLFQPQ <u>RFG</u>
	Neuropeptide SF-Gly	SQAFLFQPQ <u>RFG</u>
	Neuropeptide AF-Gly	AGEGLNSQFWSLAAPQ <u>RFG</u>
	Kisspeptin-10-Gly	YNWNSFGL <u>RFG</u>
	Kisspeptin-13-Gly	LPNYNWNSFGL <u>RFG</u>
	Kisspeptin-14-Gly	DLPNYNWNSFGL <u>RFG</u>
	Kisspeptin-Gly	GTSLSPPPESSGSPQQPGLSAPHSRQIPA PQGAVLVQREKDLPNYNWNSFGL <u>RFG</u>
	Melanotropin gamma-Gly	YVMGFHRWD <u>RFG</u>
	Neuropeptide RFRP-1-Gly	MPHSFANLPL <u>RFG</u>
	Prolactin-releasing peptide PrRP20-Gly	TPDINPAWYASRGIRPV <u>G</u> <u>RFG</u>
	Prolactin-releasing peptide PrRP31-Gly	SRTHRHSMEIRTPDINPAWYASRGIRPV <u>G</u> <u>RFG</u>
	Neuropeptide NPSF-Gly	SLNFEELKDWGPKNVIKMSTPAVNKMP HSFANLPL <u>RFG</u>
QRF-Gly	QDEGSEATGFLPAAGEKTSGPLGNLAE ELNGYSRKKGGFS <u>RFG</u>	
DFG	Cholecystokinin-5-Gly	GWMD <u>DFG</u>
	Cholecystokinin-7-Gly	YMGWMD <u>DFG</u>
	Cholecystokinin-8-Gly	DYMGWMD <u>DFG</u>
	Cholecystokinin-12-Gly	ISDRDYMGWMD <u>DFG</u>
	Cholecystokinin-18-Gly	LDPSHRISDRDYMGWMD <u>DFG</u>
	Cholecystokinin-25-Gly	YIQQARKAPSGRMSIVKNLQNLDP SHRI SDRDYMGWMD <u>DFG</u>
	Cholecystokinin-58-Gly	VSQRTDGESRAHLGALLARYIQQARKA PSGRMSIVKNLQNLDP SHRISDRDYM GWM <u>DFG</u>
	Gastrin-6-Gly	YGWMD <u>DFG</u>
	Gastrin-14-Gly	WLEEEEEAYGWMD <u>DFG</u>
	Gastrin-Gly	QGPWLEEEEEAYGWMD <u>DFG</u>
	Big gastrin-Gly	QLGPQGPPHLVADPSKKQGPWLEEEEE AYGWMD <u>DFG</u>
Gastrin-52-Gly	DLELPWLEQQGPASHHRRQLGPQGPPH LVADPSKKQGPWLEEEEEAYGWMD <u>DFG</u>	
AFG	Calcitonin gene-related peptide-Gly	ACDTATCVTHRLAGLLSRSGGVKNNF VPTNVGSK <u>AFG</u>
	Calcitonin gene-related peptide 2-Gly	ACNTATCVTHRLAGLLSRSGGMVKS NF VPTNVGSK <u>AFG</u>

Table 2.2 Proportion analysis of amino acids at the C-terminal antepenultimate position of human Gly-extended prohormones having penultimate Phe.

	Total	Arg (R)	Asp (D)	Ala (A)
Number of peptide prohormones	28	14	12	2
Number of sequence types	12	8	2	2

Since the sequence fragment -Arg-Phe-Gly-COOH appears most frequently, these amino acids were chosen as the first three of the basic consensus sequence, then being extended with three more amino acids at P3, P4, and P5. Selecting the amino acids at P3-P5 was dependent on extended sequence analysis to represent the widest variety of peptide prohormones. In the first case, after further statistical analysis, Gln (Q), Pro (P), and Gly (G) were chosen for P3-P5, respectively. *N*-Acetylation was performed at the *N*-terminus of the designed peptide sequences due to concerns that a free amino group at the *N*-terminus would be protonated under the assay conditions and hence be likely to significantly impact the binding affinity with PAM.^[120] Therefore, as illustrated in **Figure 2.1**, the peptide sequence *N*-Ac-Gly-(*S*)-Pro-(*S*)-Glu-(*S*)-Arg-(*S*)-Phe-Gly-COOH (**2-14**) was designed to be the basic consensus sequence in the present study.

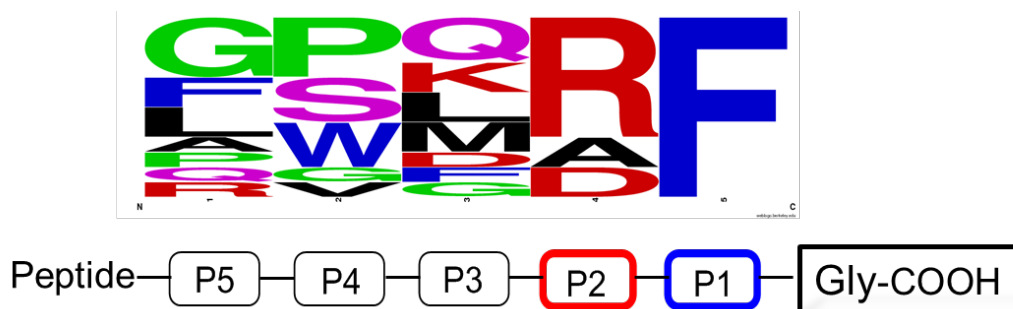


Figure 2.1 According to the human amidated peptide hormone database, *N*-Ac-Gly-(*S*)-Pro-(*S*)-Glu-(*S*)-Arg-(*S*)-Phe-Gly-COOH (**2-14**) was identified as the consensus sequence *via* mathematical analysis (the greater proportion of each amino acid at a particular position represents the more frequent occurrence of that amino acid appearing at that position, with the amino acid listed on the top of each column having the most frequent occurrence).

On the basis of the initial hexapeptide **2-14**, modifications such as decreasing the length of the sequence and substitution of Arg or Phe at P2 or P1 with amino acids representative of those found in prohormones were considered to generate nine more peptide sequences as shown in **Figure 2.2** below. Compared to consensus sequence **2-14**, its three related peptides, the penta-, tetra-, and tri-peptide prohormones **2-15 - 2-17**, with lengths decreased by one amino acid from the *N*-terminus each time, were chosen to examine the effect of extended sequence recognition on binding affinity of natural prohormones with PAM. In addition, covering the other two possibilities of -X-Phe-Gly-COOH in natural human prohormones, peptide sequences **2-18** and **2-19** were tested, to help understand the effect of antepenultimate amino acids on the binding affinity with the amidating enzyme. Though not existing in the nature, -Gly-Phe-Gly-COOH within peptide **2-20** was also examined as a control. Substitution of

Phe at P1 of the basic consensus sequence **2-14** with Pro and Gly was chosen to generate sequences **2-21** and **2-22**. The results of testing these two peptides were to be compared with the results of Easton *et al.*^[120] related to the binding affinity of procalcitonin and prooxytocin that have Pro and Gly at their respective P1 positions. Sequence fragment -Arg-Gly-Gly-COOH of peptide **2-22** also exists in two natural human peptide prohormones, Arg-vasopressin and pancreastatin. There are in total five prohormones having -Gly-Gly-COOH as shown in **Table 2.3**. Apart from -Arg-Gly-Gly-COOH possessed by two human peptides, as discussed above, a third is prooxytocin which has already been studied in the Easton Group. The other two, gonadoliberin-1 and gonadoliberin-2, both have Pro at P2. Therefore, peptide **2-23** having the -Pro-Gly-Gly-COOH fragment was also selected so that the binding affinities of all the human prohormones having -X-Gly-Gly-COOH would be covered.

Sequence recognition	Examine P1 or P2 substitution
2-14 N-Ac-GPQRF-G-CO₂H	2-18 N-Ac-GPQDF-G-CO₂H
2-15 N-Ac-PQRF-G-CO₂H	2-19 N-Ac-GPQAF-G-CO₂H
2-16 N-Ac-QRF-G-CO₂H	2-20 N-Ac-GPQGF-G-CO₂H
2-17 N-Ac-RF-G-CO₂H	2-21 N-Ac-GPQRP-G-CO₂H
	2-22 N-Ac-GPQRG-G-CO₂H
	2-23 N-Ac-GPQPG-G-CO₂H

Figure 2.2 Peptide sequences chosen to test.

Table 2.3 Human Gly-extended prohormones having penultimate Gly.

Group	Name	Sequence
LGG	Oxytocin-Gly	CYIQNCPLGG
PGG	Gonadoliberin-1-Gly	QHWSYGLRPGG
	Gonadoliberin-2-Gly	QHWSHGWYPGG
RGG	Arg-vasopressin-Gly	CYFQNCPRGG
	Pancreastatin-Gly	GESRSEALAVDGAGKPGAEAAQDPEGK GEQEHSQQKEEEEEMAVVPQGLFRGG

The amidating enzyme PAM from the growth medium of the human small cell lung carcinoma (SCLC), DMS53 cell line, was chosen for comparison with earlier studies of peptide prohormones of calcitonin and oxytocin.^[145]

2.2 Synthesis of Peptide Substrates

In order to obtain the selected Gly-extended peptide sequences, solid phase peptide synthesis (SPPS) was chosen as the method. SPPS, first established by Bruce Merrifield in 1963,^[147] is a convenient and universally adopted method for production of peptides. Its continual development related to racemisation suppression, protection group chemistry, and resin selection has made the build-up of peptide sequences more efficient and timesaving.^[148-150] In general, there are two main approaches of SPPS; one is the Boc approach, and the other is the Fmoc approach. In the former approach, the acid-labile Boc-group is well suited for temporary protection of the amino group of amino acids and is able to be removed using some acidic agents such as TFA under mild conditions; however, under these circumstances, protecting groups used for protection of the side chains of amino acids during peptide elongation and peptide-

resin linkers need to be resistant to acid hydrolysis. By contrast, when the Fmoc group is used for protecting amino groups, it is removed with base, which allows the use of more acid-labile side-chain protecting groups that may then be removed under mild acidic conditions.^[151] There are many kinds of side-chain protecting groups including Tos,^[152] Mts,^[153] and Pbf for (*S*)-Arg. The Pbf group is more acid-labile than the other two and the best Arg-protecting group for Fmoc-SPPS.^[154] Xan, Mbh and Trt can be used for protecting (*S*)-Gln. Among them, Xan and Mbh are mainly used for the Boc method^[155-156] while Trt is the best for the Fmoc method because it is more acid-labile.^[157] Therefore, the Fmoc-based SPPS method was chosen in the present synthesis.

Resins commonly used with the Fmoc approach are hydroxymethyl-based, which leads to coupling of the first amino acid by forming an ester link. Among these resins, Wang resin, as shown in **Figure 2.3**, was selected in this project because it is an unhindered one that forms esters more easily than other candidates such as Sasrin or HMPB resin.^[151] In general, aggregation of peptides can complicate coupling, therefore when preparing long peptide sequences it is better to choose a resin with low substitution to increase the yield of coupling.^[158] For instance, to prepare a long peptide (30 to 50 amino acids), a resin with a low substitution (0.1-0.4 mmol/g) is appropriate. By contrast, to prepare a short one (<10 amino acids), a higher substitution resin (1.2-2.0 mmol/g) may be used. Therefore, to make peptides **2-14 - 2-23**, the Wang resin whose estimated substitution is 1.18 mmol/g was purchased from Sigma-Aldrich Corporation and used.



Figure 2.3 The structures of Wang resin, Sasrin resin and HMPB resin.

The peptides were built up by the stepwise SPPS method on Wang resin as a solid support, which is exemplified with the synthesis of hexapeptide **2-14** *via* **Scheme 2.1**. Specifically, commercial dry Wang resin was suspended in organic solvent to swell the beads. The swelling step is essential because most of coupling sites of dry resin are not on the surface but inside the resin beads. Swelling enlarges the beads and exposes the hydroxyl groups of the Wang resin in order to maximise the coupling efficiency.^[151] The swollen Wang resin was coupled with Fmoc-Gly-COOH (2.5 eq) to produce Fmoc-Gly-Wang resin (**2-1**) using standard ester forming conditions with DIC, HOBt, and a catalytic amount of DMAP in DMF.^[158] Excess reagents at high concentration are used to drive coupling reactions, and the excess reagents and by-products are then removed simply by filtration and washing. DIC is commonly used to prepare amides or esters from carboxylic acids in SPPS, with the urea by-product being soluble in standard solvents such as DMF and washing out easily. HOBt enhances reactivity of ester or amide formation with carbodiimides.^[159] Only a small amount of DMAP was used to avoid deprotecting the Fmoc group because of its basicity. After the first coupling, a small amount of resin was used to determine the loading efficiency *via* Fmoc release and measurement by UV-Vis spectroscopy.^[151] The absorbance of samples was measured at 278 nm, from which the loading efficiency was calculated according to the following **Eq 2.1**:^[158]

$$S \text{ (mmol/g)} = (1000 \times A)/(M \times 7800 \times D) \quad \text{(Eq 2.1)}$$

S = substitution of the resin in mmol/g

A = absorbance of the sample – absorbance of the blank

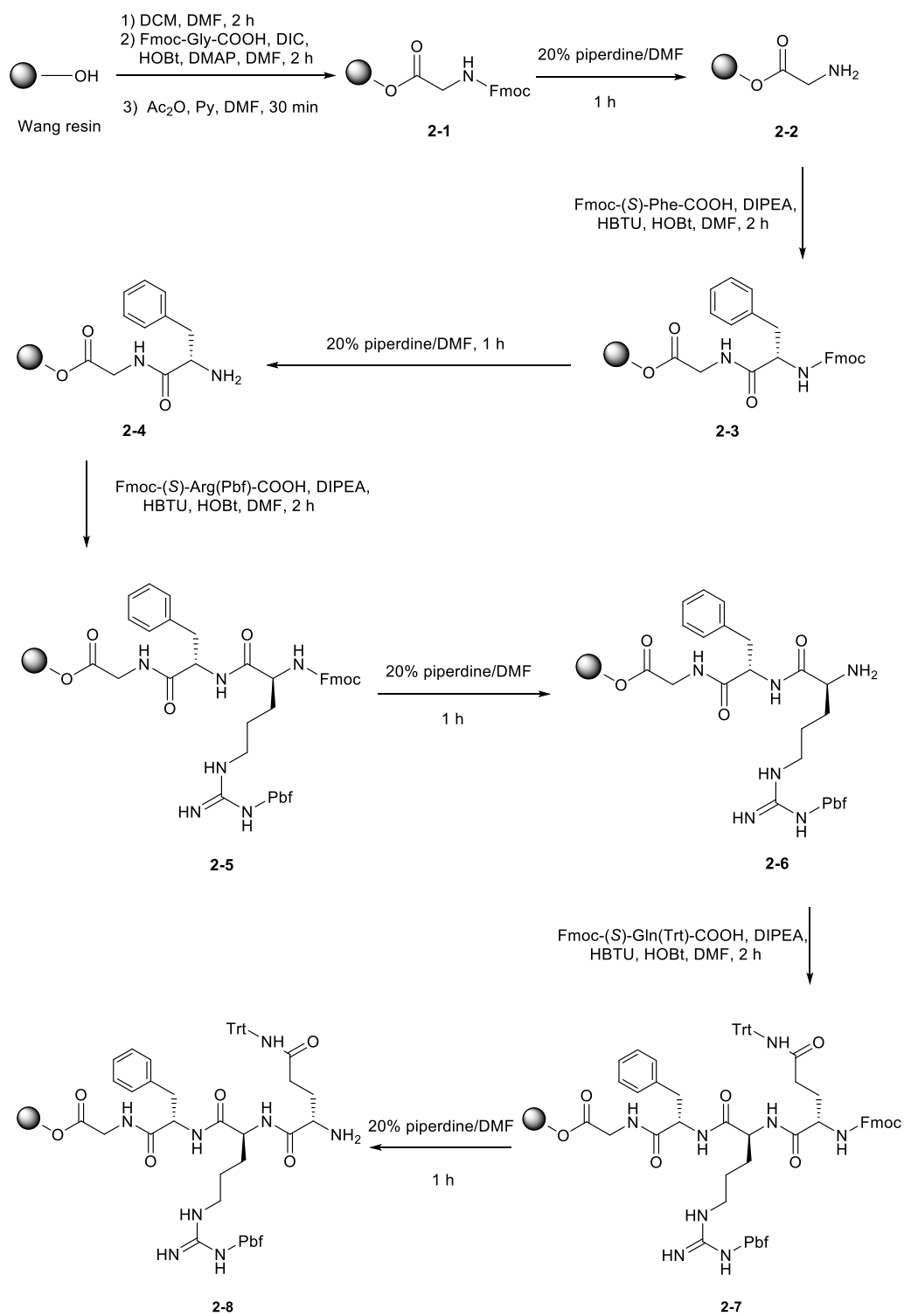
M = mass of the resin used in mg

D = dilution factor

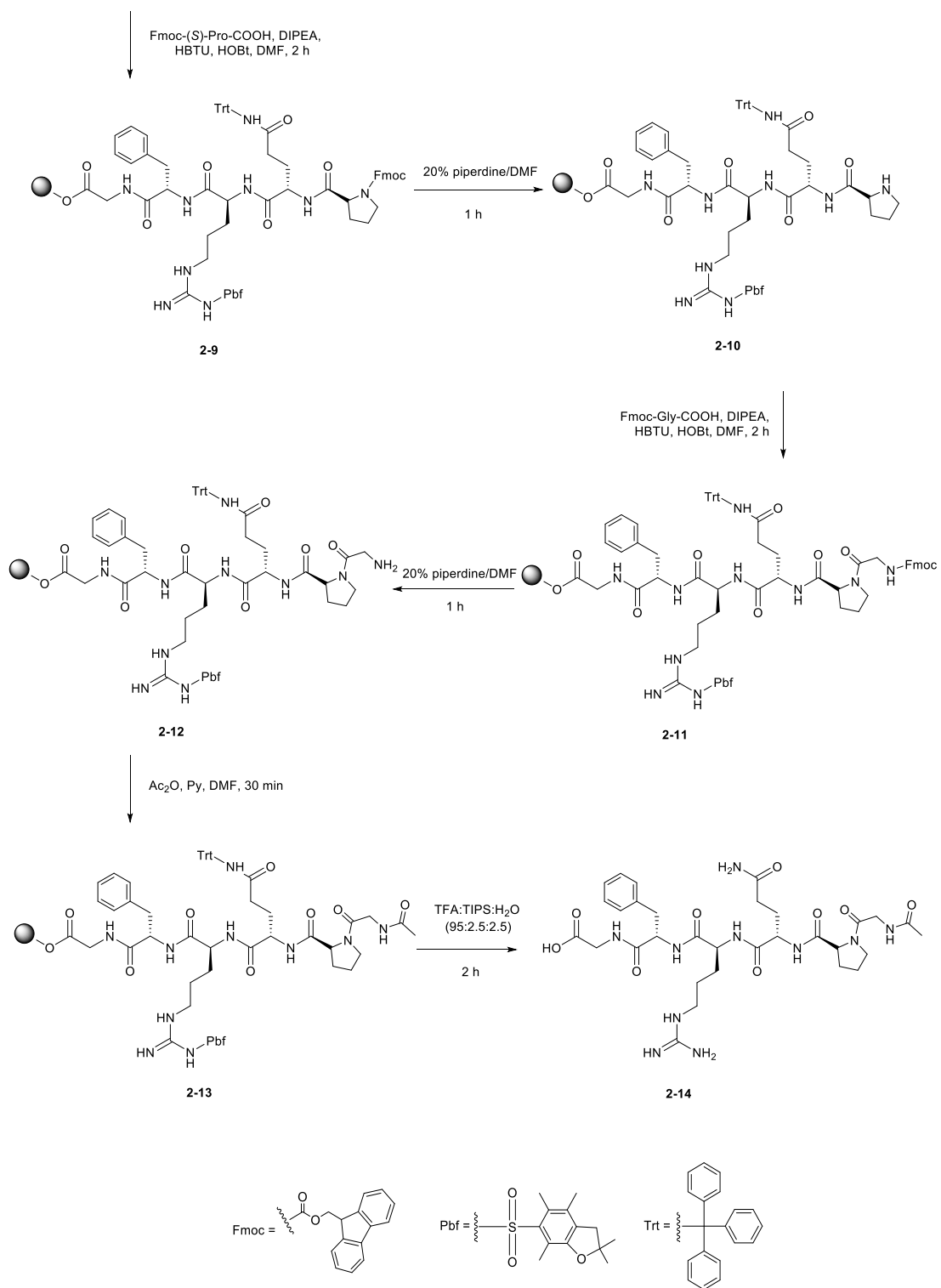
The loading efficiency test for peptide **2-1** in the synthesis of peptide **2-14** was 65% (all other target peptides were also synthesised starting by making compound **2-1** and the loading efficiencies were between 65-83%), which indicated that 35% of the hydroxyl groups were still free. Therefore, the whole resin was agitated with Ac₂O and pyridine to acetylate unreacted hydroxyl groups and hence reduce the possibility of generating undesired peptide sequences from coupling other amino acids used later in the sequence directly to the resin. Afterwards, the Fmoc-protected amino acid **2-1** underwent Fmoc deprotection by adding piperidine in DMF.

Subsequently, the resulting amine **2-2** was treated with the next Fmoc-protected amino acid, Fmoc-(*S*)-Phe-COOH, using HBTU, HOBT, and DIPEA.^[158] These reagents are more efficient than DIC/DMAP in terms of amide coupling.^[160-161] HBTU is reported to form amides rapidly with little racemisation,^[162] but requires the presence of large amounts of base such as DIPEA. After the standard Fmoc deprotection that converted peptide **2-3** to peptide **2-4**, peptide **2-4** was then elongated to the desired sequence with the following protected amino acids: Fmoc-(*S*)-Arg(Pbf)-COOH, Fmoc-(*S*)-Gln(Trt)-COOH, Fmoc-(*S*)-Pro-COOH, and Fmoc-Gly-COOH. All these coupling procedures

and the reagent quantities were as described for the second coupling described above. After the elongation and the last Fmoc deprotection, an acetylation was performed on the *N*-terminus of peptide **2-12** with Ac₂O to produce peptide **2-13**. The *N*-acetylated peptide was then cleaved from the Wang resin, at the same time removing the two side-chain protecting groups (Pbf and Trt), under acid conditions.



Continued on next page



Scheme 2.1 Synthesis of *N*-Ac-Gly-(*S*)-Pro-(*S*)-Gln-(*S*)-Arg-(*S*)-Phe-Gly-COOH (**2-14**).

A small amount of the crude peptide product was analysed by HPLC with detection using UV-Vis spectroscopy. The resulting HPLC chromatogram reproduced in **Figure 8.1** showed two dominant peaks. Separation of the materials corresponding to these peaks and MS analysis showed one corresponds to the peptide *N*-Ac-Gly-(*S*)-Pro-(*S*)-Gln-(*S*)-Arg-(*S*)-Phe-Gly-COOH (**2-14**) while the other one has mass 57 Da less. Separated compound **2-14** was analysed using high resolution MS and ¹H NMR spectroscopy for further characterization. With the exception of compound **2-19**, which was a gift from Dr. Tim Altamore, all the other peptides **2-15 - 2-18** and **2-20 - 2-23** were prepared using the same approach as described for peptide **2-14**. When preparing *N*-Ac-Gly-(*S*)-Pro-(*S*)-Gln-(*S*)-Asp-(*S*)-Phe-Gly-COOH (**2-18**), Fmoc-(*S*)-Asp(tBu)-COOH was used, wherein the tBu group protects the side chain carboxylic acid group in order to avoid production of branched peptides. Although there are other kinds of side-chain protecting groups for Asp such as Bn, cHx, and Men,^[163-164] tBu is the most used with the Fmoc method because it is the more acid-labile. In addition, the tBu group minimises side reactions because of its steric bulk.^[165] Like peptide **2-14**, the other peptides **2-15 - 2-23** were also characterised using HPLC, low and high resolution MS and ¹H NMR spectroscopy. All the NMR spectra are consistent with their structures and all the related details are shown in Chapter 8.

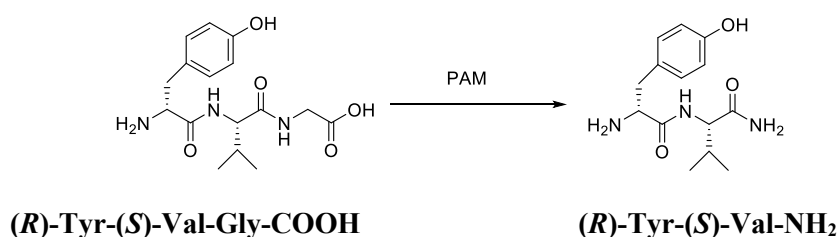
As mentioned above, two peptide products were isolated during the synthesis of peptide **2-14**, one being peptide **2-14** and the other having a mass 57 Da less. This difference is equal to loss of a glycine residue and indicates that the by-product is either *N*-Ac-Gly-(*S*)-Pro-(*S*)-Gln-(*S*)-Arg-(*S*)-Phe-COOH or *N*-Ac-(*S*)-Pro-(*S*)-Gln-(*S*)-Arg-(*S*)-Phe-Gly-COOH. A by-product was also isolated from the synthesis of *N*-Ac-(*S*)-Pro-(*S*)-Gln-(*S*)-Arg-(*S*)-Phe-Gly-COOH (**2-15**) (**Figure 8.4**); it also had a

mass 57 Da less than that of peptide **2-15**, and is therefore likely to be *N*-Ac-(*S*)-Pro-(*S*)-Gln-(*S*)-Arg-(*S*)-Phe-COOH. Due to the similarity between peptides **2-14** and **2-15**, it is probable that the by-product of the synthesis of peptide **2-14** is *N*-Ac-Gly-(*S*)-Pro-(*S*)-Gln-(*S*)-Arg-(*S*)-Phe-COOH. While these by-products could be the result of incomplete coupling of Fmoc-Gly-COOH to the resin, that seems unlikely since compound **2-1** was acetylated to avoid this potential problem. Further, analogous products were not observed in any of the other peptide syntheses. When analysing crude peptides **2-18** and **2-21**, by-products of mass corresponding to loss of two amino acid residues (Phe+Gly or Pro+Gly) were seen from the MS analysis of species. A possible explanation is that acidic peptide hydrolysis occurs in the last step of the syntheses, where a high concentration (95%) of TFA is used.^[166] Peptide hydrolysis shows a large dependence on amino acid sequence.

2.3 Measurements of Binding Affinities of Peptide Substrates with PAM

Peptides **2-14** - **2-23** were to be evaluated in terms of their binding affinities with PAM. The basic way for evaluation is to determine a K_m value, a kinetic constant, which is used widely in enzyme kinetics to determine substrate binding affinity for the enzyme. For this, the PAM assay is repeated over a range of concentrations of each peptide **2-14** - **2-23**, which is impractical and unnecessary for a simple comparative evaluation. Alternatively, an IC_{50} value, the concentration of an inhibitor that reduces the turnover of a substrate by half, was determined in a competitive PAM assay by monitoring the effect of each inhibitor on reaction of the substrate (*R*)-Tyr-(*S*)-Val-Gly-COOH. This is a more simple and convenient method, where each peptide of interest competes for binding to the active site of the PAM enzyme against the tripeptide (*R*)-Tyr-(*S*)-Val-

Gly-COOH that is converted to the corresponding product (*R*)-Tyr-(*S*)-Val-NH₂ by PAM as shown in **Scheme 2.2**.^[167-168] In this assay, the peptide of interest slows down or prevents the amidation of the above mentioned tripeptide substrate, where the relative binding affinities of the inhibitors and substrates are reflected in this competition.



Scheme 2.2 The tripeptide (*R*)-Tyr-(*S*)-Val-Gly-COOH catalysis by PAM to give the amidated product (*R*)-Tyr-(*S*)-Val-NH₂.

An IC₅₀ value is dependent on the experimental conditions. However, testing all candidates under identical conditions makes it possible to compare their binding affinities directly. The current competition assay was carried out on the basis of the reported isolated PAM assay conditions established in the Easton group.^[120, 133] To be specific, the assay sample was initially prepared with the tripeptide substrate (*R*)-Tyr-(*S*)-Val-Gly-COOH and the peptide of interest. The latter is treated in this analysis as an inhibitor though it is also expected to be a substrate. A consistent concentration of 50 mM of tripeptide substrate was used in each sample, which is smaller than the *K_m* value (360 ± 40 μM) of this tripeptide with PAM from DMS53 cell medium.^[146] Under this condition, an inhibitor or competitive substrate effectively competes for binding

the active site of PAM. In addition, PAM cofactors (ascorbic acid and copper sulphate) with bovine liver catalase were added into samples for assisting the enzyme catalysis; the function of bovine liver catalase in the assay is for stabilizing ascorbate and protecting the enzyme from damage by decomposed ascorbate.^[8, 169] Organic solvents EtOH and DMSO (a small amount) were used to increase substrate and inhibitor solubility,^[120, 133] and to maintain conditions so that these results could be compared directly with reported ones. The PAM enzyme used was from concentrated growth medium of the DMS53 cell line^[145] and was used in the binding affinity assay without further purification because PAM is the only enzyme known for catalysing the amidation of glycine-extended prohormones.^[85] The samples were incubated for 2 h at 37 °C, followed by being treated with base to quench the PAM activity, converting all the hydroxyglycine-extended intermediates to the corresponding amidated products. After being neutralised with acid, the sample mixtures were filtered with Amicon® Ultra YM-3 filters that removes compounds having molecular weights over 3000. In this case, PAM enzyme and other proteins were removed due to their high molecular weights while peptides **2-14** - **2-23**, the tripeptide (*R*)-Tyr-(*S*)-Val-Gly-COOH, and amidated products having molecular weights below 3000, passed through the membrane. The filtrates were subsequently injected onto HPLC for separation and analysis.

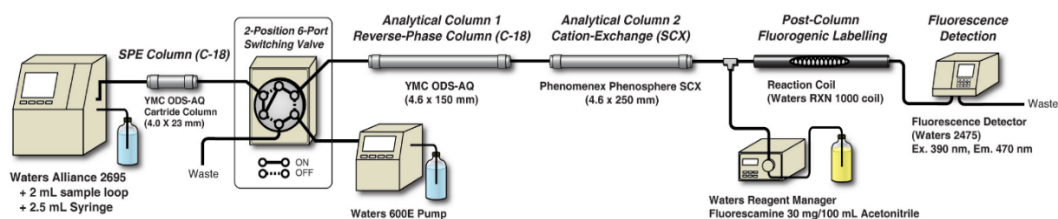


Figure 2.4 HPLC setup for the detection of (*R*)-Tyr-(*S*)-Val-Gly-COOH and its amidated product (*R*)-Tyr-(*S*)-Val-NH₂.^[133]

The detection and quantification method of HPLC used was also established in the Easton group.^[133, 146] This detection system, as illustrated in **Figure 2.4** above, consists of a Waters Alliance 2695 separation module, a Waters 600E Pump, a solid-phase extraction (SPE) column, a reverse-phase column, a cation-exchange column, a Waters reagent manager controlling the flow of fluorescamine solution, and a Waters 2475 fluorescence detector. Specifically, the prepared sample was loaded onto the SPE column and then washed with water to get rid of salts but retained peptides on the column. After that, the residual peptide material was eluted with MeCN and AccQ-Tag buffer to be separated by the C18 reverse-phase column and the cation-exchange column, followed by being labelled with fluorescamine for fluorescence detection, which gave rise to a chromatogram with the separation of (*R*)-Tyr-(*S*)-Val-Gly-COOH and (*R*)-Tyr-(*S*)-Val-NH₂. The ratio between the tripeptide substrate and the amidated product was obtained *via* Waters Empower 3 software. On this basis, the concentration of peptide of interest against the percentage of tripeptide turnover was plotted to generate an activity-concentration curve for determining an IC₅₀ value. An example HPLC trace with standard compounds is shown in **Figure 2.6** below.

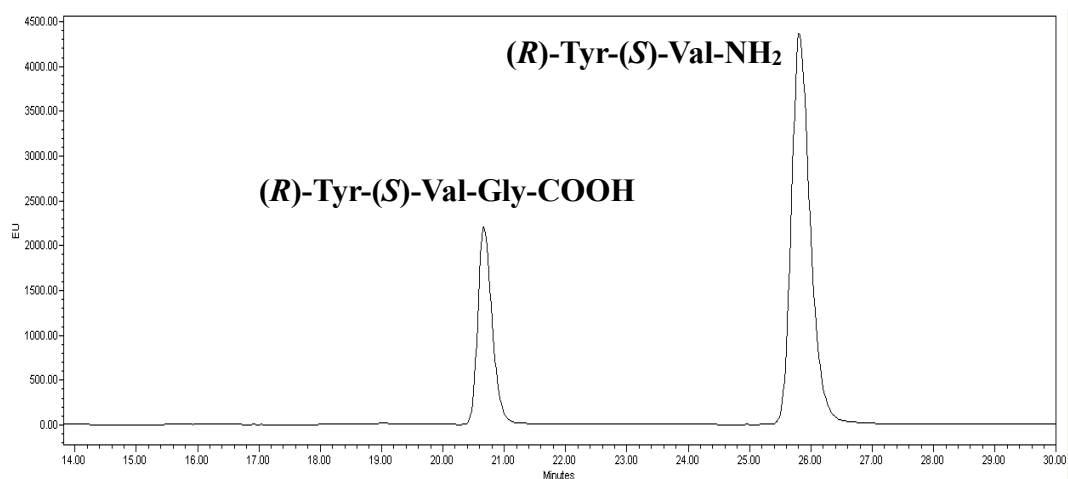


Figure 2.6 Example of HPLC trace, with commercial standards of *(R)*-Tyr-*(S)*-Val-Gly-COOH and *(R)*-Tyr-*(S)*-Val-NH₂.

Starting with the shortest peptide **2-17**, the concentration used in the assay ranged from 600 to 0 μM at 2X serial dilution, which is based on the study by Easton *et al.*^[120] that apparent K_m values of prooxytocin analogues having $-\text{Phe-Gly-COOH}$ at the C-terminus are between 9-38 μM . The assay was duplicated, and two sets of experiment data were obtained as shown in **Table 2.4**. On the basis of these data, an activity-concentration curve was fitted with SciDAVis 0.2.4 software^[120] using a sigmoidal-dose response equation: $y=b+(t-b)/(1+(x/IC_{50})^n)$ where y is percentage tripeptide turnover (after two hours), x is the peptide concentration, b is the baseline response, t is the maximum response, and n is the hill slope. All numbers calculated were corrected to two significant figures.

Table 2.4 Experiment data of binding affinity test of **2-17** from the competition assay.

Concentration of 2-17 (μM)	(R)-Tyr-(S)-Val-Gly-COOH turnover (%)	
	Experiment A	Experiment B
0	16	16
19	11	9.4
38	6.3	6.4
75	3.5	2.7
150	1.6	1.5
300	1.3	0.98
600	0.41	0.18

Experiments A and B in **Table 2.4** correspond to the competition assay using peptide **2-17**. The resulting activity-concentration curves, shown in **Figure 8.34**, had R^2 values above 0.99 and IC_{50} values in good agreement with one another; $27 \pm 1 \mu\text{M}$ and $26 \pm 2 \mu\text{M}$. The low uncertainty and R^2 values close to 0.99 indicate the data are well matched to the predicted values. The combined activity-concentration curve of these two experiments is illustrated in **Figure 2.7A**. The error bars, which are the differences between the two measurements, are relatively small. Since the most relevant part of the activity-concentration curve is from about 10-50 μM of peptide **2-17**, the high concentration data point, at 600 μM , possibly could distort the IC_{50} value calculation. Therefore, the data were reanalysed without this value at 600 μM . After recalculation, however, experiments A and B gave $IC_{50} = 26 \pm 1 \mu\text{M}$ and $IC_{50} = 26 \pm 2 \mu\text{M}$ and the combined IC_{50} value of $26 \pm 2 \mu\text{M}$, as shown in **Figure 2.8B**. The uncertainty is below 10% of the measured IC_{50} value, which is comparable with previous measurements by Easton *et al.*,^[120] indicating an accurate measurement of IC_{50} .

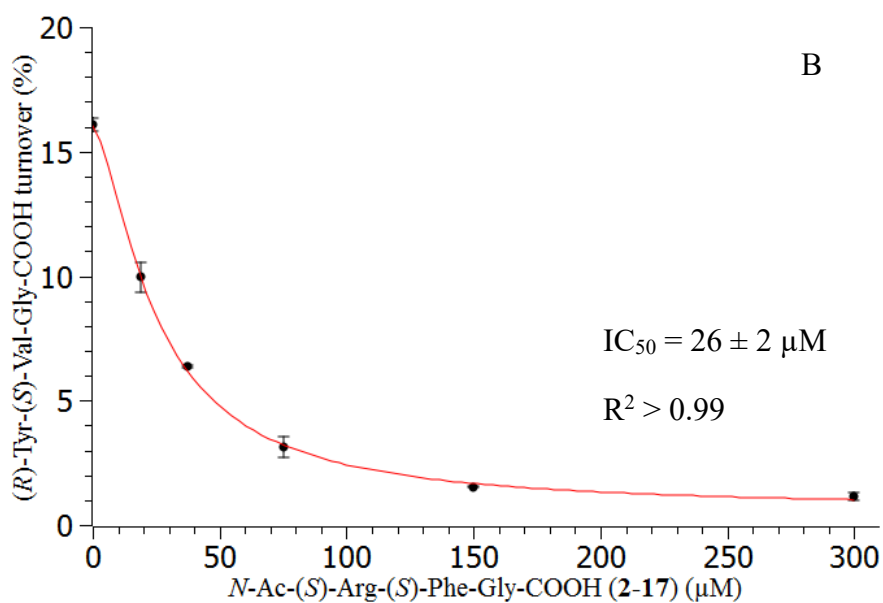
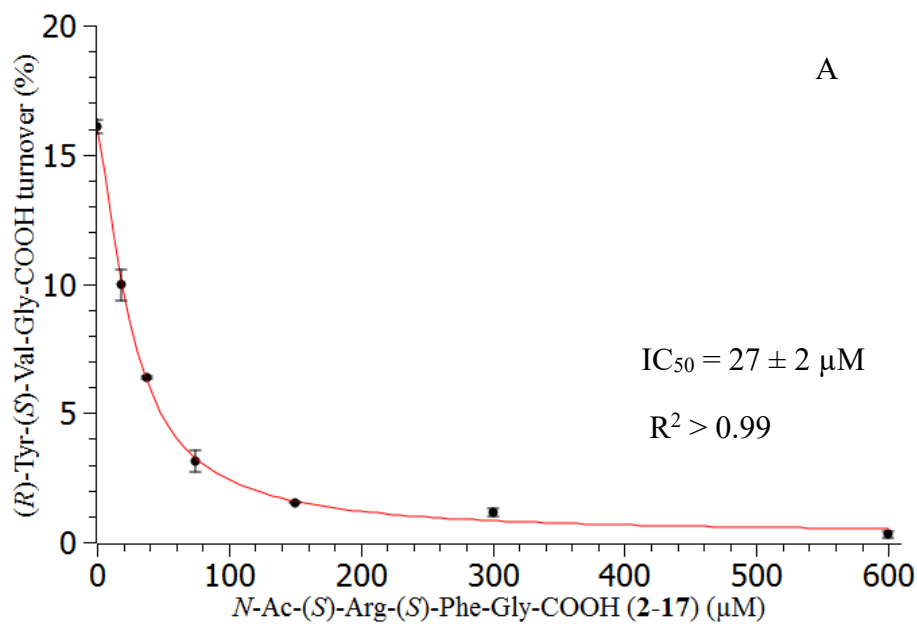


Figure 2.7 Example of the determination of an IC_{50} value, with the peptide *N*-Ac-(*S*)-Arg-(*S*)-Phe-Gly-COOH (**2-17**). The activity-concentration curve was generated by plotting the tripeptide substrate turnover percentage and inhibitor concentration ranging (**A**) from 600 to 0 μM at 2X serial dilution; and (**B**) from 300 to 0 μM at 2X serial dilution.

All other peptide candidates were tested in the same manner as described for peptide **2-17**. For peptides **2-14 - 2-16**, since their structures are similar to that of peptide **2-17**, 300 to 0 μM was used to perform the binding affinity assays and their IC_{50} values were also similar to that of peptide **2-17**, which were all below 30 μM . For peptides **2-18** and **2-19**, by reason that whether Ala or Asp at P2 would moderate IC_{50} values was not clear, the original concentration range used was 600 to 0 μM . The calculated IC_{50} values of peptides **2-18** and **2-19** were both around 70 μM , showing that the concentrations used were appropriate for the IC_{50} value calculations. For peptide **2-20**, the initial concentration range of 300 to 0 μM was used for the assay. Since 300 μM of peptide **2-20** had decreased the tripeptide turnover by over 95%, no larger concentration was required. By contrast, for peptides **2-21 - 2-23**, 600 was not enough. For example, as shown in **Figure 2.8A** below, the maximum concentration of 600 μM of peptide **2-22**, only reduced the tripeptide substrate turnover by around 30%. This indicated that more peptide **2-22** should be used in the assay. Therefore, a range from 6000 to 0 μM of peptide **2-22** was used and the combined IC_{50} value was determined as $1200 \pm 190 \mu\text{M}$ as shown in **Figure 2.8B**. For peptides **2-21** and **2-23**, a concentration range of 2000 to 0 μM , not higher due to the lack of material. In the assay of peptide **2-21**, even the maximum concentration, 2 mM, only reduced the tripeptide substrate turnover by around 40%. This is not enough to accurately calculate the IC_{50} , but it is clear that the value must be over 2 mM. Under the same conditions, the IC_{50} value of peptide **2-23** was calculated as $1500 \pm 210 \mu\text{M}$. All the data related to these ten target peptides are illustrated in Chapter 8.

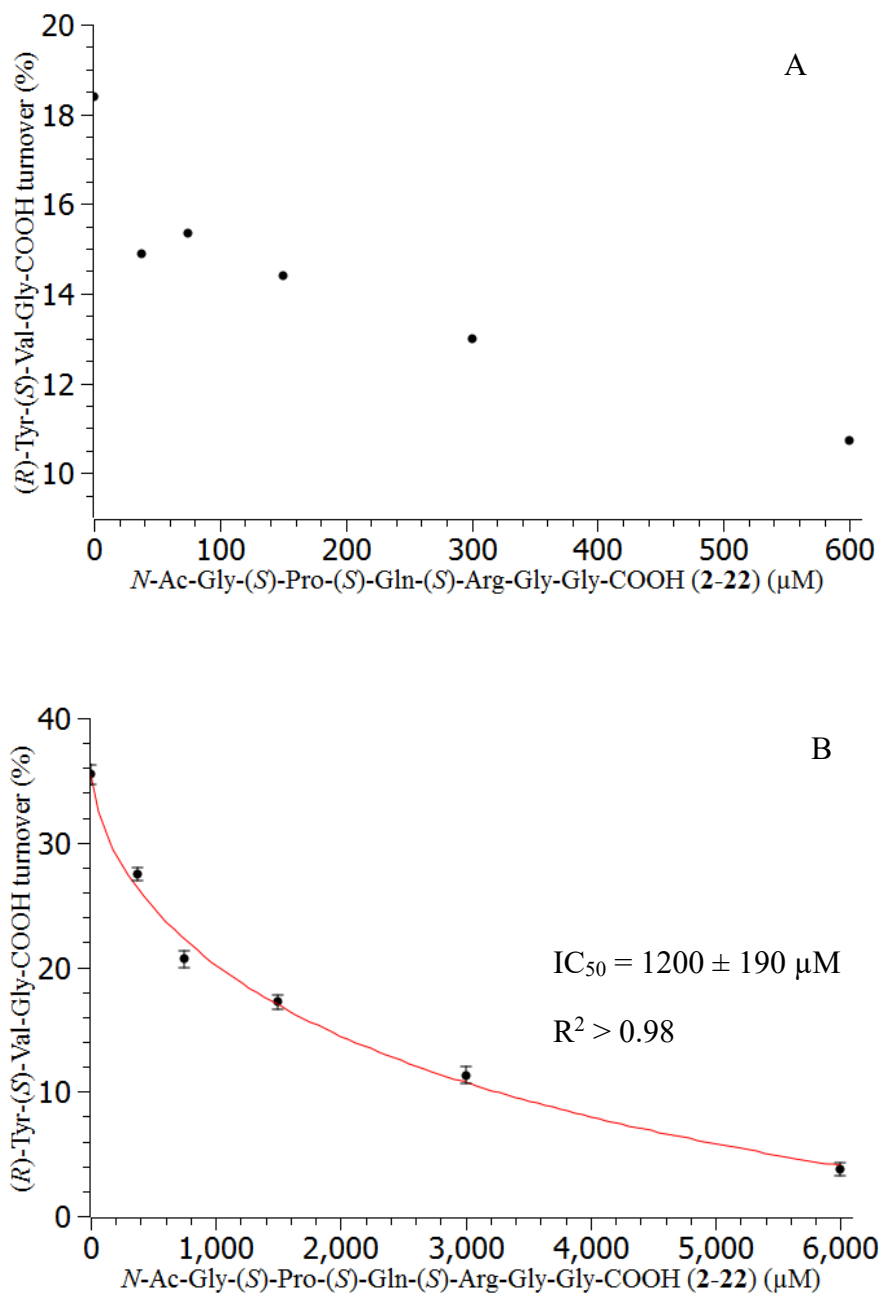


Figure 2.8 Example of the determination of an IC₅₀ value, with the peptide *N*-Ac-Gly-(*S*)-Pro-(*S*)-Gln-(*S*)-Arg-Gly-Gly-COOH (**2-22**). The activity-concentration curve was generated by plotting the tripeptide substrate turnover percentage and inhibitor concentration ranging (**A**) from 600 to 0 μM at 2X serial dilution; and (**B**) from 6000 to 0 μM at 2X serial dilution (different batches of concentrated PAM used caused different substrate turnovers for these two experiments).

Table 2.5 IC₅₀ values of the peptide substrates (all assays were duplicated).

No.	Peptide of interest	IC ₅₀ (μM)	
2-14	<i>N</i> -Ac-Gly-(<i>S</i>)-Pro-Gln-(<i>S</i>)-Arg-(<i>S</i>)-Phe-Gly-COOH	16 ± 3	20 ± 1
2-15	<i>N</i> -Ac-(<i>S</i>)-Pro-(<i>S</i>)-Gln-(<i>S</i>)-Arg-(<i>S</i>)-Phe-Gly-COOH	17 ± 2	21 ± 5
2-16	<i>N</i> -Ac-(<i>S</i>)-Gln-(<i>S</i>)-Arg-(<i>S</i>)-Phe-Gly-COOH	20 ± 2	17 ± 1
2-17	<i>N</i> -Ac-(<i>S</i>)-Arg-(<i>S</i>)-Phe-Gly-COOH	26 ± 1	26 ± 2
2-18	<i>N</i> -Ac-Gly-(<i>S</i>)-Pro-Gln-(<i>S</i>)-Asp-(<i>S</i>)-Phe-Gly-COOH	69 ± 9	62 ± 8
2-19	<i>N</i> -Ac-Gly-(<i>S</i>)-Pro-Gln-(<i>S</i>)-Ala-(<i>S</i>)-Phe-Gly-COOH	69 ± 10	71 ± 8
2-20	<i>N</i> -Ac-Gly-(<i>S</i>)-Pro-Gln-Gly-(<i>S</i>)-Phe-Gly-COOH	10 ± 1	12 ± 1
2-21	<i>N</i> -Ac-Gly-(<i>S</i>)-Pro-Gln-(<i>S</i>)-Arg-(<i>S</i>)-Pro-Gly-COOH	> 2000	> 2000
2-22	<i>N</i> -Ac-Gly-(<i>S</i>)-Pro-Gln-(<i>S</i>)-Arg-Gly-Gly-COOH	1200 ± 200	1300 ± 200
2-23	<i>N</i> -Ac-Gly-(<i>S</i>)-Pro-Gln-(<i>S</i>)-Pro-Gly-Gly-COOH	1400 ± 160	1500 ± 260

From **Table 2.5**, the IC₅₀ values of peptides **2-14** - **2-17** having -Arg-Phe-Gly-COOH were all between 10-30 μM, which is similar to those of prooxytocin analogues with penultimate Phe in the early study.^[120] The similar values of peptides **2-14** - **2-17** illustrate that when Phe is at the penultimate position from the *C*-terminus, there is little sequence recognition of amino acids at P3 - P5. Therefore, these natural prohormone models show the same trend as observed previously with unnatural peptides,^[120] that there is negligible sequence recognition of amino acids from P3 to the *N*-terminus of peptide substrates having penultimate Phe.^[120] Based on this consensus sequence study, it is anticipated that, the first group of human prohormones shown in **Table 2.1**, having -Arg-Phe-Gly-COOH, are likely to bind to PAM effectively in living bodies with IC₅₀ values around 20 μM.

Considering then the effect of different amino acids at P2 on the binding affinities of human prohormones having penultimate Phe, based on **Table 2.5**, compared to peptide **2-14** with Arg at P2, the IC₅₀ values of peptides **2-18** and **2-19** with Asp and Ala, respectively, were around four times higher (70 μM) while the value of peptide **2-20**

with Gly was slightly lower (10 μM). This indicates that Asp and Ala at P2 slightly disrupt binding affinity with PAM compared to Arg. By contrast, Gly at P2 helps binding. The contributions from these antepenultimate amino acids probably reflect their properties. Among these four amino acids (Arg, Asp, Ala, and Gly), Gly gives the highest binding affinity and is the smallest. The marginal decrease with Arg indicates that its positive charged side chain fits the active site of the enzyme. By contrast, negatively charged Asp and uncharged Ala give lower binding affinity. The trend found in the present study is supported by Caron^[146] who found that the K_i value (25 μM) of γ -MSH with $-\text{Arg-Phe-Gly-COOH}$ was 3.5 times lower than that (85 μM) of CCK8-Gly with $-\text{Asp-Phe-Gly-COOH}$. Based on the results above, it is expected that human prohormones having $-\text{Asp-Phe-Gly-COOH}$ and $-\text{Ala-Phe-Gly-COOH}$, shown in the second and third groups of **Table 2.1**, are likely to have slightly lower binding with PAM than those having $-\text{Arg-Phe-Gly-COOH}$, but are still likely to bind to PAM effectively with IC_{50} values around 70 μM .

Further to this, the P1 amino acid was considered. The peptide substrates **2-21** - **2-23** having penultimate Pro and Gly had IC_{50} values all at the millimolar level. Their IC_{50} values were all over 60 times higher than peptide **2-14**, indicating that penultimate Pro or Gly, compared with Phe, gives much poorer binding affinities with PAM. So in the current study modification of the natural prohormone sequence $-\text{Arg-Phe-Gly-COOH}$, by replacing the Phe with Pro or Gly disrupts binding, just as substitution of the penultimate Pro and Gly in the natural sequences of the prohormones procalcitonin and prooxytocin with Phe increases binding.^[120] The combined results indicate that the penultimate amino acids predominantly determine the binding affinities with PAM.

The fact that K_m values of natural prohormones are usually much higher than their concentrations implies that amidation significantly depends on the binding affinity with PAM. The study in this Chapter suggests that penultimate amino acid of human prohormones mainly determines the binding affinity with PAM. Therefore, penultimate amino acid is likely to be an important factor of the selectivity of amidation of peptide hormones. To further investigate this, literature research was performed on the correlation between the penultimate amino acids and the functions of hormones. It was found that hormones having -Arg-Phe-NH₂ are mostly neuropeptides that play important role in body temperature homeostasis, pain modulation, and the control of transmission of nociceptive information.^[170-171] Asp-Phe-amides are either cholecystokinin (CCK) or gastrin, and their main functions are both related to dietary digestion in stomach.^[172-174] While the Ala-Phe-amide, calcitonin gene-related peptide, is a potent peptide vasodilator that also plays a vital role in the transmission of pain.^[175-176] These reviews suggest that hormones with Phe-NH₂ are produced rapidly in bodies. By contrast, amidated hormones having -Pro-NH₂ or -Gly-NH₂ serve as growth hormones in humans and show relatively low preference on release. For example, calcitonin (Pro-NH₂) plays a role in blood calcium regulation,^[22] and oxytocin (Gly-NH₂) mainly plays a role in sexual reproduction.^[177] Combining the current results and the literature work, it is concluded that there might be a correlation between penultimate amino acid and the release rate of amidated peptide hormones. It is likely that prohormones having penultimate amino acid that enhance binding are possibly amidated by PAM relatively preferentially and *vice versa*. In future, new models related to human prohormones with other penultimate amino acids should be studied to further investigate this.

Chapter Three

Synthesis and Evaluation of Interactions of Glycine Derivatives of Medicinal Agents with Peptidylglycine α -Amidating Monooxygenase

3.1 Introduction

PAM is found in many types of tumours and has potential in cancer therapy.^[178-180] Anti-sense expression of PAM in tumour cell lines is reported to inhibit tumour growth efficiently.^[180] Moreover, the potent PAM inhibitor, PBA (**1-17**), is reported to reduce the growth of some particular types of cancer cells.^[129-130, 181] On this basis, the work in this Chapter involves derivatives of antineoplastic drugs which were considered to be potential PAM substrates or inhibitors. The hypothesis was that these compounds would not only inhibit PAM activity, but also undergo reaction to produce a cytotoxic agent. The aim of this work was to examine some modified anticancer drugs and see whether an improvement in the anticancer effect was achieved. As shown in **Figure 3.1**, the cytotoxic agents, bexarotene (**3-1**) and temozolomide (**3-2**), which are clinically available, were chosen for investigation.

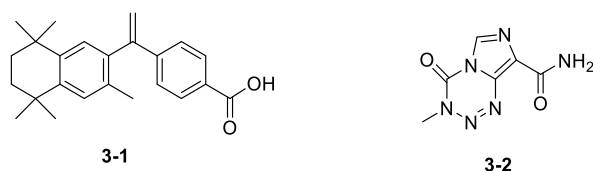
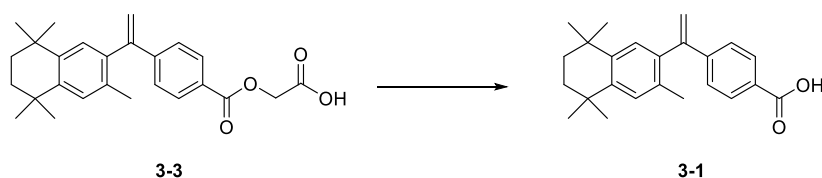


Figure 3.1 Structures of bexarotene (**3-1**) and temozolomide (**3-2**).

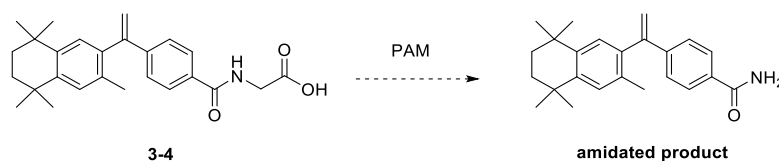
Bexarotene (Bex, **3-1**) is a selective retinoid type-X receptor (RXR) agonist,^[182] where activation of RXR gives rise to the formation of homodimeric (RXR-RXR) or heterodimeric complexes (RXR-RAR (retinoic acid receptors)).^[183] The RXR-RAR heterodimeric complexes can bind DNA and hence induce apoptosis and differentiation of tumours,^[184] which indicates that Bex (**3-1**) might play an important role in cancer prevention or treatment. Therapeutically, Bex (**3-1**) has already been widely used in the treatment of cutaneous T-cell lymphoma,^[185] and also has promising effects on the treatment of non-small cell lung cancer (NSCLC).^[186]

The glycolate analogue of Bex (Bex-glycolate, **3-3**) is a competitive PAM inhibitor (IC₅₀ value = 17.7 μM) and no significant reaction was observed during the PAM assay (**Scheme 3.1**).^[187] It was also evaluated in terms of cytotoxicity for DMS53 cells and its LD₅₀ value (40 μM) was slightly better than that (60 μM) of the parent cytotoxic agent **3-1**, indicating that it is also a promising cytotoxic agent for SCLC.^[187]



Scheme 3.1 Bex-glycolate (**3-3**) and its potential hydrolysis to produce Bex (**3-1**).

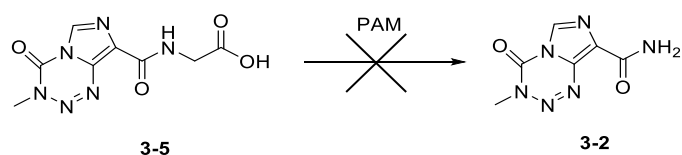
In the present study, another analogue of Bex (**3-1**), Bex-glycine (**3-4**), was assessed in the same way as Bex-glycolate (**3-3**). It was expected that Bex (**3-1**) could be synthetically extended as a glycine derivative to operate as a PAM substrate, the intent being that the PAM would recognise and cleave it to produce the amide (**Scheme 3.2**) which hopefully would have similar cytotoxicity to Bex (**3-1**). In this case, compound **3-4** would not only inhibit the PAM, but also react to produce a cytotoxic drug. The PAM source, the DMS53 cell strain (a human SCLC), was used as the cancer cell candidate for cytotoxicity assays.



Scheme 3.2 Bex-glycine (**3-4**) and its expected amidated PAM product.

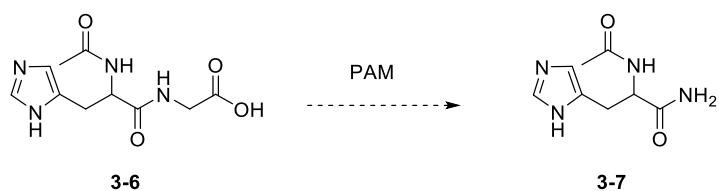
Another antineoplastic agent, temozolomide (Tmz, **3-2**), is a methylating agent used for cancer treatment that works through DNA damage.^[188] Recent studies have shown that Tmz (**3-2**) is a very effective agent in recurrent metastatic SCLC,^[189] where all standard therapies operate *via* DNA damage. However, both Tmz (**3-2**) and its glycine-

extended analogue (Tmz-glycine, **3-5**) were found to be ineffective against DMS53 cells (LD_{50} value > 2 mM).^[187] More surprisingly, Tmz-glycine (**3-5**), with a good binding affinity (IC_{50} value = 17.7 μ M) to medium PAM, did not undergo PAM-mediated cleavage (**Scheme 3.3**), and it could be recovered after the assay.^[187] This suggests that Tmz-glycine (**3-5**) serves as a PAM inhibitor rather than a PAM substrate.



Scheme 3.3 No Tmz (**3-2**) was produced in the PAM assay using Tmz-glycine (**3-5**).

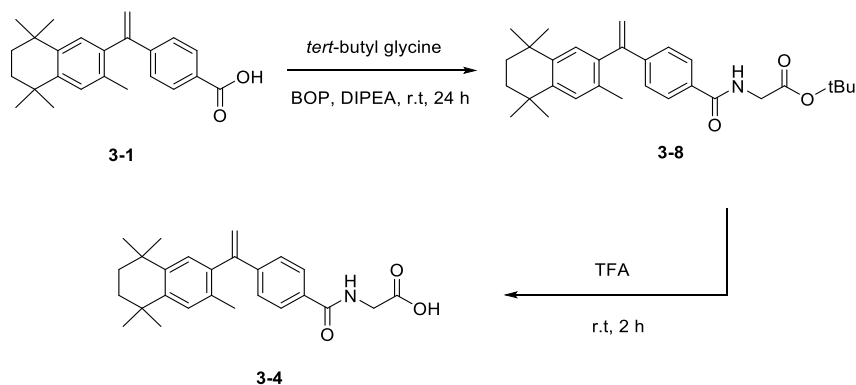
Based on this, another aim of the work in this Chapter was to attempt to find out why Tmz-glycine (**3-5**) is not converted into Tmz (**3-2**) by PAM. Recent studies suggest that the reaction of Tmz with $CdCl_2 \cdot 2H_2O$ produces the complex $[Cd(Tmz)Cl_2]_n$,^[190] as Tmz is an organic ligand with abundant coordinating sites. Therefore, the working hypothesis for the inability of PAM to process Tmz-glycine (**3-5**) is that it may coordinate to the enzyme cofactor Cu(II) during the assay, resulting in inactive enzyme. In order to test this, a structurally-similar molecule *N*-Ac-(*S*)-His-Gly-COOH (**3-6**) was prepared. Both compound **3-6** and Tmz-glycine (**3-5**) have the imidazole moiety, for copper coordination.^[191] Hence, it was of interest to examine whether *N*-Ac-(*S*)-His-Gly-COOH (**3-6**) would be converted to *N*-Ac-(*S*)-His-NH₂ (**3-7**) through enzyme-mediated cleavage.



Scheme 3.4 *N*-Ac-(*S*)-His-Gly-COOH (**3-6**) and the corresponding possible amidated product *N*-Ac-(*S*)-His-NH₂ (**3-7**).

3.2 Synthesis of Bex-glycine (**3-4**)

It was anticipated that *tert*-butyl glycine could be installed onto Bex (**3-1**) through coupling in the presence of the BOP and DIPEA reagents, followed by deprotection of the *tert*-butyl group with TFA (**Scheme 3.5**).



Scheme 3.5 Synthesis of Bex-glycine (**3-4**).

As expected, Bex (**3-1**) coupled with *tert*-butyl glycine hydrochloride in the presence of BOP and DIPEA at room temperature to produce the ester **3-8**, which was indicated by the appearance of a singlet peak at δ_{H} 1.50 and a doublet peak at δ_{H} 4.13 in the ¹H

NMR spectrum, corresponding to the *tert*-butyl and glycine methylene protons, respectively. Deprotection of the ester **3-8** under acidic condition was performed to produce Bex-glycine (**3-4**), as evident from the loss of the singlet peak related to *tert*-butyl protons in the ¹H NMR spectrum. The product was purified by preparative HPLC. More synthesis details are presented in Chapter 8.

3.3 Interaction of Bex-glycine (3-4) with Medium PAM

Initially the binding affinity of Bex-glycine (**3-4**) with PAM was examined by determining the IC₅₀ value in a competitive assay with the tripeptide (*R*)-Tyr-(*S*)-Val-Gly-COOH as discussed in Chapter 2. This way, the present results are comparable with the earlier study of the analogue Bex-glycolate (**3-3**), wherein the binding affinity assay was performed using the same assay conditions. Due to the similarity of the structures of compounds **3-3** and **3-4**, they were expected to have similar binding affinities. Since the IC₅₀ value of compound **3-3** is reported to be 17.7 μM with the medium PAM from DMS53 cells,^[187] the initial concentration range for testing compound **3-4** in the competitive assay was from 300-0 μM and the corresponding experimental data are shown in **Table 3.1** below.

Table 3.1 Preliminary experimental data of binding affinity of Bex-glycine (**3-4**) from a competition assay.

Concentration of Bex-glycine (3-4) (μM)	<i>(R)</i> -Tyr- <i>(S)</i> -Val-Gly-COOH turnover (%)	
	Experiment A	Experiment B
0	20	18
19	19	18
38	17	17
75	17	17
150	15	14
300	14	14

From the Table above, up to 300 μM of compound **3-4** only reduced turnover of *(R)*-Tyr-*(S)*-Val-Gly-COOH by around 20%. Therefore, higher concentrations (4800-0 μM) were used in the competitive assay and the data are provided in **Table 3.2**. After plotting the concentration of compound **3-4** against the percentage turnover of the tripeptide, the activity-concentration curve (**Figure 3.2**) gave the IC_{50} value as $1300 \pm 300 \mu\text{M}$.

Table 3.2 Second experimental data of binding affinity of Bex-glycine (3-4) from a competition assay.

Concentration of Bex-glycine (3-4) (μM)	<i>(R)</i> -Tyr- <i>(S)</i> -Val-Gly-COOH turnover (%)	
	Experiment A	Experiment B
0	20	19
75	19	18
150	16	16
300	16	16
600	14	13
1200	9.2	10
2400	5.4	5.1
4800	4.0	3.5

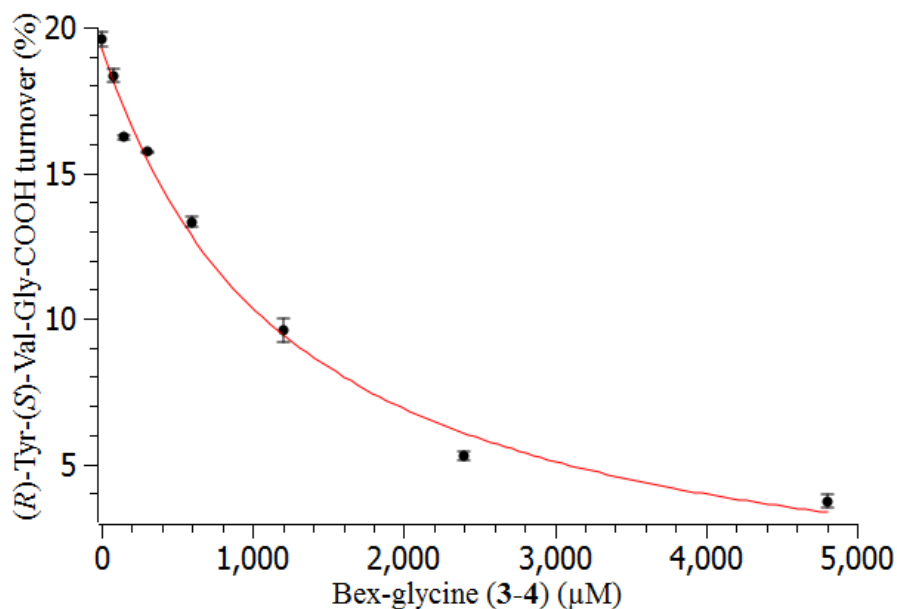
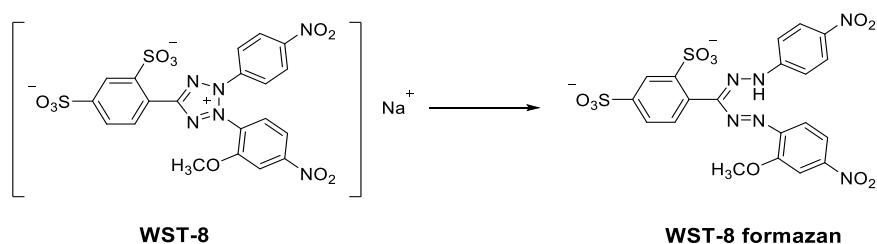


Figure 3.2 Activity-concentration curve for the assessment of binding affinity of Bex-glycine (3-4) with medium PAM.

The millimolar IC₅₀ value shows that this Bex analogue **3-4** has poor binding affinity with PAM and it is therefore anticipated that when doped into cancer cells no significant amount of corresponding amidated product would form. However, it was still of interest to test its cytotoxicity profile because of its structural similarity with the medicinal agent Bex (**3-1**).

3.4 Cytotoxicity Profile of Bex (**3-1**) and Bex-glycine (**3-4**)

To evaluate the cytotoxicity of Bex (**3-1**) and Bex-glycine (**3-4**) with the DMS53 cell line, their LD₅₀ values were to be determined. LD stands for lethal dose and the LD₅₀ value is the concentration of the tested compound required to produce a fifty percent decrease in cell viability.^[192] In the present work, this value was calculated by plotting the concentration of the test compound against the fraction of cell viability using SciDAVis 0.2.4 software. The method used a Cell Counting Kit-8 (CCK-8), which provides convenient and sensitive colorimetric assays for determination of cell viability in cell proliferation and cytotoxicity assays. It relies on Dojindo's highly water-soluble tetrazolium salt, WST-8 [2-(2-methoxy-4-nitrophenyl)-3-(4-nitrophenyl)-5-(2,4-disulfophenyl)-2*H*-tetrazolium, monosodium salt]. This salt, as shown in **Scheme 3.6**, is reduced by dehydrogenase activities in cells to give an orange-colour formazan dye, which is soluble in the tissue culture medium and proportional to the numbers of living cells.^[193] The detection sensitivity of WST-8 is higher than that of other tetrazolium salts such as MTT, XTT, MTS or WST-1.^[194]



Scheme 3.6 WST-8 is reduced by dehydrogenase activities to give formazan dye.

The assay involved pre-incubated DMS53 cells in a 96-well plate. Each well was treated with various concentrations of compounds **3-1** or **3-4** and incubated in a humidified incubator, followed by the addition of CCK-8 solution and further incubation. The concentration range was chosen from 160-0 μM at 2X serial dilution and 640 μM due to the fact that the LD_{50} value of compound **3-1** in an early study was found to be 60 μM .^[187] The plate was finally analysed using a microplate reader. Each compound was tested twice, and the averaged results are presented in **Figure 3.3**. The data provided LD_{50} values for compounds **3-1** and **3-4** of $60 \pm 9 \mu\text{M}$ and $80 \pm 9 \mu\text{M}$, respectively. As discussed in Chapter 2, the error was generated from the software program. This analysis indicates that the relative cytotoxic efficacies of Bex (**3-1**) and Bex-glycine (**3-4**) are not substantially different.

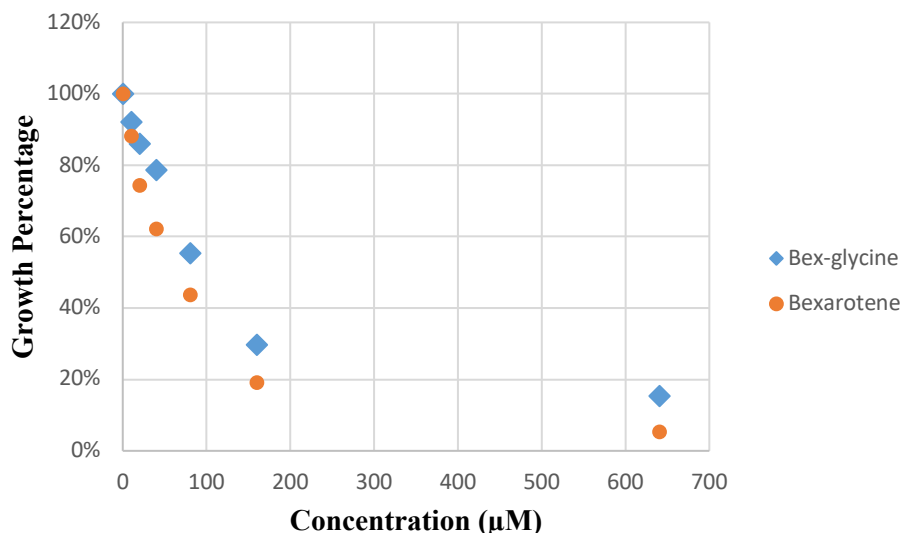
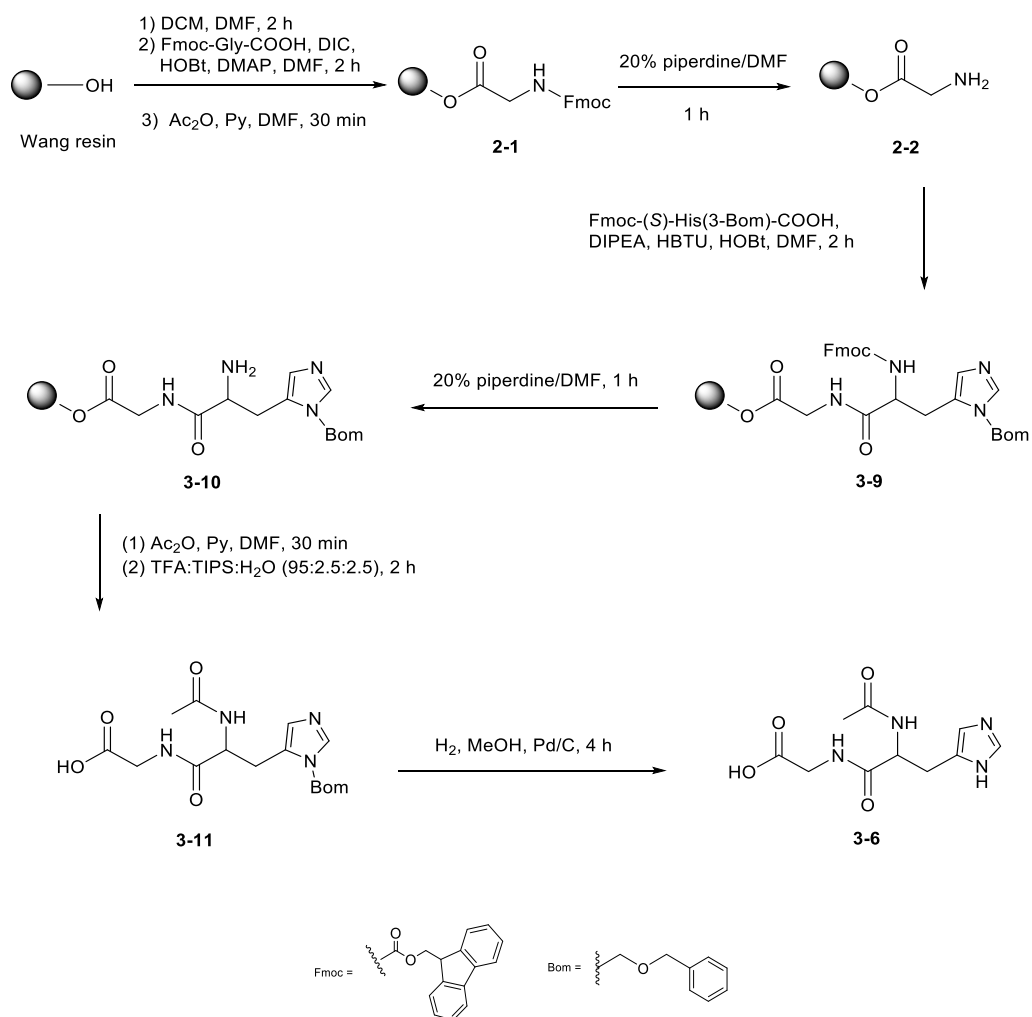


Figure 3.3 Antiproliferation effects of Bex (**3-1**) and Bex-glycine (**3-4**) on DMS53 cells.

3.5 Synthesis of *N*-Ac-(*S*)-His-Gly-COOH (**3-6**) and *N*-Ac-(*S*)-His-NH₂ (**3-7**)

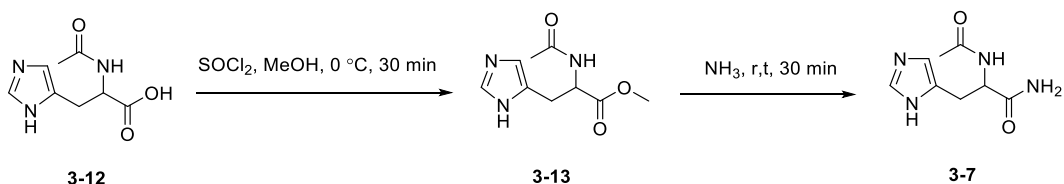
Another aspect of the work described in this Chapter was to examine whether the potential PAM substrate **3-6** would be converted to compound **3-7** through enzyme-mediated cleavage to attempt to find an explanation for why Tmz-glycine (**3-5**) is not converted to Tmz (**3-2**) by PAM. To obtain the peptide **3-6**, solid phase peptide synthesis was carried out using standard Fmoc protocols (**Scheme 3.7**) with Wang resin in a similar manner as described for the synthesis of peptide **2-14**. The swollen resin was treated with Fmoc-Gly-COOH in the presence of DIC and DMAP to give peptide **2-1** with 70% loading efficiency, followed by deprotection of the Fmoc group to give peptide **2-2**. The resulting resin was then coupled with Fmoc-(*S*)-His(Bom)-COOH. After Fmoc deprotection, an acetylation was performed with Ac₂O and pyridine, followed by cleavage from the resin under acidic conditions, to give compound **3-11**. It is noteworthy that the side-chain Bom group, attached to the

imidazole moiety, is stable to TFA but would be removed by a stronger acid such as HF. Considering HF is extremely hazardous and requires particular equipment to conduct deprotection of the Bom group, instead a mild method was chosen, that is hydrogenation using palladium on carbon under hydrogen.^[195] After hydrogenation, a small amount of the crude peptide product was analysed by HPLC with detection using UV-Vis spectroscopy. The resulting HPLC chromatogram reproduced in **Figure 8.46** showed two dominant peaks. Separation of the materials corresponding to these peaks and MS analysis showed one corresponds to compound **3-6**. The other one has mass 120 Da more, which corresponds to compound **3-11**. Separated compound **3-6** was analysed using high resolution MS and ¹H NMR spectroscopy.



Scheme 3.7 Synthesis of *N*-Ac-(*S*)-His-Gly-COOH (**3-6**)

In order to get a standard sample for HPLC detection, compound **3-7** was also synthesised. As shown in **Scheme 3.8**, esterification of *N*-Ac-(*S*)-His-COOH (**3-12**) was performed to produce the ester **3-13**. Then, ammonia was used to convert the ester **3-13** to the amide **3-7** at room temperature. The crude product was purified using HPLC and analysed using high resolution MS and ¹H NMR spectroscopy before use.



Scheme 3.8 Synthesis of *N*-Ac-(*S*)-His-NH₂ (**3-7**)

3.6 Interaction of *N*-Ac-(*S*)-His-Gly-COOH (**3-6**) with Medium PAM

Before examining whether compound **3-6** would be converted to compound **3-7** through enzyme-mediated oxidative cleavage, the binding affinity of compound **3-6** was measured in a competitive assay under the same conditions as described for peptide **2-14**, because this is a relatively quick way to check whether *N*-Ac-(*S*)-His-Gly-COOH (**3-6**) binds to PAM. The concentration of compound **3-6** and the tripeptide substrate turnover percentage were plotted to generate the activity-concentration curve (**Figure 3.4**) and the average IC₅₀ value of compound **3-6** was calculated as 70 ± 11 μM. This establishes that *N*-Ac-(*S*)-His-Gly-COOH (**3-6**) binds to PAM tightly. To determine if it is also a PAM substrate, standard assays were performed with *N*-Ac-(*S*)-His-Gly-COOH (**3-6**).

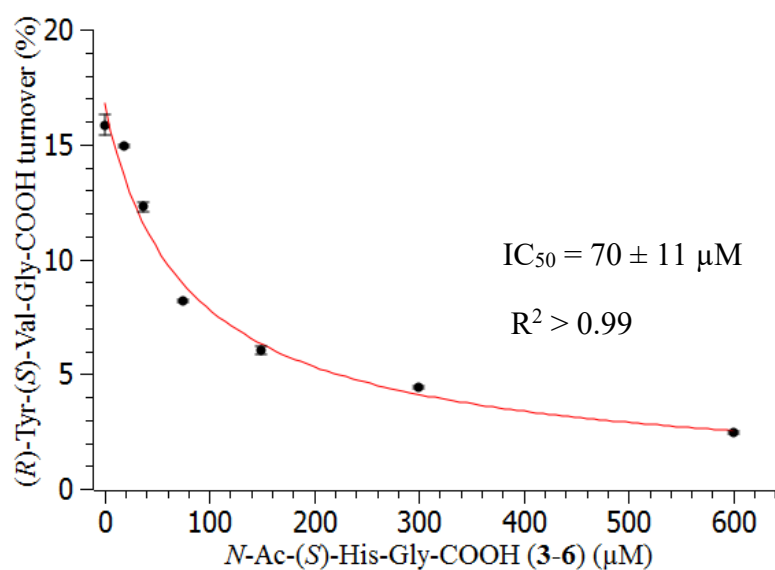


Figure 3.4 PAM binding affinity assay of *N*-Ac-(*S*)-His-Gly-COOH (**3-6**).

The investigation of **3-6** as a possible substrate of PAM was performed under the same conditions as described for the above competitive assay, but with no tripeptide (*R*)-Tyr-(*S*)-Val-Gly-COOH. The concentration of **3-6** used was 75 μM because this is close to the IC₅₀ value determined above and hence enzyme binding occurs. After incubation, the solution was passed through an Amicon® Ultra YM-3 filter, then it was analysed using analytical HPLC, with detection and quantification of *N*-Ac-(*S*)-His-Gly-COOH (**3-6**) and *N*-Ac-(*S*)-His-NH₂ (**3-7**) by UV-Vis spectroscopy. The analytical standards had retention times of 10.8 min for compound **3-7** and 11.8 min for compound **3-6** (**Figure 3.5A**). The analysis of the PAM assay sample shown in **Figure 3.5B** shows a peak at 10.8 min corresponding to *N*-Ac-(*S*)-His-NH₂ (**3-7**). It was thus concluded that *N*-Ac-(*S*)-His-Gly-COOH (**3-6**) is converted to the amidated product *N*-Ac-(*S*)-His-NH₂ (**3-7**) by PAM.

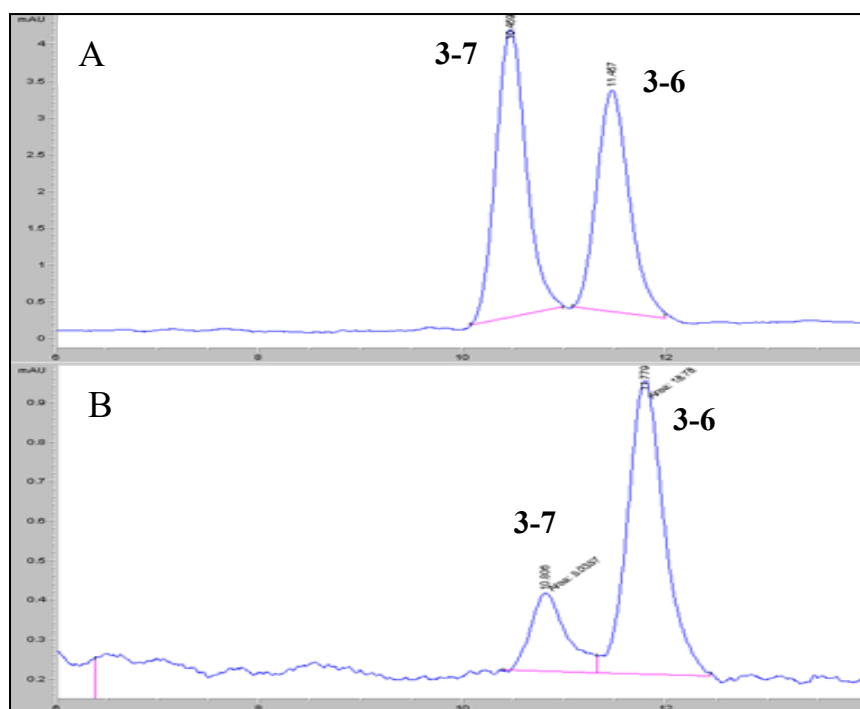


Figure 3.5 (A) HPLC trace of 100 μM *N*-Ac-(*S*)-His-Gly-COOH (**3-6**) and *N*-Ac-(*S*)-His-NH₂ (**3-7**) standards; (B) HPLC trace of the sample from the PAM assay with 75 μM *N*-Ac-(*S*)-His-Gly-COOH (**3-6**) (the small variation in retention time is likely due to the different solvents used, which were water (A) and MES buffer containing EtOH and DMSO (B), respectively).

3.7 Discussion

Bex-glycine (**3-4**) had an IC₅₀ value at the micromolar level in the competition assay, indicating that it is a poor PAM substrate with weak enzyme binding. Therefore, compound **3-4** would not have dual activity as proposed, *i.e.* inhibiting PAM and then producing a cytotoxic drug for cancer cells. However, the cytotoxicity assay showed that compound **3-4** itself had good activity against DMS53 cells, similar to its analogue

3-3 and the parent agent **3-1**. This indicates that compound **3-4** still has potential in cancer therapy but not through the dual activity anticipated.

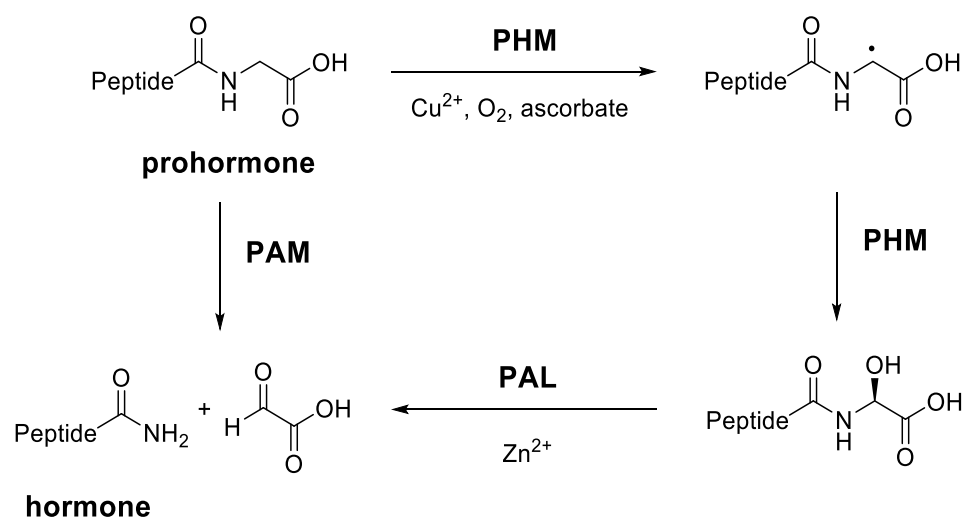
The fact that the reaction of *N*-Ac-(*S*)-His-Gly-COOH (**3-6**) is catalysed by PAM shows that its imidazole moiety does not inactivate the enzyme through copper coordination. Therefore, it is unlikely that Tmz-glycine (**3-5**) possessing the similar imidazole moiety inhibits PAM by metal chelation. Instead, other possibilities should be considered to explain why Tmz-glycine (**3-5**) is not converted to Tmz (**3-2**) by PAM. For example, compound **3-5** might bind to the active site of PAM in a different orientation other than that required for reaction.

Chapter Four

Investigation of the Subunit Activity of Peptidylglycine α -Amidating Monooxygenase

4.1 Introduction

PAM consists of two subunits, PHM and PAL. As shown in **Scheme 4.1** (which is reproduced from **Scheme 1.1** in Chapter 1), PHM catalyses reaction of glycine-extended peptides to give α -hydroxyglycine intermediates, and PAL then catalyses cleavage of the intermediates to give amidated products. The latter step also occurs through non-enzyme-catalysed hydrolysis, particularly on treatment with base.^[196] In the work described in the previous Chapters, base was used in the work-up of PAM assays, so any PAL activity was masked and the activity being measured was actually that of the PHM subunit. In this Chapter, the aim was to unmask the PAL activity. Without non-enzymatic hydrolysis, PHM activity corresponds to the amount of the glycine-extended peptide reacted and the sum of the quantities of the hydroxylated intermediate and amidated product formed, while PAL activity corresponds only to the amount of formation of the amidated product.



Scheme 4.1 Mechanism of PAM catalysis.

Within the past thirty years, a number of groups have studied both PHM activity and PAL activity using various assay conditions and detection methods. Eipper and her colleagues performed radioactivity assays with ^{125}I -labelled *N*-Ac-(*R*)-Tyr-(*S*)-Val-Gly-COOH and *N*-Ac-(*R*)-Tyr-(*S*)-Val- α -hydroxyglycine as distinct substrates to determine PHM and PAL activities, respectively.^[125] This assay had a few shortcomings. Apart from involving radioactivity, separate investigations of PHM and PAL activities complicated the experiment. Furthermore, hydroxyglycine derivatives are hard to synthesise and store due to chemical instability.^[196]

The Merkler group also conducted separate assays of PHM and PAL activities.^[127] In their study, PHM activity was determined by measuring either oxygen consumption, using acetic acid as an oxidisable substrate, or measuring *N*-dansyl-Tyr-Val-Gly amidation. PAL activity was determined by measuring glyoxylate production from (*R,S*)- α -hydroxyhippuric acid by the spectrophotometric method of Christman *et*

al.,^[197] modified by Katopodis and May.^[102] The drawbacks mentioned above encouraged us to consider a single assay to investigate both PHM and PAL at the same time. Mounier *et al.* monitored PHM and PAL activities in a time-dependent assay with the PAM from *X. laevis*,^[126] using HPLC with a UV-Vis detector. We instead developed an assay based on HPLC-MS.

4.2 Investigation of PHM and PAL Activities Using HPLC-MS

To develop an efficient method for detecting universal PAM substrates, intermediates, and amidated products at the same time, HPLC-MS was considered because it involves rapid method development. The HPLC-MS setup, as illustrated in **Figure 4.1** below, consists of a Waters Alliance 2695 separation module, a reverse-phase C18 column, a Waters flow splitter, a Waters TQD mass detector (ESI), and a Waters Fraction Collector. For analysis, samples are injected onto the reverse-phase column, eluted with MeCN, water and formic acid, followed by detection with the ESI mass detector. The percent conversion from peptide substrates to intermediates and products is then calculated *via* MassLynx 4.1 software.

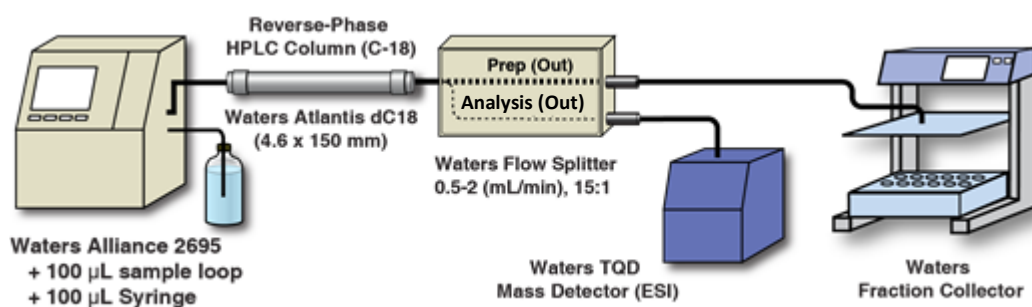
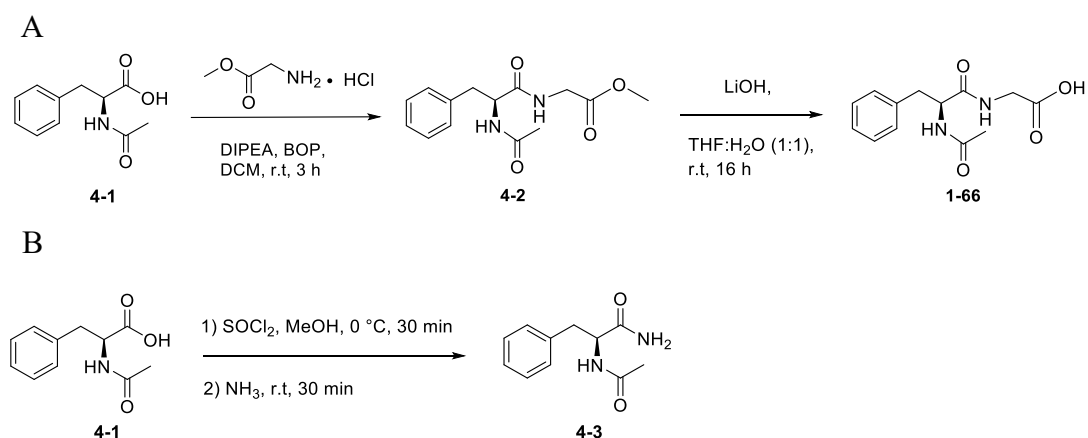


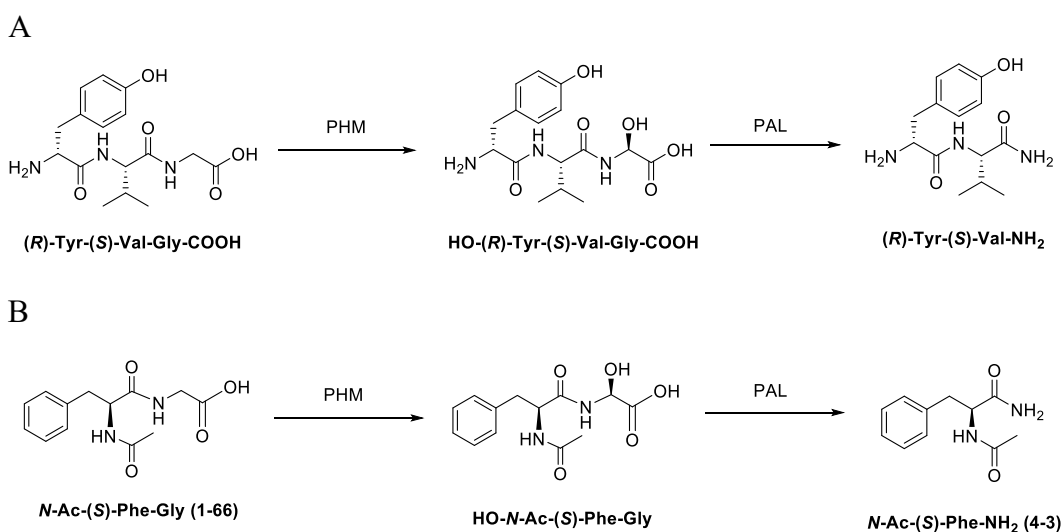
Figure 4.1 HPLC-MS setup for detection of PAM substrates, intermediates, and products.

The PAM enzyme used in this work was medium PAM as used in Chapter 2 and Chapter 3, which is most relevant to humans. In this work, the first PAM substrate studied was the tripeptide (*R*)-Tyr-(*S*)-Val-Gly-COOH, which had already been used before where it was detected by fluorescence after labelling the free amine group with fluorescamine. The second substrate selected was *N*-Ac-(*S*)-Phe-Gly-COOH (**1-66**). This compound was expected to bind PAM better than the tripeptide because it has Phe at its penultimate position from the *C*-terminus. Compound **1-66** was synthesised through a coupling reaction between *N*-Ac-(*S*)-Phe-COOH (**4-1**) and glycine methyl ester hydrochloride, followed by ester deprotection, as described in the literature (**Scheme 4.2A**).^[133] The corresponding amidated product **4-3** was also made to facilitate the development of the detection method. As shown in **Scheme 4.2B**, it was synthesised through an esterification, followed by adding ammonia.



Scheme 4.2 Synthesis of (A) *N*-Ac-(*S*)-Phe-Gly-COOH (**1-66**) and (B) *N*-Ac-(*S*)-Phe-NH₂ (**4-3**).

PAM assays in this Chapter were performed under the same conditions as described in Chapter 2 except that no base was used after the sample incubation. Both compound **1-66** and the tripeptide substrate were used with the same concentration so that the data can be compared directly. Under these circumstances, the hydroxylated intermediate produced by PHM catalysis but not yet processed by PAL should be detectable. The substrates, hydroxylated intermediates and amidated products are shown in **Scheme 4.3**.



Scheme 4.3 PAM processing of **(A)** (R)-Tyr-(S)-Val-Gly-COOH and **(B)** N-Ac-(S)-Phe-Gly-COOH (1-66).

After being incubated and filtered, assay mixtures were injected on to the HPLC-MS system. The substrates, intermediates and products were successfully separated by HPLC and quantified by the mass detector (ESI). The quantification was conducted through Multiple Reaction Monitoring (MRM) mass spectrometry (**Figure 4.2** and **Figure 4.3**) comparing peak areas of the three components. PHM activity is reflected by the sum of hydroxylated intermediate and amidated product while PAL activity plus chemical hydrolysis of hydroxylated intermediate are reflected by only the amount of amidated product.

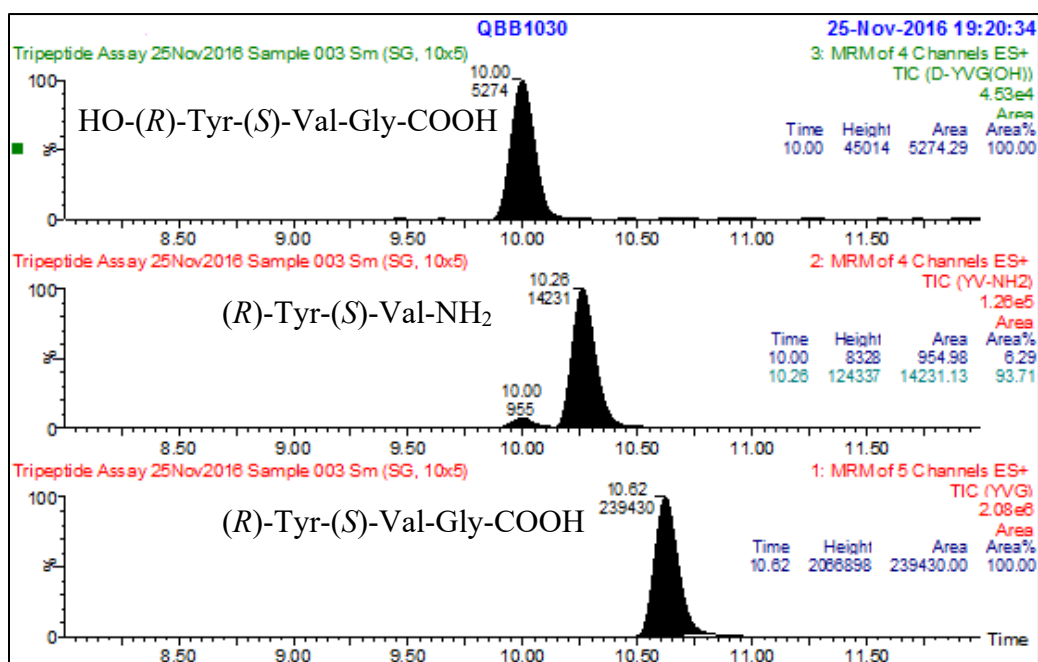


Figure 4.2 Representative HPLC-MS analysis of HO-(*R*)-Tyr-(*S*)-Val-Gly-COOH, (*R*)-Tyr-(*S*)-Val-NH₂ and (*R*)-Tyr-(*S*)-Val-Gly-COOH.

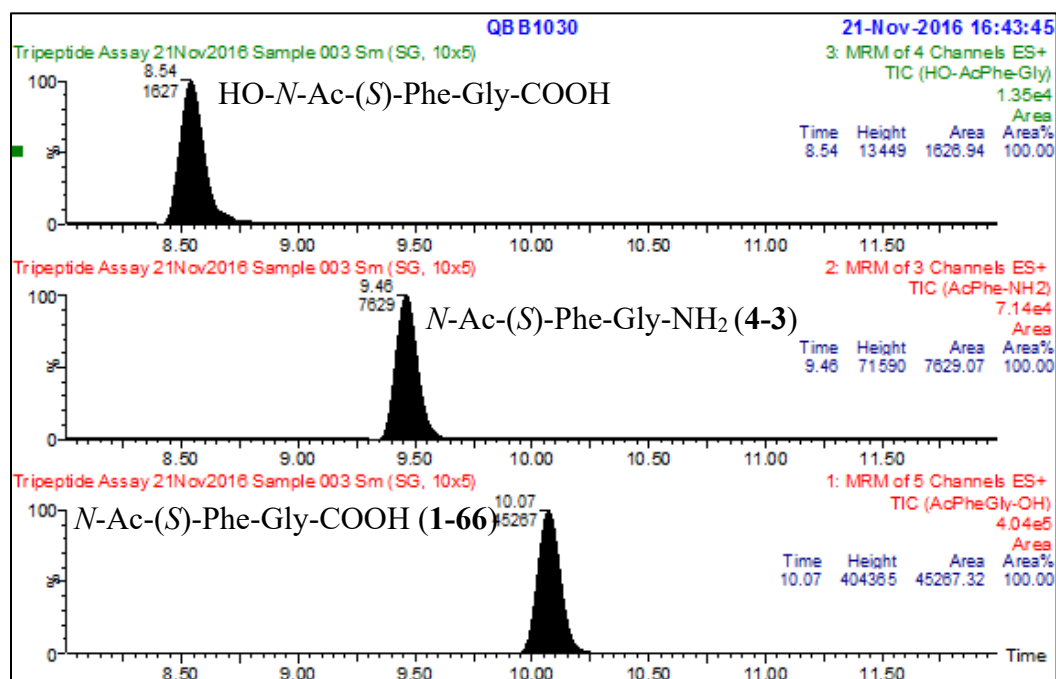


Figure 4.3 Representative HPLC-MS analysis of HO-*N*-Ac-(*S*)-Phe-Gly-COOH, *N*-Ac-(*S*)-Phe-NH₂ (4-3) and *N*-Ac-(*S*)-Phe-Gly-COOH (1-66).

The relative amounts of substrates, intermediates, and products in the samples with (*R*)-Tyr-(*S*)-Val-Gly-COOH and *N*-Ac-(*S*)-Phe-Gly-COOH (**1-66**) are illustrated in **Figure 4.4**. The substrate and hydroxylated intermediate turnovers were calculated and are shown in **Table 4.1**. Under identical assay conditions, the substrate turnover of **1-66** was 10% higher than that of (*R*)-Tyr-(*S*)-Val-Gly-COOH, reflecting that PHM activity for compound **1-66** was higher than for the tripeptide. This is likely due to the Phe at the penultimate position from the *C*-terminus which increases the binding affinity with PAM as described in Chapter 2. Additionally, the free amino group at the *N*-terminus of (*R*)-Tyr-(*S*)-Val-Gly-COOH would be protonated under the assay conditions, which likely negatively impacts the binding affinity;^[120] in contrast, *N*-Ac-(*S*)-Phe-Gly-COOH (**1-66**) is *N*-acetylated so is neutral/uncharged. Hydroxylated intermediate turnover in the case of compound **1-66** was 9% higher than that of the tripeptide. The HPLC-MS detection method is rapid and efficient.

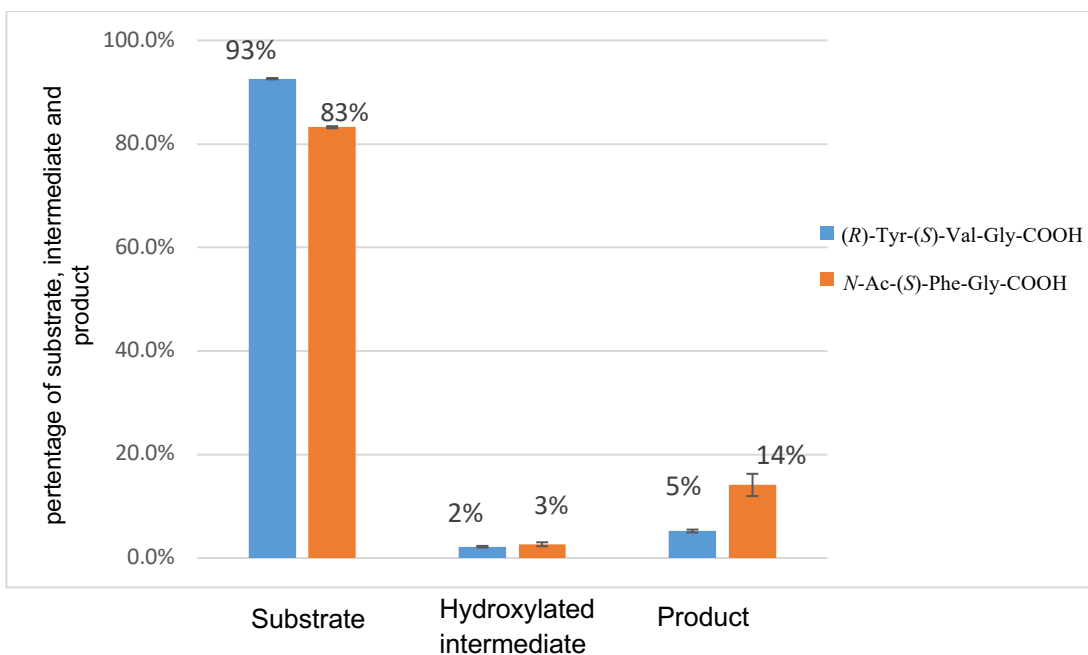


Figure 4.4 Ratios of substrates, intermediates, and products in assays using (*R*)-Tyr-(*S*)-Val-Gly-COOH and *N*-Ac-(*S*)-Phe-Gly-COOH (**1-66**) with PAM (both assays were duplicated).

Table 4.1 Substrate and hydroxylated intermediate turnover in assays using (*R*)-Tyr-(*S*)-Val-Gly-COOH and *N*-Ac-(*S*)-Phe-Gly-COOH (**1-66**).

Substrate	Substrate Turnover (%)	Hydroxylated Intermediate Turnover (%)
(<i>R</i>)-Tyr-(<i>S</i>)-Val-Gly-COOH	7	5
<i>N</i> -Ac-(<i>S</i>)-Phe-Gly-COOH	17	14

Having established a method for assessing intermediate turnover, it was now feasible to further investigate the hydrolysis of hydroxylated intermediates during the PAM reaction. As discussed in **Section 4.1**, the hydrolysis occurs due to PAL catalysis and chemical instability. However, the proportion of these two processes was unknown. Chemical instability of hydroxyglycine derivatives increases with increasing pH (from pH 5),^[196] and a kinetic study by Mounier *et al.* reported chemical hydrolysis of hydroxyglycine derivatives increases approximately 2 fold from pH 5.0 to 6.5.^[126] Considering this, the effect of pH on the PAM assay was investigated. The PAM assay was conducted across the effective pH range (5.5 - 6.7) of MES buffer.^[198] It was expected that, if chemical hydrolysis dominates the conversion of hydroxylated intermediates, the amount of amidated product would increase with increasing pH.

The pH-dependent assays using (*R*)-Tyr-(*S*)-Val-Gly-COOH and *N*-Ac-(*S*)-Phe-Gly-COOH (**1-66**) were performed under the same conditions as described above except the pH was varied. Relative amounts of substrates, intermediates, and products with (*R*)-Tyr-(*S*)-Val-Gly-COOH and *N*-Ac-(*S*)-Phe-Gly-COOH (**1-66**) are illustrated in **Figure 4.5** and **Figure 4.6**, respectively. **Figure 4.5** shows the relative amounts of each component in the assays with (*R*)-Tyr-(*S*)-Val-Gly-COOH are similar from pH 5.5 to 6.7. This indicates that, for (*R*)-Tyr-(*S*)-Val-Gly-COOH, PHM activity is constant across this pH range. The similar amounts of product and intermediate across the pH range suggest that chemical hydrolysis is at least not solely responsible for the conversion of hydroxylated intermediate. Otherwise, the amount of intermediate at pH 5.5 would be expected to be around double the amount at pH 6.7 due to the pH dependency of chemical hydrolysis.^[126] Based on this, either PAL activity is mostly responsible for conversion of the hydroxylated intermediate, or a decrease of PAL

activity with increasing pH offsets the expected increase in chemical hydrolysis. Based on the kinetic study by Mounier *et al.*^[126] that half-lives of hydroxyglycine derivatives are typically several days, it is more likely but not proven that PAL activity is mostly responsible for hydrolysis of the intermediate.

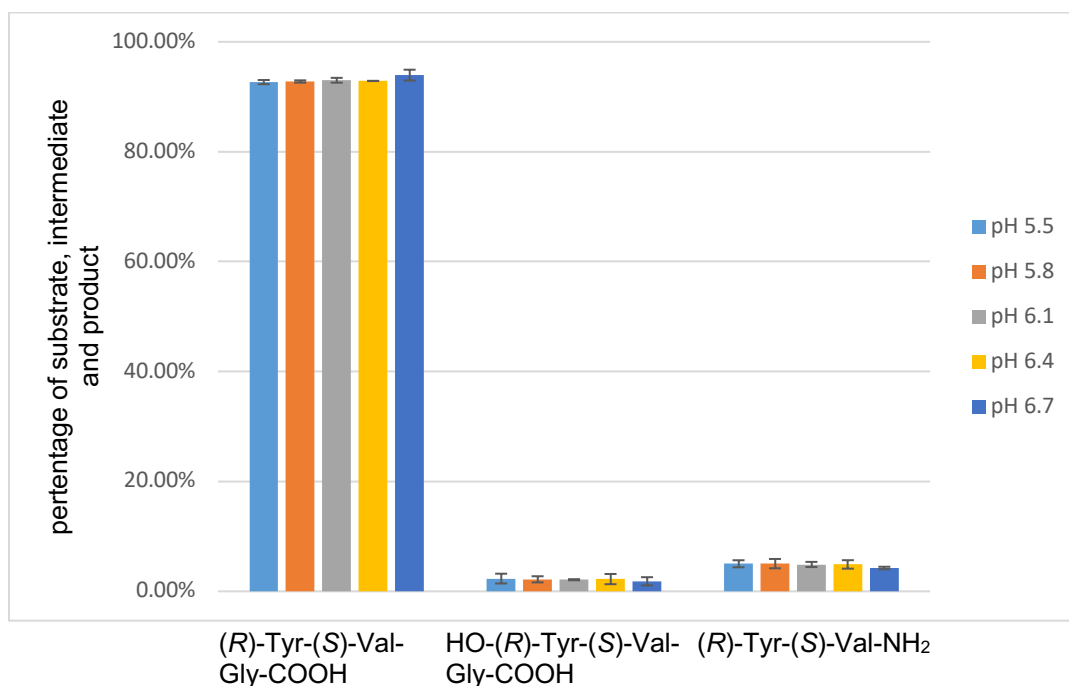


Figure 4.5 Ratios of substrates, intermediates, and products in pH-dependent assays using (R)-Tyr-(S)-Val-Gly-COOH with PAM.

As shown in **Figure 4.6** and **Table 4.2**, *N*-Ac-(*S*)-Phe-Gly-COOH (**1-66**) turnover decreased with increasing pH, showing a decreasing PHM activity. So after the first step of the PAM reaction, more hydroxylated intermediate is produced at lower pH. But the observed relative amounts of hydroxylated intermediate were constant and the observed relative amounts of amidated product decreased with increasing pH,

demonstrating that hydrolysis of intermediate (PAL activity plus chemical hydrolysis) decreases with increasing pH. As discussed above, chemical hydrolysis would be expected to increase with increasing pH from pH 5, which again means that PAL activity is likely to be much greater than chemical hydrolysis.

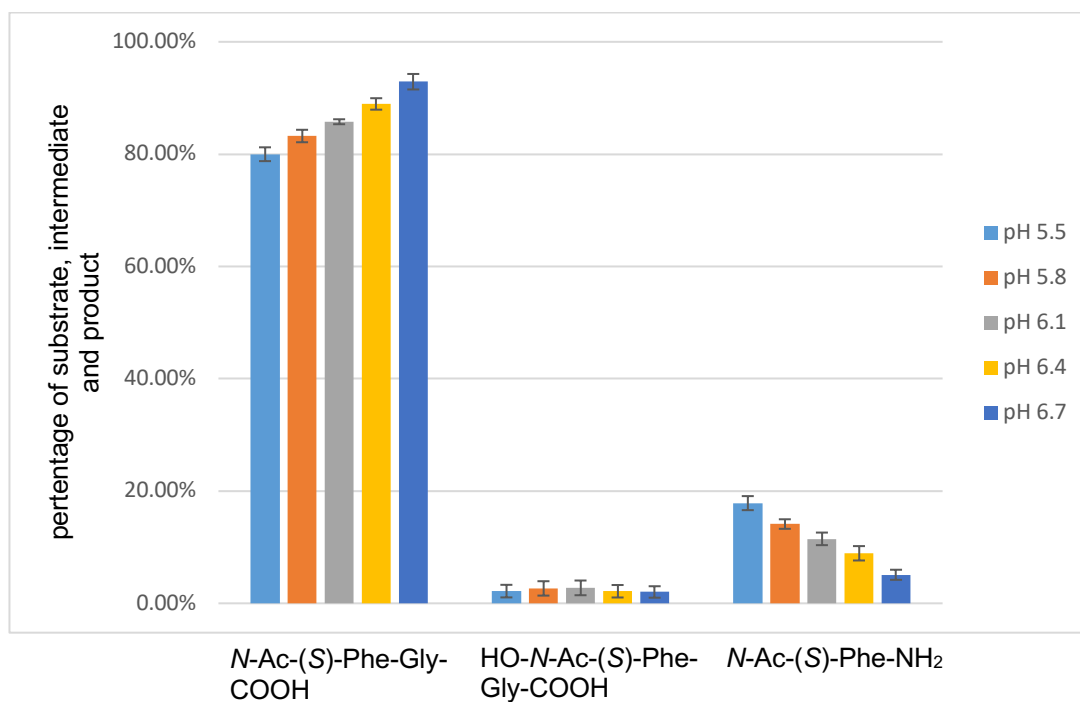


Figure 4.6 Ratios of substrates, intermediates, and products in pH-dependent assays using *N*-Ac-(*S*)-Phe-Gly-COOH (**1-66**) with PAM.

Table 4.2 Substrate and hydroxylated intermediate turnover in pH-dependent assays using *N*-Ac-(*S*)-Phe-Gly-COOH with PAM.

pH	Substrate Turnover (%)	Hydroxylated Intermediate Turnover (%)
5.5	20	18
5.8	17	14
6.1	14	11
6.4	11	9
6.7	7	5

4.3 Conclusion

In the present study, an efficient and rapid HPLC-MS method was developed, which enables the detection and quantification of substrate, hydroxylated intermediate and product in PAM catalysis and hence investigation of both substrate turnover and hydroxylated intermediate turnover simultaneously. With this new method, the proportion of PAL catalysis and chemical hydrolysis of hydroxylated intermediates were investigated through pH-dependent assays. It was found that no increase of amidated product was observed with increasing pH, showing that PAL activity is likely to be mostly responsible for the hydrolysis of hydroxylated intermediate while the proportion of chemical hydrolysis is expected to be quite low. Nevertheless, to assess this more accurately, PAL inhibition assays were considered.

Chapter Five

Structure-Activity Relationship Study for Peptidyl- α -Hydroxyglycine α -Amidating Lyase Inhibition

5.1 Introduction

The work described in the previous Chapter comprised a bifunctional PAM assay using HPLC-MS which enables simultaneous investigation of PHM activity and PAL activity. With this newly established assay, it is feasible to investigate the inhibition of both PHM and PAL activities at the same time with PAM inhibitors. Considerable effort has been made to develop PAM inhibitors with potential to treat diseases associated with amidated peptide production imbalances. To date, many studies have focused on PHM inhibition,^[16, 102, 121, 124-125, 127-128, 131, 133-139, 142-144] but only a few PAL inhibitors have been reported.^[119, 126-127] With two components, PHM and PAL, there are several possible modes of inhibition for a PAM inhibitor: (1) only PHM inhibition; (2) only PAL inhibition; or (3) inhibition of PAL and PHM. To find out which mode of inhibition is applicable for a range of candidate molecules, PAM inhibitory potency is assessed in this Chapter. Specifically, a known PAL inhibitor **1-143** was investigated alongside a number of structural analogues, as shown in **Figure 5.1**, to build a structure activity relationship revealing the modes of inhibition and which structural elements are responsible for PAL inhibition.

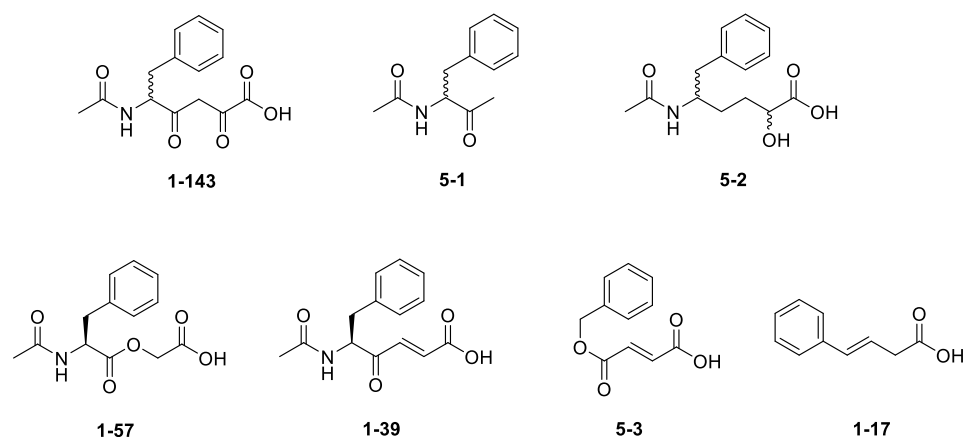
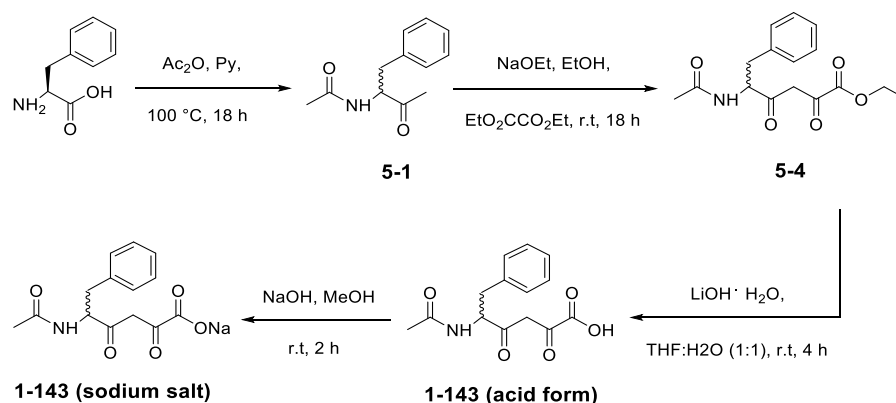


Figure 5.1 Compounds for structure-activity relationship study in PAM inhibition.

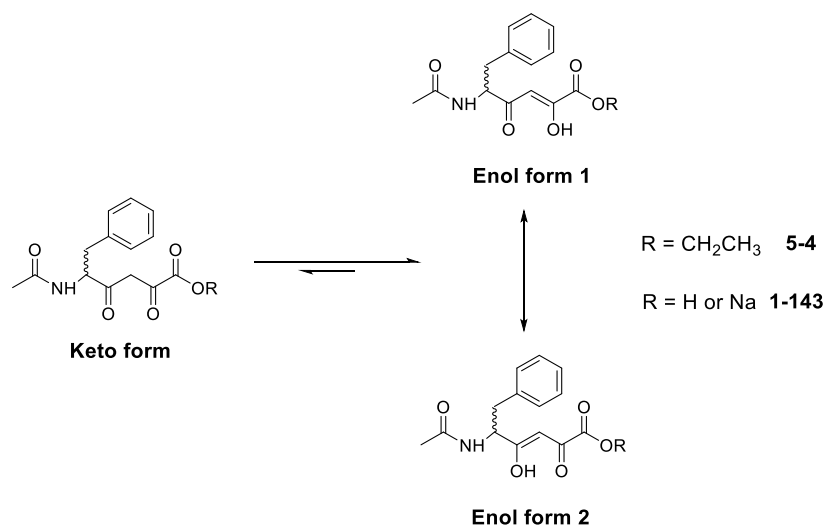
5.2 Synthesis of Candidate Molecules for PAM Inhibition Assay

N-Ac-Phe-pyruvate (**1-143**) was prepared on the basis of the protocol described by Mounier *et al.*^[126] As shown in **Scheme 5.1**, (*S*)-Phe-COOH reacted with acetic anhydride through a Dakin-West reaction using pyridine as the base at elevated temperature delivering a racemic ketone mixture **5-1** upon liberation of CO₂.^[199] The proposed mechanism^[200-201] is that acylation of (*S*)-Phe-COOH on the carboxylic acid group as well as the amine forms an anhydride, which then cyclises to give an oxazolone intermediate. Deprotonation of the oxazolone by the base leads to a resonance-stabilised 1,3-oxazol-5-olate. Subsequent acetylation followed by ring opening gives rise to a racemic anhydride. After transacylation decarboxylation finally furnishes the product **5-1**. Its structure was confirmed by ¹H NMR spectroscopy which showed two singlets at δ 1.98 and δ 2.15 corresponding to the methyl groups. ESI-MS showed an [M+H]⁺ ion at *m/z* 206.2. The resulting product **5-1** then reacted with diethyl oxalate through condensation in sodium ethoxide solution as the base at room temperature overnight.^[126] The crude product was treated with decolorizing carbon to

remove a yellowish impurity, and then further purified by silica-gel chromatography to yield compound **5-4** as a colourless oil. The structure of compound **5-4** was confirmed by ^1H NMR spectroscopy which showed a triplet and a quartet at δ 1.37 and δ 4.35 with coupling constants of 7.1 Hz. These two peaks were attributed to the ester group in compound **5-4**. A singlet peak at δ 6.40 corresponds to an olefinic proton, with an integration for one proton, indicating that compound **5-4** in this solvent CDCl_3 is mainly the enol form of the keto-enol tautomerism, as shown in **Scheme 5.2**. It is worth noting that Mounier *et al.* reported the synthesis of compound **5-4** and their ^1H NMR spectrum in CDCl_3 showed peaks related to every proton in compound **5-4** except the olefinic proton for the enol form (or the methylene protons for the keto form). The structure of compound **5-4** was also confirmed by ESI-MS which showed an $[\text{M}+\text{H}]^+$ ion at m/z 306.2. Hydrolysis of the ester **5-4** using lithium hydroxide in THF mixed with water gave the acid form of compound **1-143**,^[202] which was finally converted to the sodium salt using sodium hydroxide. The ^1H NMR spectrum of the final product **1-143** (sodium form) in D_2O showed a singlet peak at δ 1.82, corresponding to the methyl group. Two doublets of doublets at δ 2.79 and δ 3.21 with coupling constants of 14.0 Hz correspond to the benzylic methylene. The methine resonance of the phenylalanine moiety is expected to be masked by the HOD peak at δ 4.79. The fact that the two protons of the benzylic methylene both show doublets of doublets instead of simply doublets suggests they are both affected by a proton on an adjacent carbon. The phenyl resonances centre around δ 7.36. The methylene resonance of the pyruvate moiety was not seen, which is expected to be due to deuterium exchange through keto-enol equilibration. ESI-MS of compound **1-143** showed an $[\text{M}-\text{H}]^-$ ion at m/z 276.4. Both the ^1H NMR and MS spectra are consistent with data reported by Mounier *et al.*^[126]



Scheme 5.1 Synthesis of *N*-Ac-Phe-Pyruvate (**1-143**).

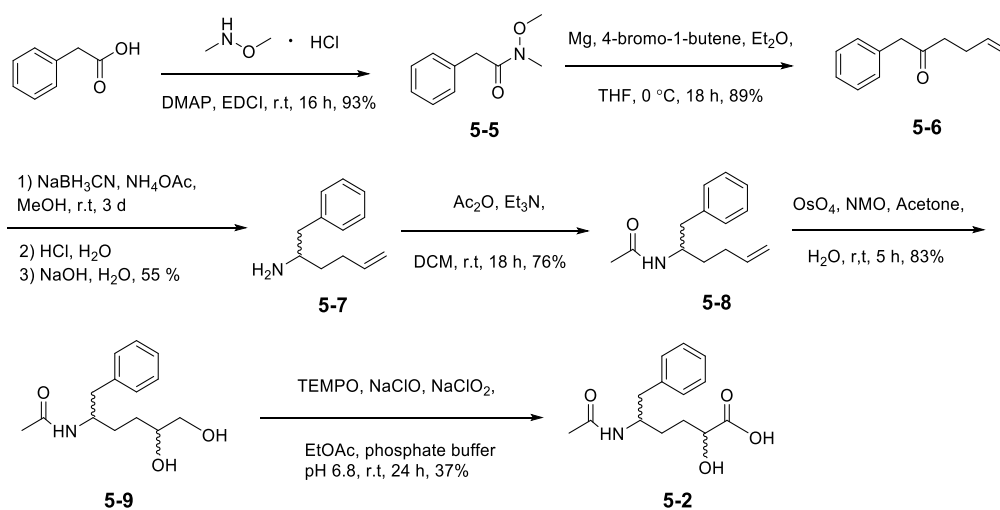


Scheme 5.2 Keto-enol tautomerism.

The α -hydroxy acid **5-2** was previously unreported. Its synthesis was accomplished in six steps from phenylacetic acid as shown in **Scheme 5.3**. The first step involved activation of phenylacetic acid with EDCI and cross-coupling with *N,O*-dimethylhydroxylamine to give the amide **5-5**.^[203] ESI-MS showed an $[M+H]^+$ ion at m/z 180.1. Then compound **5-5** underwent a Grignard reaction delivering the ketone

5-6,^[204] wherein the Grignard reagent formed *via* the reaction of 4-bromo-1-butene with magnesium metal, functioned as a nucleophile, substituting at the electrophilic carbon of the carbonyl group of compound **5-5**. The product structure was confirmed by ¹H NMR spectroscopy which showed a triplet peak at δ 2.55, corresponding to a methylene in the butenyl group of compound **5-6**. EI-MS showed an M⁺ ion at *m/z* 174.1. The ketone **5-6** then underwent reductive amination to deliver the primary amine **5-7**.^[205] In the reaction, ammonium acetate first reacts with compound **5-6** to form an imine losing a molecule of H₂O. Under the acidic conditions, the imine is protonated as the iminium ion, which is reduced to give the amine **5-7** by the reducing agent, NaBH₃CN. The singlet at δ 3.69 in the ¹H NMR spectrum of compound **5-6** in CDCl₃, corresponding to the benzylic methylene, is completely missing from the ¹H NMR spectrum of compound **5-7** in CDCl₃. Instead, two doublets of doublets appear at δ 2.78 and δ 2.91, and a broad singlet appears at δ 3.60, corresponding to the benzylic methylene and amino group, indicating that the amine **5-7** is obtained. The product structure was further confirmed by ESI-MS which showed an [M+H]⁺ ion at *m/z* 176.2. Since no stereoselective reagents were used, the resulting compound **5-7** is expected to be a racemic mixture. After acetylation of the amine **5-7** to form the amide **5-8**, dihydroxylation was performed using osmium tetroxide as a catalyst and a stoichiometric amount of NMO as oxidant to convert the amide **5-8** to the 1,2-diol **5-9**.^[206] Peaks corresponding to olefinic protons in the ¹H NMR spectrum of compound **5-8** in CDCl₃ are completely missing from the ¹H NMR spectrum of the diol **5-9** in CDCl₃, suggesting the olefin group in compound **5-8** was oxidised. Many peaks in the spectrum are duplicated, suggesting the compound is a mixture of diastereomers as compound **5-9** has two chiral centres. Two singlets at δ 1.91 and δ 1.92 are attributed to the *N*-acetyl methyl group, the equal height of which indicated the ratio of

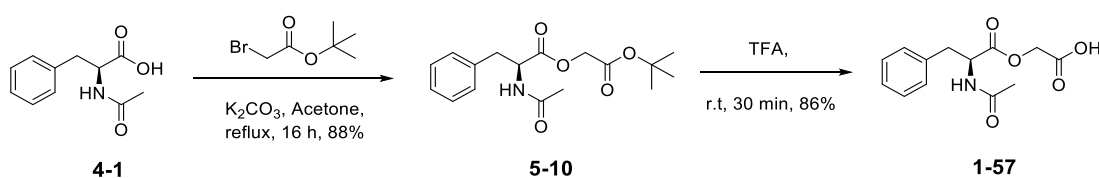
diastereomers is 1:1. This can be explained by the reaction mechanism that after the cycloaddition of osmium tetroxide to the olefinic bond in compound **5-8**, water attacks the epoxy intermediate from both sides with equal chance to give the mixture of diastereomers in the ratio 1:1. ESI-MS showed an $[M+H]^+$ ion at m/z 252.2. The terminal alcohol of the diol **5-9** was later oxidised, catalysed by TEMPO, to achieve the target product **5-2**.^[207] The ^1H NMR spectrum of the final product in D_2O shows resonances of α -carboxy and α -acetamido methine groups, at δ 4.21 and δ 4.03, respectively. Four doublets of doublets with the same coupling of 13.4 Hz are all attributed to benzylic methylenes, again suggesting the product is a mixture of diastereomers. The product structure was also confirmed by ^{13}C NMR spectroscopy and ESI-MS which showed an $[M+\text{Na}]^+$ ion at m/z 344.2.



Scheme 5.3 Synthesis of the α -hydroxy acid **5-2**.

The glycolate **1-57** was prepared according to the protocol described by Easton *et al.*^[133] As shown in **Scheme 5.4**, an alkylation of *N*-Ac-(*S*)-Phe-COOH (**4-1**) was performed to give compound **5-10**, involving dissolving compound **4-1** and *tert*-butyl

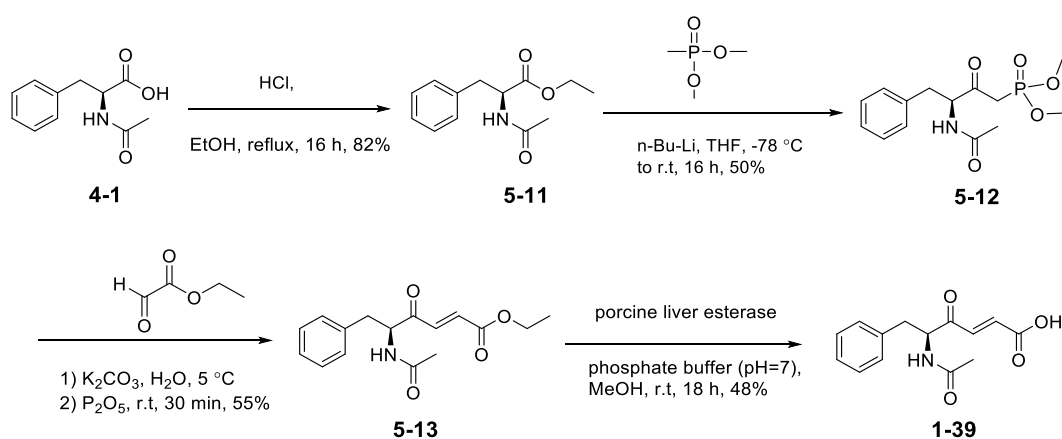
bromoacetate in acetone with excess K_2CO_3 added as an insoluble component. The reaction was run at reflux. The product structure was confirmed by ESI-MS which showed an $[M+Na]^+$ ion at m/z 344.2. The final product **1-57** was obtained through removal of the *tert*-butyl group using strong acid at room temperature. The product structure was confirmed by 1H NMR spectroscopy, which showed a singlet at δ 1.99, corresponding to the *N*-acetyl methyl group, and the ESI-MS which showed an $[M-H]^-$ ion at m/z 264.1.



Scheme 5.4 Synthesis of the glycolate **1-57**.

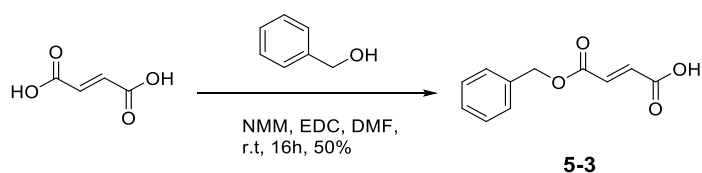
The α,β -unsaturated γ -keto acid **1-39** was prepared according to the protocol described by Mounier *et al.*^[140] As shown in **Scheme 5.5**, *N*-Ac-(*S*)-Phe-COOH (**4-1**) was esterified using acid and EtOH at reflux to give the ester **5-11**. The resulting ester then reacted with *n*-BuLi and dimethyl methylphosphonate (DMMP, $CH_3PO(OCH_3)_2$) to give a ketophosphonate.^[208-209] This reaction involves the deprotonation of DMMP using *n*-BuLi at -78 °C to give $LiCH_2PO(OCH_3)_2$, which then reacts with the ester **5-11** through a condensation to give the product **5-12**. This product structure was confirmed by 1H NMR spectroscopy which showed two multiplets at δ 3.23 and δ 3.75 with an integration value of two protons for each. These two multiplets are attributed to the overlapping of two methylene groups, *i.e.* phosphate methylene and benzylic methylene groups, suggesting that the phosphate methylene has two magnetically nonequivalent protons. ESI-MS showed an $[M+Na]^+$ ion at m/z 336.1. A Horner–

Wadsworth–Emmons (HWE) reaction between ethyl glyoxalate and compound **5-12**, using K_2CO_3 as the base at $5\text{ }^\circ\text{C}$, was then performed to give the alkene **5-13**.^[140] This reaction involves deprotonation of the phosphonate **5-12** to give a phosphonate carbanion. Nucleophilic addition of the carbanion onto ethyl glyoxalate, followed by elimination, produces the *E*-alkene **5-13**. This reaction produces predominantly *E*-alkenes due to the fact that bulky aldehydes and bulky electron-withdrawing groups enhance *E*-alkene selectivity of HWE reactions.^[210] The structure of the ester **5-13** was confirmed by ^1H NMR spectroscopy which showed two doublets at δ 6.77 and δ 7.13 with coupling constants of 15.8 Hz, corresponding to *trans*-olefinic protons. ESI-MS showed an $[\text{M}+\text{Na}]^+$ ion at m/z 312.1. Following the reported procedure^[140] which conveniently converts the ester **5-13** to the carboxylic acid **1-39** using pig liver esterase in phosphate buffer that maintains the pH around 7, crude compound **1-39** was obtained then purified by preparative HPLC to afford the final the product as a colourless powder. ESI-MS showed an $[\text{M}-\text{H}]^-$ ion at m/z 260.2. Both the ^1H NMR and MS spectra are consistent with data reported by Mounier *et al.*^[140]



Scheme 5.5 Synthesis of the α,β -unsaturated γ -keto acid **1-39**.

Synthesis of the fumaric acid **5-3** was based on the method by Ekici *et al.*^[211] As shown in **Scheme 5.6**, ester coupling was performed between fumaric acid and benzyl alcohol using NMM as a coupling reagent and EDC as an activating reagent for ester formation in DMF solvent. The product structure was confirmed by ¹H NMR spectroscopy which showed two doublets at δ 6.88 and δ 6.98 with coupling constants of 15.8 Hz, corresponding to the *trans*-olefinic protons. ESI-MS showed an $[M+Na]^+$ ion at m/z 229.1.



Scheme 5.6 Synthesis of the fumaric acid **5-3**.

5.3 Measurements of PAM Inhibition Potencies of Molecules

N-Ac-Phe-pyruvate (**1-143**) was chosen as the first candidate to test for PAM inhibition potency because it has the most potent PAL inhibition ever reported and has relatively weak PHM inhibition.^[126] Therefore, evaluating the pyruvate **1-143** was to check whether the HPLC-MS system works for investigation of PHM and PAL inhibition potencies of PAM inhibitors. The evaluation was performed through a PAM inhibition assay using the substrate (*R*)-Tyr-(*S*)-Val-Gly-COOH with the addition of varying concentrations of the compound **1-143**. The assay conditions were the same as described in **Section 4.2**. The concentrations of compound **1-143** used initially were from 0.4 to 0 μ M at 2X serial dilution and 4 μ M, based on the report by Mounier *et al.*^[126] of a K_i value of compound **1-143** for competitive PAL inhibition of 0.24 μ M.

The ratios of substrate, intermediate and product of the PAM catalysis are shown in **Table 5.1**. The Table shows increasing percentage of hydroxylated intermediate and decreasing percentage of amidated products with increasing concentrations of compound **1-143**, consistent with compound **1-143** having PAL inhibition. The constant percentages of substrate show that compound **1-143** has no PHM inhibition in this concentration range.

Table 5.1 Ratios of substrate, intermediate, and product in PAM assays using (*R*)-Tyr- (*S*)-Val-Gly-COOH with concentrations of *N*-Ac-Phe-pyruvate (**1-143**) ranging from 0-4 μ M.

Concentration of <i>N</i> -Ac-Phe-pyruvate (1-143) (μ M)	Substrate (%)	Intermediate (%)	Product (%)
0	91.5	5.0	3.5
0.012	91.6	5.6	2.9
0.025	91.1	6.2	2.7
0.05	91.4	6.1	2.4
0.1	92.0	6.4	1.6
0.2	92.6	6.3	1.1
0.4	91.6	7.6	0.8
4	92.7	7.0	0.3

In this assay, the inhibitor-free sample is the control, and the hydroxylated intermediate turnover (percentage of amidated product) of the control, reflecting PAL activity, is therefore set as one hundred percent. The IC₅₀ value for PAL inhibition was then calculated as the concentration of compound **1-143** that reduced hydroxylated

intermediate turnover of the control by 50%. The activity-concentration curves were generated by plotting the hydroxylated intermediate turnover (percentage of control) and compound **1-143** concentration. The activity-concentration curves for duplicate PAL inhibition assays are shown in **Figure 5.2**. As a result, compound **1-143** was found to show good PAL inhibition with an IC_{50} value of $0.09 \pm 0.02 \mu\text{M}$, in the same range as the K_i value of $0.24 \mu\text{M}$ reported by Mounier *et al.*^[126]

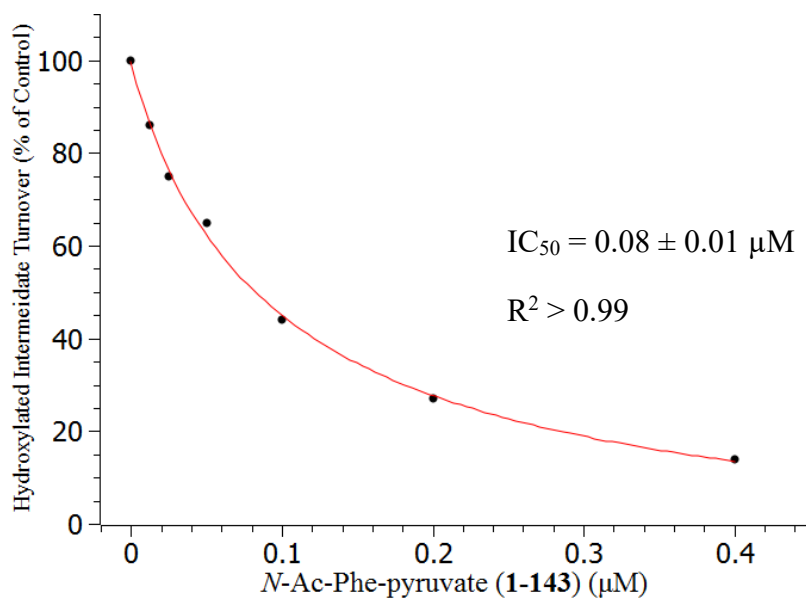
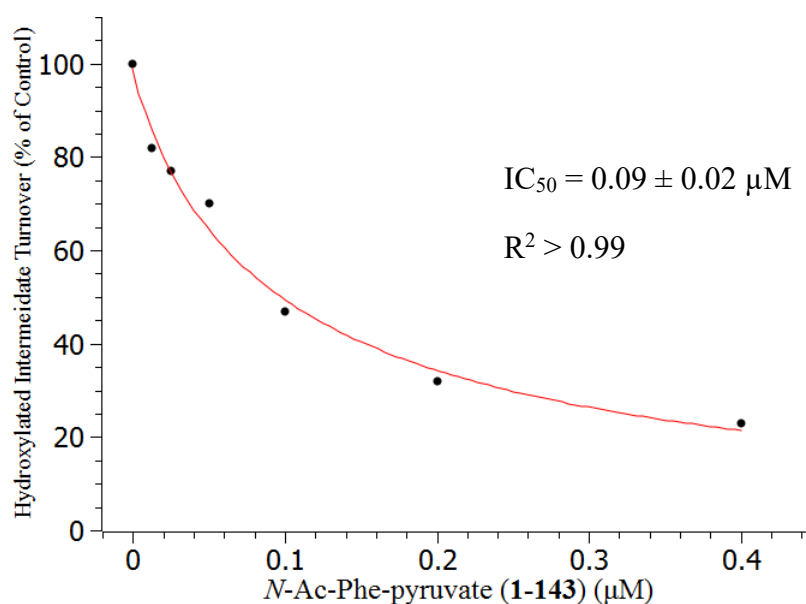


Figure 5.2 Determination of IC_{50} values of *N*-Ac-(*S*)-Phe-Gly-COOH (**1-143**) for PAL inhibition in duplicate assays.

A PAM inhibition assay was then performed using concentrations of compound **1-143** from 100 to 0 μ M at 2X serial dilution for further investigation due to the fact that the K_i value of compound **1-143** toward PHM is known to be two orders of magnitude higher than that toward PAL.^[126] The data, shown in **Table 5.2**, demonstrate that the percentage of hydroxylated intermediate increases going from 0-6.25 μ M of compound **1-143** and then goes down with further increasing concentration of compound **1-143**. This indicates compound **1-143** shows mainly PAL inhibition at low concentration but also shows PHM inhibition with further increasing concentration. The percentage of amidated product keeps decreasing till to zero with increasing compound **1-143** due to PAL inhibition, confirming that PAL activity is indeed mostly responsible for the hydrolysis of the intermediate and little chemical hydrolysis occurs in this two-hour PAM assay.

Table 5.2 Ratios of substrate, intermediate, and product in assays using (*R*)-Tyr-(*S*)-Val-Gly-COOH with concentrations of *N*-Ac-Phe-pyruvate (**1-143**) ranging from 0-100 μ M.

Concentration of <i>N</i> -Ac-Phe-pyruvate (1-143) (μ M)	Substrate (%)	Intermediate (%)	Product (%)
0	92.2	4.7	3.1
6.25	93.5	6.3	0.2
12.5	95.2	4.6	0.2

25	96.9	3.0	0.1
50	97.4	2.5	0.1
100	98.3	1.7	0

Like the determination of IC₅₀ values for PAL inhibition, the substrate turnover (percentage of the sum of intermediate and product) of the control, reflecting PHM activity, was set as one hundred percent, and the IC₅₀ value for PHM was then calculated as the concentration of compound **1-143** that reduced substrate turnover of the control by 50%. The activity-concentration curves generated by plotting the substrate turnover (percentage of control) and compound **1-143** concentration for PHM inhibition are shown in **Figure 5.3**. As a result, compound **1-143** was found to have micromolar PHM inhibition with an IC₅₀ value of $14 \pm 3 \mu\text{M}$. The PHM and PAL inhibition results of compound **1-143** are consistent with the results by Mounier *et al.*,^[126] indicating that the bifunctional PAM assay using the HPLC-MS system is suitable for the evaluation of PAM inhibitory potency of molecules.

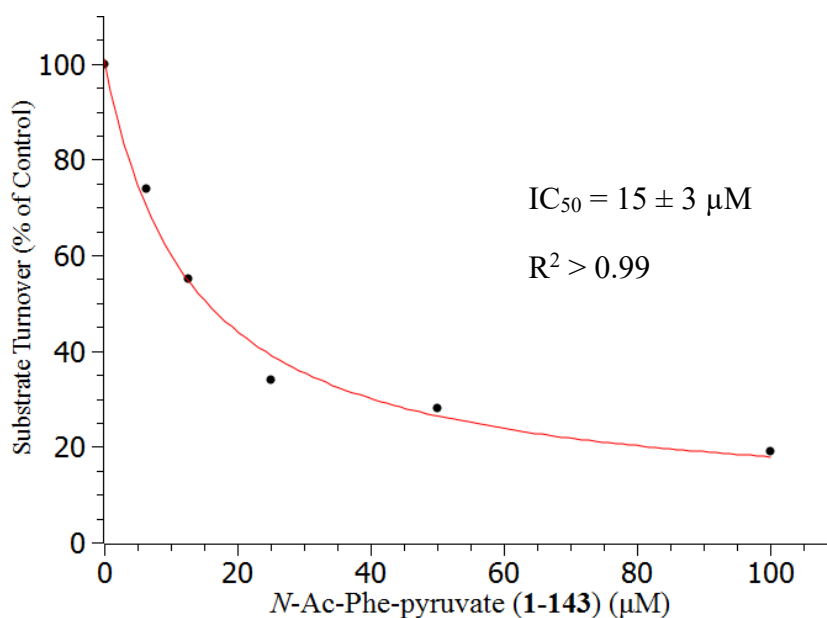
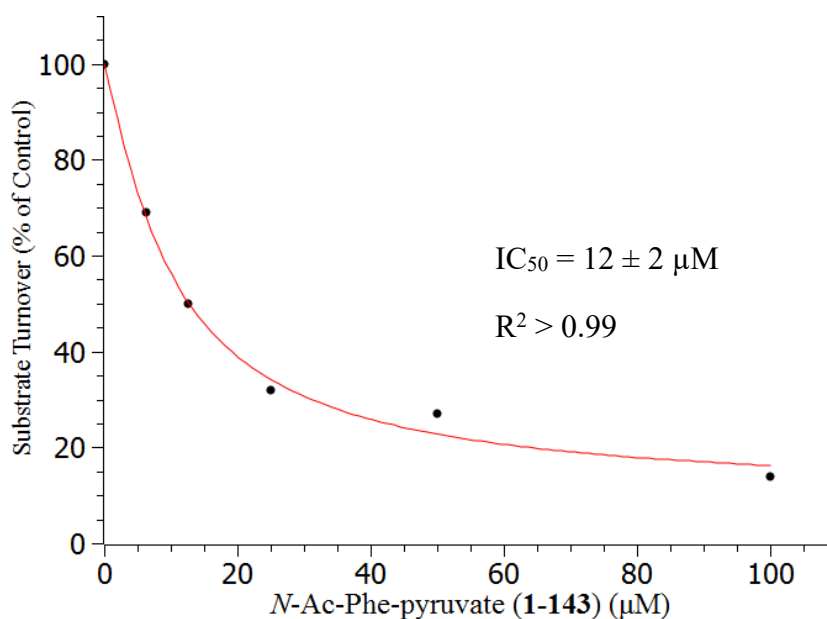


Figure 5.3 Determination of IC_{50} values of *N*-Ac-(*S*)-Phe-Gly-COOH (**1-143**) for PHM inhibition in duplicate assays.

After testing compound **1-143** and confirming that the HPLC-MS PAM assay is suitable for investigating PHM and PAL inhibitory potency simultaneously, the other inhibitor candidates in **Figure 5.1** were then evaluated using the assay conditions as described for compound **1-143**, except with different concentrations used for each molecule. PBA (**1-17**) was tested over the concentration range from 20 to 0 μM at 2X

serial dilution and 100 μM due to the fact that PBA (**1-17**) has reported PHM-inhibition-related K_i values of 0.096 μM (human) and 19 μM (porcine).^[128, 138] The data in **Table 5.3** illustrate the increasing percentage of substrate and the decreasing percentage of intermediate and product with increasing concentration of PBA (**1-17**), indicating that PBA has PHM inhibition. At 20 μM PBA, the percentage of the intermediate is around 28% of the control while the percentage of the amidated product is around 57% of the control. This is expected when PHM activity is inhibited leading to less of the hydroxylated intermediate. This observation is consistent with the study by Eipper *et al.*^[125] that PBA has only PHM inhibition and no PAL inhibition. Its IC_{50} value for PHM inhibition was determined as $14 \pm 5 \mu\text{M}$ through analysis of the activity-concentration curve.

Table 5.3 Ratios of substrate, intermediate, and product in assays using (*R*)-Tyr-(*S*)-Val-Gly-COOH with concentrations of PBA **1-17** ranging from 100-0 μM .

Concentration of PBA 1-17 (μM)	Substrate (%)	Intermediate (%)	Product (%)
0	94.7	2.5	2.8
0.05	95.3	2.0	2.7
0.5	95.7	1.6	2.7
1	95.8	2.0	2.2
5	96.1	1.9	2.0
10	97.0	1.1	1.9
20	97.7	0.7	1.6
100	99.2	0.2	0.6

Compounds **5-1** and **5-2** were tested at 400-0 μM at 10X serial dilution to quickly assess any PAL and PHM inhibition since no related information was available. No reduction of substrate or intermediate turnover with increasing concentrations was observed with compounds **5-1** and **5-2**, suggesting neither of these two compounds is a PHM or PAL inhibitor up to a concentration of 400 μM .

Since its IC_{50} value for inhibition of PAM enzyme extracted from H889 small cell lung carcinoma cells is 6 μM ,^[133] the initial concentration of compound **1-57** used for this PAM inhibition assay was 100-0 μM at 2X serial dilution. **Table 5.4** shows the ratios among substrate, intermediate and product are constant with compound **1-57** concentrations from 0 to 20 μM . 100 μM *N*-Ac-Phe-glycolate (**1-57**) only reduced the tripeptide substrate turnover by 21%, suggesting compound **1-57** has PHM inhibition but requires higher concentrations for IC_{50} calculation. Therefore, higher concentrations, 0-2000 μM , were used and the data are shown in **Table 5.5**.

Table 5.4 Ratios of substrate, intermediate, and product in assays using (*R*)-Tyr-(*S*)-Val-Gly-COOH with concentrations of *N*-Ac-Phe-glycolate (**1-57**) ranging from 0-100 μ M.

Concentration of <i>N</i> -Ac-Phe-glycolate (1-57) (μ M)	Substrate (%)	Intermediate (%)	Product (%)
0	94.7	2.4	2.9
0.05	94.0	2.6	3.4
0.5	94.1	2.6	3.3
1	93.8	2.7	3.5
5	94.3	2.3	3.4
10	94.2	2.5	3.3
20	95.0	2.1	2.9
100	95.8	1.5	2.7

The data in **Table 5.5** show the increasing percentage of substrate and the decreasing percentage of intermediate and product with increasing concentrations of compound **1-57**. Similar to the scenario with PBA **1-17**, the decrease of the intermediate is greater than that of the product, indicating that PHM inhibition by compound **1-57** is greater than its PAL inhibition. Under these circumstances, it is not practical to determine an IC_{50} value for PAL inhibition but that for PHM inhibition was determined to be $139 \pm 23 \mu$ M through analysis of the activity-concentration curve, and the PAL IC_{50} must be higher.

Table 5.5 Ratios of substrate, intermediate, and product in assays using (*R*)-Tyr-(*S*)-Val-Gly-COOH with concentrations of *N*-Ac-Phe-glycolate (**1-57**) ranging from 0-2000 μ M.

Concentration of <i>N</i> -Ac-Phe-glycolate (1-57) (μ M)	Substrate (%)	Intermediate (%)	Product (%)
0	94.2	2.1	3.7
100	96.9	1.0	2.1
250	97.5	0.6	1.9
500	98.4	0.3	1.3
1000	99.0	0.2	0.8
2000	99.4	0.1	0.5

For compound **1-39**, the concentration range used was 20-0 μ M at 2X serial dilution and 100 μ M since its IC_{50} value against frog PAM is 57 μ M.^[131] The data in **Table 5.6** show the increasing percentage of substrate and the decreasing percentage of intermediate and product with increasing concentrations of compound **1-39**. At lower concentrations of compound **1-39** the decrease in the percentage of amidated product is greater than that of substrate turnover, showing selective PAL inhibition. Though the corresponding IC_{50} value could not be determined due to the complicated dual-step assay, the IC_{50} value of compound **1-39** for PHM inhibition was determined through analysis of the activity-concentration curve to be $3 \pm 1 \mu$ M.

Table 5.6 Ratios of substrate, intermediate, and product in assays using (*R*)-Tyr-(*S*)-Val-Gly-COOH with concentrations of compound **1-39** ranging from 100-0 μM .

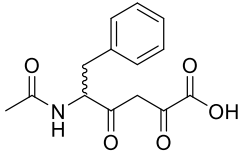
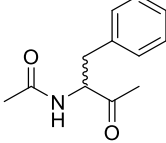
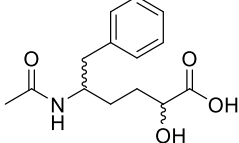
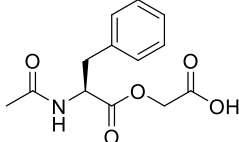
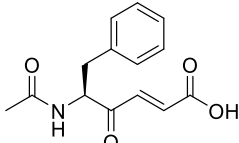
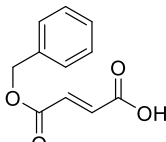
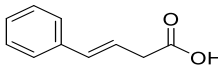
Concentration of compound 1-39 (μM)	Substrate (%)	Intermediate (%)	Product (%)
0	94.6	1.7	3.7
0.05	94.9	2.0	3.2
0.5	95.8	1.7	2.5
1	96.1	1.5	2.4
5	97.7	0.8	1.5
10	98.7	0.4	0.9
20	99.4	0.1	0.5
100	99.9	0	0.1

Although there is no study related to PAM inhibition for the fumaric acid **5-3**, 150-0 μM at 2X serial dilution was used based on analogy to compound **1-39** because they are structurally similar. The data in **Table 5.7** illustrate the increasing percentage of substrate and the decreasing percentage of intermediate and product with increasing concentrations of the fumaric acid **5-3**, indicating that it has PHM inhibition. The decrease of the intermediate is greater than that of the product, showing that PHM inhibition is greater than PAL inhibition. The IC_{50} value for PHM inhibition was determined as $139 \pm 23 \mu\text{M}$, and the IC_{50} value for PAL inhibition is greater.

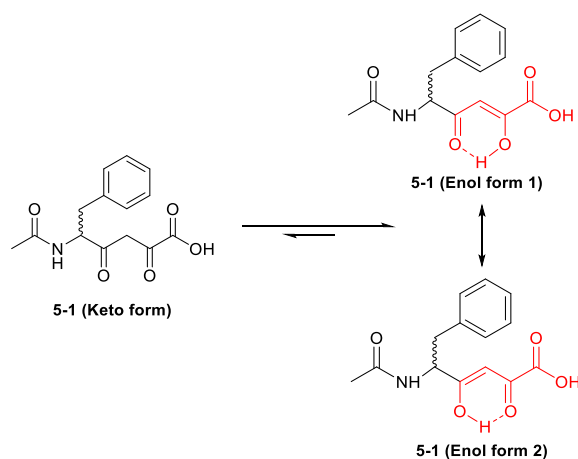
Table 5.7 Ratios of substrate, intermediate, and product in assays using (*R*)-Tyr-(*S*)-Val-Gly-COOH with concentrations of the fumaric acid **5-3** ranging from 150-0 μ M.

Concentration of the fumaric acid 5-3 (μM)	Substrate (%)	Intermediate (%)	Product (%)
0	92.4	4.8	2.8
1.9	92.4	4.6	3.0
19	94.7	2.9	2.4
38	96.7	1.6	1.7
75	98.6	0.7	0.7
150	100	0	0

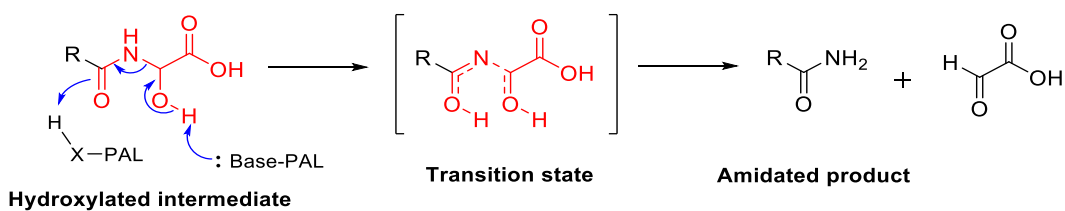
Table 5.8 Summary of the assessment of PHM and PAL inhibition with selected compounds.

Compound No.	Compound Structure	PHM Inhibition IC ₅₀	PAL Inhibition IC ₅₀
1-143		14 ± 3 μM	0.09 ± 0.02 μM
5-1		>> 400 μM	>> 400 μM
5-2		>> 400 μM	>> 400 μM
1-57		139 ± 23 μM	> 139 μM
1-39		3 ± 1 μM	< 3 μM
5-3		32 ± 1 μM	> 32 μM
1-17		14 ± 5 μM	—

The PHM and PAL inhibition potencies are summarised in **Table 5.8**. Compound **1-143** shows PAL inhibition at the nanomolar level and its pyruvate moiety must play an important role in this since compound **5-1** lacking the pyruvate moiety shows no PHM or PAL inhibition up to 400 μM . As discussed in **Section 5.2**, keto-enol tautomerism is likely for compound **1-143**. Compound **1-143** is expected to be mainly the enol forms based on the study by Burdett *et al.*^[212] that tautomeric equilibria for β -diketones favours the enol tautomers. Intramolecular hydrogen bonding between a hydroxyl group and a carbonyl group stabilizes the enol forms, as shown in **Scheme 5.7**. It is more likely that the enol forms of compound **1-143** instead of the keto form are responsible for PAL inhibition because the keto form of compound **1-143** is even less like α -hydroxyglycine PAM intermediates. Its enol forms have similar geometry (red parts in **Scheme 5.7**) to both the hydroxylated intermediate and the corresponding transition state in the PAL catalysed reaction as shown in **Scheme 5.8**.



Scheme 5.7 Keto-enol tautomerism of *N*-Ac-(*S*)-Phe-Gly-COOH (**1-143**) in solution.



Scheme 5.8 PAL catalysis pathway.

The glycolate **1-57** shows only PHM inhibition with an IC_{50} value of $139 \pm 23 \mu\text{M}$. No PAL inhibition is observed probably because compound **1-57** more closely resembles PHM substrates than PAL substrates. The α,β -unsaturated acids **1-39** and **5-3** both show PHM inhibition at the micromolar level. This is consistent with the study by May *et al.*^[131] of the K_i value for competitive PHM inhibition by compound **1-39** of $54 \mu\text{M}$. Their molecular docking studies illustrate that compound **1-39** docks and binds to the active site of PHM in a similar manner to the corresponding PAM substrate *N*-Ac-(*S*)-Phe-Gly-COOH.

5.4 pH-Dependent PAM Inhibition Assays with *N*-Ac-Phe-Pyruvate

Having confirmed that the diketone **1-143** is a PAL inhibitor and that the more active form is likely to be the enol rather than the ketone, this was further investigated by monitoring the effect of pH on PAL inhibition. The pH-dependent PAM inhibition competitive assay was conducted using (*R*)-Tyr-(*S*)-Val-Gly-COOH with various concentrations of compound **1-143** across the effective pH range (5.5 - 6.7) of MES buffer.^[198] The concentrations used were from 0.4 to 0 μM at 2X serial dilution. **Tables 5.9 – 5.12** show the ratios of substrate, intermediate, and product in PAM

inhibition assays at pH 5.5, 6.1, 6.4 and 6.7. The data for pH 5.8 have been shown above in **Table 5.1**.

Table 5.9 Ratios of substrate, intermediate, and product in PAM assays at pH 5.5, using (*R*)-Tyr-(*S*)-Val-Gly-COOH with concentrations of *N*-Ac-(*S*)-Phe-Gly-COOH (**1-143**) ranging from 0-0.4 μ M.

Concentration of <i>N</i>-Ac-(<i>S</i>)-Phe- Gly-COOH (1- 143) (μM)	Substrate (%)	Intermediate (%)	Product (%)
0	93.4	4.1	2.5
0.012	93.2	4.4	2.4
0.025	93.0	4.8	2.2
0.05	93.2	5.1	1.7
0.1	93.3	5.5	1.2
0.2	93.5	5.6	0.9
0.4	94.5	5.1	0.4

Table 5.10 Ratios of substrate, intermediate, and product in PAM assays at pH 6.1, using (*R*)-Tyr-(*S*)-Val-Gly-COOH with concentrations of *N*-Ac-(*S*)-Phe-Gly-COOH (1-143) ranging from 0-0.4 μ M.

Concentration of <i>N</i>-Ac-(<i>S</i>)-Phe-Gly-COOH (1-143) (μM)	Substrate (%)	Intermediate (%)	Product (%)
0	88.5	6.9	4.6
0.012	89.3	6.7	4.0
0.025	89.5	6.6	3.9
0.05	89.9	7.1	3.0
0.1	88.8	8.7	2.5
0.2	88.9	9.5	1.6
0.4	88.6	10.1	1.3

Table 5.11 Ratios of substrate, intermediate, and product in PAM assays at pH 6.4, using (*R*)-Tyr-(*S*)-Val-Gly-COOH with concentrations of *N*-Ac-(*S*)-Phe-Gly-COOH (1-143) ranging from 0-0.4 μ M.

Concentration of <i>N</i>-Ac-(<i>S</i>)-Phe-Gly-COOH (1-143) (μM)	Substrate (%)	Intermediate (%)	Product (%)
0	85.7	8.5	5.8
0.012	88.0	7.6	4.4
0.025	87.5	8.4	4.1
0.05	88.5	8.0	3.5
0.1	87.6	9.4	3.0
0.2	88.1	9.8	2.1
0.4	86.9	11.7	1.4

Table 5.12 Ratios of substrate, intermediate, and product in PAM assays at pH 6.7, using (*R*)-Tyr-(*S*)-Val-Gly-COOH with concentrations of *N*-Ac-(*S*)-Phe-Gly-COOH (**1-143**) ranging from 0-0.4 μ M.

Concentration of <i>N</i> -Ac-(<i>S</i>)-Phe-Gly-COOH (1-143) (μ M)	Substrate (%)	Intermediate (%)	Product (%)
0	88.6	6.0	5.4
0.012	87.3	8.1	4.6
0.025	87.5	8.0	4.5
0.05	86.4	9.6	4.0
0.1	86.9	9.6	3.5
0.2	87.2	10.2	2.6
0.4	87.7	10.7	1.6

Table 5.1 and **Tables 5.9 – 5.12** show that, in each data set, an increasing percentage of hydroxylated intermediate and a decreasing percentage of amidated product are seen with increasing concentrations of compound **1-143** from 0 to 0.4 μ M. The activity-concentration curves were generated, as described in **Section 5.3**, by plotting the hydroxylated intermediate turnover and compound **1-143** concentration. The corresponding IC₅₀ values for PAL inhibition at each pH were determined through analysis of the corresponding activity-concentration curves and are shown in **Figure 5.4**. It was impractical to prepare and analyse all the assay samples on the same day. Therefore, compound **1-143**-concentration-dependent PAM inhibition assays at different pH values were performed on different days. Since the enzyme activity decreases with the passage of time, it is not meaningful to compare the substrate and

intermediate turnovers at different pH values, but this does not affect the relative IC_{50} values.

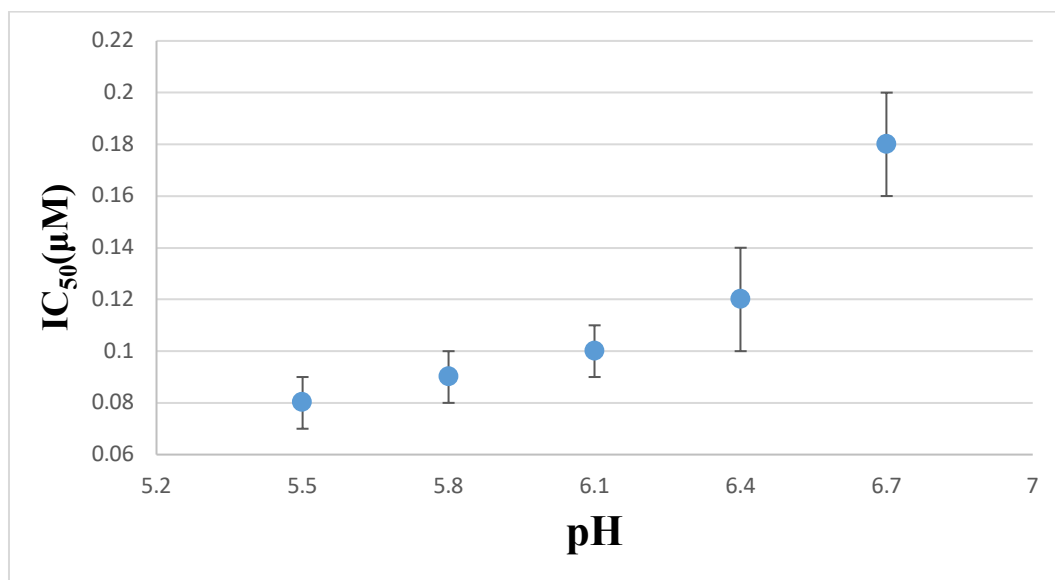


Figure 5.4 The IC_{50} values for PAL inhibition of *N*-Ac-Phe-pyruvate (**1-143**) against the medium PAM from DMS53 cells at the pH ranging from 5.5 to 6.7.

Figure 5.4 shows that the IC_{50} value increases by around two times on increasing the pH from 5.5 to 6.7, indicating that compound **1-143** shows decreasing PAL inhibition. This can be attributed to the increase in pH decreasing the amount of enol and increasing the amount of the corresponding enolate, A study by Bunting *et al.*^[213] showed that the acidities of the enols (pK_a) of β -diketones range from three to eight depending on the substituents. The corresponding pK_a of compound **1-143**, though unknown, is therefore expected to be in this range. On the basis of this, when the pH increases from 5.5 to 6.7, which is around the estimated pK_a value, more deprotonation

of the enol form of compound **1-143** is expected. Presumably this binds less readily to PAL.

5.5 Conclusion

To summarise, the established HPLC-MS system enables simultaneous evaluation of PHM and PAL inhibition by molecules, which significantly facilitates structure-activity relationship studies and the development of PAM inhibitors for pharmaceutical and medical applications. In the present study, *N*-Ac-Phe-pyruvate (**1-143**) was confirmed to be a PAL inhibitor at the nanomolar level against the medium PAM from DMS53 cells. The PAM inhibition assay with compound **1-143** also confirms that PAL activity dominates the conversion of hydroxylated intermediates to amidated products within two hours. The pH-dependent PAM inhibition assay implies that the deprotonation of the enol form of compound **1-143** results in a decrease of PAL inhibition by compound **1-143**.

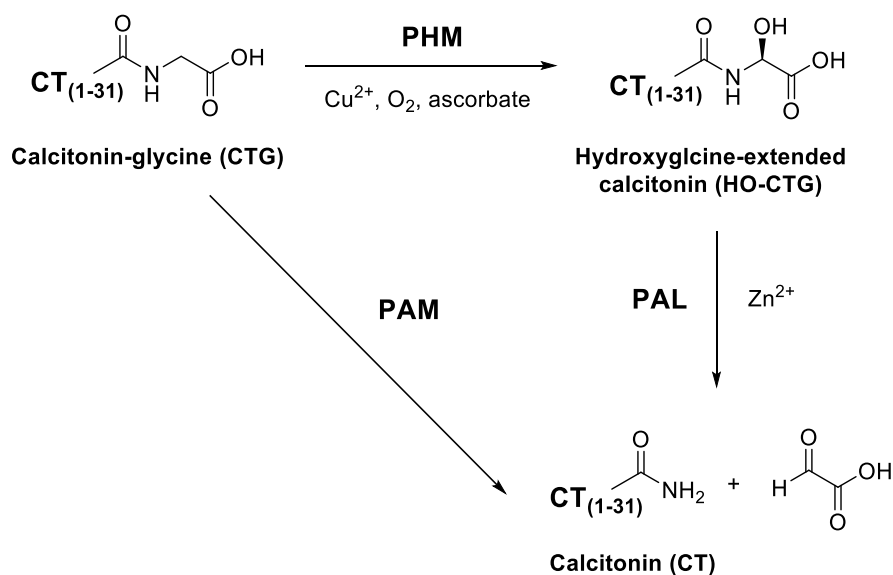
Chapter Six

Detection of an α -Hydroxyglycine-extended Peptide Hormone Produced by Human Small Cell Lung Cancer Cells

6.1 Introduction

To date, the role of α -hydroxyglycine-extended peptide hormones in humans is not well understood. To investigate this requires the detection and quantification of α -hydroxyglycine-extended peptide hormones. So far, Eipper and her colleagues^[214] are the only research group that has ever detected an α -hydroxyglycine peptide in a biological sample, wherein hydroxyglycine-extended joining peptide from mouse pituitary was measured. They reported that the level of hydroxylated joining peptide (HO-JPG) is around 70-fold lower than that of the corresponding precursor (JPG), which suggested that PAL catalysis is much faster than PHM catalysis in animals. In this Chapter, human α -hydroxyglycine-extended calcitonin (HO-CTG) was chosen as a candidate for detection. Its corresponding amidated product, calcitonin (CT) is a typical human amidated polypeptide hormone and mainly functions to reduce blood calcium (Ca^{2+}).^[215] In terms of medical science, CT is usually used for the treatment of osteoporosis or hypercalcemia.^[216] Increased concentration of CT is closely associated with many human cancers such as lung cancer, breast cancer, and pancreatic cancer.^[217-219] It is also used as an important clinical marker for monitoring medullary thyroid carcinoma.^[220] Due to the biological and medical importance of CT, understanding the relationship between the precursor glycine-extended calcitonin

(CTG), intermediate α -hydroxyglycine-extended calcitonin (HO-CTG) and product CT is of considerable interest (**Scheme 6.1**).



Scheme 6.1 Proposed PAM activity with CTG.

In the present study, the cancer cell line selected was DMS53 due to its unusually high expression of CT (43 ng/mL).^[145] Previously, CT and its glycine-extended precursor CTG secreted from the DMS53 cells were successfully identified by the Easton Group^[221] *via* HPLC with a fluorescence detector. After incubation of DMS53 cells, they analysed the culture medium and found that two peaks matched those of commercial authentic CT and CTG standards on the HPLC trace. These two peaks were then identified as CT and CTG through collection and ESI-MS analysis. However, the intermediate HO-CTG had not been investigated.

Given the expected low level and chemical instability of hydroxylated intermediates,^[196] PAL inhibition was considered as a possible strategy to cause the accumulation of HO-CTG in order to facilitate its detection and quantification. The work described in the previous Chapter demonstrated that *N*-Ac-Phe-pyruvate (**1-143**) is an effective PAL inhibitor with nanomolar potency against the medium PAM from the DMS53 cell line. Therefore, compound **1-143** was chosen in the present work to help the detection of HO-CTG. Further, to develop the analytical method, an authentic sample of HO-CTG was prepared through using isolated PAM and CTG, through HPLC and analysis by MS.

The work in this Chapter has been published in Analytical Chemistry, and is copied on the following pages. My contribution to this multiauthored paper involved the preparation of an authentic sample of HO-CTG and the detection of HO-CTG produced by DMS53 cells. My work showed that concentrated medium from DMS53 cells injected onto HPLC provided a sample that was positively identified by HPLC-MS. However, with or without the PAL inhibitor **1-143** (up to 2 mM), analysis of the medium samples showed that the concentration of HO-CTG was below the fluorescence detection limit (< 0.1 ng/mL), indicating that the concentration of HO-CTG is more than two orders of magnitude lower than those of the CTG and CT. This means PAL catalysis is much faster than PHM catalysis, and PHM catalysis is the rate-limiting step of amidation of calcitonin in human. The following pages are the copied paper and the contents highlighted with yellow are my work.

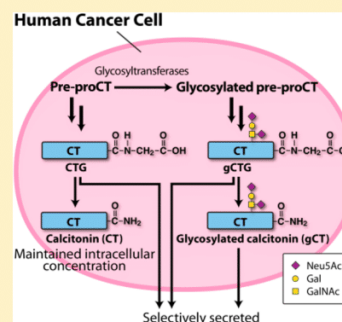
Detection of Biosynthetic Precursors, Discovery of Glycosylated Forms, and Homeostasis of Calcitonin in Human Cancer Cells

Feihua Cao, Allan B. Gamble,^{1b} Hideki Onagi,^{1b} Joanna Howes, James E. Hennessy, Chen Gu, Jeremy A. M. Morgan, and Christopher J. Easton*^{1b}

Research School of Chemistry, Australian National University, Canberra, ACT 2601, Australia

S Supporting Information

ABSTRACT: The peptide hormone calcitonin is intimately connected with human cancer development and proliferation. Its biosynthesis is reasoned to proceed via glycine-, α -hydroxyglycine-, glycyllysine-, and glycyllslylsine-extended precursors; however, as a result of the limitations of current analytical methods, until now, there has been no procedure capable of detecting these individual species in cell or tissue samples. Therefore, their presence and dynamics in cancer had not been established. Here, we report the first methodology for the separation, detection, and quantification of calcitonin and each of its precursors in human cancer cells. We also report the discovery and characterization of *O*-glycosylated calcitonin and its analogous biosynthetic precursors. Through direct and simultaneous analysis of the glycosylated and nonglycosylated species, we interrogate the hormone biosynthesis. This shows that the cellular calcitonin level is maintained to mitigate effects of biosynthetic enzyme inhibitors that substantially change the proportions of calcitonin-related species released into the culture medium.



Calcitonin (CT), which normally functions to regulate physiological calcium levels,¹ is closely associated with various forms of human cancer. It is used as a marker for medullary thyroid carcinoma,^{2–4} and elevated levels are seen with lung, pancreatic, and other tumors.^{5–8} It has also been correlated with cancer cell proliferation and tumor growth, as well as disease recurrence following medical treatment.^{9–13} Given the pathological relevance of CT, an improved understanding of its biological chemistry and a connection with disease progression are of considerable interest.^{14,15}

The biosynthesis of CT is thought to occur as shown in Figure 1a, proposed based on transcribed nucleotide sequence analysis for preprocalcitonin (prepro-CT)¹⁶ and by analogy with the formation of other amidated peptide hormones from their corresponding prohormones.¹⁷ However, until now, none of the glycine-, α -hydroxyglycine-, glycyllsine-, and glycyllslylsine-extended peptides (CTG, HO-CTG, CTGK, and CTGKK), which are the proposed precursors of CT, has been directly detected in cells. Analyses with immunoassays have detected only CT, or they have been incapable of distinguishing the individual precursors from CT and each other, because of their very similar overall chemical and physical characteristics.^{18,19} Peptide hormone immunoassays are also subject to interference from other species.^{20–22}

Therefore, it has not been possible to interrogate CT biosynthesis, examine the effects of inhibitors of the biosynthetic enzymes, peptidylglycine α -amidating monooxygenase (PAM), and carboxypeptidase E (CPE), and investigate the relationship between increased CT levels and carcinogenesis and metastasis. It has previously been reported

that CPE is upregulated in many cancer cell lines and tumor tissues, and directly implicated in their tumorigenesis.^{23–25} Potent PAM inhibitors including *E*-4-phenyl-3-butenic acid (PBA, Figure 2) are also known to inhibit growth of some cancer cell types,^{26–28} while other cell lines display a curious resistance to high concentrations of PBA and other very effective inhibitors of PAM, even though they are readily taken up by the cells.²⁹

Here, we present the development of analytical methods that enable close analysis of the biosynthetic behavior of CT. For the first time, they allow the separation, detection, and quantification of CT, HO-CTG, CTG, CTGK, and CTGKK, produced by human cancer cells. Application of the methods directly establishes the biosynthetic relationships between these species, and the effects of PAM and CPE inhibitors. Through this study, we also discovered *O*-glycosylated calcitonin (gCT) and its parallel biosynthetic precursors gCTG, gCTGK, and gCTGKK (Figure 1). In addition, we developed procedures for direct analyses of the levels of the glycosylated and nonglycosylated species in both the culture medium and within the corresponding cells, requiring little or no sample pretreatment. These show that the cellular level and proportion of fully processed nonglycosylated CT is largely unresponsive to PAM and CPE inhibitors, even though they change the ratios of CT-related species secreted from the cells.

Received: February 6, 2017

Accepted: June 7, 2017

Published: June 7, 2017

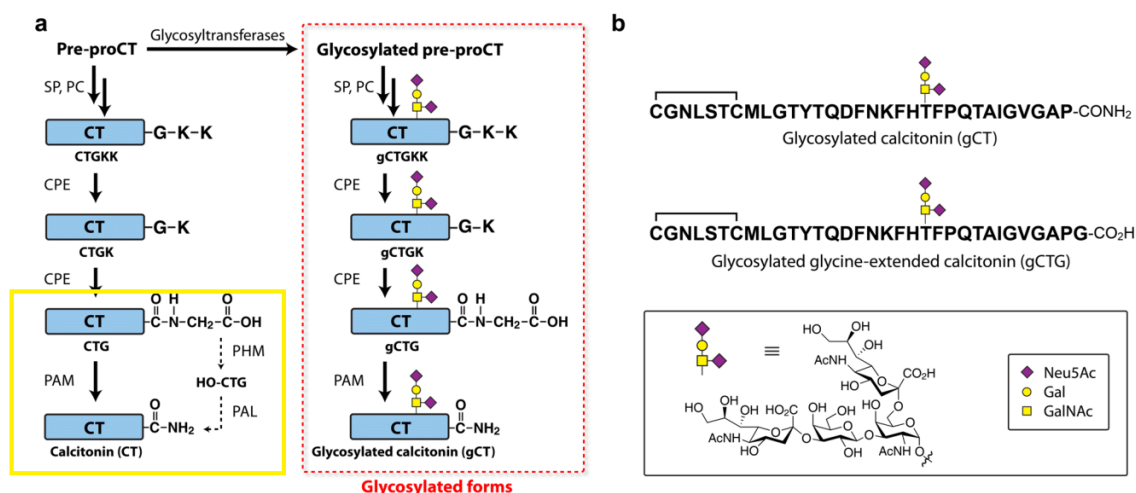


Figure 1. (a) Calcitonin (CT) biosynthesis pathway (shown on left) and parallel biosynthesis of *O*-glycosylated calcitonin (gCT) (shown on right) discovered during the course of this work. (b) Structures of gCT and the glycine-extended form (gCTG). [Legend: SP, signal peptidase; PC, prohormone convertase; CPE, carboxypeptidase E; PAM, peptidylglycine α -amidating monooxygenase; PHM, peptidylglycine α -hydroxylating monooxygenase; and PAL, peptidylamidoglycolate lyase.]

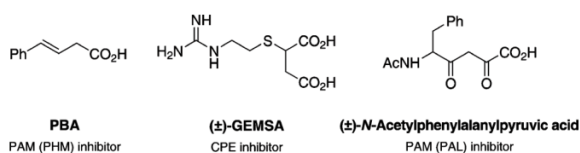


Figure 2. Enzyme inhibitors used in this study.

EXPERIMENTAL SECTION

General. The DMS53 human small cell lung cancer cell line was obtained from the American Type Culture Collection (Manassas, VA, USA). Cells were cultured in Gibco RPMI

1640 medium supplemented with 10% fetal bovine serum and 1% penicillin-streptomycin (10,000 U mL⁻¹), incubated under 5% CO₂ in air, at 37 °C. They were counted using a Bio-Rad TC20 automated cell counter with Trypan Blue stain.

Analysis for CT, CTG, CTGK, and CTGKK. Samples of CT, CTG, CTGK, and CTGKK were purchased from GL Biochem (Shanghai, China) and used to develop the analytical method that is illustrated in Figure 3. The method employs a Waters Alliance 2695 separation module fitted with a large volume sample loop and is fully automated using Waters Empower 3 software. The analyte is injected onto an online solid-phase extraction cartridge column (Waters Oasis HLB, 25 μ m, 2.1 \times

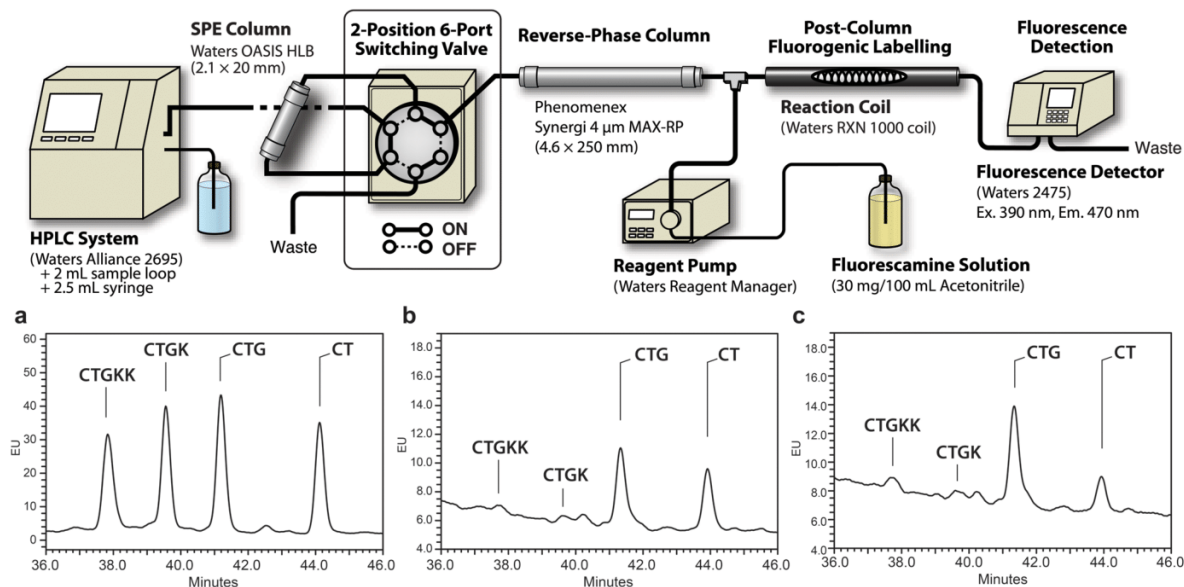


Figure 3. HPLC system overview and traces: (a) of calcitonin (CT) and precursor standards, (b) of culture medium from incubation of DMS53 cells without PBA, and (c) of medium from incubation of the cells with 400 μ M PBA.

20 mm) maintained at 40 °C, which is then flushed with water at 3 mL min⁻¹ for 4 min and 20% MeCN in buffer for 1 min; before the flow rate is reduced to 1.2 mL min⁻¹, the two-position, six-port valve is switched to divert the flow from waste to a reverse-phase column (Phenomenex Synergi MAX-RP, 4 μm, 4.6 × 250 mm) also maintained at 40 °C, and the mobile phase is adjusted with a solvent gradient over 35 min to 30% MeCN in buffer. Buffer refers to 2.5% Waters AccQ.Tag eluent A in water. Material eluting from the reverse-phase column is mixed with a solution of fluorescamine (Sigma–Aldrich, 30 mg) in acetonitrile (100 mL) delivered at 0.2 mL min⁻¹ by a Waters Reagent Manager, before passing through a Waters RXN 1000 reaction coil maintained at 25 °C, then detection with a Waters 2475 fluorescence detector (excitation 390 nm, emission 470 nm).

DMS53 cell-culture medium was analyzed directly after centrifugation at 4 °C and 10 000 g for 5 min. In addition to fluorescence detection, samples of CT, CTG, CTGK, and CTGKK produced by the cells were isolated by manually collecting fractions eluting from the reverse-phase column without treatment with fluorescamine. The separated fractions were then concentrated and desalted, by loading onto a solid-phase extraction cartridge column (Waters Oasis HLB), followed by elution with 50% aqueous acetonitrile. The isolated samples were analyzed using electrospray ionization–mass spectrometry (ESI-MS).

Analysis for HO-CTG. PAM extracted from DMS53 cells²⁹ was used to prepare HO-CTG from CTG, in order to develop the analytical method. A mixture of CTG (0.1 mg) and PAM solution (5 μL) in MES buffer (100 μL, 150 mM, pH 5.8) containing 1.25 mM ascorbic acid, 10 μM copper sulfate, 0.2 mg mL⁻¹ bovine liver catalase, 1% ethanol, and 1% dimethylsulfoxide (DMSO) was incubated at 37 °C for 2 h, before being filtered using an Amicon Ultra-0.5 mL centrifugal filter fitted with an Ultracel-3 membrane (Merck Millipore), at 12 000 g for 30 min. HPLC of the filtrate was used to isolate HO-CTG.

The method used for the analysis of CT, CTG, CTGK, and CTGKK in a cell-culture medium was also used for analysis for HO-CTG, except that tandem separation columns were employed (column 1: YMC ODS-AQ, 3 μm, 4.6 × 100 mm; column 2: Phenomenex Phenosphere SCX, 5 μm, 4.6 × 250 mm) (see Figure S1 in the Supporting Information), and the solvent gradient was introduced over 95 min instead of 35 min. A sample of HO-CTG produced by the cells was isolated, by manually collecting fractions eluting from the separation columns before treatment with fluorescamine, and was characterized using ESI-MS.

Identification and Characterization of gCT, gCTG, gCTGK, and gCTGKK. Samples of the compounds corresponding to two unidentified peaks in HPLC traces from analyses of DMS53 cell-culture medium were isolated using the protocol described above for analysis for HO-CTG, but with the solvent gradient introduced over 65 min instead of 95 min, and without fluorescent derivatization. The isolation was performed using 120 mL of medium from cells grown to 50%–90% confluency, after it had been concentrated by lyophilization, reconstituted in Milli-Q water to 10% of its original volume and centrifuged at RT and 10 000 g for 5 min.

Each of the isolated compounds was analyzed by MS using an Agilent 6530 Accurate-Mass Q-TOF LC/MS system, treated systematically with deglycosylation enzymes using the CarboRelease Kit from QA-Bio (Palm Desert, CA, USA), as per the

manufacturer's instructions, treated with trypsin in Tris-HCl buffer (100 mM, pH 7.8) at 37 °C for 6 h, and analyzed using electron transfer dissociation–tandem mass spectrometry (ETD-MS/MS). ETD-MS/MS data were matched using the Mascot program (Matrix Sciences). The results of these analyses, detailed below, established the species to be glycosylated CT and CTG (gCT and gCTG).

Direct MS analysis (LC-MS/MS-MRM) of the culture medium was used to confirm the presence of glycosylated CTGK and CTGKK (gCTGK and gCTGKK). gCTGK was identified on the basis of analyzing for the parent molecular ions, e.g., at calculated m/z 1138.2584 ($[M+4H]^{4+}$), as well as daughter ions at m/z 70.0107, 86.1058, 86.5681, and 136.0684. The daughter ions were expected based on the structure as well as the observation of identical fragmentations with CTGK. Similarly, gCTGKK was identified on the basis of analyzing for the parent molecular ions, e.g., at calculated m/z 936.4273 ($[M+5H]^{5+}$), as well as daughter ions at m/z 70.0107, 86.1058, 86.5681, and 129.1146. Again, the daughter ions were expected on the basis of the structure and the observation of identical fragmentations with CTGKK.

Analysis for CT, CTG, gCT, and gCTG in Cell Lysate and Culture Medium in the Presence and Absence of PBA and GEMSA.

Cells were grown to confluency and then lifted with trypsin-EDTA (0.05%), before being suspended in RPMI 1640 medium supplemented with 10% fetal bovine serum and 1% penicillin–streptomycin (10 000 U mL⁻¹), and counted. This suspension was used to initiate subcultures with ~10⁶ cells mL⁻¹ in 10 mL of the medium in 75 cm² flasks. To examine the effect of PBA, these subcultures were prepared in quadruplicate, then incubated for 72 h to reach confluency (~25 × 10⁶ cells per flask). The medium in each flask was then replaced, in two with the standard medium (10 mL) containing 0.1% DMSO as the control, and in the other two with a medium containing PBA (Sigma–Aldrich, 400 μM) added as a solution in the DMSO, and the flasks were incubated for 48 h. The cell-culture medium was then collected, and centrifuged at 4 °C and 10 000 g for 5 min, before being analyzed by HPLC. For analysis of the cell lysate, cells were trypsinized from the culture flask, pelleted by centrifugation at 2500 g for 5 min, washed with DPBS, and re-pelleted, before being re-suspended in 400 μL of the medium. The suspension was snap-frozen in liquid nitrogen then quickly thawed in hot water for 7 min. Lysates prepared in this manner were filtered using an Amicon Ultra-0.5 mL centrifugal filter fitted with an Ultracel-50 membrane (Merck Millipore) that had been deactivated by presoaking in 50% fetal bovine serum for 48 h. Filtration was carried out at 12 000 g for 30 min. The membrane was washed with additional medium (3 × 200 μL) and the combined filtrates were analyzed by HPLC. The same procedure was used to examine the effect of GEMSA (Santa Cruz Biotechnology, Inc., 100 μM) except that DMSO was not used. A similar protocol was also used to examine the effect of incubation time and volume of medium used, except that, for the final cultures, either 10 or 30 mL of fresh medium was used, and incubation was carried out for either 24 or 72 h.

RESULTS

Separation, Detection, and Quantification of CT and Biosynthetic Precursors. The DMS53 small cell lung cancer cell line was chosen for use in this investigation, because (i) it was established from an untreated biopsy, (ii) it shows excellent correlation in hormone production between cell cultures and in

vivo transplants, and (iii) it exhibits unusually stable hormone production characteristics and high expression of the CT-producing gene.^{9,30} The protocol developed for the separation, detection, and quantification of CT, CTG, CTGK, and CTGKK, in a cell-culture medium (Figure 3) involves direct analysis of the medium through HPLC, using online solid-phase extraction to preclean and preconcentrate the analytes, before their passage onto a reverse-phase column, with online post-column fluorogenic derivatization to detect the separated species and determine the amounts present. The solid-phase extraction enables the direct injection of up to 10 mL of complex culture medium, without any pretreatment. The retention times of CT, CTG, CTGK, and CTGKK were determined using authentic commercial samples of the peptides (Figure 3a), which were also used to measure calibration curves and determine that all four compounds show very similar fluorescence detection response ratios. The detector response of each peptide was found to be due to reaction of the N-terminal primary amino group with fluorescamine. Side-chain amino groups of lysine residues present in peptides do not generate a measurable response under the assay conditions. This was established by analysis of free and *N*-acetylated peptides, both with and without lysine residues, and is attributable to the lysine amines being more extensively protonated and, therefore, several orders of magnitude less reactive. The method was shown to provide reliable quantification with a lower limit of 1 ng mL⁻¹ for analysis of 1 mL of medium. Even greater sensitivity is achieved with larger injection volumes, by concentration of the medium prior to injection, and/or by detection using MS in place of fluorescent derivatization.

A representative chromatogram of 1 mL of medium sampled after 48 h from $\sim 10 \times 10^6$ DMS53 cells cultured in 10 mL is shown in Figure 3b. The quality of the chromatogram is remarkably good given such low concentrations of the analytes in the complex culture mixture. CT, CTG, CTGK, and CTGKK were all detected, and the identity of each of these species was confirmed by collecting fractions eluting from the separation column, then analyzing them without fluorescent labeling using ESI-MS (see Figures S2–S5 in the Supporting Information). CT and CTG were also identified by direct HPLC-MS analysis of the medium. The concentrations of the individual species CT, CTG, CTGK, and CTGKK in the medium were measured through HPLC with fluorescence detection and determined to be ~ 10 , 13, 1, and 1 ng mL⁻¹, respectively, under these conditions.

Having separately detected CT, CTG, CTGK, and CTGKK, we then probed their biosynthetic relationships using inhibitors of the enzymes that are understood to catalyze their interconversion. As would be anticipated, culturing the DMS53 cells in the presence of the PAM inhibitor PBA (400 μ M) resulted in a decrease in the CT to CTG ratio in the medium, from 1:1.3 to 1:3 (Figure 3c). Use of the CPE inhibitor GEMSA²³ (Figure 2) (100 μ M) increased the CTGK and CTGKK concentrations, and decreased that of CTG, as is discussed in more detail below.

PAM is a two-component enzyme comprising peptidylglycine α -hydroxylating monooxygenase (PHM), which catalyzes hydroxylation of glycine-extended peptide hormone precursors, and peptidylamidoglycolate lyase (PAL), which facilitates lysis of the hydroxylated materials, to give the physiologically active, amidated peptide hormones (Figure 4). The PAM inhibitor PBA, referred to above, interacts with PHM. The procedures

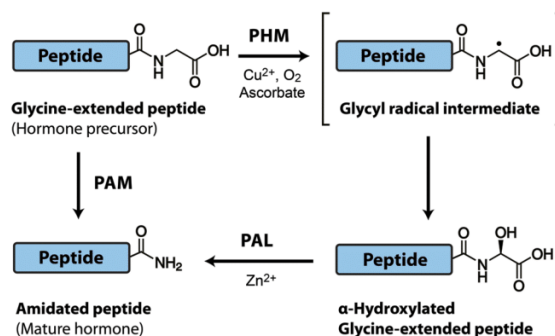


Figure 4. Production of amidated peptides from glycine-extended precursors, catalyzed by peptidylglycine α -amidating monooxygenase (PAM). [Legend: PHM, peptidylglycine α -hydroxylating monooxygenase; PAL, peptidylamidoglycolate lyase.]

used to detect CT, CTG, CTGK, and CTGKK were adapted to also analyze for the corresponding hydroxylated glycine-extended calcitonin (HO-CTG) in the cell-culture medium. Initially, an authentic sample of HO-CTG was prepared by treatment of CTG with isolated PAM,²⁹ purified through HPLC and analyzed by MS. This material was then utilized to develop the analytical method, which mainly involved introduction of an additional online ion-exchange column to the protocol used for CT, CTG, CTGK, and CTGKK, in a similar manner to two-dimensional (2D) liquid chromatography, for adequate resolution of the components in the medium (Figure S1 in the Supporting Information). Analysis of the medium sampled from cells cultured in the presence or absence of the PAL inhibitor *N*-acetylphenylalanylpyruvate³¹ (up to 2 mM) (Figure 2), which would be expected to increase the amount of HO-CTG, then established that, in both cases, its concentration was below the fluorescence detection limit of <0.1 ng mL⁻¹ (see Figure S6 in the Supporting Information). Even so, blind fractionation of medium by HPLC provided a sample that was unambiguously identified using ESI-MS (Figure S7 in the Supporting Information).

Identification and Characterization of gCT and gCTG.

HPLC analyses of DMS53 cell-culture medium indicated the presence of two unidentified major components. Using a protocol adapted from the analysis for HO-CTG resulted in improved resolution of these species, marked with asterisks in Figure 5a. The addition of PBA changed their ratio, as it did with CT and CTG (Figure 5b), suggesting them to also be an amidated peptide and its biosynthetically related, glycine-extended precursor. HPLC enabled isolation of pure samples for structure determination.

MS analysis of the separated materials (see Figures S8 and S9 in the Supporting Information) showed ions with m/z 1092.2 and 1456.0 in one case, and 1106.7 and 1475.3 in the other, corresponding to $[M+4H]^{4+}$ and $[M+3H]^{3+}$ ions of species with molecular weights of 4365 and 4423 Da, respectively. The molecular weight difference of 58 Da confirmed the relationship between the two species of amidated peptide and its glycine-extended precursor. MS/MS analysis performed on the parent ions (see Figures S10 and S11 in the Supporting Information) provided the first indication that these species are the glycosylated derivatives of CT and CTG: gCT and gCTG. This was corroborated by enzymatic deglycosylation and MS of the product peptides, together with considerations of biosynthetic pathways. In particular, treatment with PNGase

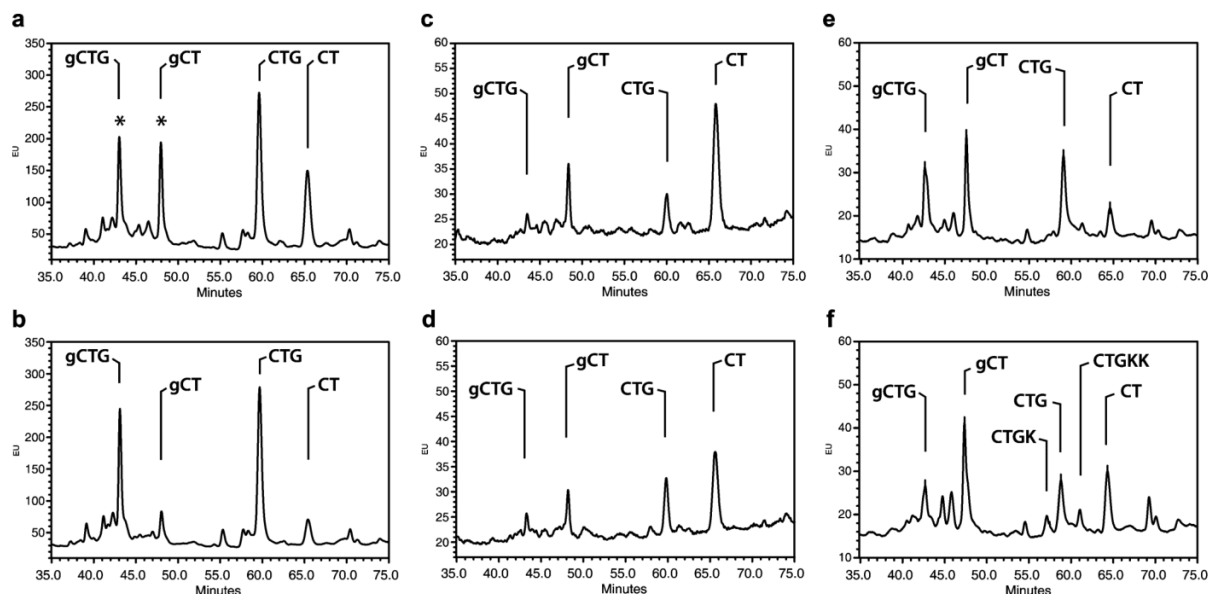


Figure 5. HPLC traces of culture medium and cell lysate from incubation of DMS53 cells: (a) medium (5 mL) without PBA, (b) medium (5 mL) with 400 μM PBA, (c) lysate (entire sample) without PBA, (d) lysate (entire sample) with 400 μM PBA, (e) medium (1 mL) without GEMSA, and (f) medium (1 mL) with 100 μM GEMSA. (Retention times of CT, CTG, CTGK, and CTGKK were recalibrated with standards under these conditions.)

Table 1. Proportions of Calcitonin (CT), Glycine-Extended Calcitonin (CTG) and the Glycosylated Forms (gCT and gCTG) in a Cell-Culture Medium and Lysate

entry	CT (%) ^{a,b}	CTG (%) ^{a,b}	gCT (%) ^{a,b}	gCTG (%) ^{a,b}	glycosylated (%) ^{a,c}	amidated (%) ^{a,d}
Experiment 1: Effect of PBA (400 μM) with DMS53 Cells Grown in 10 mL of Medium for 48 h						
(i) medium (– PBA)	25	38	18	19	37	43
(ii) medium (+ PBA)	11	51	8	30	38	19
(iii) lysate (– PBA)	63	16	16	5	21	79
(iv) lysate (+ PBA)	53	28	13	6	19	66
Experiment 2: Effect of GEMSA (100 μM) with DMS53 Cells Grown in 10 mL of Medium for 48 h						
(v) medium (– GEMSA)	22	36	23	19	42	45
(vi) medium (+ GEMSA)	32	25	31	11	42	63
(vii) lysate (– GEMSA)	69	9	17	6	23	86
(viii) lysate (+ GEMSA)	72	7	16	6	22	88
Experiment 3: Effects of Volume of Culture Medium and Incubation Time with DMS53 Cells						
(ix) 24 h, 10 mL medium	31	30	29	10	39	60
(x) 24 h, 30 mL medium	24	41	23	12	35	47
(xi) 72 h, 10 mL medium	18	25	29	28	57	47
(xii) 72 h, 30 mL medium	14	31	16	39	55	30

^aAverage of incubations carried out at least in duplicate and HPLC analyses performed at least in duplicate. ^bProportion as a percentage of the total quantities of CT, CTG, gCT, and gCTG. ^cProportion of gCT and gCTG as a percentage of the total quantities of CT, CTG, gCT, and gCTG. ^dProportion of CT and gCT as a percentage of the total quantities of CT, CTG, gCT, and gCTG.

F, sialidase, β -galactosidase, glucosaminidase, and O-glycosidase, to remove all N- and O-linked oligosaccharides, afforded product peptides that were shown by MS to be identical to CT and CTG. Alone, PNGase F failed to catalyze the deglycosylation, when it would have removed any N-linked glycan, while O-glycosidase and sialidase did so, in a stepwise manner, showing that the glycopeptides have the disialylated core 1 O-glycan, NeuAc(α 2–3)Gal(β 1–3)[NeuAc(α 2–6)]-GalNAc.^{32,33}

Having identified the tetrasaccharide, enzyme-catalyzed peptide digestion and ETD-MS/MS were then employed to ascertain the site of peptide glycosylation. Treatment of each

species with trypsin gave products identified through LC/MS analysis as nonglycosylated CT(1–18) and glycosylated CT(19–32), and nonglycosylated CTG(1–18) and glycosylated CTG(19–33). This corresponds to peptide cleavage between Lys18 and Phe19. CT and CTG each have one Ser and five Thr residues that are possible O-glycosylation sites but the retention of the glycan on the C-terminal fragments limits these to either Thr21 or Thr25. Finally, ETD-MS/MS was used in each case to determine Thr21 as the O-glycosylation site and confirm the identities of both gCT and gCTG. Data matched using the Mascot program showed, for example, peaks for the series of *c* ions. In particular, for both gCT and gCTG, peaks at

m/z 1147.0 and 1671.2 correspond to c_{20}^{++} and c_{21}^{++} , with the difference being the mass of Thr plus the glycan, whereas peaks at m/z 1857.3 and 1907.8 correspond to c_{24}^{++} and c_{25}^{++} , differing only by the mass of Thr. The complete analysis was carried out separately on gCT and gCTG, and their structures were therefore independently determined to be those illustrated in Figure 1b.

Having identified gCT and gCTG, by analogy with the biosynthesis of CT from CTG, CTGK, and CTGKK, it seemed logical that gCT and gCTG would be derived via a parallel route from the corresponding glycosylated lysine-extended precursors: gCTGK and gCTGKK (Figure 1). MS analysis (LC-MS/MS-MRM) of a cell-culture medium confirmed the presence of both species, in concentrations much lower than those of gCT and gCTG (see the Supporting Information for details).

Direct Comparative Analyses of CT, CTG, gCT, and gCTG, and Homeostasis of Cellular Calcitonin Levels. As described above, among CT, gCT and their biosynthetic precursors, CT, gCT, CTG, and gCTG are predominant in the cell-culture medium. Therefore, we monitored the relative proportions of these four compounds in the medium under a variety of conditions. The HPLC method used in these analyses, and particularly the online solid-phase extraction process, is sufficiently robust that it was also possible to monitor the intracellular proportions of these species by direct injection of the entire lysate of ~ 30 million cells, following simple filtration to remove cellular debris. The results of typical duplicate experiments are illustrated in Figure 5, and the relative proportions of CT, CTG, gCT, and gCTG are summarized in Table 1.

The concentrations of CT, CTG, gCT, and gCTG are dependent on several factors, such as the number of cells, the passage of the cells used for inoculation, the volume of the culture medium, and the time of incubation. Within each experiment, a common inoculate of cells was used but, because of practical limitations, it was necessary to use different inoculates for Experiments 1 and 2 in Table 1. This accounts for the differences between the outcomes of the corresponding controls (see entries (i) and (v), and entries (iii) and (vii) in the table). HPLC-MS analysis showed that $(^2\text{H}_{10}\text{-Leu})_2\text{-CTG}$ was not converted to $(^2\text{H}_{10}\text{-Leu})_2\text{-CT}$ in the medium, either during or after incubation with cells. When both $(^2\text{H}_{10}\text{-Leu})_2\text{-CTG}$ and $(^2\text{H}_{10}\text{-Leu})_2\text{-CT}$ were added, they remained in the same ratio. These experiments show that there is no turnover of CT and CTG in the medium, so the results in Table 1 correspond to materials produced in the cells then released. Further control experiments established that there was no change in the proportions of CT, CTG, gCT, and gCTG in cells after they were harvested.

With reference to Table 1 and the proportions of CT, CTG, gCT, and gCTG, with cells cultured in the absence of any enzyme inhibitor, the intracellular species are $\sim 20\%$ glycosylated (gCT and gCTG) and $\sim 80\text{--}90\%$ amidated or processed by PAM (CT and gCT), and CT is dominant (63 and 69%, entries (iii) and (vii) in the table). By comparison, in the corresponding culture media (entries (i) and (v) in the table), the amount glycosylated is approximately doubled (to $\sim 40\%$) and the amount processed by PAM is halved (to $\sim 45\%$). Neither PBA nor GEMSA affects the proportion of glycosylated species, which remains at $\sim 20\%$ in the cells (see entries (iv) and (viii) in the table) and $\sim 40\%$ in the medium (entries (ii) and (vi) in the table). PBA only reduces the

cellular proportion of CT from 63% to 53%, which is a small reduction for the high concentration of PAM inhibitor used ($400 \mu\text{M}$). The same concentration of PBA more than halves the fraction of CT in the medium, reducing its proportion from 25% to 11% (entries (i) and (ii) in the table). Maintenance of the cellular CT level is also seen with GEMSA (69% and 72%, entries (vii) and (viii) in the table). In the medium, GEMSA increases the proportion of CT by ~ 1.5 -fold (entries (v) and (vi) in the table, from 22% to 32%). This increase is a consequence of the CPE inhibitor increasing the CTGK and CTGKK concentrations, and decreasing that of CTG (and gCTG), as would be predicted, but without a corresponding decrease in CT (Figures 5e and 5f). In all experiments with GEMSA, the concentration of CT in the medium was the same or higher than with the corresponding controls. When results from experiments with different incubation times and volumes of culture medium are compared (entries (ix)–(xii) in the table), the proportion of the amidated species in the medium varies from 60% to 30%. The proportion of the glycosylated species increases, from 35%–40% to 55%–60%, with time but is not significantly affected by the change in the volume of the medium.

DISCUSSION

Despite the close association that links CT with cancer, before now, no method had been reported to separate, detect, and quantify CT and the peptides understood to be its biosynthetic precursors, CTG, CTGK, and CTGKK. The HPLC analysis illustrated in Figure 3 provided the original tool for this purpose and established that all four species are present in DMS53 cell-culture medium, this being the first direct observation of CTG, CTGK, or CTGKK in a cell or tissue sample. Adaptation of the analytical method also enabled the detection of HO-CTG, the intermediate between CTG and CT, using HPLC-MS. There has been no previous report of the detection of HO-CTG produced by cells and, indeed, the only other account of any hydroxylated, glycine-extended precursor of any amidated peptide in a biological specimen was the finding of the hydroxylated precursor of joining peptide in pituitary lysates from mice.³⁴

The discovery of the *O*-glycosylated gCT, gCTG, gCTGK, and gCTGKK was unexpected. Not only were these glycopeptides previously unknown, as a group or individually, a much earlier investigation looking for the production of any *N*- or *O*-linked glycosylated form of CT by DMS53 cells yielded negative results.³⁵ The core 1 *O*-glycan of gCT has been found attached to many other glycopeptides produced by both normal and cancer cells, including the gonadotropin hormone family,³⁶ MUC-1,³⁷ and von Willebrand factor,³⁸ but it has not been associated before now with CT. The production of gCT, gCTG, gCTGK, and gCTGKK most logically proceeds through a biosynthetic pathway parallel to that for production of CT from CTG, CTGK, and CTGKK, that branches from the known pathway through glycosylation of prepro-CT in the Golgi apparatus, before CTGKK is excised (Figure 1a). We have used our analytical methods (HPLC fractionation; LC/MS - MRM) to discover identically glycosylated gCT and gCTG, in addition to CT and its precursors, produced by TT cells, so it is apparent that this glycosylation also occurs with the human medullary thyroid cancer cell line.

The studies summarized in Table 1 show selective intracellular retention of CT, compared to its biosynthetic precursor CTG, and the corresponding glycosylated forms gCT and

gCTG. They also show selective maintenance of CT levels in the cells in response to the PAM and CPE inhibitors, PBA and GEMSA, which, at the same time, bring about relatively large variations in the proportions of CT and gCT that are released into the medium. The accumulation of CTG and gCTG demonstrates that catalytic turnover by PAM limits the production of CT and gCT. More specifically, it is the limiting activity of the PHM component of PAM, since there is no buildup of HO-CTG. The anomalous effect of the CPE inhibitor GEMSA, already discussed above, to reduce the concentration of CTG, as expected, but without a corresponding decrease in CT, further shows that catalytic turnover by PAM is not proportional to substrate concentration in a typical manner.

CONCLUSION

In summary, the protocols reported here constitute sophisticated and sensitive, yet straightforward methods, that enable direct analysis of CT and its biosynthetic processes in biological samples. We expect that the techniques will be generally applicable for screening inhibitors of the associated biosynthetic enzymes, as well as for analysis of other amidated peptide hormones. Already, we have developed closely analogous procedures to analyze for oxytocin (OT) and its precursors (OTG, OTGK, and OTGKK).

The identification and full characterization of gCT, gCTG, gCTGK, and gCTGKK provides the platform for further studies to understand the function of the glycosylation pathway for CT. Glycopeptides are generally recognized as playing important and various roles in cancer.^{39,40} O-Glycans control cellular trafficking and the metabolism of hormones, in particular, through affecting their processing by prohormone convertase.^{41–43} They are also known to regulate hormone serum levels, confer peptides with resistance to degradation, and direct them to cell surface receptors,^{33,44} as well as affect the cellular passaging of PAM.⁴⁵ In any event, already the studies described above and summarized in Table 1 establish that CT is selectively retained in the cells, while larger fractions of CTG and the glycosylated species gCT and gCTG are released. It is clear that there is a complex interplay of regulatory processes that maintain the intracellular concentration of CT, even when cells are challenged with the PAM and CPE inhibitors, PBA and GEMSA. Understanding them will be key to delineating the correlation between CT and cancer, and a prerequisite to developing therapies that seek to regulate the production of CT or other amidated peptide hormones associated with disease.

ASSOCIATED CONTENT

Supporting Information

The Supporting Information is available free of charge on the ACS Publications website at DOI: 10.1021/acs.analchem.7b00457.

Supplementary mass spectra, the HPLC separation and detection method for HO-CTG, gCT, gCTG, CT, CTG, CTGK, and CTGKK and details of LC-MS/MS-MRM analysis for gCTGK and gCTGKK (PDF)

AUTHOR INFORMATION

Corresponding Author

*E-mail: Chris.Easton@anu.edu.au.

ORCID

Allan B. Gamble: 0000-0001-5440-8771

Hideki Onagi: 0000-0003-0085-7349

Christopher J. Easton: 0000-0002-2263-1204

Notes

The authors declare no competing financial interest.

ACKNOWLEDGMENTS

We thank the Australian Research Council for financial support, the University of New South Wales, Bioanalytical Mass Spectrometry Facility (Assoc. Prof. Mark Raftery) for performing ETD-MS experiments, Dr. Hye-Kyung Kim for establishing the tissue culture laboratory, and Dr. Apostolos Alissandratos for performing ESI-MS experiments.

REFERENCES

- (1) Findlay, D. M.; Sexton, P. M.; Martin, T. J. In *Endocrinology: Adult & Pediatric*, 7th Edition; Jameson, J. L., De Groot, L. J., de Kretser, D. M., Giudice, L. C., Grossman, A. B., Melmed, S., Potts, J. T., Weir, G. C., Eds.; Elsevier: Philadelphia, PA, 2016; pp 1004–1017.
- (2) Williams, G. A.; Hargis, G. K.; Galloway, W. B.; Henderson, W. J. *Exp. Biol. Med.* **1966**, *122*, 1273–1276.
- (3) Trimboli, P.; Giovanella, L.; Crescenzi, A.; Romanelli, F.; Valabrega, S.; Spriano, G.; Cremonini, N.; Guglielmi, R.; Papini, E. *Head Neck* **2014**, *36*, 1216–1223.
- (4) Jung, K. Y.; Kim, S. M.; Yoo, W. S.; Kim, B. W.; Lee, Y. S.; Kim, K. W.; Lee, K. E.; Jeong, J. J.; Nam, K. H.; Lee, S. H.; Hah, J. H.; Chung, W. Y.; Yi, K. H.; Park, D. J.; Youn, Y. K.; Sung, M. W.; Cho, B. Y.; Park, C. S.; Park, Y. J.; Chang, H. S. *Clin. Endocrinol.* **2016**, *84*, 587–597.
- (5) Baylin, S. B.; Weisburger, W. R.; Eggleston, J. C.; Mendelsohn, G.; Beaven, M. A.; Abeloff, M. D.; Ettinger, D. S. *N. Engl. J. Med.* **1978**, *299*, 105–110.
- (6) Schneider, R.; Waldmann, J.; Swaid, Z.; Ramaswamy, A.; Fendrich, V.; Bartsch, D. K.; Schlosser, K. *Pancreas* **2011**, *40*, 213–221.
- (7) Kovacova, M.; Filkova, M.; Potocarova, M.; Kinova, S.; Pajvani, U. *Endocr. Pract.* **2014**, *20*, e140–e144.
- (8) Nozieres, C.; Chardon, L.; Goichot, B.; Borson-Chazot, F.; Hervieu, V.; Chikh, K.; Lombard-Bohas, C.; Walter, T. *Eur. J. Endocrinol.* **2016**, *174*, 335–341.
- (9) Cate, C. C.; Duple, E. B.; Andrews, K. M.; Pettengill, O. S.; Curphey, T. J.; Sorenson, G. D.; Maurer, L. H. *Cancer Res.* **1984**, *44*, 949–954.
- (10) Chigurupati, S.; Kulkarni, T.; Thomas, S.; Shah, G. *Cancer Res.* **2005**, *65*, 8519–8529.
- (11) Sabbisetti, V. S.; Chirugupati, S.; Thomas, S.; Vaidya, K. S.; Reardon, D.; Chiriva-Internati, M.; Iczkowski, K. A.; Shah, G. V. *Int. J. Cancer* **2005**, *117*, 551–560.
- (12) Shah, G. V.; Thomas, S.; Muralidharan, A.; Liu, Y.; Hermonat, P. L.; Williams, J.; Chaudhary, J. *Endocr.-Relat. Cancer* **2008**, *15*, 953–964.
- (13) Hadoux, J.; Pacini, F.; Tuttle, R. M.; Schlumberger, M. *Lancet Diabetes Endocrinol.* **2016**, *4*, 64–71.
- (14) Lee, S. M.; Hay, D. L.; Pioszak, A. A. *J. Biol. Chem.* **2016**, *291*, 8686–8700.
- (15) Opsahl, E. M.; Brauckhoff, M.; Schlichting, E.; Helset, K.; Svartberg, J.; Brauckhoff, K.; Maehle, L.; Engebretsen, L. F.; Sigstad, E.; Groholt, K. K.; Akslen, L. A.; Jorgensen, L. H.; Varhaug, J. E.; Bjoro, T. *Thyroid* **2016**, *26*, 1225–1238.
- (16) Le Moulec, J. M.; Jullienne, A.; Chenais, J.; Lasmoles, F.; Guliana, J. M.; Milhaud, G.; Moukhtar, M. S. *FEBS Lett.* **1984**, *167*, 93–97.
- (17) Douglass, J.; Civelli, O.; Herbert, E. *Annu. Rev. Biochem.* **1984**, *53*, 665–715.
- (18) Kratzsch, J.; Petzold, A.; Raue, F.; Reinhardt, W.; Brocker-Preuss, M.; Gorges, R.; Mann, K.; Karges, W.; Morgenthaler, N.;

- Luster, M.; Reiners, C.; Thiery, J.; Dralle, H.; Fuhrer, D. *Clin. Chem.* **2011**, *57*, 467–474.
- (19) Alves, T. G.; Kasamatsu, T. S.; Yang, J. H.; Meneghetti, M. C. Z.; Mendes, A.; Kunii, I. S.; Lindsey, S. C.; Camacho, C. P.; Dias da Silva, M. R.; Maciel, R. M. B.; Vieira, J. G. H.; Martins, J. R. M. J. *Clin. Endocrinol. Metab.* **2016**, *101*, 653–658.
- (20) Gulbahar, O.; Konca Degertekin, C.; Akturk, M.; Yalcin, M. M.; Kalan, I.; Atikeler, G. F.; Altinova, A. E.; Yetkin, I.; Arslan, M.; Toruner, F. *J. Clin. Endocrinol. Metab.* **2015**, *100*, 2147–2153.
- (21) Schiettecatte, J.; Strasser, O.; Anckaert, E.; Smits, J. *Clin. Biochem.* **2016**, *49*, 929–931.
- (22) Kwon, H.; Kim, W. G.; Choi, Y. M.; Jang, E. K.; Jeon, M. J.; Song, D. E.; Baek, J. H.; Ryu, J. S.; Hong, S. J.; Kim, T. Y.; Kim, W. B.; Shong, Y. K. *Clin. Endocrinol.* **2015**, *82*, 598–603.
- (23) Murthy, S. R. K.; Dupart, E.; Al-Sweel, N.; Chen, A.; Cawley, N. X.; Loh, Y. P. *Cancer Lett.* **2013**, *341*, 204–213.
- (24) Liu, A.; Shao, C. H.; Jin, G.; Liu, R.; Hao, J.; Shao, Z.; Liu, Q. Y.; Hu, X. G. *Tumor Biol.* **2014**, *35*, 12459–12465.
- (25) Huang, S. F.; Wu, H. D. I.; Chen, Y. T.; Murthy, S. R. K.; Chiu, Y. T.; Chang, Y.; Chang, I. C.; Yang, X. Y.; Loh, Y. P. *Tumor Biol.* **2016**, *37*, 9745–9753.
- (26) Iwai, N.; Martinez, A.; Miller, M. J.; Vos, M.; Mulshine, J. L.; Treston, A. M. *Lung Cancer-J. Iaslc* **1999**, *23*, 209–222.
- (27) Sunman, J. A.; Foster, M. S.; Folsie, S. L.; May, S. W.; Matesic, D. F. *Mol. Carcinog.* **2004**, *41*, 231–246.
- (28) Ali, A.; Burns, T. J.; Lucrezi, J. D.; May, S. W.; Green, G. R.; Matesic, D. F. *Invest. New Drugs* **2015**, *33*, 827–834.
- (29) Cao, F. H.; Gamble, A. B.; Kim, H. K.; Onagi, H.; Gresser, M. J.; Kerr, J.; Easton, C. J. *MedChemComm* **2011**, *2*, 760–763.
- (30) Sorenson, G. D.; Pettengill, O. S.; Brinck-Johnsen, T.; Cate, C. C.; Maurer, L. H. *Cancer* **1981**, *47*, 1289–1296.
- (31) Mounier, C. E.; Shi, J.; Sirimanne, S. R.; Chen, B. H.; Moore, A. B.; GillWoznichak, M. M.; Ping, D. S.; May, S. W. *J. Biol. Chem.* **1997**, *272*, 5016–5023.
- (32) Capon, C.; Laboisie, C. L.; Wieruszkeski, J. M.; Maoret, J. J.; Augeron, C.; Fournet, B. *J. Biol. Chem.* **1992**, *267*, 19248–19257.
- (33) Hang, H. C.; Bertozzi, C. R. *Bioorg. Med. Chem.* **2005**, *13*, 5021–5034.
- (34) Yin, P.; Bousquet-Moore, D.; Annangudi, S. P.; Southey, B. R.; Mains, R. E.; Eipper, B. A.; Sweedler, J. V. *PLoS One* **2011**, *6*, e28679.
- (35) Cate, C. C.; Pettengill, O. S.; Sorenson, G. D. *Cancer Res.* **1986**, *46*, 812–818.
- (36) Harrd, K.; Damm, J. B. L.; Spruijt, M. P. N.; Bergwerff, A. A.; Kamerling, J. P.; Van Dedem, G. W. K.; Vliegenthart, J. F. G. *Eur. J. Biochem.* **1992**, *205*, 785–798.
- (37) Lloyd, K. O.; Burchell, J.; Kudryashov, V.; Yin, B. W. T.; Taylor-Papadimitriou, J. *J. Biol. Chem.* **1996**, *271*, 33325–33334.
- (38) van Schooten, C. J. M.; Denis, C. V.; Lisman, T.; Eikenboom, J. C. J.; Leebeek, F. W.; Goudemand, J.; Fressinaud, E.; van den Berg, H. M.; de Groot, P. G.; Lenting, P. J. *Blood* **2007**, *109*, 2430–2437.
- (39) Chia, J.; Goh, G.; Bard, F. *Biochim. Biophys. Acta, Gen. Subj.* **2016**, *1860*, 1623–1629.
- (40) Zeng, Q. H.; Zhao, R. X.; Chen, J. F.; Li, Y. N.; Li, X. D.; Liu, X. L.; Zhang, W. M.; Quan, C. S.; Wang, Y. S.; Zhai, Y. X.; Wang, J. W.; Youssef, M.; Cui, R. T.; Liang, J. Y.; Genovese, N.; Chow, L. T.; Li, Y. L.; Xu, Z. X. *Proc. Natl. Acad. Sci. U. S. A.* **2016**, *113*, 9333–9338.
- (41) Gram Schjoldager, K. T.-B.; Vester-Christensen, M. B.; Goth, C. K.; Petersen, T. N.; Brunak, S.; Bennett, E. P.; Levery, S. B.; Clausen, H. *J. Biol. Chem.* **2011**, *286*, 40122–40132.
- (42) Zhang, L. P.; Syed, Z. A.; van Dijk Hard, I.; Lim, J. M.; Wells, L.; Ten Hagen, K. G. *Proc. Natl. Acad. Sci. U. S. A.* **2014**, *111*, 7296–7301.
- (43) Tagliabracchi, V. S.; Engel, J. L.; Wiley, S. E.; Xiao, J. Y.; Gonzalez, D. J.; Nidumanda Appaiah, H.; Koller, A.; Nizet, V.; White, K. E.; Dixon, J. E. *Proc. Natl. Acad. Sci. U. S. A.* **2014**, *111*, 5520–5525.
- (44) Ellies, L. G.; Ditto, D.; Levy, G. G.; Wahrenbrock, M.; Ginsburg, D.; Varki, A.; Le, D. T.; Marth, J. D. *Proc. Natl. Acad. Sci. U. S. A.* **2002**, *99*, 10042–10047.
- (45) Vishwanatha, K. S.; Bäck, N.; Lam, T. T.; Mains, R. E.; Eipper, B. A. *J. Biol. Chem.* **2016**, *291*, 9835–9850.

Supporting Information

Detection of Biosynthetic Precursors, Discovery of Glycosylated Forms and Homeostasis of Calcitonin in Human Cancer Cells

Feihua Cao, Allan B. Gamble, Hideki Onagi, Joanna Howes, James E. Hennessy, Chen Gu, Jeremy A. M. Morgan and Christopher J. Easton*

Research School of Chemistry, Australian National University

Canberra, ACT 2601, Australia.

*email: Chris.Easton@anu.edu.au

ABSTRACT: The peptide hormone calcitonin is intimately connected with human cancer development and proliferation. Its biosynthesis is reasoned to proceed via glycine-, α -hydroxyglycine-, glycyllysine- and glycyllslylsine-extended precursors though, as a result of limitations of current analytical methods, until now there has been no procedure capable of detecting these individual species in cell or tissue samples. Therefore their presence and dynamics in cancer had not been established. Here we report the first methodology for the separation, detection and quantification of calcitonin and each of these precursors in human cancer cells. We also report the discovery and characterization of O-glycosylated calcitonin and its analogous biosynthetic precursors. Through direct and simultaneous analysis of the glycosylated and non-glycosylated species, we interrogate the hormone biosynthesis, to observe that the cellular calcitonin level is maintained to mitigate effects of biosynthetic enzyme inhibitors that substantially change the proportions of calcitonin-related species released into the culture medium.

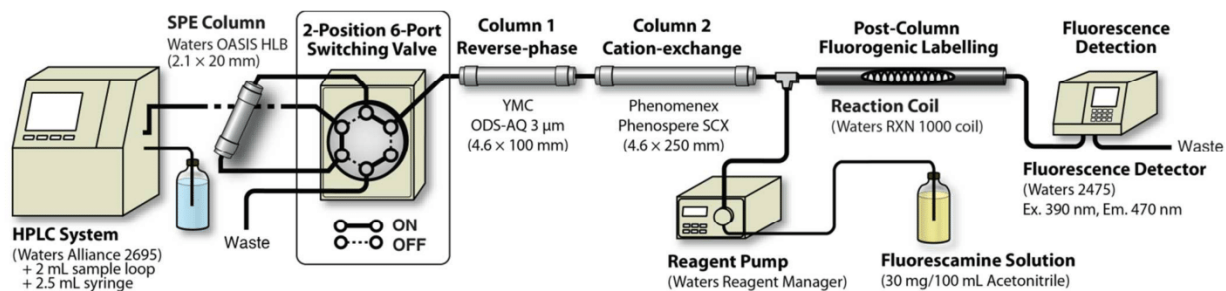


Figure S1. Hardware configuration of the HPLC separation and detection method for HO-CTG, gCT, gCTG, CT, CTG, CTGK and CTGKK.

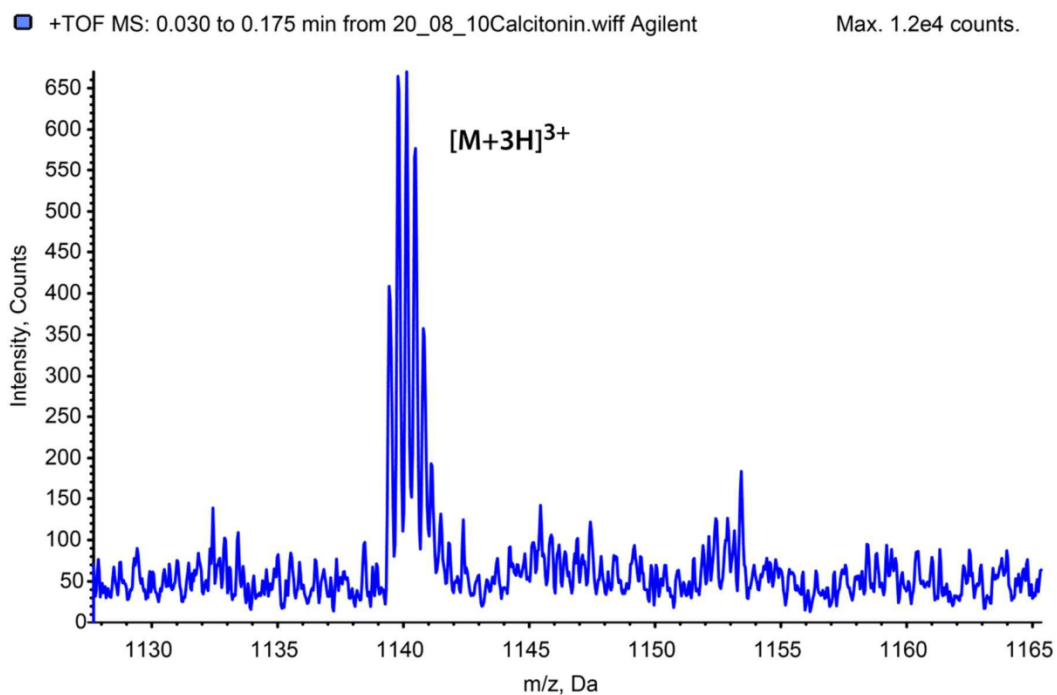


Figure S2. ESI-Mass spectrum of CT (mass 3418 Daltons) produced by DMS53 cells.

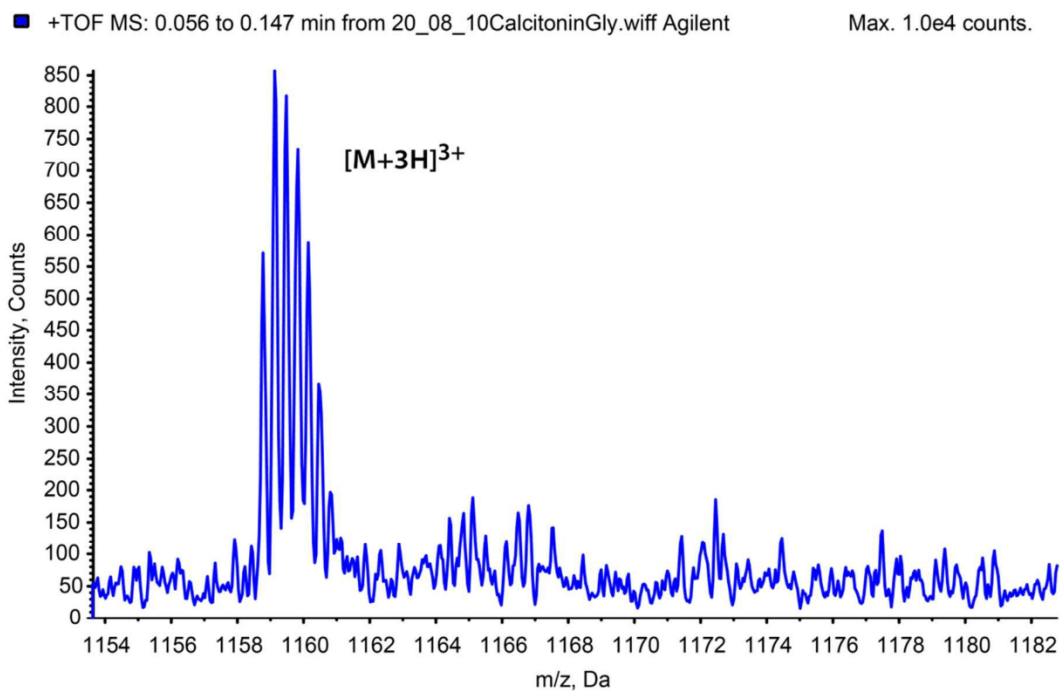


Figure S3. ESI-Mass spectrum of CTG (mass 3476 Daltons) produced by DMS53 cells.

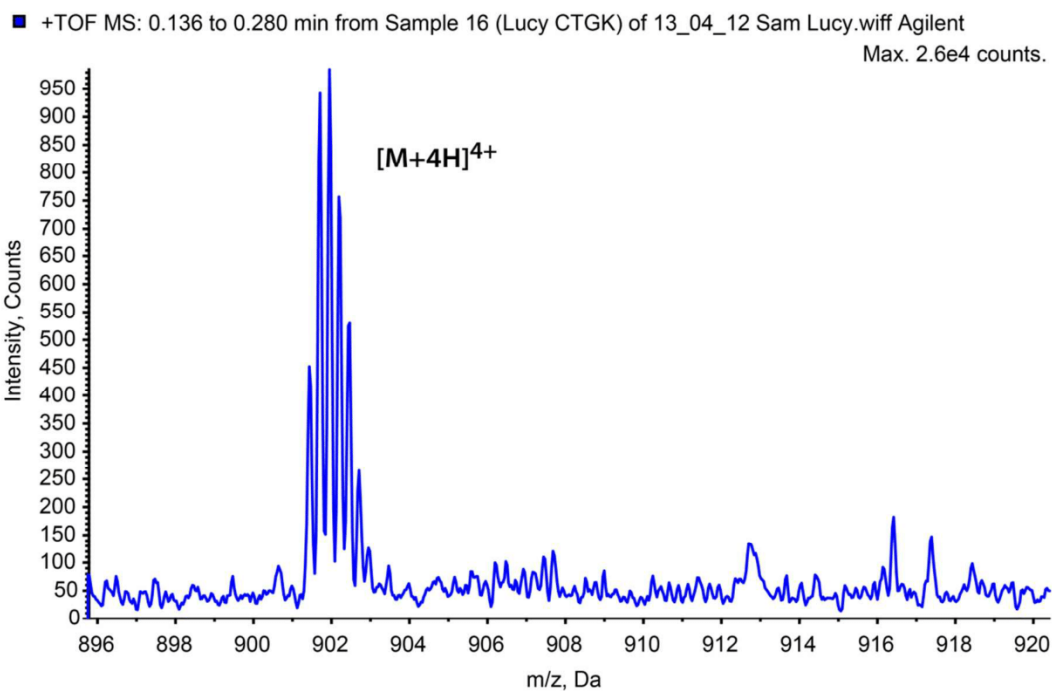


Figure S4. ESI-Mass spectrum of CTGK (mass 3604 Daltons) produced by DMS53 cells.

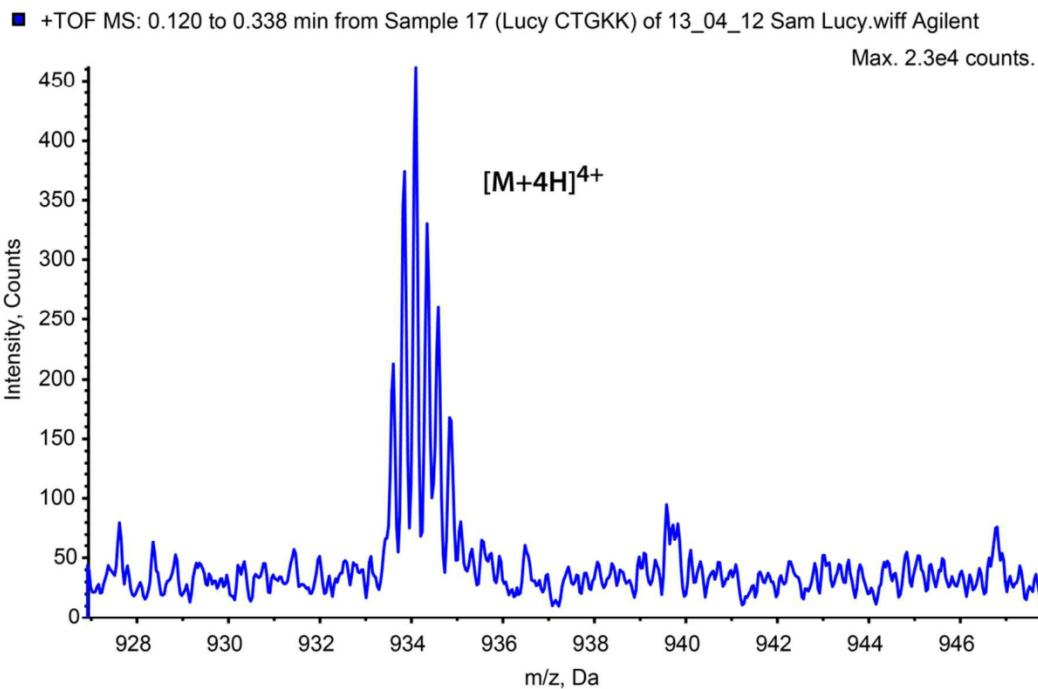


Figure S5. ESI-Mass spectrum of CTGKK (mass 3732 Daltons) produced by DMS53 cells.

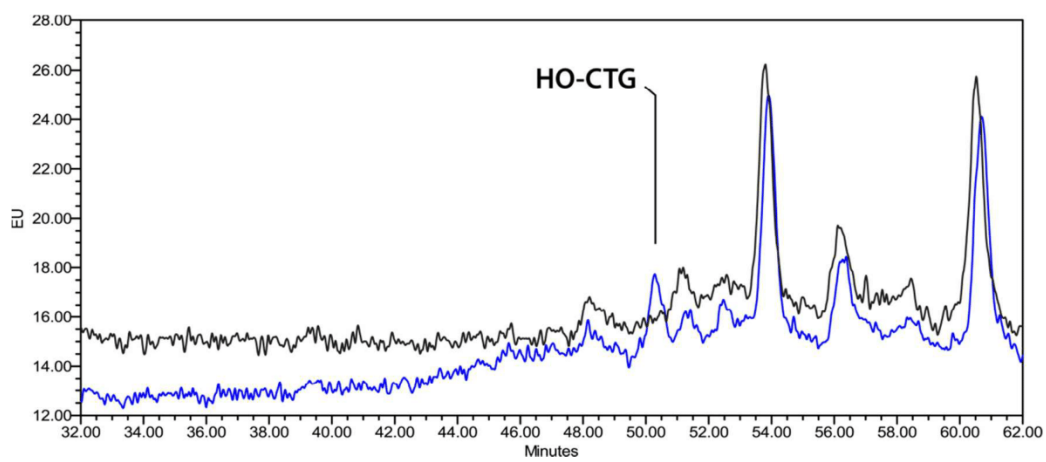


Figure S6. HPLC trace of DMS53 cell culture medium (black) overlaid with trace of medium to which HO-CTG standard has been added (blue).

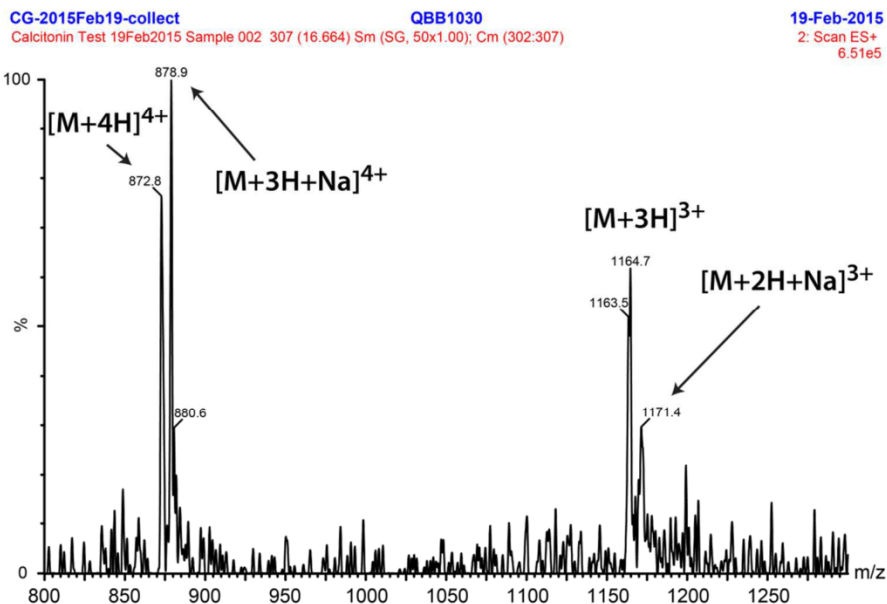


Figure S7. ESI mass spectrum (Waters Alliance 2695 separation module coupled to Waters TQD detector) of HO-CTG produced by DMS53 cells.

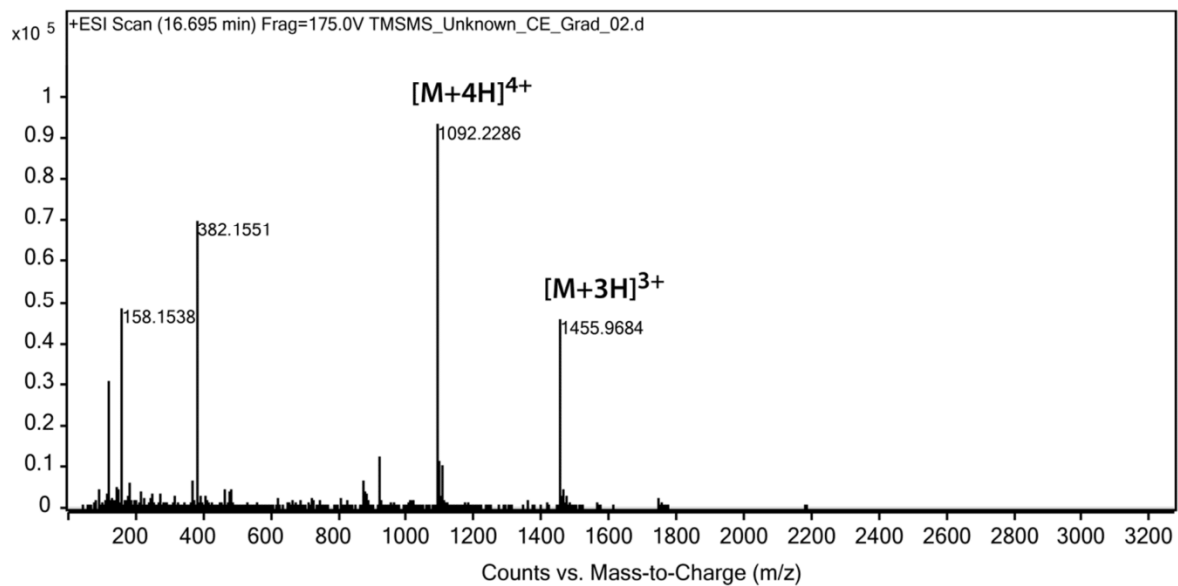


Figure S8. ESI mass spectrum (Agilent 6530 Accurate-Mass Q-TOF LC/MS) of gCT produced by DMS53 cells.

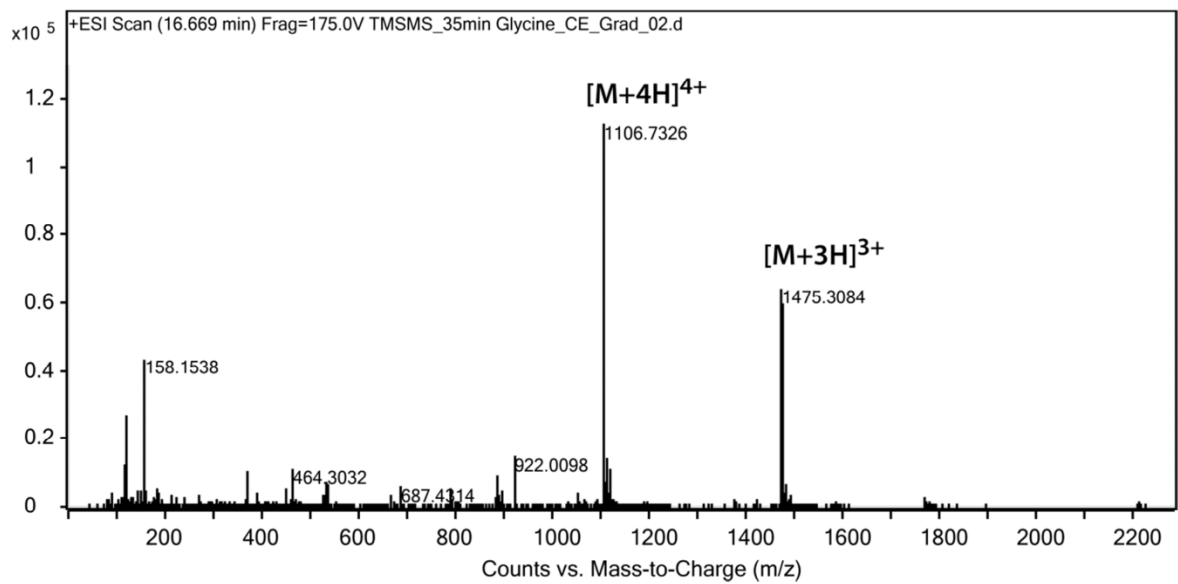


Figure S9. ESI mass spectrum (Agilent 6530 Accurate-Mass Q-TOF LC/MS) of gCTG produced by DMS53 cells.

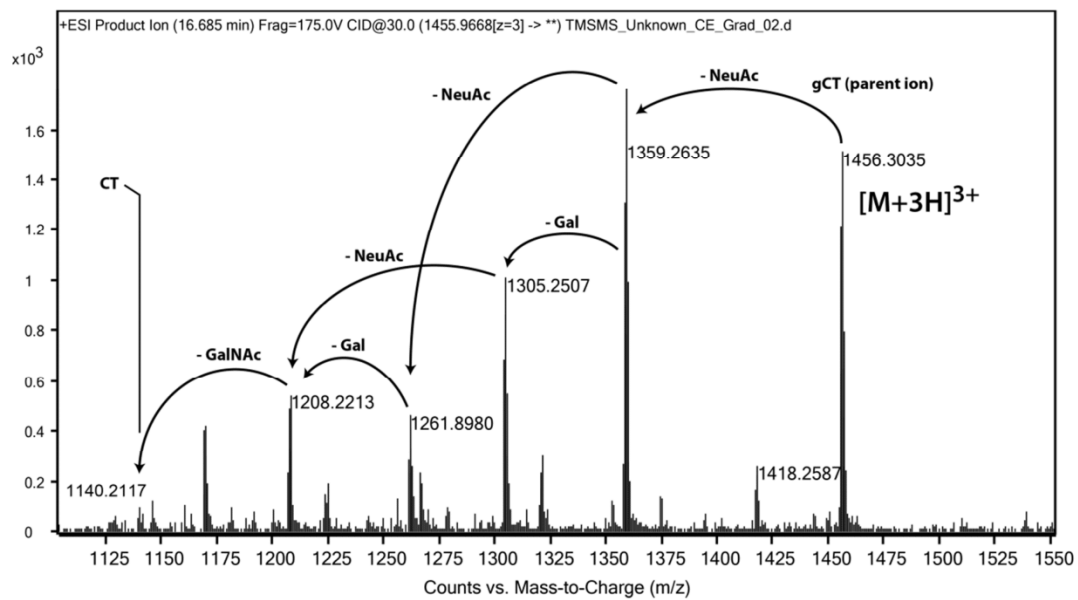


Figure S10. Q-TOF MS/MS spectrum (Agilent 6530 Accurate-Mass Q-TOF LC/MS) of gCT.

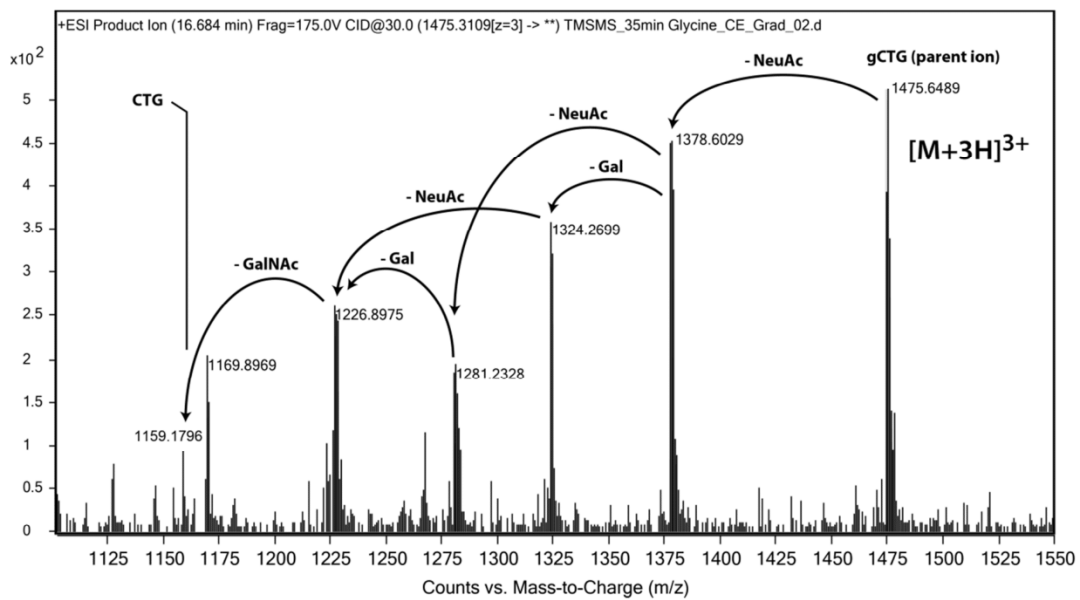


Figure S11. Q-TOF MS/MS spectrum (Agilent 6530 Accurate-Mass Q-TOF LC/MS) of gCTG.

LC-MS/MS MRM Analysis for gCTGK and gCTGKK

Analysis was performed using a Waters Alliance 2695 separation module coupled to a Waters TQD detector. HPLC Column: Waters Sunfire C18, 5 μ m, 4.6 \times 150 mm, heated at 30°C. Flow: 0.7 mL/min (15:1 flow splitter). Eluent: acetonitrile/water 5/95 (0-1 min), acetonitrile/water 30/70 (1-30 min, linear), both eluents contain 0.1% formic acid.

gCTGK

Channel 1: Parent (m/z): 1138.2584, Daughter (m/z): 70.0107, Dwell (s): 0.025, Cone (V): 40, Collision (V): 80; Channel 2: Parent (m/z): 1138.2584, Daughter (m/z): 86.1058, Dwell (s): 0.025, Cone (V): 40, Collision (V): 78; Channel 3: Parent (m/z): 1138.2584, Daughter (m/z): 86.5681, Dwell (s): 0.025, Cone (V): 40, Collision (V): 80; Channel 4: Parent (m/z): 1138.2584, Daughter (m/z): 136.0684, Dwell (s): 0.025, Cone (V): 40, Collision (V): 80.

gCTGKK

Channel 1: Parent (m/z): 936.4273, Daughter (m/z): 70.0107, Dwell (s): 0.025, Cone (V): 50, Collision (V): 74; Channel 2: Parent (m/z): 936.4273, Daughter (m/z): 86.1159, Dwell (s): 0.025, Cone (V): 50, Collision (V): 74; Channel 3: Parent (m/z): 936.4273, Daughter (m/z): 86.698, Dwell (s): 0.025, Cone (V): 50, Collision (V): 78; Channel 4: Parent (m/z): 936.4273, Daughter (m/z): 129.1146, Dwell (s): 0.025, Cone (V): 50, Collision (V): 76.

Chapter Seven

Conclusions and Future Directions

PAM is considered to be a key enzyme for regulation of amidated peptide hormones because more than a half of human peptide hormones are amidated peptide hormones, which are produced only through PAM catalysis. The consensus sequence study shows that C-terminal glycine-extended prohormone having penultimate Phe are expected to have strong binding affinity with PAM. It also shows amino acids at the antepenultimate position from the C-terminus has much smaller effect than those at the penultimate position on binding with PAM. The assay of Bex-glycine (**3-4**) illustrates that compound **3-4** is a poor PAM substrate but itself has good activity against DMS53 cells, similar to the parent agent **3-1**, indicating compound **3-4** has potential in cancer therapy but not through the dual activity anticipated.

A new bifunctional PAM assay with HPLC-MS system was developed, which enables simultaneous investigation of PHM and PAL activity. With this new assay, it was demonstrated that compound **1-143** has strong PAL inhibition and relatively low PHM inhibition. The results of structure-activity study show that the pyruvate moiety in compound **1-143** is responsible for PAL inhibition. The pH-dependent PAM inhibition assay with compound **1-143** implies that deprotonation of the enol form of compound **1-143** results in a decrease of PAL inhibition by compound **1-143**. The PAM inhibition assay with compound **1-143** also confirms that PAL activity dominates the conversion of hydroxylated intermediates to amidated products within two hours. The subsequent

stability study of compound **1-143** illustrated that compound **1-143** decomposes to compound **5-1** almost completely in aqueous solution over two days. This may inform the design of more stable PAL inhibitors in the future.

The results that the intermediate HO-CTG in the culture medium of DMS53 cells is below the detection limit of fluorescence detector and over one hundred times lower than CTG and CT, suggests PAL catalysis is much better than PHM catalysis in human cells. Under these circumstances, the accumulation of CTG demonstrates that catalytic turnover by PHM limits the production of CT. In other words, PHM activity is the rate-limiting step of PAM activity. In future, the focus should be the cofactors of PHM activity such as ascorbate. Preliminary results in Appendix shows that ascorbate levels play a role in PHM activity through the isolated PAM competitive assay, and that SIN-1 is likely to inactivate PHM activity through inhibiting semidehydroascorbate reductase (SDR) that is responsible for reducing semidehydroascorbate back to ascorbate during ascorbate recycling.

Chapter Eight

Experimental

8.1 General

Melting points measuring method was established using a Stanford Research Systems MPA 100 OptiMelt automated melting point system with digital image processing technology operated with Meltview software.

NMR spectra were recorded on Varian Mercury 300 (300 MHz for ^1H and 75 MHz for ^{13}C), Bruker AscendTM 400 (400 MHz for ^1H and 100 MHz for ^{13}C), and Bruker Avance 700 (700 MHz for ^1H and 150 MHz for ^{13}C) spectrometers. The NMR solvent Chloroform-D (99.8% D) and DMSO-D₆ (99.9% D) were purchased from Cambridge Isotope Laboratories Inc, and D₂O (99.8% D) and CD₃OD (99.8%) were purchased from Sigma-Aldrich Co.

The HPLC-MS method about isolated PAM assay was conducted on Waters Alliance 2690 liquid chromatography (plus flow splitter) and Waters ACQUITY TQ mass detector. ESI mass spectra were recorded using a Micromass LC-ZMD single quadrupole liquid chromatograph mass spectrometer for low resolution (LR).

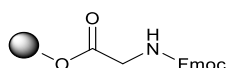
The DMS53 cell line were grown in GIBCO[®] RPMI-1640 medium supplemented with 10% fetal bovine serum obtained from Invitrogen. The tripeptide substrate (*R*)-Tyr-

(*S*)-Val-Gly-COOH used in isolated enzyme assays was obtained from Bachem AG. Fmoc-Gly-OH, Fmoc-(*S*)-Arg(Pbf)-OH, Fmoc-(*S*)-Phe-OH, Fmoc-(*S*)-Gln(Trt)-OH, Fmoc-(*S*)-Asp(OtBu)-OH, Fmoc-(*S*)-His(Bom)-OH, BOP and sodium were purchased from Merck Pty. Ltd. Bexarotene were purchased from Atomole Scientifica Co. Ltd. HBTU, Fmoc-(*S*)-Pro-OH, Fmoc-Ala-OH and BOP were purchased from Auspep Pty Ltd. NaOH, NaHCO₃, NaCl, K₂CO₃, NH₄Cl, Et₃N, CuSO₄ and ammonium acetate were purchased from Ajax Finechem Pty Ltd. Na₂S₂O₅ were purchased from May & Baker Ltd. Ethyl glyoxalate solution (50% w/w in toluene) were purchased from Thermo Fisher Scientific Inc. HOBt, DMAP, DIC, DMAP, DIPEA, TIPS, TFA, NMO, TEMPO, EDC, PBA, Pd/C, Wang resins, piperidine, thionyl chloride, diethyl oxalate, *n*-Butyl-lithium, lithium hydroxide monohydrate, NaClO₂, NaClO, OsO₄, MgSO₄, NaBH₃CN, Ac₂O, (*S*)-Phe, NMM, *N*-Acetyl-(*S*)-Histidine, *tert*-butyl glycine hydrochloride, 4-Bromo-1-butene, *tert*-butyl bromoacetate, phenylacetic acid, *N*, *O*-Dimethylhydroxylamine hydrochloride, molecular sieves 3Å, dimethyl methylphosphonate, esterase from porcine liver, fumaric acid, benzyl alcohol, SIN-1, ascorbate, bovine liver catalase and fluorescamine were purchased from Sigma Aldrich Chemical Co. Glycyl-extended calcitonin and calcitonin were purchased from GL Biochem (Shanghai) Ltd. Unless otherwise noted, all reagents were obtained from commercial suppliers and used without further purification.

8.2 Experimental for Chapter 2: Study of Sequence Recognition by PAM

8.2.1 Synthesis Work Described in Chapter 2

Fmoc-Gly-Wang resin (2-1)

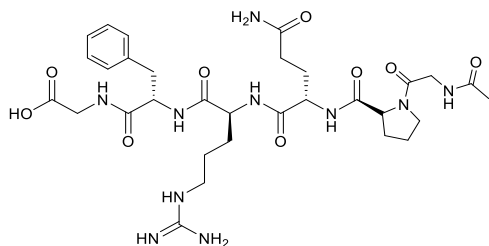


2-1

Commercial dry Wang resin (339 mg, 0.40 mmol) was placed in a manual reaction vessel with DCM (4.5 mL) and DMF (0.5 mL) for 2 h. The organic solvent was then removed by filtration and the swollen Wang resin was treated with DMF (3 mL) containing Fmoc-Gly-COOH (297 mg, 1.00 mmol, 2.5 eq), DIC (160 μ L, 1.00 mmol, 2.5 eq), HOBt (135 mg, 1.00 mmol, 2.5 eq), and DMAP (5 mg, 0.04 mmol, 0.04 eq). The mixture was agitated gently with a nitrogen flow for 2 h. The solvent was then removed by filtration and the resin was washed with DMF (3×5 mL), MeOH (3×5 mL) and dried *in vacuo*. A sample of the resin (10 mg) was used for testing the loading efficiency of Fmoc-Gly through Fmoc determination. It was added to piperidine in DMF (50 μ L, 20%, v/v) to conduct Fmoc deprotection, followed by dilution with DMF (4.95 mL). The solution was analysed by UV-Vis spectroscopy at 278 nm against a blank sample that contained piperidine in DMF (50 μ L, 20%, v/v) with DMF (4.95 mL). The loading efficiency of Fmoc-Gly to the resin of 65% was calculated based on literature.^[158] The loaded Fmoc-Gly-Wang resin **2-1** was again treated with DCM (4.5 mL) and DMF (0.5 mL) for 2 h, then DMF (3 mL), Ac₂O (80 μ L, 0.80 mmol, 2.0 eq), and pyridine (70 μ L, 0.80 mmol, 2.0 eq) were added. The mixture was agitated with a

nitrogen flow for 30 min. The solution was then filtered off and the resin was washed with DMF (3×5 mL).

***N*-Ac-Gly-(*S*)-Pro-(*S*)-Gln-(*S*)-Arg-(*S*)-Phe-Gly-COOH (2-14)**



2-14

To Fmoc-Gly-Wang resin **2-1** was added piperidine in DMF (3.4 mL, 20%, v/v) and the mixture was agitated with a nitrogen flow at room temperature for 1 h to produce compound **2-2**. The solvent was then filtered off and the resin was washed with DMF (3×5 mL). The glycine-substituted resin **2-2** was elongated to peptide **2-12** with the following protected amino acids: Fmoc-(*S*)-Phe-COOH, Fmoc-(*S*)-Arg(Pbf)-COOH, Fmoc-(*S*)-Gln(Trt)-COOH, Fmoc-(*S*)-Pro-COOH, and Fmoc-Gly-COOH. Each amino acid was used in 2-fold excess and was coupled in the presence of HOBt (108 mg, 0.80 mmol, 2.00 eq), HBTU (303 mg, 0.80 mmol, 2.00 eq), and DIPEA (280 μ L, 1.60 mmol, 4.00 eq) in DMF (3.0 mL). Each coupling reaction mixture was agitated with a nitrogen flow at room temperature for 2 h, filtered in order to remove excess reagents, and then washed with DMF (3×5 mL). Fmoc deprotection was achieved by addition of piperidine in DMF (3.4 mL, 20%, v/v), agitation with a nitrogen flow at room temperature for 1 h, and washing with DMF (3×5 mL). After all the desired coupling and Fmoc deprotection reactions, to the crude compound **2-12** was added a mixture of excess Ac_2O (500 μ L), pyridine (500 μ L), and DMF (5 mL), and the

mixture was agitated with a nitrogen flow at room temperature for 30 min to give acetylated peptide on the Wang resin **2-13**. After filtration, the resin **2-13** was added to a mixture of TFA (3.2 mL), TIPS (0.1 mL) and H₂O (0.1 mL) and then agitated at room temperature for 2 h. The mixture was filtered and the filtrate was transferred into cold Et₂O (80 mL) in two Falcon tubes and placed in a -20 °C freezer overnight. The tubes were then centrifuged at 5000 g, the supernatant was removed, and a sample (approx. 3 mg) of the product precipitate was dissolved in 10% aqueous MeOH solution (50 µL) and analysed by HPLC using an Alltima C18 5µ (22 × 250 mm) column, at a flow rate of 8 mL/min with a UV-Vis spectroscopy at 210 nm. The analysis was carried out with a linear gradient elution of 40:60 (MeOH: H₂O (0.1% TFA), v/v) to 50:50 between 0-20 min, followed by a gradient elution of 50:50 to 95:5 between 20-31 min and a gradient elution of 95:5 to 40:60 between 31-36 min. Finally, the solvent system was maintained at 40:60 for 4 min more. The resulting HPLC is reproduced in **Figure 8.1**, and showed two dominant peaks at 29.50 and 31.90 min. Samples corresponding to each of these two peaks were isolated through HPLC. Mass spectrometry of the peak at 29.50 min displayed ions at m/z 703.7, which corresponds to the $[M+H]^+$ for hexapeptide **2-14**; the peak at 31.90 min displayed ions at m/z 646.7, which is 57 less than that of the former peak, the difference being equal to the mass of a glycine residue. Based on this analysis, preparative HPLC was used to isolate compound **2-14**. The column fractions were concentrated *via* freeze drying to give compound **2-14** (10 mg, 3.6%) as a colourless powder.

¹H NMR (400 MHz, D₂O): δ7.35 (m, 5H), 4.73 (dd, $J = 9.6, 5.7$ Hz, 1H), 4.43 (dd, $J = 8.6, 5.0$ Hz, 1H), 4.26 (m, 2H), 4.09 (s, 2H), 3.96 (d, $J = 17.9$ Hz, 1H), 3.92 (d, $J = 17.9$ Hz, 1H), 3.65 (m, 2H), 3.23 (dd, $J = 14.0, 5.7$ Hz, 1H), 3.13 (t, $J = 6.9$ Hz, 2H),

3.00 (dd, $J = 14.0, 9.6$ Hz, 1H), 2.30 (m, 3H), 2.06 (m, 8H), 1.67 (m, 2H), 1.47 (m, 2H); **MS (ESI) (+ve)**: m/z 703.7 $[M+H]^+$. **HRMS (ESI)** calcd. for $C_{31}H_{47}N_{10}O_9$ $[M+H]^+$ m/z 703.3527, found m/z 703.3528 (**Figure 8.2**).

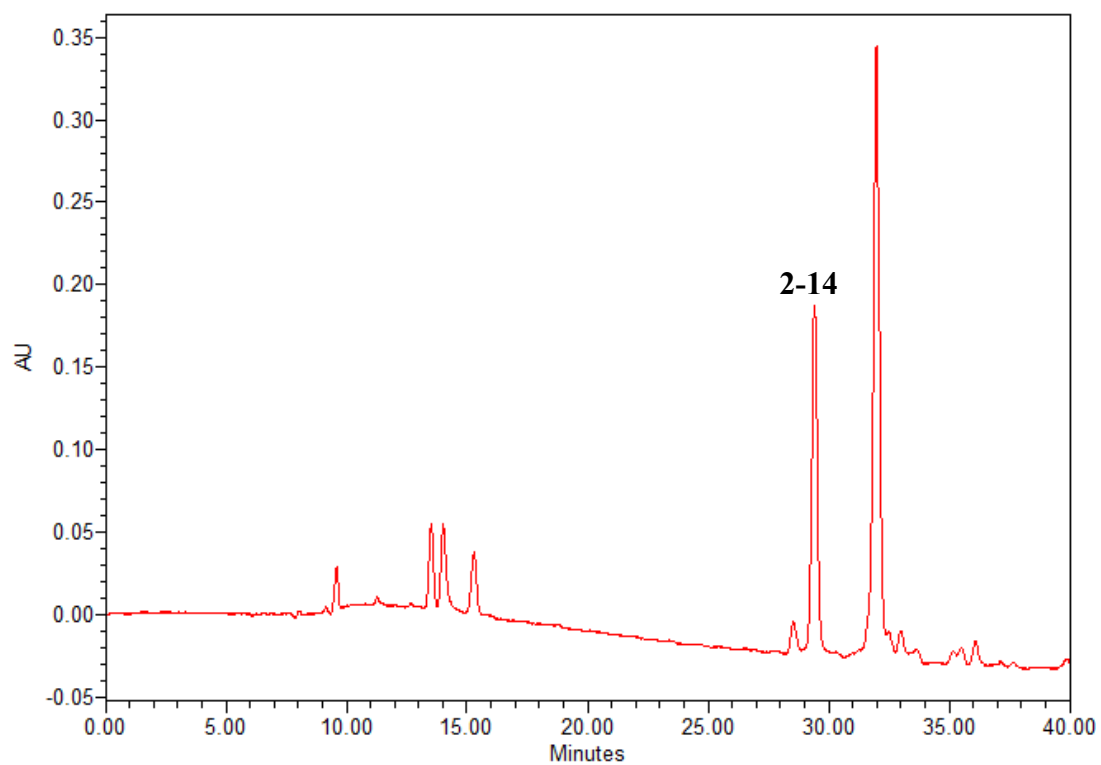


Figure 8.1 HPLC chromatogram of crude *N*-Ac-Gly-(*S*)-Pro-(*S*)-Gln-(*S*)-Arg-(*S*)-Phe-Gly-COOH (**2-14**).

Single Mass Analysis

Tolerance = 3.0 PPM / DBE: min = -1.5, max = 20.0

Element prediction: Off

Number of isotope peaks used for i-FIT = 3

Monoisotopic Mass, Even Electron Ions

105 formula(e) evaluated with 1 results within limits (all results (up to 1000) for each mass)

Elements Used:

C: 0-31 H: 0-48 N: 0-10 O: 0-9

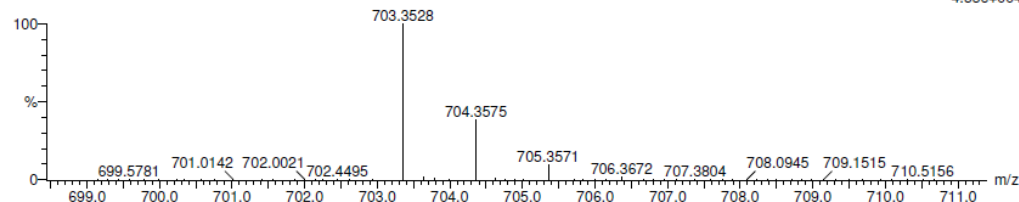
ACNH-GPQRFG-COOH^{EO}

30630

0023 48 (2.097)

KE375

08-Jan-2014 12:02:36

1: TOF MS ES+
4.53e+004

Minimum:				-1.5		
Maximum:		5.0	3.0	20.0		
Mass	Calc. Mass	mDa	PPM	DBE	i-FIT	Formula
703.3528	703.3527	0.1	0.1	13.5	5.8	C31 H47 N10 O9

Figure 8.2 High resolution MS of isolated *N*-Ac-Gly-(*S*)-Pro-(*S*)-Gln-(*S*)-Arg-(*S*)-Phe-Gly-COOH (**2-14**).

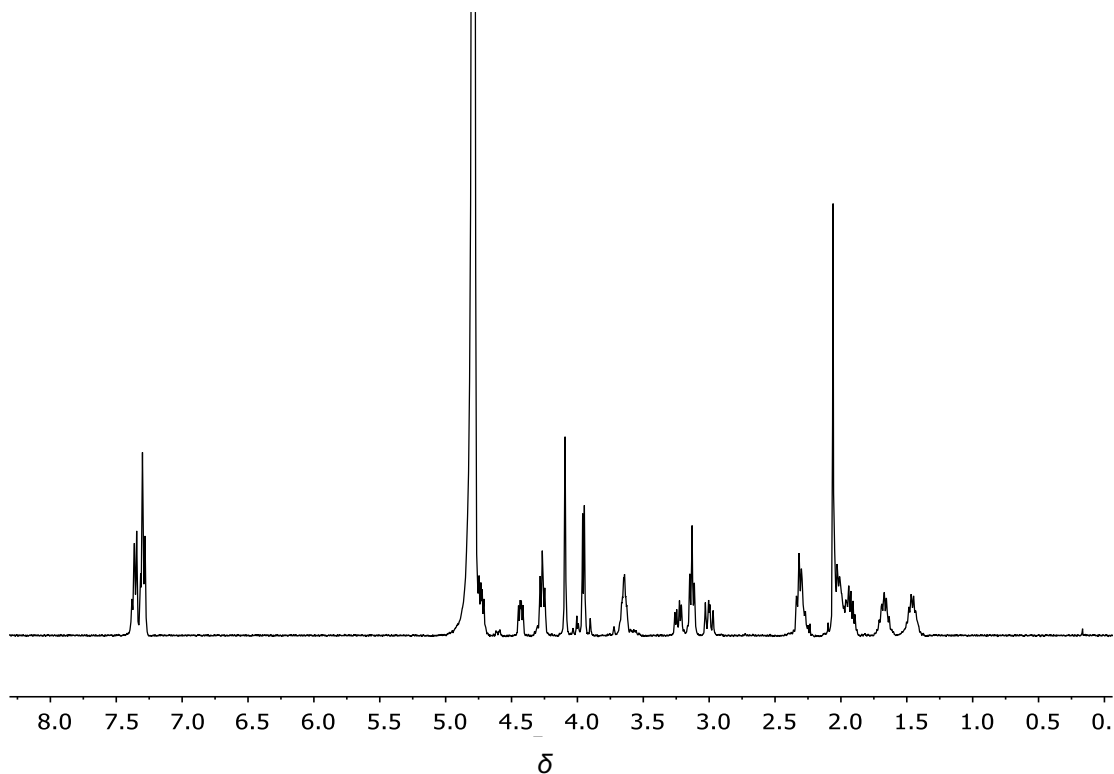
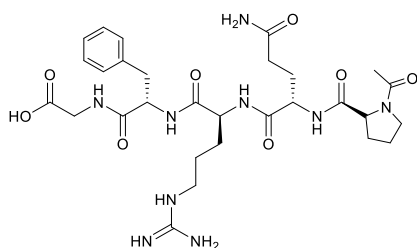


Figure 8.3 ¹H NMR of spectrum of compound **2-14**.

***N*-Ac-(*S*)-Pro-(*S*)-Gln-(*S*)-Arg-(*S*)-Phe-Gly-COOH (2-15)**



2-15

Peptide **2-15** was synthesised using the same quantities and techniques described for compound **2-14**. After the elongation from compounds **2-1** to **2-10** with Fmoc-(*S*)-Phe-COOH, Fmoc-(*S*)-Arg(Pbf)-COOH, Fmoc-(*S*)-Gln(Trt)-COOH, and Fmoc-(*S*)-Pro-COOH, compound **2-10** was acetylated, acidified, and precipitated in cold Et₂O in exactly the same manner as described for compound **2-12**. The analysis of a small amount of product precipitate was then carried out with a linear gradient elution of 30:70 (MeOH: H₂O (0.1% TFA), v/v) to 40:60 between 0-20 min. The resulting HPLC chromatogram is reproduced in **Figure 8.4** and showed several dominant peaks. Samples corresponding to each of these were isolated through HPLC. Mass spectrometry of the peak at 11.40 min displayed ions at *m/z* 646.8, which corresponds to the [M+H]⁺ for pentapeptide **2-15**; the peak at 12.70 min displayed ions at *m/z* 589.7, which is 57 less than that of the former peak, the difference being equal to the mass of a glycine residue. Based on this analysis, preparative HPLC was used to isolate compound **2-15**. The column fractions were concentrated *via* freeze drying to give compound **2-15** (8 mg, 3.2%) as a colourless powder.

¹H NMR (400 MHz, D₂O): δ 7.33 (m, 5H), 4.73 (dd, J = 9.4, 5.9 Hz, 1H), 4.38 (dd, J = 8.7, 4.9 Hz, 1H), 4.27 (m, 2H), 4.00 (d, J = 17.9 Hz, 1H), 3.96 (d, J = 17.9 Hz, 1H), 3.65 (m, 2H), 3.23 (dd, J = 14.0, 5.9 Hz, 1H), 3.14 (t, J = 7.0 Hz, 2H), 3.00 (dd, J = 14.0, 9.4 Hz, 1H), 2.32 (m, 3H), 2.13 (s, 3H), 1.96 (m, 5H), 1.67 (m, 2H), 1.47 (m, 2H); **MS (ESI) (+ve):** m/z 646.8 [M+H]⁺. **HRMS (ESI) calcd.** for C₂₉H₄₄N₉O₈ [M+H]⁺ m/z 646.3313, found m/z 646.3314 (**Figure 8.5**).

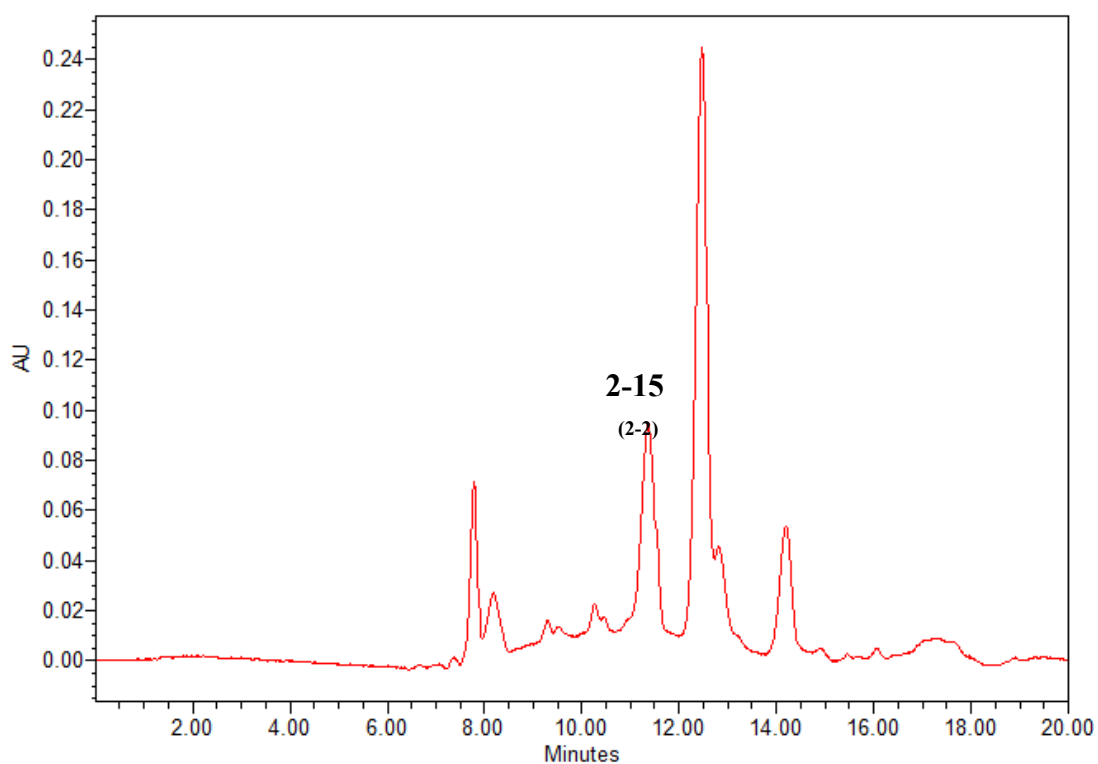


Figure 8.4 HPLC chromatogram of crude *N*-Ac-(*S*)-Pro-(*S*)-Gln-(*S*)-Arg-(*S*)-Phe-Gly-COOH (**2-15**).

Single Mass Analysis

Tolerance = 3.0 PPM / DBE: min = -1.5, max = 20.0

Element prediction: Off

Number of isotope peaks used for i-FIT = 3

Monoisotopic Mass, Even Electron Ions

58 formula(e) evaluated with 1 results within limits (all results (up to 1000) for each mass)

Elements Used:

C: 0-29 H: 0-45 N: 3-9 O: 0-8

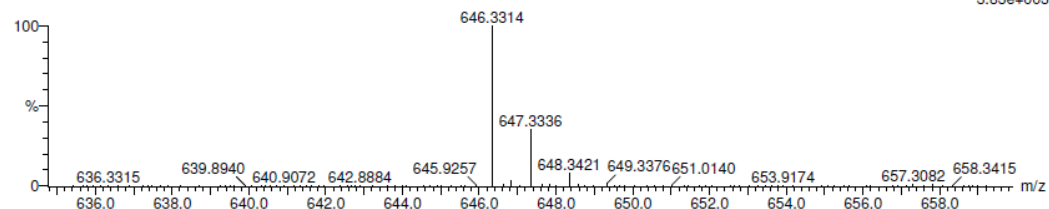
PQFPG2/EO

30504

1684 31 (1.364)

KE375

17-Dec-2013 14:59:29

1: TOF MS ES+
3.83e+003Minimum: -1.5
Maximum: 5.0 3.0 20.0

Mass	Calc. Mass	mDa	PPM	DBE	i-FIT	Formula
646.3314	646.3313	0.1	0.2	12.5	1.1	C29 H44 N9 O8

Figure 8.5 High resolution MS of isolated *N*-Ac-(*S*)-Pro-(*S*)-Gln-(*S*)-Arg-(*S*)-Phe-Gly-COOH (**2-15**).

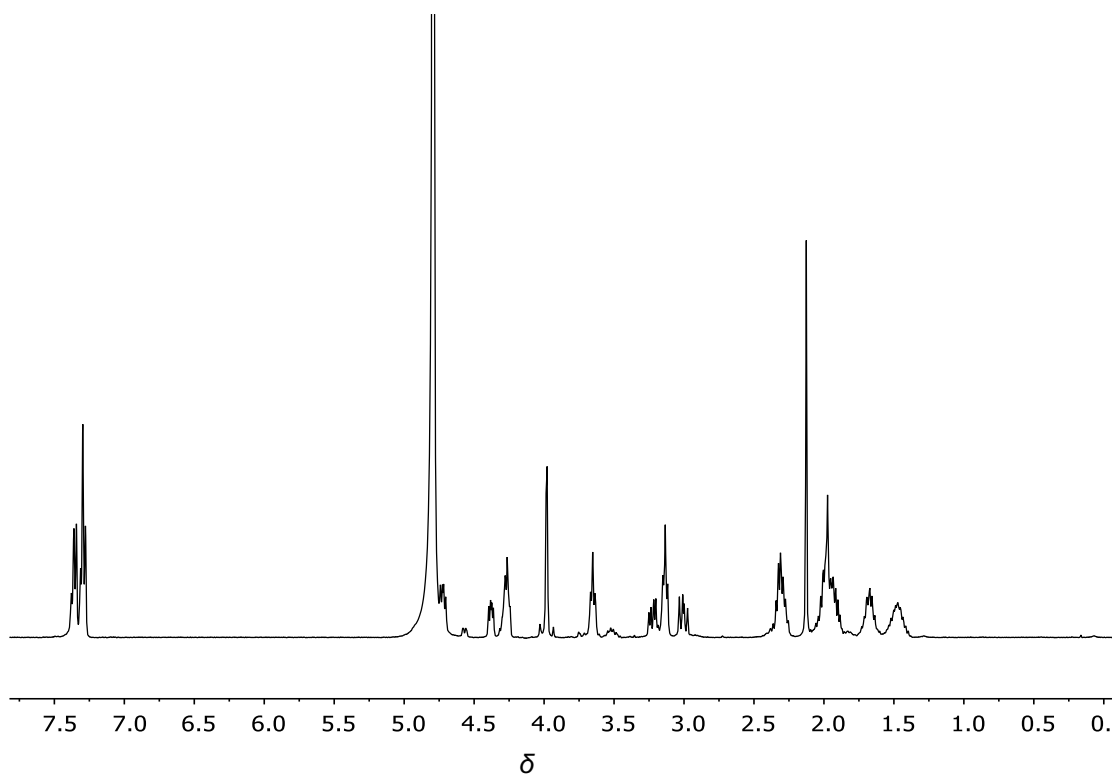
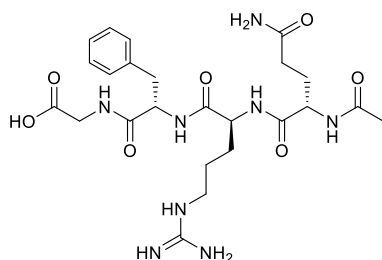


Figure 8.6 ^1H NMR of spectrum of compound **2-15**.

***N*-Ac-(*S*)-Gln-(*S*)-Arg-(*S*)-Phe-Gly-COOH (2-16)**



2-16

Peptide **2-16** was synthesised using the same quantities and techniques described for compound **2-14**. After the elongation from compounds **2-1** to **2-8** with Fmoc-(*S*)-Phe-COOH, Fmoc-(*S*)-Arg(Pbf)-COOH, and Fmoc-(*S*)-Gln(Trt)-COOH, compound **2-8** was acetylated, acidified, and precipitated in cold Et₂O in exactly the same manner as described for compound **2-12**. The analysis of a small amount of product precipitate was then carried out with a linear gradient elution of 45:55 (MeOH: H₂O (0.1% TFA), v/v) to 60:40 between 0-15 min, followed by maintenance of 95:5 between 15-20 min. The resulting HPLC chromatogram is reproduced in **Figure 8.7** and showed several dominant peaks. Samples corresponding to each of these were isolated through HPLC. Mass spectrometry of the peak at 8.30 min displayed ions at *m/z* 549.7, which corresponds to the [M+H]⁺ for tetrapeptide **2-16**. Based on this analysis, preparative HPLC was used to isolate **2-16**. The column fractions were concentrated *via* freeze drying to give compound **2-16** (15 mg, 6.7%) as a colourless powder.

¹H NMR (400 MHz, D₂O): δ7.35 (m, 5H), 4.70 (dd, *J* = 9.4, 5.7 Hz, 1H), 4.29 (dd, *J* = 8.2, 6.1 Hz, 1H), 4.22 (dd, *J* = 8.4, 6.2 Hz, 1H), 3.99 (d, *J* = 17.9 Hz, 1H), 3.94 (d,

$J = 17.9$ Hz, 1H), 3.23 (dd, $J = 13.9, 5.7$ Hz, 1H), 3.14 (t, $J = 6.9$ Hz, 2H), 3.00 (dd, $J = 13.9, 9.4$ Hz, 1H), 2.27 (m, 2H), 2.03 (s, 3H), 1.93 (m, 2H), 1.68 (m, 2H), 1.48 (m, 2H); **MS (ESI) (+ve):** m/z 549.7 [M+H]⁺. **HRMS (ESI)** calcd. for C₂₄H₃₇N₈O₇ [M+H]⁺ m/z 549.2785, found m/z 549.2785 (**Figure 8.8**).

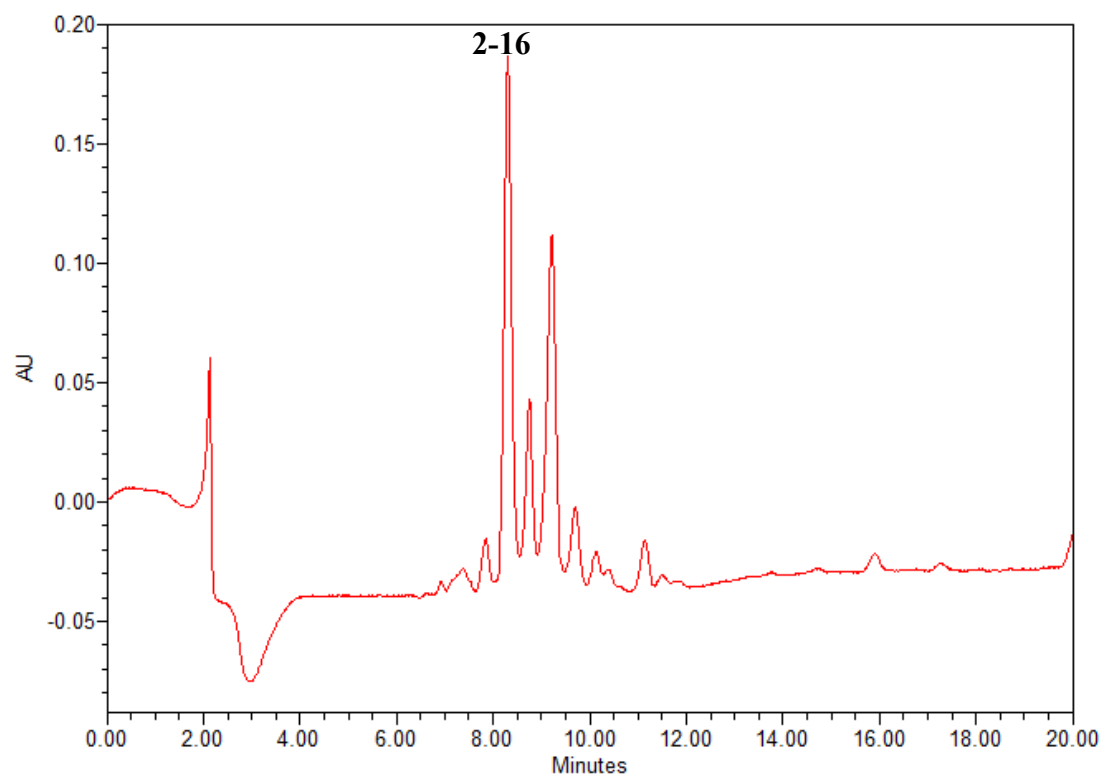


Figure 8.7 HPLC chromatogram of crude *N*-Ac-(*S*)-Gln-(*S*)-Arg-(*S*)-Phe-Gly-COOH (**2-16**).

Single Mass Analysis

Tolerance = 3.0 PPM / DBE: min = -1.5, max = 60.0

Element prediction: Off

Number of isotope peaks used for i-FIT = 3

Monoisotopic Mass, Even Electron Ions

416 formula(e) evaluated with 1 results within limits (all results (up to 1000) for each mass)

Elements Used:

C: 0-100 H: 0-100 N: 1-8 O: 0-7

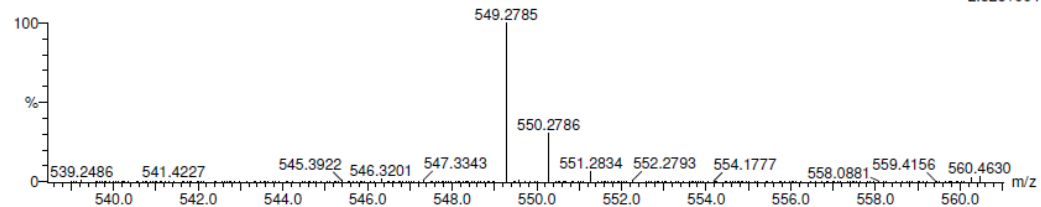
ORFG/AJ

30302

1619 15 (0.664) Cm (13:16)

KE375

03-Dec-2013 12:55:07

1: TOF MS ES+
2.52e+004

Minimum:

Maximum:

5.0

3.0

-1.5

60.0

Mass	Calc. Mass	mDa	PPM	DBE	i-FIT	Formula
549.2785	549.2785	0.0	0.0	10.5	4.0	C24 H37 N8 O7

Figure 8.8 High resolution MS of isolated *N*-Ac-(*S*)-Gln-(*S*)-Arg-(*S*)-Phe-Gly-COOH (2-16).

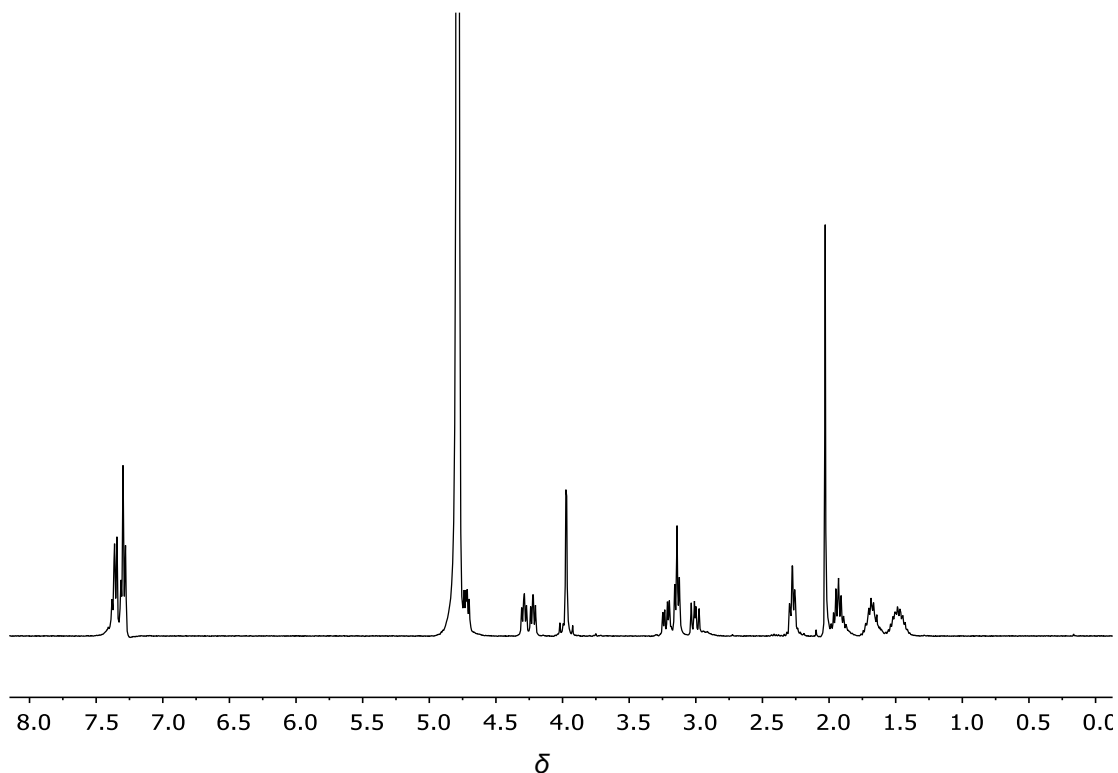
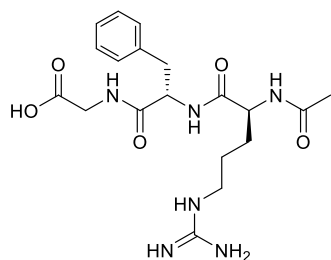


Figure 8.9 ^1H NMR of spectrum of compound 2-16.

***N*-Ac-(*S*)-Arg-(*S*)-Phe-Gly-COOH (2-17)**



2-17

Peptide **2-17** was synthesised using the same quantities and techniques described for compound **2-14**. After the elongation from peptides **2-1** to **2-6** with Fmoc-(*S*)-Phe-COOH and Fmoc-(*S*)-Arg(Pbf)-COOH, compound **2-6** was acetylated, acidified, and precipitated in cold Et₂O in exactly the same manner as described for compound **2-12**. The analysis of a small amount of product precipitate was then carried out with a linear gradient elution of 5:95 (MeOH: H₂O (0.1% TFA), v/v) to 40:60 between 0-50 min, followed by maintenance of 5:95 between 50-55 min. The resulting HPLC chromatogram is reproduced in **Figure 8.10** and showed only one dominant peak at 47.60 min. Sample corresponding to this peak was isolated through HPLC. Mass spectrometry of the peak displayed ions at *m/z* 421.7, which corresponds to the [M+H]⁺ for tripeptide **2-17**. Based on this analysis, the whole precipitate was concentrated *via* freeze drying to give compound **2-17** (15 mg, 9.0 %) as a colourless powder.

¹H NMR (400 MHz, D₂O): δ7.35 (m, 5H), 4.73 (m, 1H), 4.21 (dd, *J* = 7.9, 6.4 Hz, 1H), 4.04 (d, *J* = 17.9 Hz, 1H), 3.99 (d, *J* = 17.9 Hz, 1H), 3.28 (dd, *J* = 14.0, 5.7 Hz,

1H), 3.14 (td, $J = 7.0, 1.8$ Hz, 2H), 3.01 (dd, $J = 14.0, 9.6$ Hz 1H), 2.02 (s, 3H), 1.63 (m, 2H), 1.45 (m, 2H); **MS (ESI) (+ve):** m/z 421.1 $[M+H]^+$. **HRMS (ESI)** calcd. for $C_{19}H_{29}N_6O_5$ $[M+H]^+$ m/z 421.2199, found m/z 421.2206 (**Figure 8.11**).

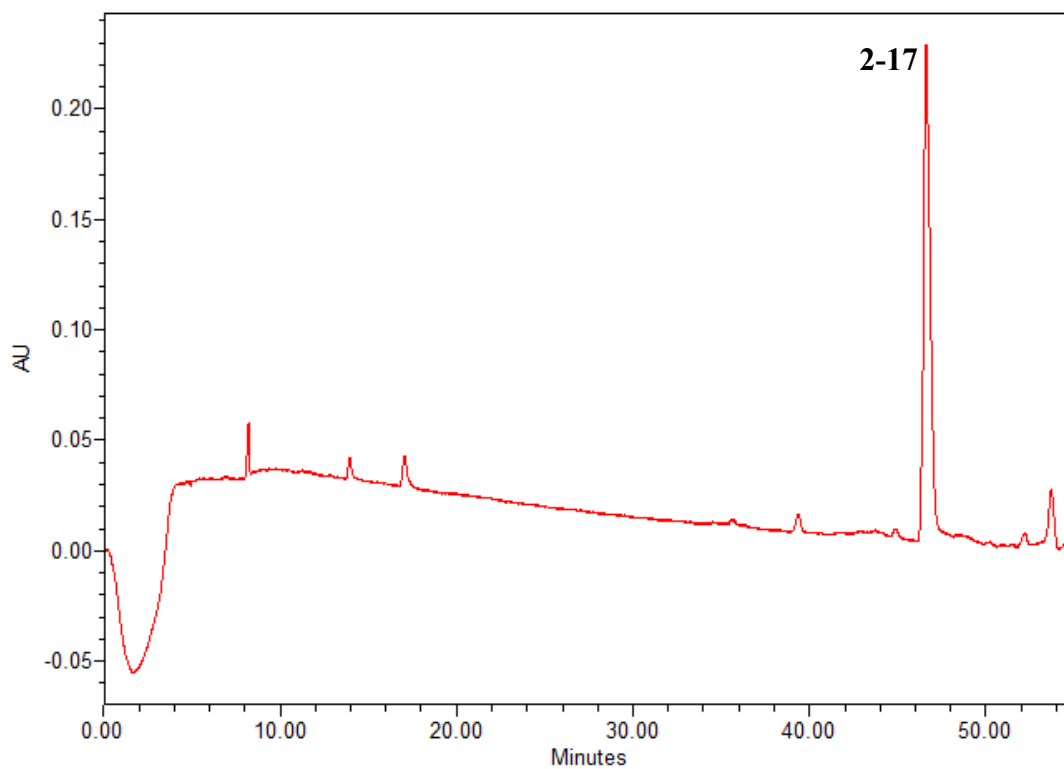


Figure 8.10 HPLC chromatogram of crude *N*-Ac-(*S*)-Arg-(*S*)-Phe-Gly-COOH (**2-17**).

Single Mass Analysis

Tolerance = 3.0 PPM / DBE: min = -1.5, max = 20.0

Element prediction: Off

Number of isotope peaks used for i-FIT = 3

Monoisotopic Mass, Even Electron Ions

40 formula(e) evaluated with 1 results within limits (all results (up to 1000) for each mass)

Elements Used:

C: 0-19 H: 0-30 N: 0-6 O: 0-5

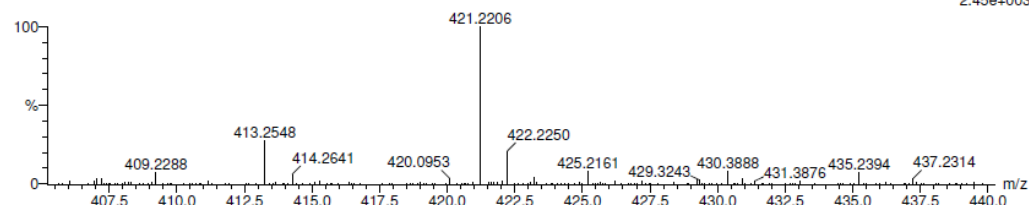
RFG1/EO

29243

1328 44 (1.922)

KE375

14-Oct-2013 4:6:30

1: TOF MS ES+
2.45e+003

Minimum:

Maximum:

Mass

Calc. Mass

421.2206

mDa

PPM

DBE

i-FIT

Formula

-1.5

20.0

5.0

3.0

0.7

1.7

8.5

5.9

C19

H29

N6

O5

Figure 8.11 High resolution MS of isolated *N*-Ac-(*S*)-Arg-(*S*)-Phe-Gly-COOH (2-17).

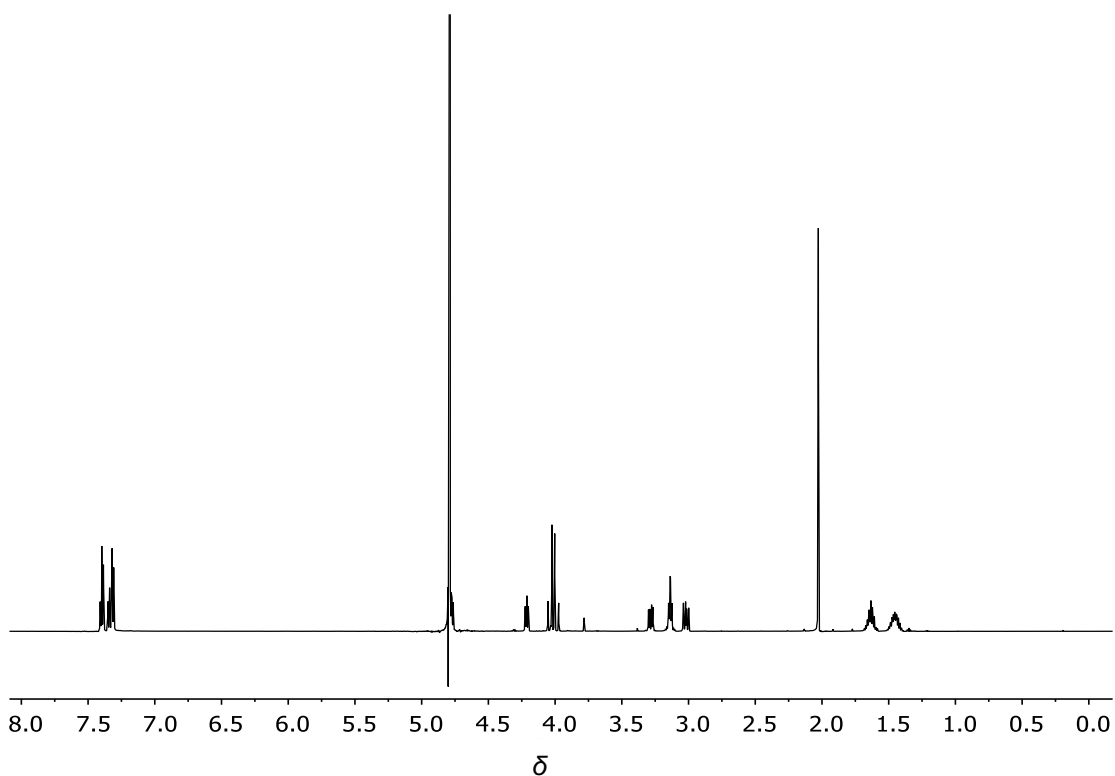
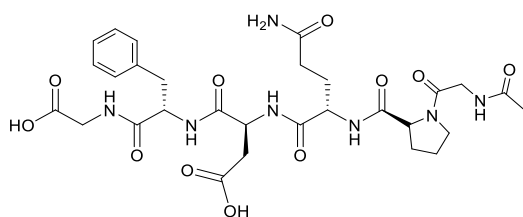


Figure 8.12 ¹H NMR of spectrum of compound 2-17.

***N*-Ac-Gly-(*S*)-Pro-(*S*)-Gln-(*S*)-Asp-(*S*)-Phe-Gly-COOH (2-18)**



2-18

Peptide **2-18** was synthesised and precipitated in Et₂O in the same manner as described for compound **2-14**, except that the Fmoc protected amino acid used for the third coupling was Fmoc-(*S*)-Asp(OtBu)-COOH instead of Fmoc-(*S*)-Arg(Trt)-COOH. The analysis of a small amount of product precipitate was carried out with a linear gradient elution of 5:95 (MeOH: H₂O (0.1% TFA), v/v) to 60:40 between 0-50 min, followed by maintenance of 5:95 between 50-65 min. The resulting HPLC chromatogram is reproduced in **Figure 8.13** and showed two dominant peaks. Samples corresponding to each of these were isolated through HPLC. Mass spectrometry of the peak at 48.10 min displayed ions at *m/z* 663.4, which corresponds to the [M+H]⁺ for hexapeptide **2-18**; the peak at 23.20 min displayed ions at *m/z* 458.6, which is 204 less than that of the former peak, the difference being equal to a sum of the mass of glycine and phenylalanine residues. Based on this analysis, preparative HPLC was used to isolate compound **2-18**. The column fractions were concentrated *via* freeze drying to give compound **2-18** (19 mg, 7.2%) as a colourless powder.

¹H NMR (400 MHz, D₂O): δ7.36 (m, 5H), 4.71 (m, 1H), 4.40 (dd, *J* = 8.7, 5.2 Hz, 1H), 4.27 (dd, *J* = 9.4, 5.1 Hz, 1H), 4.12 (d, *J* = 17.6 Hz, 1H), 4.07 (d, *J* = 17.6 Hz,

1H), 3.99 (s, 2H), 3.64 (m, 2H), 3.26 (dd, $J = 14.1, 5.7$ Hz, 1H), 3.03 (dd, $J = 14.1, 9.0$ Hz, 1H), 2.88 (dd, $J = 17.0, 6.2$ Hz, 1H), 2.75 (dd, $J = 17.0, 7.7$ Hz, 1H), 2.30 (m, 3H), 2.05 (m, 8H); **MS (ESI) (+ve):** m/z 663.4 [M+H]⁺. **HRMS (ESI)** calcd. for C₂₉H₃₉N₇O₁₁Na [M+Na]⁺ m/z 684.2605, found m/z 684.2601 (**Figure 8.14**).

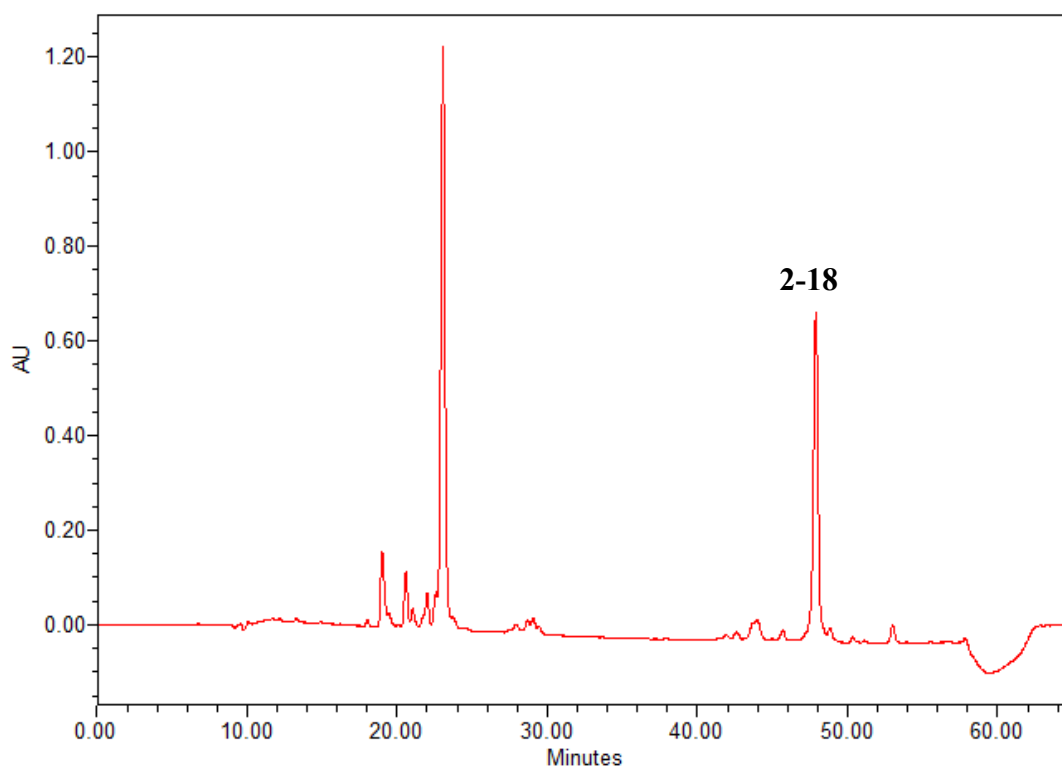


Figure 8.13 HPLC chromatogram of *N*-Ac-Gly-(*S*)-Pro-(*S*)-Gln-(*S*)-Asp-(*S*)-Phe-Gly-COOH (**2-18**).

Single Mass Analysis

Tolerance = 3.0 PPM / DBE: min = -1.5, max = 20.0

Element prediction: Off

Number of isotope peaks used for i-FIT = 3

Monoisotopic Mass, Even Electron Ions

1170 formula(e) evaluated with 1 results within limits (all results (up to 1000) for each mass)

Elements Used:

C: 0-50 H: 0-50 N: 0-10 O: 0-12 23Na: 0-1

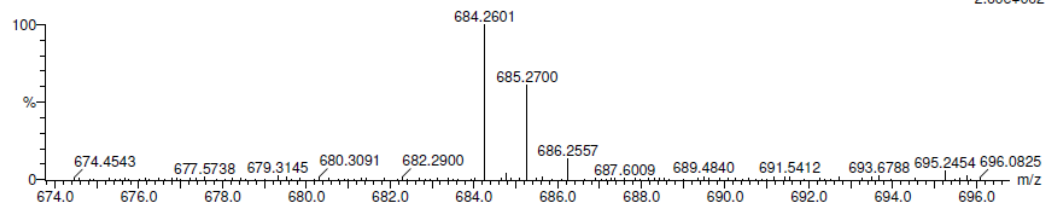
CG_DFG/AJ

41170

1495 66 (2.907)

KE375

05-Aug-2015 09:55:00

1: TOF MS ES+
2.60e+002

Minimum:

Maximum:

5.0 3.0 -1.5

Maximum: 5.0 3.0 20.0

Mass	Calc. Mass	mDa	PPM	DBE	i-FIT	Formula
684.2601	684.2605	-0.4	-0.6	13.5	12.2	C29 H39 N7 O11 23Na

Figure 8.14 High resolution MS of isolated *N*-Ac-Gly-(*S*)-Pro-(*S*)-Gln-(*S*)-Asp-(*S*)-Phe-Gly-COOH (**2-18**).

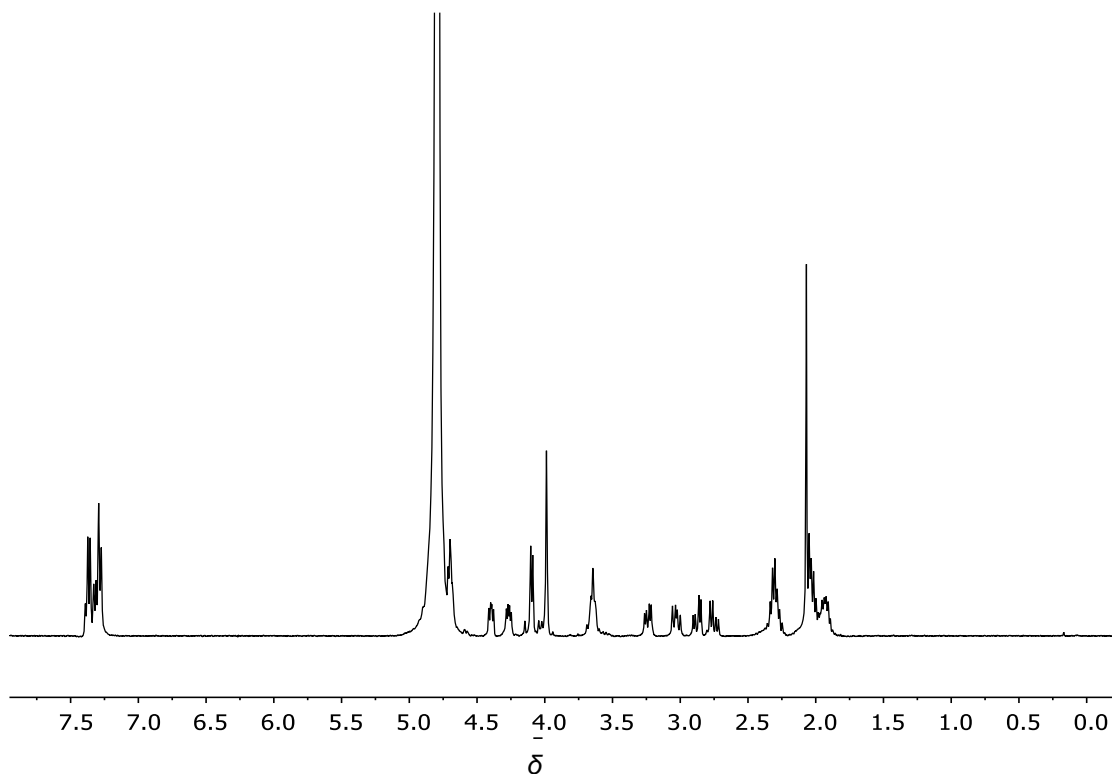
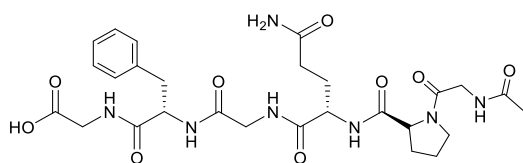


Figure 8.15 ^1H NMR of spectrum of compound **2-18**.

***N*-Ac-Gly-(*S*)-Pro-(*S*)-Gln-(*S*)-Ala-(*S*)-Phe-Gly-COOH (2-19)**



2-19

Peptide **2-19** (5 mg) was generously given by Dr. Tim Altamore. The purity of this peptide was checked with a linear gradient elution of 5:95 (MeOH: H₂O (0.1% TFA), v/v) to 60:40 between 0-30 min, followed by maintenance of 5:95 between 30-35 min at 210 nm. The peak retention time of compound **2-19** was 32.70 min.

¹H NMR (400 MHz, D₂O): δ 7.33 (m, 5H), 4.68 (dd, J = 8.9, 5.8 Hz, 1H), 4.42 (dd, J = 8.6, 5.2 Hz, 1H), 4.27 (m, 2H), 4.10 (s, 2H), 3.90 (d, J = 17.6 Hz, 1H), 3.84 (d, J = 17.6 Hz, 1H), 3.66 (m, 2H), 3.25 (dd, J = 14.0, 5.8 Hz, 1H), 3.02 (dd, J = 14.0, 8.9 Hz, 1H), 2.33 (m, 3H), 2.06 (m, 8H), 1.30 (d, J = 7.2 Hz, 3H); **MS (ESI) (+ve):** m/z 640.6 [M+Na]⁺. **HRMS (ESI)** calcd. for C₂₈H₃₉N₇O₉Na [M+Na]⁺ m/z 640.2707, found m/z 640.2707 (**Figure 8.17**).

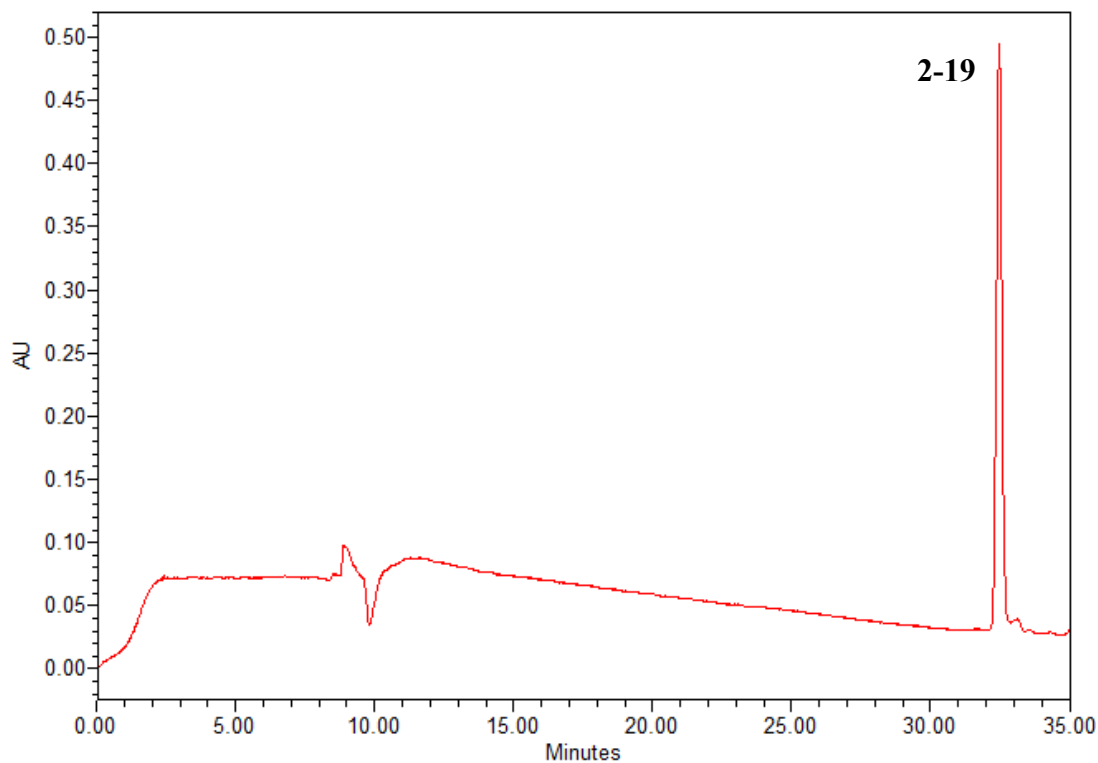


Figure 8.16 HPLC chromatogram of crude *N*-Ac-Gly-(*S*)-Pro-(*S*)-Gln-(*S*)-Ala-(*S*)-Phe-Gly-COOH (**2-19**).

Elemental Composition Report

Page 1

Single Mass Analysis

Tolerance = 3.0 PPM / DBE: min = -1.5, max = 15.0
 Element prediction: Off
 Number of isotope peaks used for i-FIT = 3

Monoisotopic Mass, Even Electron Ions
 1040 formula(e) evaluated with 1 results within limits (all results (up to 1000) for each mass)

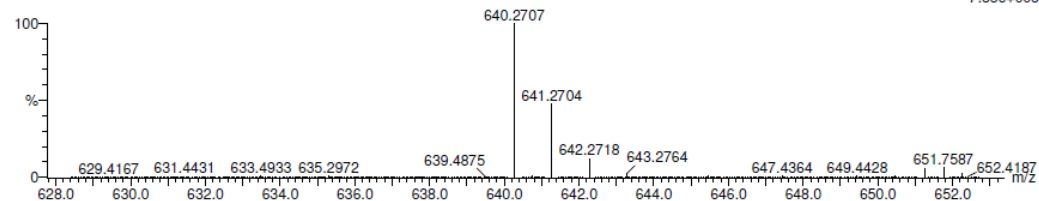
Elements Used:
 C: 0-50 H: 0-50 N: 0-10 O: 0-10 23Na: 0-1

CG_AFG/AJ
 41169
 1494 38 (1.680) Cm (34:46)

KE375

05-Aug-2015 09:41:24

1: TOF MS ES+
 7.88e+003



Minimum: -1.5
 Maximum: 5.0 3.0 15.0

Mass	Calc. Mass	mDa	PPM	DBE	i-FIT	Formula
640.2707	640.2707	0.0	0.0	12.5	161.2	C28 H39 N7 O9 23Na

Figure 8.17 High resolution MS of isolated *N*-Ac-Gly-(*S*)-Pro-(*S*)-Gln-(*S*)-Ala-(*S*)-Phe-Gly-COOH (**2-19**).

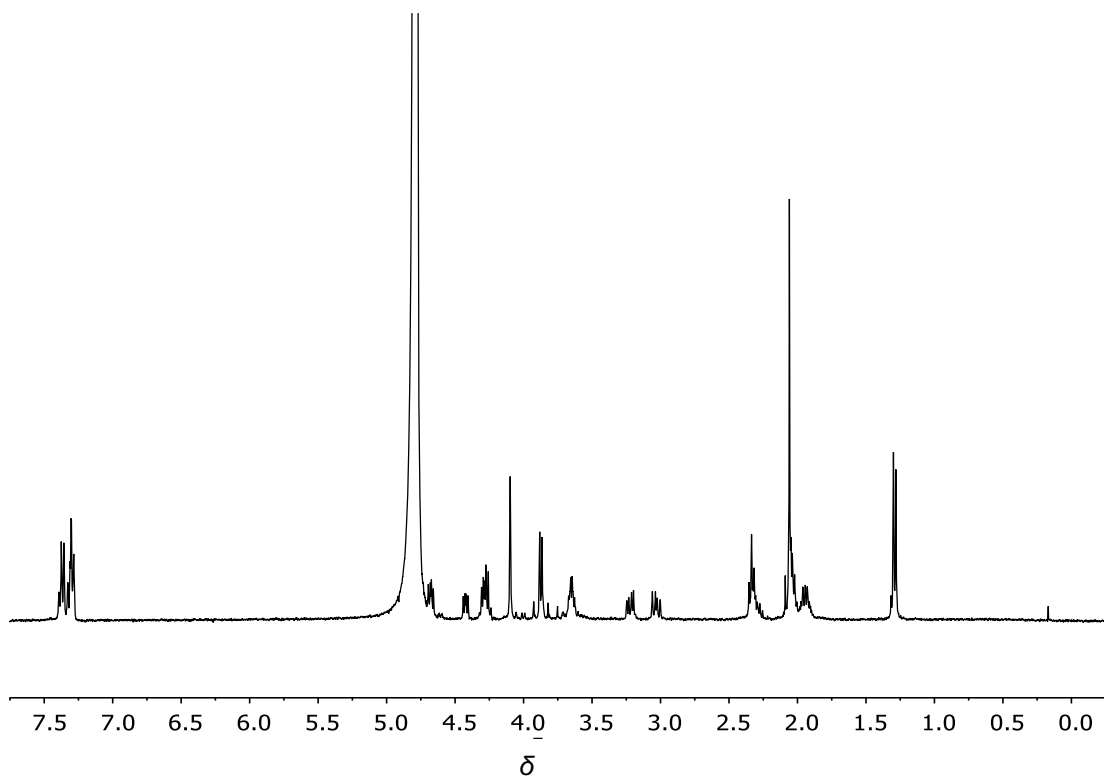
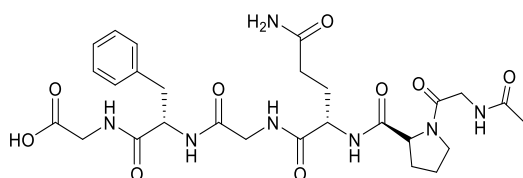


Figure 8.18 ^1H NMR of spectrum of compound **2-19**.

***N*-Ac-Gly-(*S*)-Pro-(*S*)-Gln-Gly-(*S*)-Phe-Gly-COOH (**2-20**)**



2-20

Peptide **2-20** was synthesised and precipitated in cold Et_2O in the same manner as described for compound **2-14**, except that the Fmoc protected amino acid used for the third coupling was Fmoc-Gly-COOH instead of Fmoc-(*S*)-Arg(Trt)-COOH. The analysis of a small amount of product precipitate was carried out with a linear gradient elution of 5:95 (MeOH: H_2O (0.1% TFA), v/v) to 60:40 applied between 0-50 min, followed by maintenance of 5:95 between 50-65 min. The resulting HPLC

chromatogram is reproduced in **Figure 8.19** and showed two dominant peaks. Samples corresponding to each of these were isolated through HPLC. Mass spectrometry of the peak at 21.70 min displayed ions at m/z 626.7, which corresponds to the $[M+Na]^+$ for hexapeptide **2-20**; the peak at 20.50 min displayed ions at m/z 422.5, which is 204 less than that of the former peak, the difference being equal to a sum of the mass of glycine and phenylalanine residues. Based on this analysis, preparative HPLC was used to isolate compound **2-20**. The column fractions were concentrated *via* freeze drying to give compound **2-20** (20 mg, 8.4%) as a colourless powder.

1H NMR (400 MHz, D_2O): δ 7.35 (m, 5H), 4.69 (dd, $J = 8.8, 5.9$ Hz, 1H), 4.43 (dd, $J = 8.6, 5.1$ Hz, 1H), 4.33 (m, 1H), 4.12 (d, $J = 17.2$ Hz, 1H), 4.07 (d, $J = 17.2$ Hz, 1H), 4.00 (d, $J = 17.9$ Hz, 1H), 3.95 (d, $J = 17.9$ Hz, 1H), 3.88 (m, 2H), 3.63 (m, 2H), 3.23 (dd, $J = 14.0, 5.9$ Hz, 1H), 3.02 (dd, $J = 14.0, 8.8$ Hz, 1H), 2.49 (m, 1H), 2.37 (m, 2H), 2.29 (m, 1H), 2.06 (m, 7H); **MS (ESI) (+ve):** m/z 626.7 $[M+Na]^+$. **HRMS (ESI)** calcd. for $C_{27}H_{37}N_7O_9Na$ $[M+Na]^+$ m/z 626.2550, found m/z 626.2559 (**Figure 8.20**).

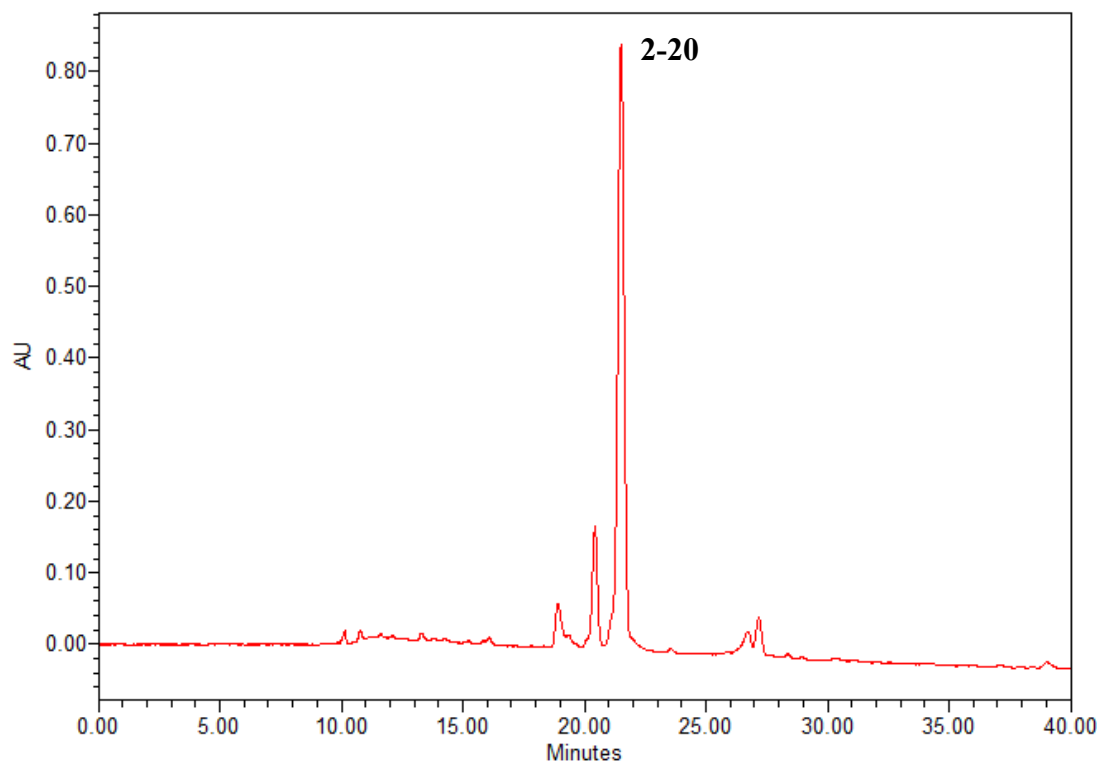


Figure 8.19 HPLC chromatogram of crude *N*-Ac-Gly-(*S*)-Pro-(*S*)-Gln-Gly-(*S*)-Phe-Gly-COOH (**2-20**).

Elemental Composition Report

Page 1

Single Mass Analysis

Tolerance = 3.0 PPM / DBE: min = -1.5, max = 20.0

Element prediction: Off

Number of isotope peaks used for i-FIT = 3

Monoisotopic Mass, Even Electron Ions

154 formula(e) evaluated with 1 results within limits (all results (up to 1000) for each mass)

Elements Used:

C: 0-27 H: 0-39 N: 0-7 O: 0-9 23Na: 0-1

GPOGFGI/EO

KE375

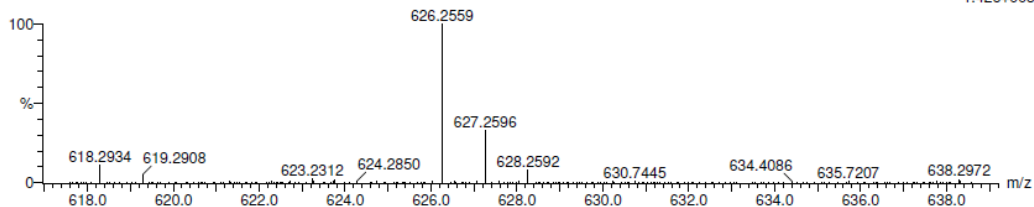
02-Dec-2013 15:10:35

30287

1614 25 (1.122) Cm (23:25)

1: TOF MS ES+

1.42e+003



Minimum:

Maximum: 5.0 3.0 -1.5

Mass Calc. Mass mDa PPM DBE i-FIT Formula

626.2559 626.2550 0.9 1.4 12.5 0.4 C27 H37 N7 O9 23Na

Figure 8.20 High resolution MS of isolated *N*-Ac-Gly-(*S*)-Pro-(*S*)-Gln-(*S*)-Gly-(*S*)-Phe-Gly-COOH (**2-20**).

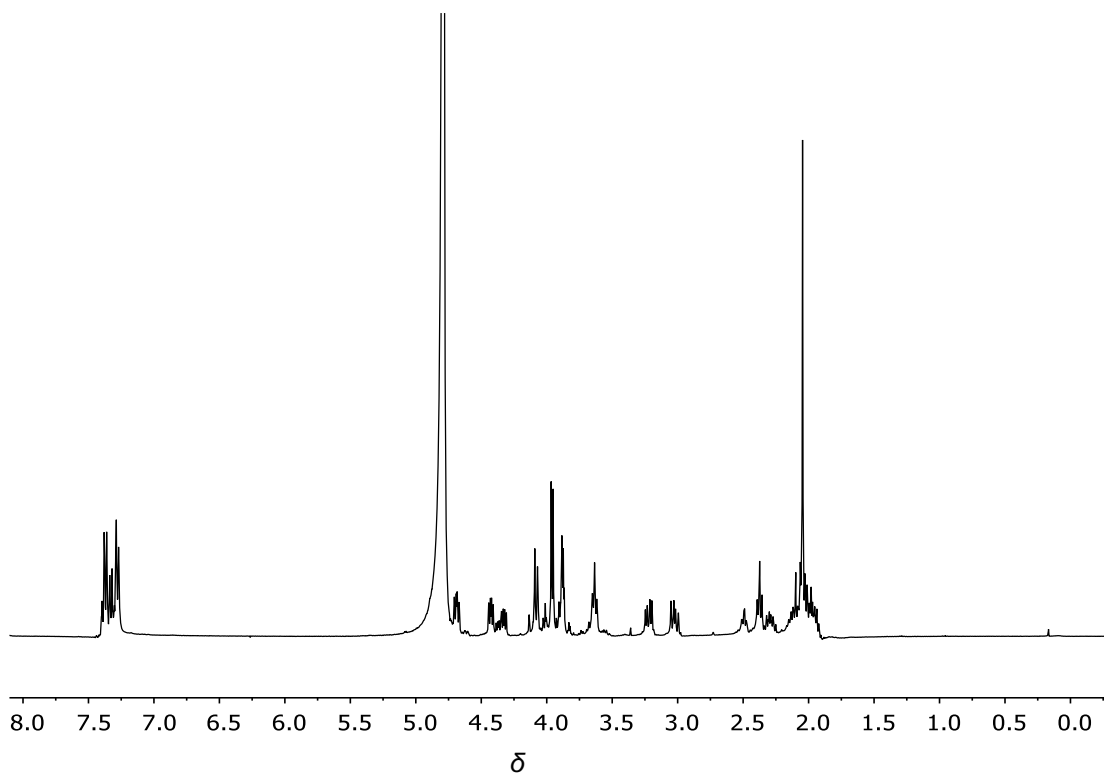
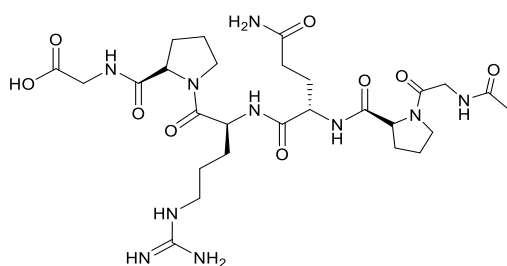


Figure 8.21 ^1H NMR of spectrum of compound **2-20**.

***N*-Ac-Gly-(*S*)-Pro-(*S*)-Gln-(*S*)-Arg-(*S*)-Pro-Gly-COOH (**2-21**)**



2-21

Peptide **2-21** was synthesised and precipitated in cold Et_2O in the same manner as described for compound **2-14**, except that the Fmoc protected amino acid used for the second coupling was Fmoc-(*S*)-Pro-COOH instead of Fmoc-(*S*)-Phe-COOH. The

analysis of a small amount of product precipitate was carried out with a linear gradient elution of 5:95 (MeOH: H₂O (0.1% TFA), v/v) to 35:65 between 0-32 min, followed by maintenance of 5:95 between 32-35 min. The resulting HPLC chromatogram is reproduced in **Figure 8.22** and showed two dominant peaks. Samples corresponding to each of these were isolated through HPLC. Mass spectrometry of the peak at 19.20 min displayed ions at m/z 653.3, which corresponds to the $[M+H]^+$ for hexapeptide **2-21**; the peak at 13.30 min displayed ions at m/z 499.5, which is 154 less than that of the former peak, the difference being equal to a sum of the mass of glycine and proline residues. Based on this analysis, preparative HPLC was used to isolate compound **2-21**. The column fractions were concentrated *via* freeze drying to give compound **2-21** (7 mg, 2.7%) as a colourless powder.

¹H NMR (400 MHz, D₂O): δ 4.65 (m, 1H), 4.45 (m, 2H), 4.31 (m, 1H), 4.08 (s, 2H), 4.05 (d, $J = 18.1$ Hz, 1H), 3.95 (d, $J = 18.1$ Hz, 1H), 3.81 (m, 1H), 3.64 (m, 3H), 3.22 (t, $J = 6.9$ Hz, 2H), 2.38 (m, 2H), 2.30 (m, 2H), 2.06 (m, 12H), 1.69 (m, 3H); **MS (ESI) (+ve):** m/z 653.6 $[M+H]^+$. **HRMS (ESI)** calcd. for C₂₇H₄₅N₁₀O₉ $[M+H]^+$ m/z 653.3371, found m/z 653.3385 (**Figure 8.23**).

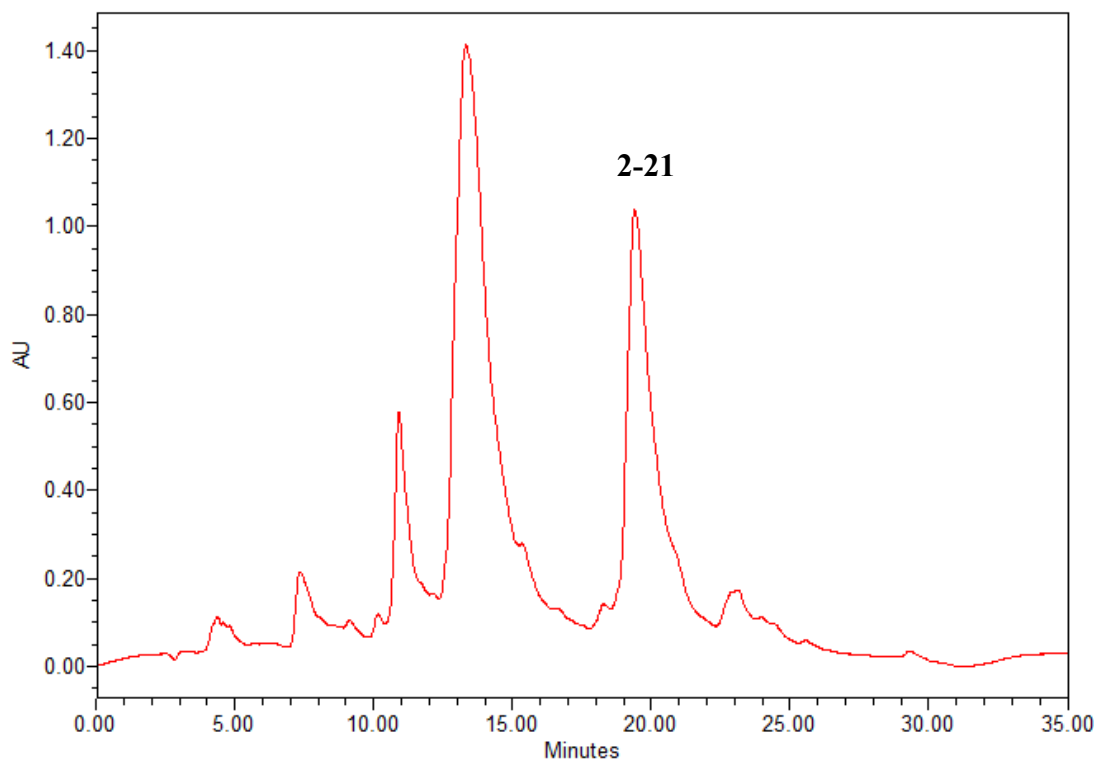


Figure 8.22 HPLC chromatogram of crude *N*-Ac-Gly-(*S*)-Pro-(*S*)-Gln-(*S*)-Arg-(*S*)-Pro-Gly-COOH (**2-21**).

Elemental Composition Report

Page 1

Single Mass Analysis

Tolerance = 3.0 PPM / DBE: min = -1.5, max = 20.0

Element prediction: Off

Number of isotope peaks used for i-FIT = 3

Monoisotopic Mass, Even Electron Ions

461 formula(e) evaluated with 1 results within limits (all results (up to 1000) for each mass)

Elements Used:

C: 0-50 H: 0-50 N: 0-10 O: 0-9

GPORPG1/AJ

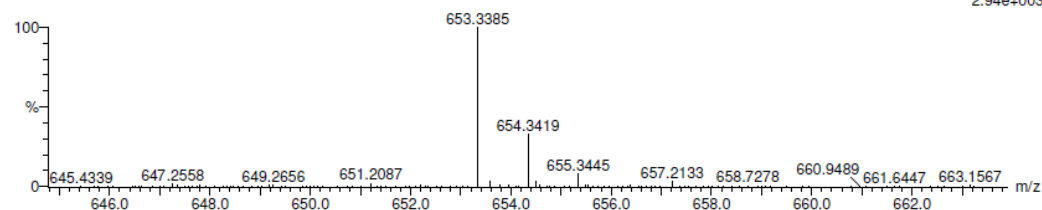
28579

1182 32 (1.397)

KE375

20-Aug-2013 14:15:38

1: TOF MS ES+
2.94e+003



Mass	Calc. Mass	mDa	PPM	DBE	i-FIT	Formula
653.3385	653.3371	1.4	2.1	10.5	1.9	C27 H45 N10 O9

Figure 8.23 High resolution MS of isolated *N*-Ac-Gly-(*S*)-Pro-(*S*)-Gln-(*S*)-Arg-(*S*)-Pro-Gly-COOH (**2-21**).

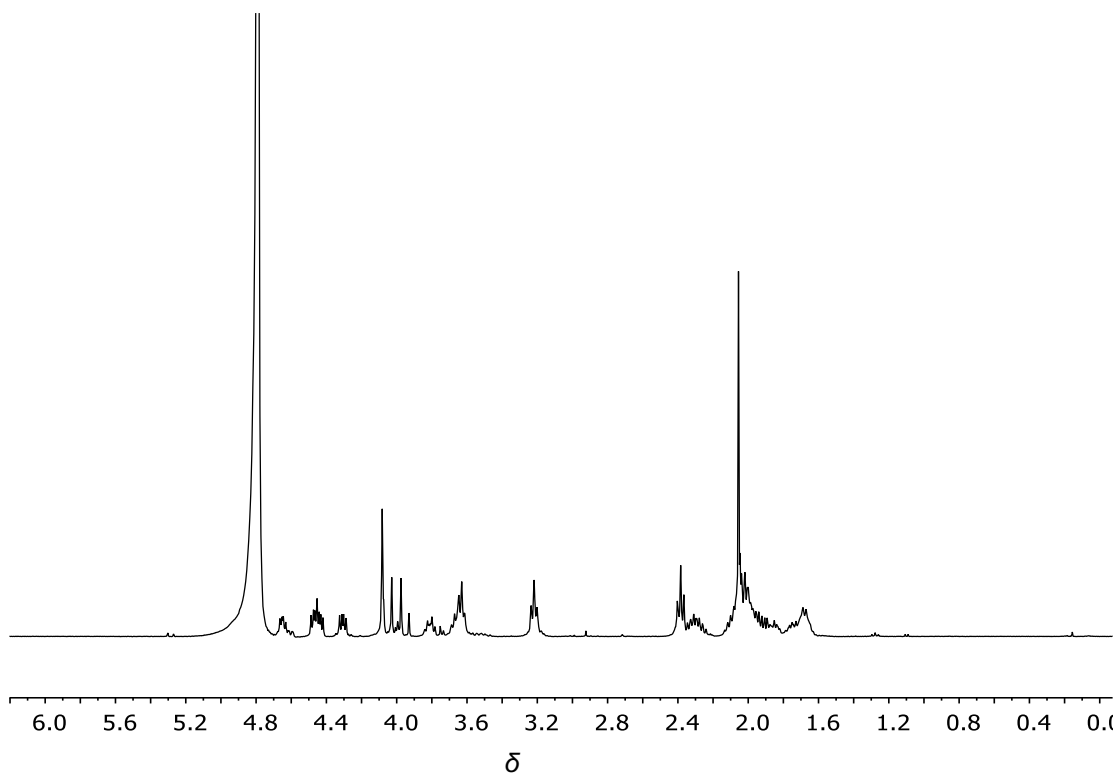
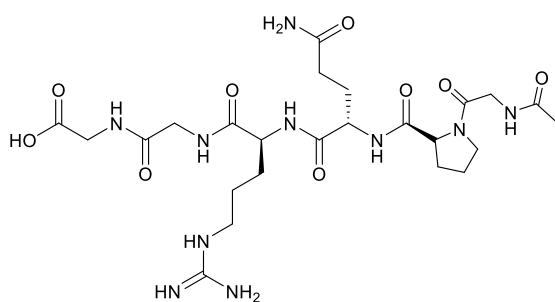


Figure 8.24 ^1H NMR of spectrum of compound **2-21**.

***N*-Ac-Gly-(*S*)-Pro-(*S*)-Gln-(*S*)-Arg-Gly-Gly-COOH (**2-22**)**



2-22

Peptide **2-22** was synthesised and precipitated in cold Et_2O in the same manner as described for compound **2-14**, except that the Fmoc protected amino acid used for the second coupling was Fmoc-Gly-COOH instead of Fmoc-(*S*)-Phe-COOH. The analysis

of a small amount of product precipitate was carried out with a linear gradient elution of 5:95 (MeOH: H₂O (0.1% TFA), v/v) to 22:78 between 0-20 min, followed by maintenance of 5:95 between 20-28 min. The resulting HPLC chromatogram is reproduced in **Figure 8.25** and showed only one dominant peak at 25.60 min. Sample corresponding to the peak was isolated through HPLC. Mass spectrometry of the peak displayed ions at m/z 611.6, which corresponds to the [M-H]⁻ for hexapeptide **2-22**. Based on this analysis, the whole precipitate, was concentrated *via* freeze drying to give compound **2-22** (15 mg, 6.2%) as a colourless powder.

¹H NMR (400 MHz, D₂O): δ4.30 (m, 3H), 4.01 (s, 2H), 3.91 (m, 2H), 3.88 (d, J = 3.4 Hz, 1H), 3.86 (d, J = 3.4 Hz, 1H), 3.56 (m, 2H), 3.14 (t, J = 6.9 Hz, 2H), 2.31 (m, 2H), 2.20 (m, 1H), 1.98 (m, 8H), 1.71 (m, 1H), 1.58 (m, 2H); **MS (ESI) (-ve):** m/z 611.6 [M-H]⁻. **HRMS (ESI)** calcd. for C₂₄H₃₉N₁₀O₉ [M-H]⁻ m/z 611.2901, found m/z 611.2900 (**Figure 8.26**).

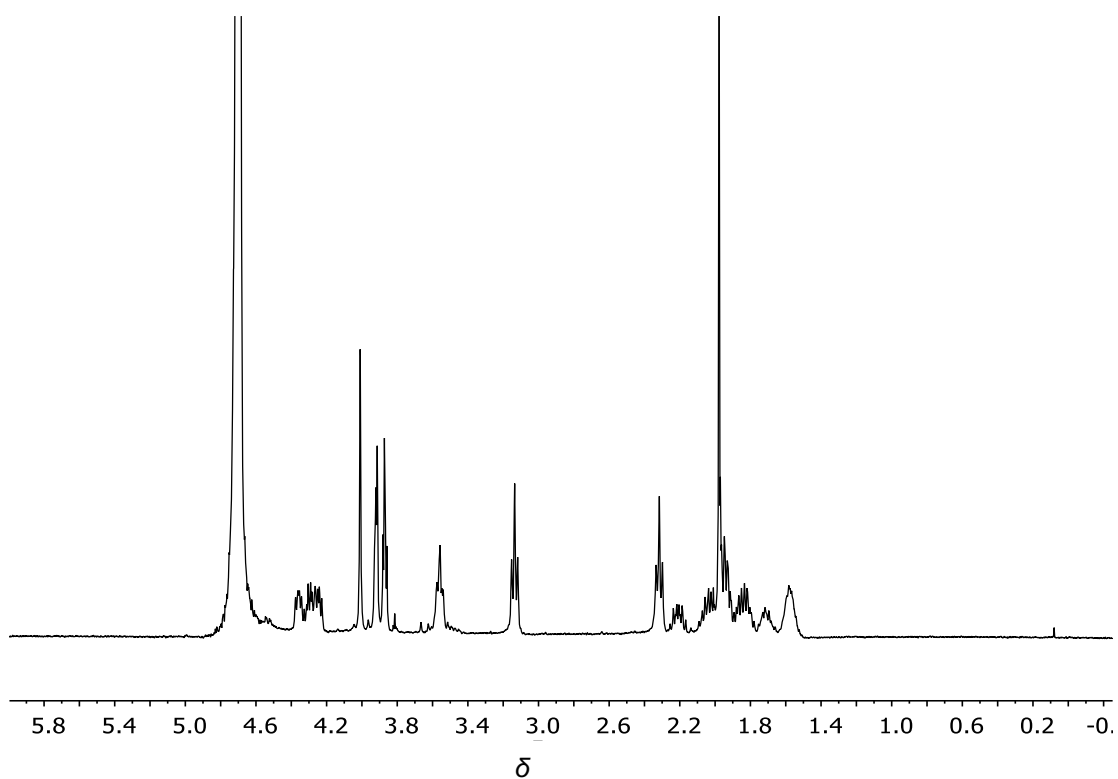
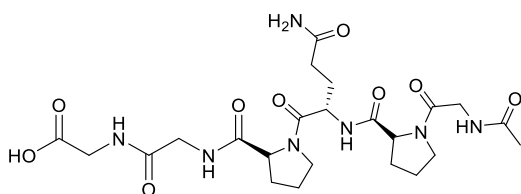


Figure 8.27 ^1H NMR of spectrum of compound **2-22**.

***N*-Ac-Gly-(*S*)-Pro-(*S*)-Gln-(*S*)-Pro-Gly-Gly-COOH (**2-23**)**



2-23

Peptide **2-23** was synthesised and precipitated in cold Et_2O in the same manner as described for **2-22**, except that the Fmoc protected amino acid used for the third coupling was Fmoc-(*S*)-Pro-COOH instead of Fmoc-(*S*)-Arg(Trt)-COOH. The analysis of a small amount of product precipitate was carried out with a linear gradient

elution of 25:75 (MeOH: H₂O (0.1% TFA), v/v) to 38:62 between 0-25 min, followed by maintenance of 25:75 between 25-30 min. The resulting HPLC chromatogram is reproduced in **Figure 8.28** and showed only one dominant peak at 12.60 min. Sample corresponding to the peak was isolated through HPLC. Mass spectrometry of the peak displayed ions at m/z 576.6, which corresponds to the $[M+Na]^+$ for hexapeptide **2-23**. Based on this analysis, the whole precipitate was concentrated *via* freeze drying to give compound **2-23** (16 mg, 7.3%) as a colourless powder.

¹H NMR (400 MHz, D₂O): δ 4.48 (dd, $J = 9.6, 4.7$ Hz, 1H), 4.29 (m, 2H), 3.88 (m, 6H), 3.65 (m, 1H), 3.53 (m, 1H), 3.47 (t, $J = 6.6$ Hz, 2H), 2.26 (t, $J = 7.2$ Hz, 2H), 2.13 (m, 2H), 1.90 (m, 11H); **MS (ESI) (+ve):** m/z 576.6 $[M+Na]^+$. **HRMS (ESI) calcd.** for C₂₃H₃₅N₇O₉Na $[M+Na]^+$ m/z 576.2394, found m/z 576.2394 (**Figure 8.29**).

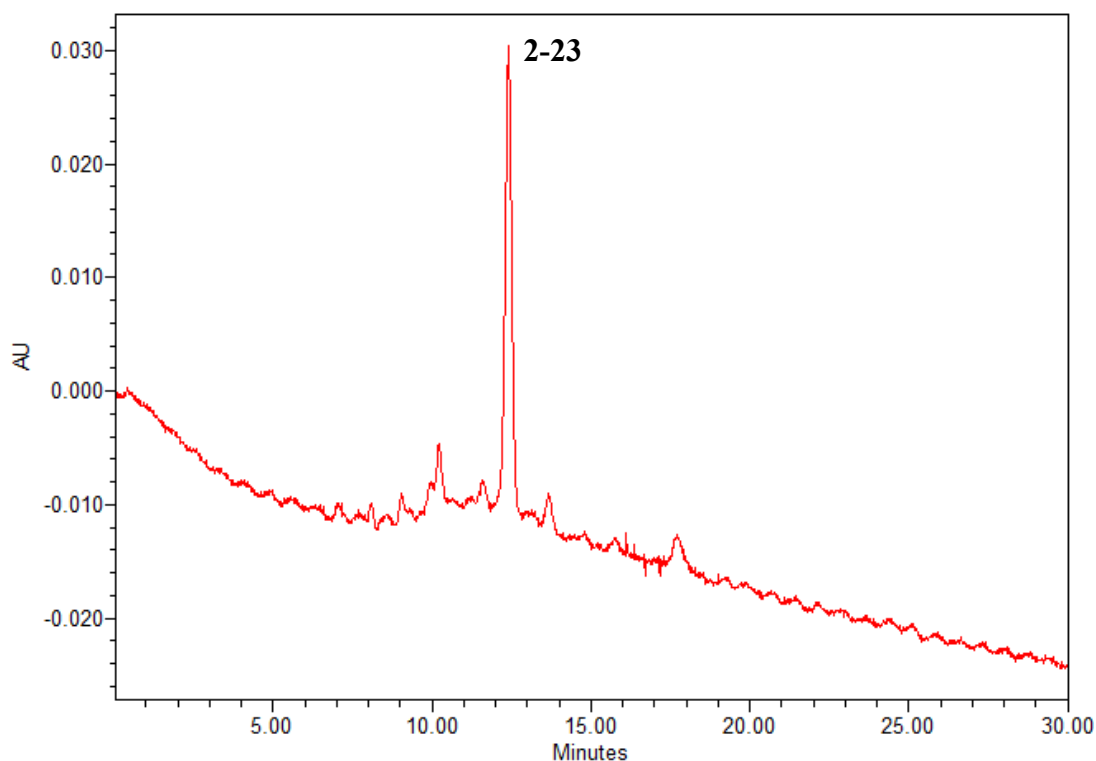


Figure 8.28 HPLC chromatogram of crude *N*-Ac-Gly-(*S*)-Pro-(*S*)-Gln-(*S*)-Pro-Gly-Gly-COOH (**2-23**).

Elemental Composition Report

Page 1

Single Mass Analysis

Tolerance = 3.0 PPM / DBE: min = -1.5, max = 20.0
 Element prediction: Off
 Number of isotope peaks used for i-FIT = 3

Monoisotopic Mass, Odd and Even Electron Ions

136 formula(e) evaluated with 1 results within limits (all results (up to 1000) for each mass)

Elements Used:

C: 0-23 H: 10-37 N: 1-7 O: 0-9 23Na: 0-1

GPOPGGEO

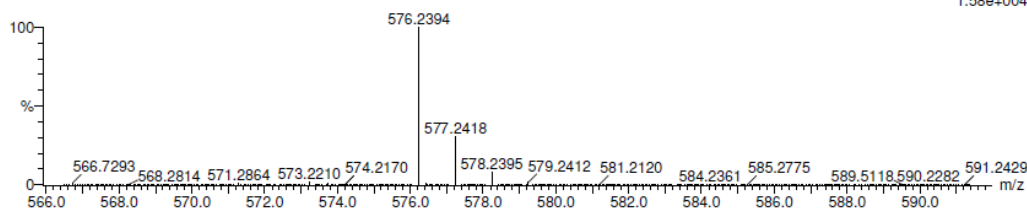
KE375

23-Apr-2014 15:06:41

32239

1: TOF MS ES+
1.58e+004

0548 15 (0.663) Cm (5:15)



Minimum:

Maximum: 5.0 3.0 -1.5

Mass	Calc. Mass	mDa	PPM	DBE	i-FIT	Formula
576.2394	576.2394	0.0	0.0	9.5	30.9	C23 H35 N7 O9 23Na

Figure 8.29 High resolution MS of isolated *N*-Ac-Gly-(*S*)-Pro-(*S*)-Gln-(*S*)-Pro-Gly-Gly-COOH (**2-23**).

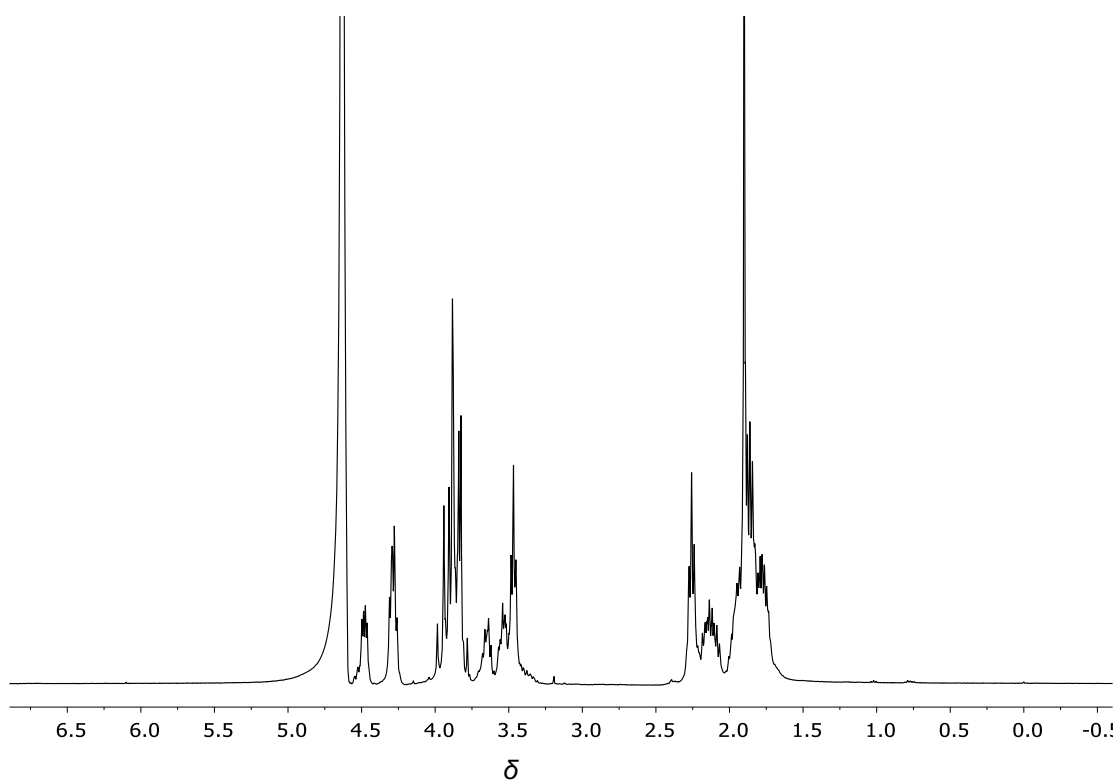


Figure 8.30 ^1H NMR of spectrum of compound **2-23**.

8.2.2 Cell Culture Maintenance and PAM Enzyme Preparation

Cell culture was performed using a modified literature procedure.^[138] DMS53 cells (ATCC[®] CRL-2062[™]) were seeded into fresh Nunc Cell Culture T25 flasks at 37 °C under a moist atmosphere of 5% CO₂ /95% air in a Memmert incubator, with RPMI medium (3 mL) that was changed every 48 h. Once cells were grown to about 80% density (estimated by microscope), they were washed thrice with Dulbecco's phosphate-buffered saline (DPBS) (3 mL for each time), lifted with 0.05% trypsin-EDTA (1 mL) and incubation for 10 min. The resulting cell suspensions were then diluted with fresh medium (6 mL) and transferred into Nunc Cell Culture T175 flasks, followed by addition of more medium (40 mL) for further growth under the same temperature and air environment, as mentioned above. The cell medium (50 mL) was changed every 48 h.

Once cells were grown close to 90% density, the last batch of growth medium (which had been used for growing cells for 48 h) was collected, centrifuged at 5000 g for 20 min by using a Millipore Amicon® Ultra YM-10 filter, and concentrated 100 times. The PAM enzyme concentrate was snap-frozen and stored at -80 °C for use later.

8.2.3 Procedure for Determination of IC₅₀ Values of Peptide Prohormones with PAM

Assays were performed with 1.25 mM ascorbic acid, 10 µM copper sulphate, 0.2 mg/mL bovine liver catalase, 1% EtOH, 1% DMSO, 50 µM tripeptide substrate (*R*)-Tyr-(*S*)-Val-Gly-COOH and 600-0 µM at 2X serial dilution of peptide **2-17** in 150 mM MES buffer at pH 5.8. For the concentration selection of other peptides, compounds **2-18** and **2-19** were tested with the same concentration range as described above; peptides **2-14** - **2-16** and **2-20** were tested with 300-0 µM at 2X serial dilution; peptides **2-21** - **2-22** and **2-23** were examined with 2000-0 µM and 6000-0 µM at 2X serial dilution, respectively. Assays were initiated through the addition of concentrated medium PAM (5 µL) to give a final volume of 100 µL. The mixtures were incubated in a Lab Companion Model SI-600R open-air shaker at 37 °C for 2 h, with agitation at 80 rpm. At the end of the incubation, the reaction mixture was treated with 1 M NaOH (25 µL) and incubated at 37 °C for 2 min, followed by neutralisation with 1 M HCl (25 µL). The solutions were then passed through Amicon® Ultra YM-3 filters using a centrifuge for 15 min at 12000 rpm at room temperature, and the filtrates were then analysed by using analytical HPLC. The competition assays were run at least in duplicate.

8.2.4 HPLC Method for Detection and Quantification of (*R*)-Tyr-(*S*)-Val-Gly-COOH and (*R*)-Tyr-(*S*)-Val-NH₂ in IC₅₀ Assays

HPLC detection of (*R*)-Tyr-(*S*)-Val-Gly-COOH and (*R*)-Tyr-(*S*)-Val-NH₂ used a Waters Alliance 2695 separation module and a Waters 600E Pump connected to a two position, six port switching valve, a Waters Reagent Manager containing fluorescamine (30 mg/100 mL MeCN) and a Waters 2475 Fluorescence Detector. Injected sample underwent an online solid phase extraction on a YMC-Pack ODS AQ cartridge column S-5 μm (4.0 × 23 mm) with the switching valve open to waste. After 5 min, flow was diverted to a YMC-Pack ODS-AQ column (4.6 × 150 mm) and a Phenosphere 5 μm CN 80Å column (4.6 × 250 mm) for 30 min. To allow fluorescent labelling of the *N*-terminus of substrate and product, a fluorescamine solution (0.33 mg/mL in MeCN) was mixed with the eluent in a post-column Waters 1000 RXN coil at 25 °C, before detection with a Waters 2475 Fluorescence Detector ($\lambda_{\text{ex.}} = 390 \text{ nm}$, $\lambda_{\text{em.}} = 470 \text{ nm}$). The solvent and gradient system for the analysis is illustrated in **Table 8.1**. A 30-minute cleaning routine was applied between each sample injection using the solvent and gradient system shown in **Table 8.2**.

Table 8.1 Solvent and gradient system for separation of (*R*)-Tyr-(*S*)-Val-Gly-COOH and (*R*)-Tyr-(*S*)-Val-NH₂.

Time (min)	Flow (mL/min)	MeCN (%)	Buffer A [*] (%)
0	3	0	100
3	3	10	90
30	3	10	90

*Buffer A: 100 mL Waters AccQ.Tag™ and 1000 mL Water

Table 8.2 Solvent and gradient system used for cleaning routine.

Time (min)	Flow (mL/min)	MeCN (%)	Buffer A [*] (%)
0	0.5	50	50
6	0.8	50	50
16	0.8	50	50
18	0.8	10	90
24	0.8	10	90
25	0.8	0	100
30	0.8	0	100

*Buffer A: 100 mL Waters AccQ.Tag™ and 1000 mL Water

Data were collected and processed with Waters Empower 3 software wherein the peak areas of (*R*)-Tyr-(*S*)-Val-Gly-COOH and (*R*)-Tyr-(*S*)-Val-NH₂ were determined and the proportion of (*R*)-Tyr-(*S*)-Val-NH₂ was calculated as the percentage substrate turnover by PAM. For each peptide candidate **2-14** - **2-23**, its concentration was

plotted as a function of percentage tripeptide substrate turnover using SciDAVis 0.2.4, and used to calculate IC_{50} values, as shown in **Figure 8.31-Figure 8.40**.

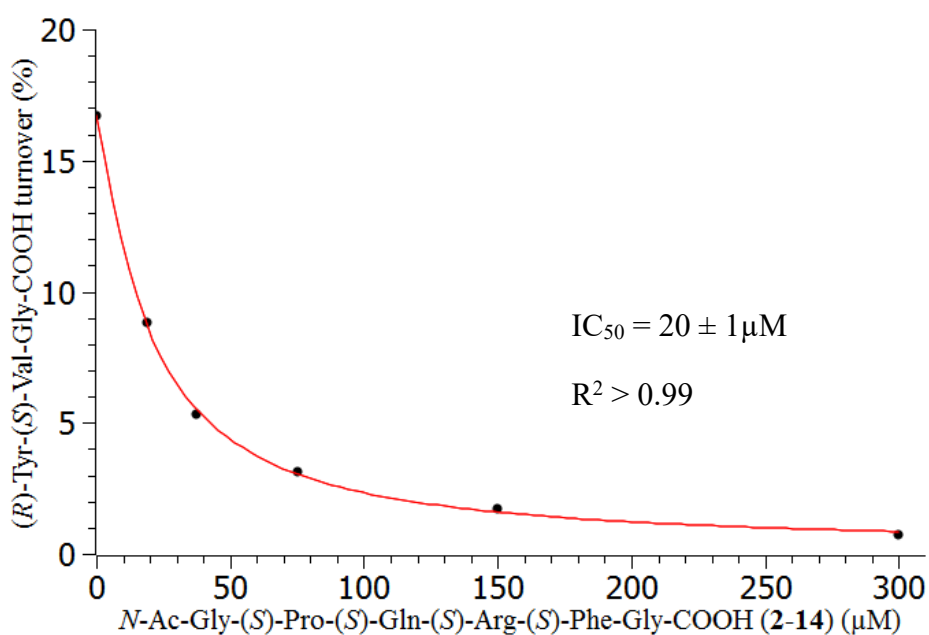
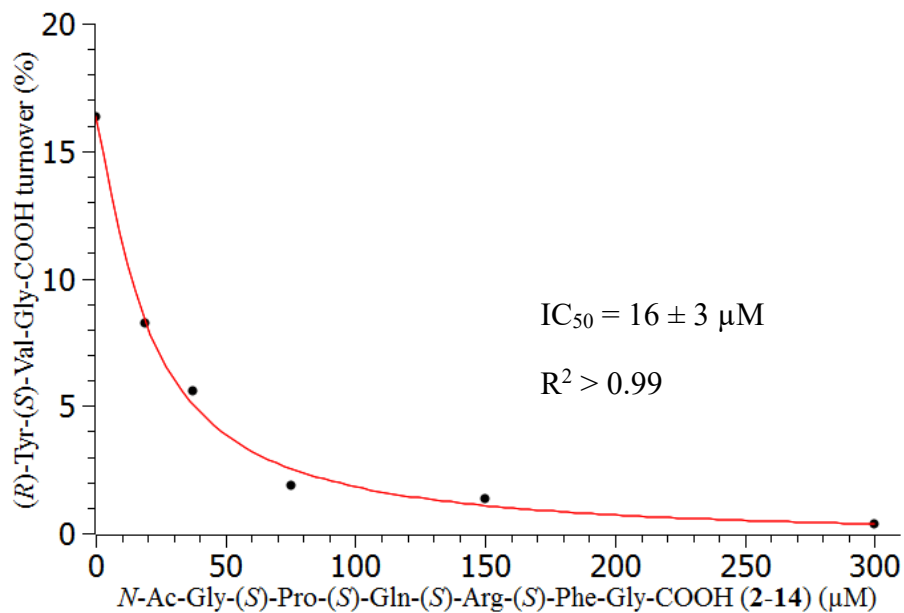


Figure 8.31 Determination of IC_{50} for $N\text{-Ac-Gly-(S)-Pro-(S)-Gln-(S)-Arg-(S)-Phe-Gly-COOH (2-14) (\mu\text{M})$

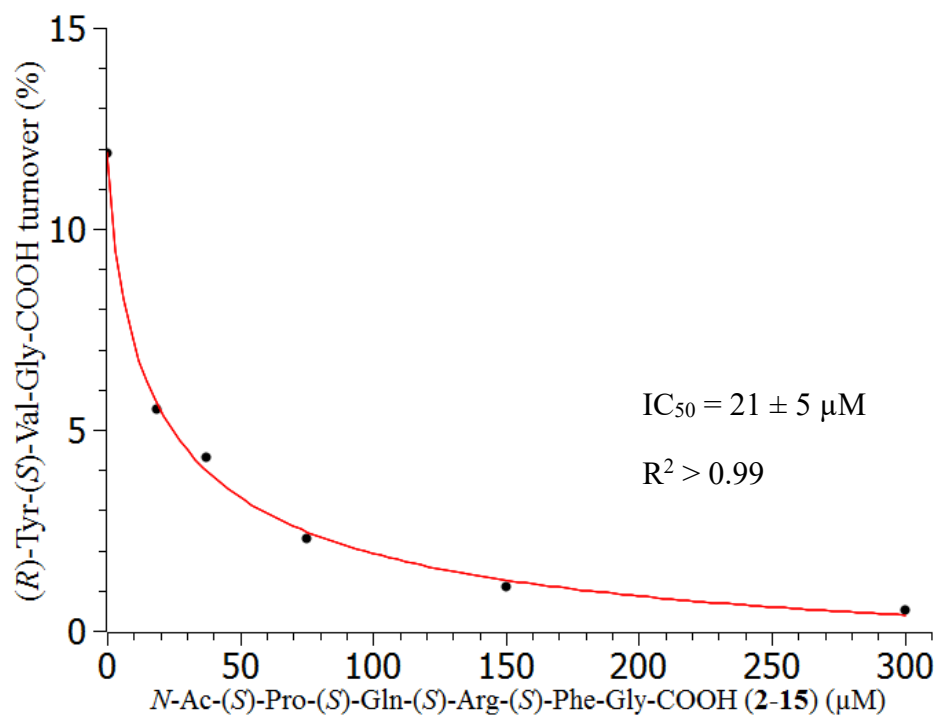
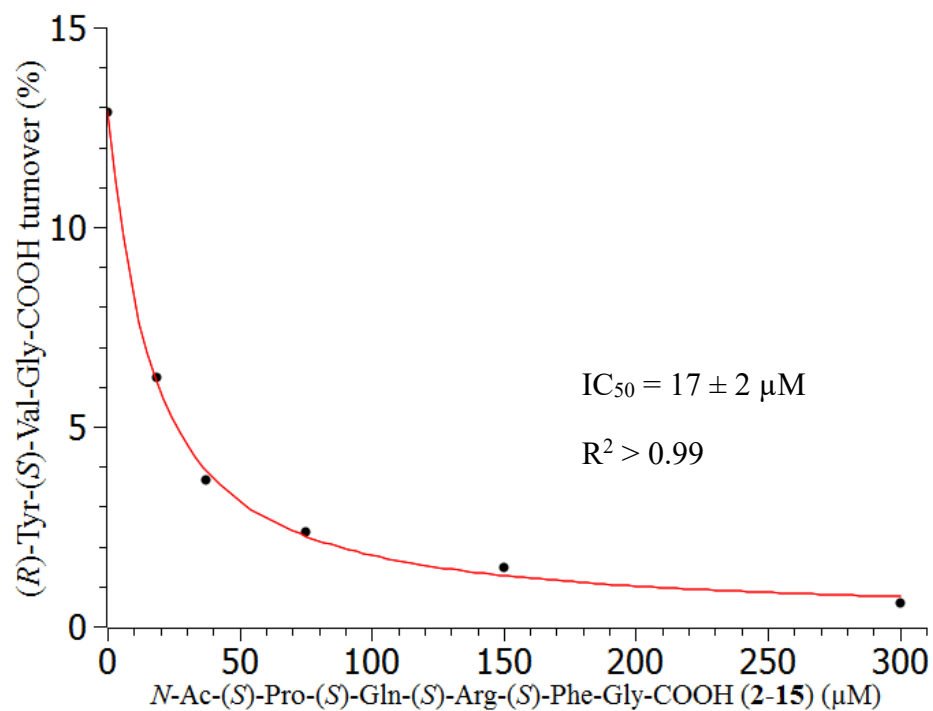


Figure 8.32 Determination of IC_{50} for N -Ac-(S)-Pro-(S)-Gln-(S)-Arg-(S)-Phe-Gly-COOH (2-15) (μ M)

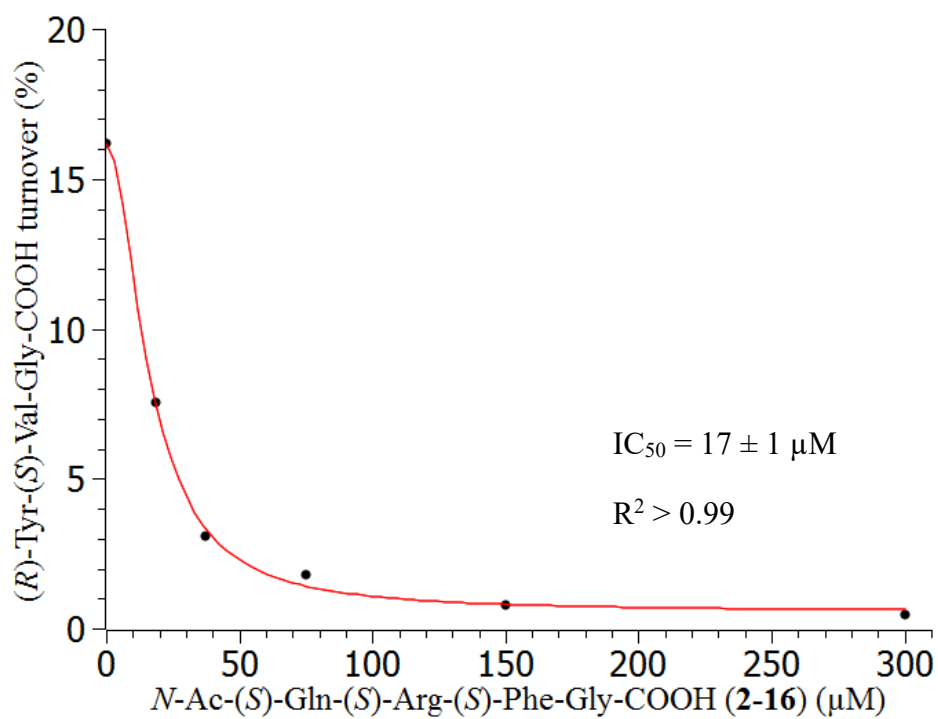
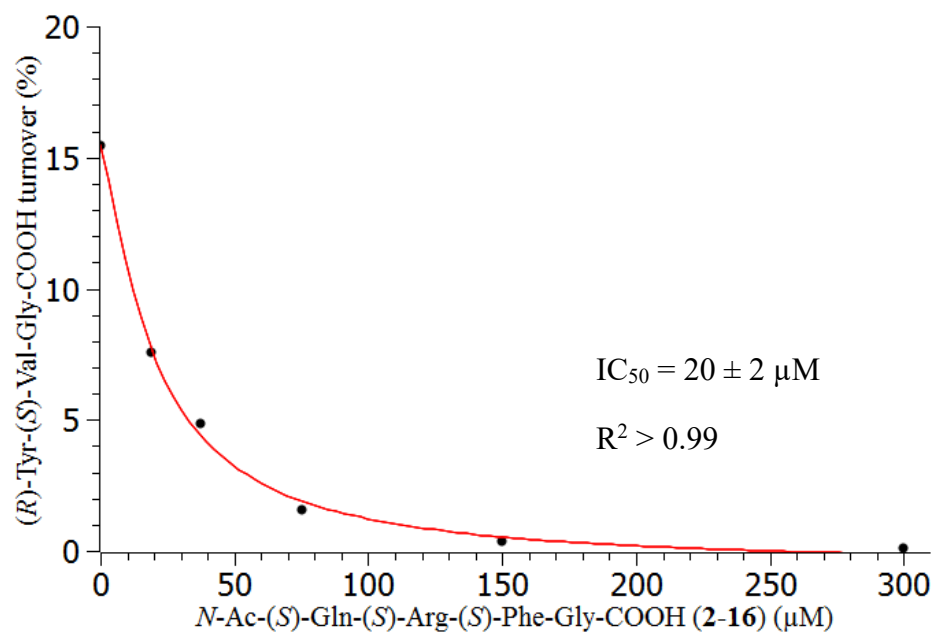


Figure 8.33 Determination of IC_{50} for N -Ac-(S)-Gln-(S)-Arg-(S)-Phe-Gly-COOH (**2-16**) (μ M)

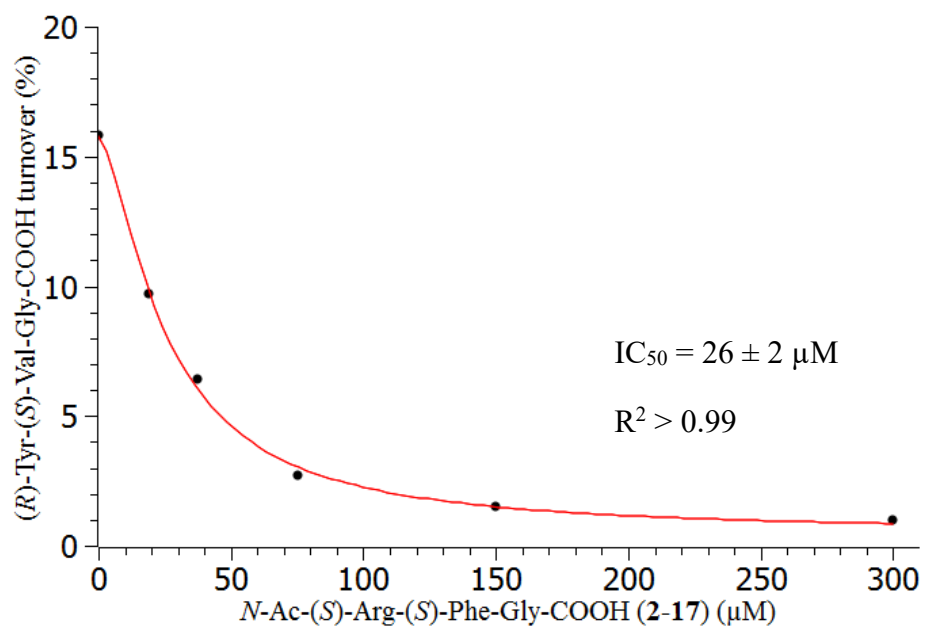
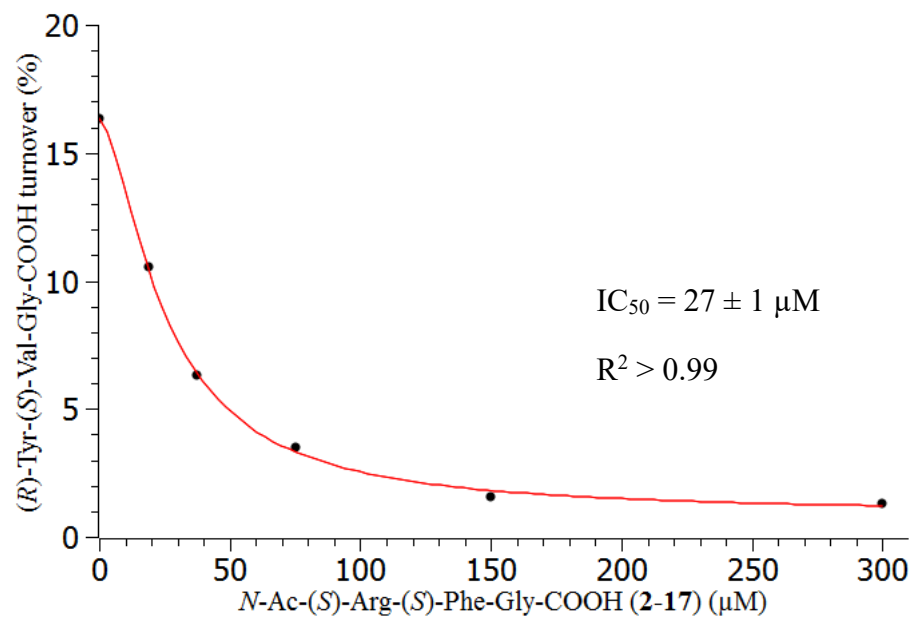


Figure 8.34 Determination of IC_{50} for *N*-Ac-(*S*)-Arg-(*S*)-Phe-Gly-COOH (2-17) (μM)

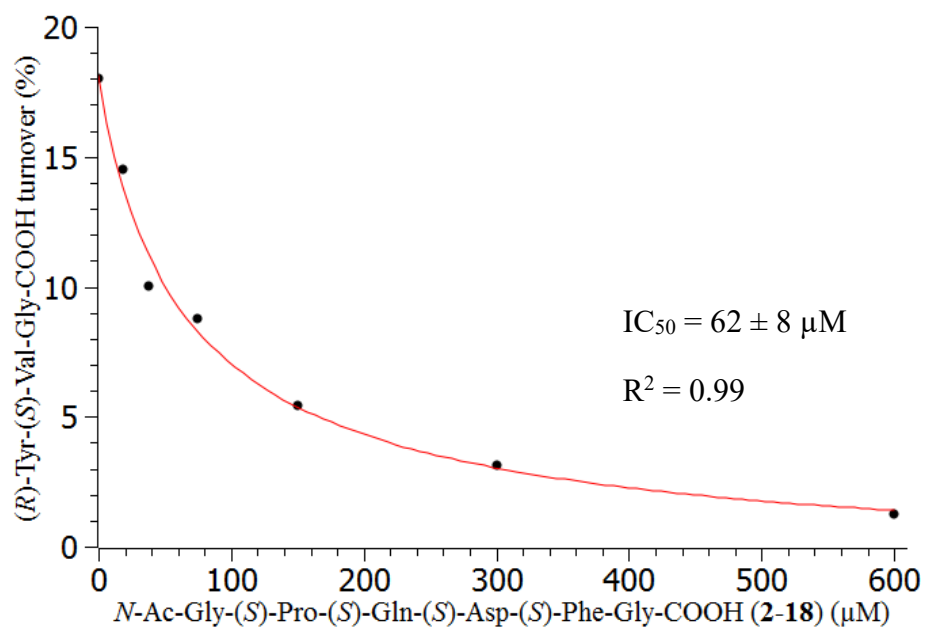
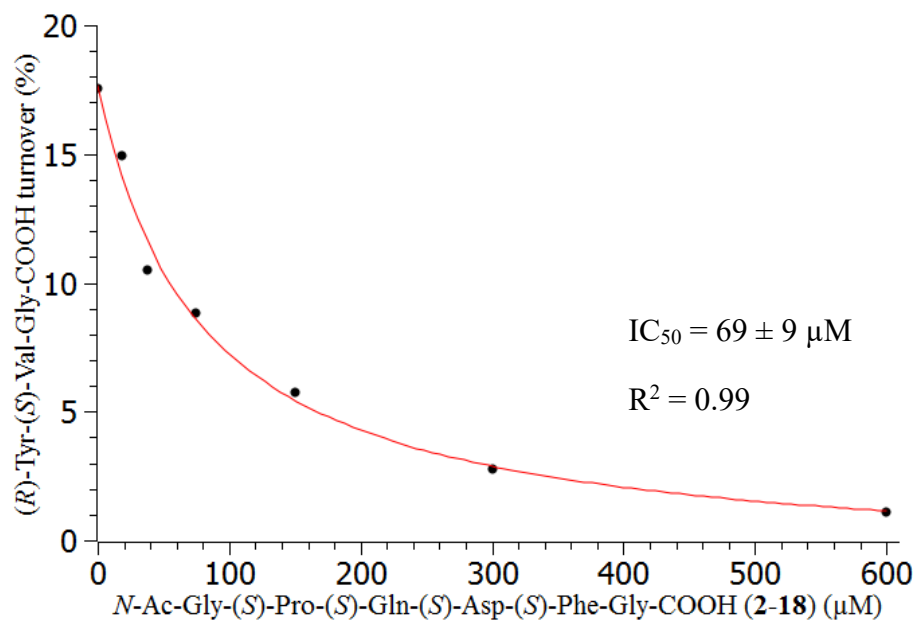


Figure 8.35 Determination of IC_{50} for N -Ac-Gly-(S)-Pro-(S)-Gln-(S)-Asp-(S)-Phe-Gly-COOH (**2-18**) (μ M)

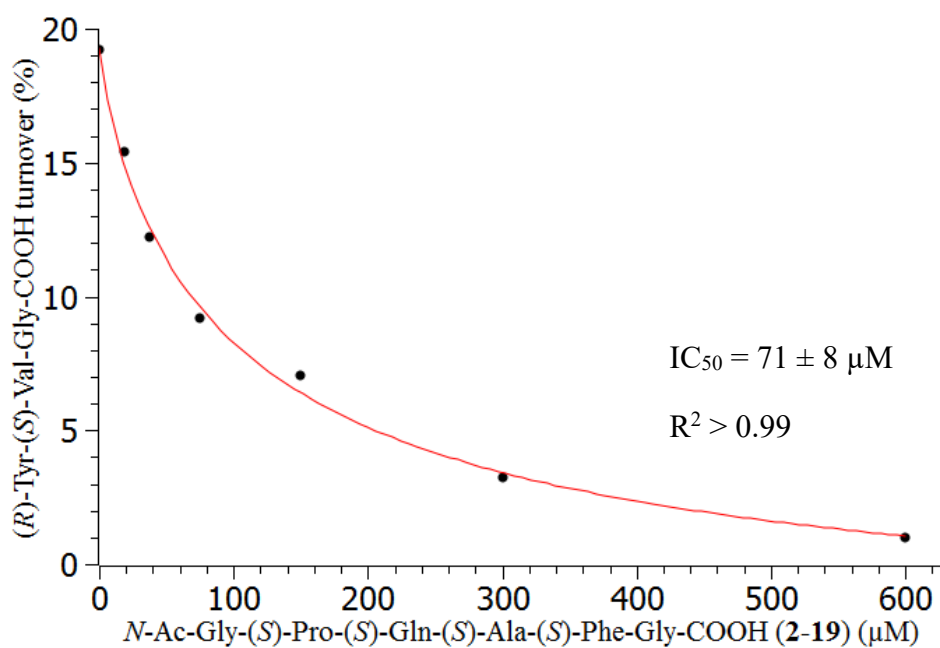
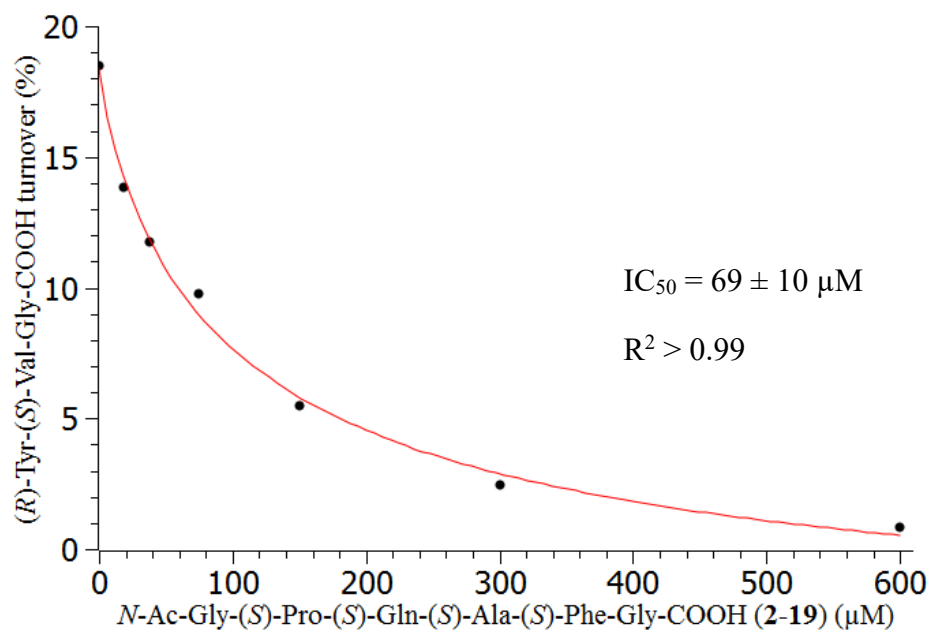


Figure 8.36 Determination of IC_{50} for *N*-Ac-Gly-(*S*)-Pro-(*S*)-Gln-(*S*)-Ala-(*S*)-Phe-Gly-COOH (2-19) (μM)

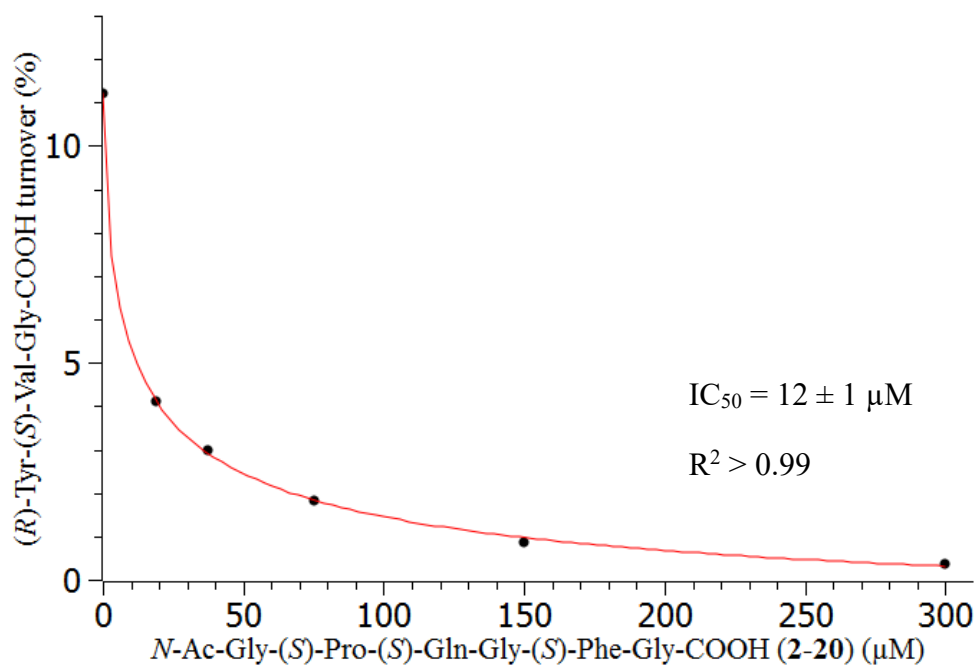
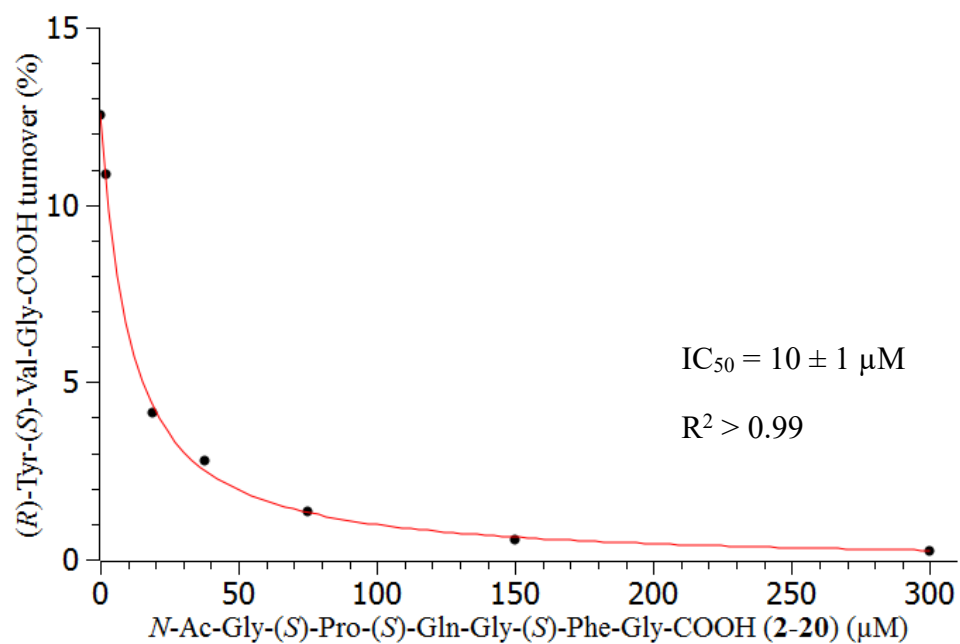


Figure 8.37 Determination of IC_{50} for *N*-Ac-Gly-(*S*)-Pro-(*S*)-Gln-Gly-(*S*)-Phe-Gly-COOH (2-20) (μM)

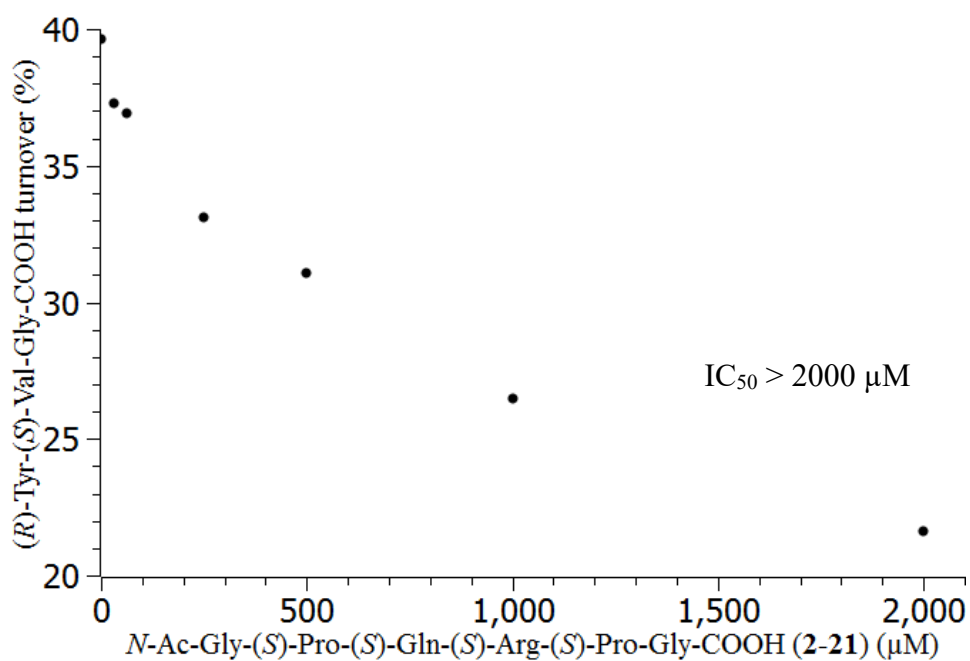
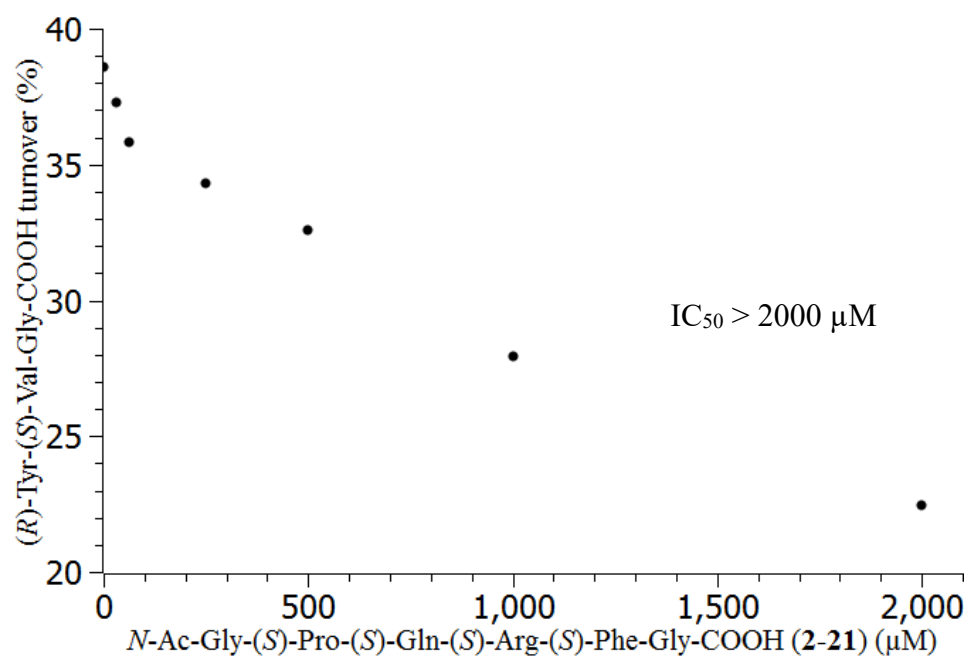


Figure 8.38 Determination of IC_{50} for *N*-Ac-Gly-(*S*)-Pro-(*S*)-Gln-(*S*)-Arg-(*S*)-Pro-Gly-COOH (2-21) (μ M)

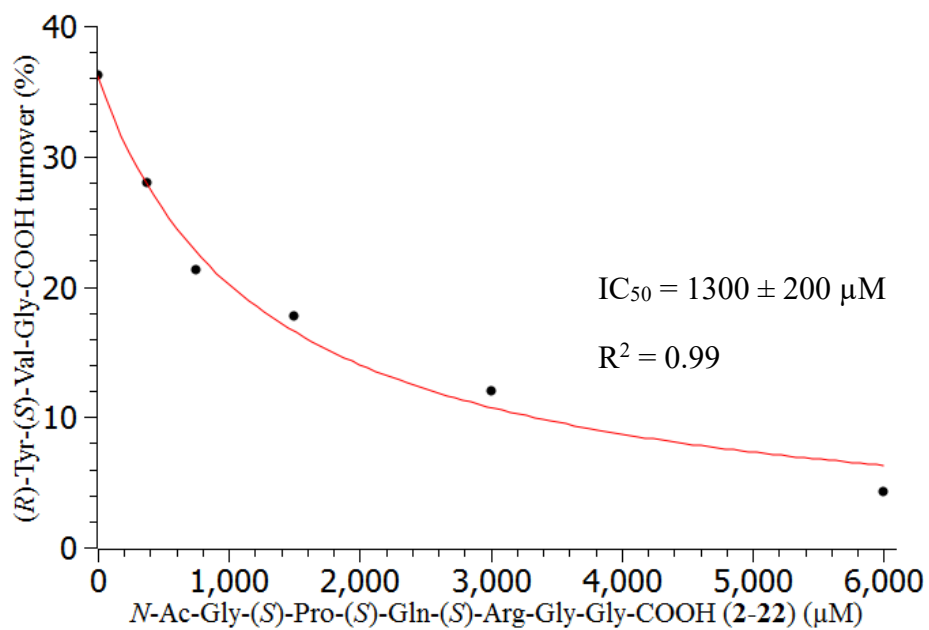
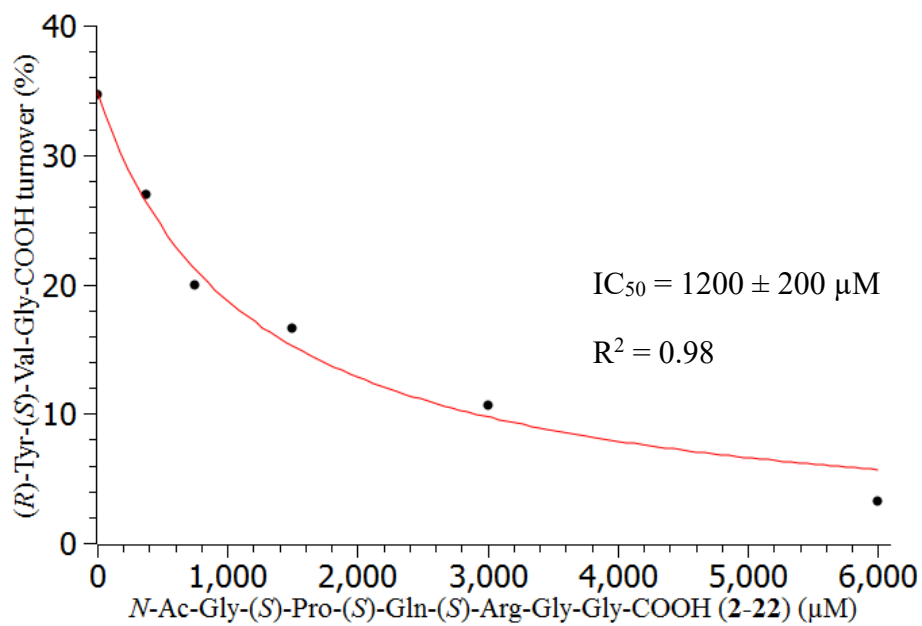


Figure 8.39 Determination of IC_{50} for N -Ac-Gly-(S)-Pro-(S)-Gln-(S)-Arg-Gly-Gly-COOH (**2-22**) (μM)

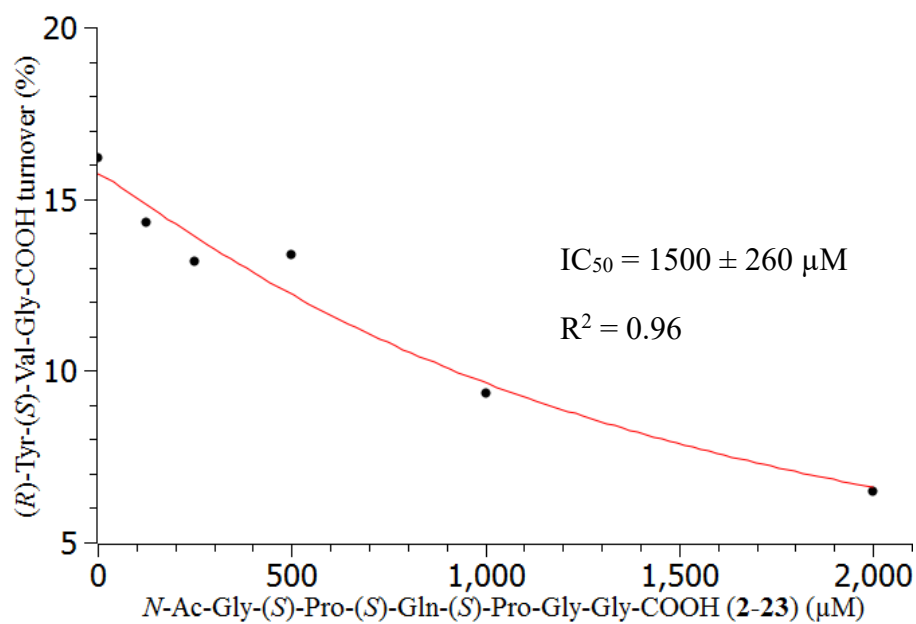
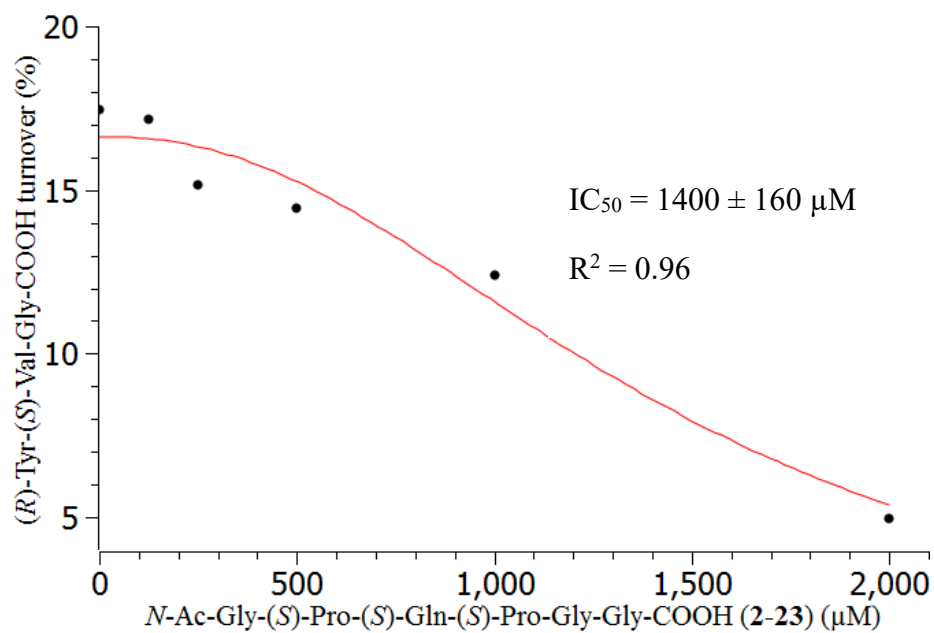
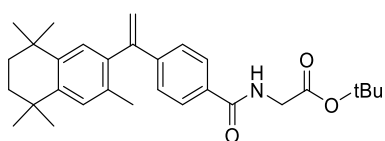


Figure 8.40 Determination of IC_{50} for *N*-Ac-Gly-(*S*)-Pro-(*S*)-Gln-(*S*)-Pro-Gly-Gly-COOH (2-23) (μM)

8.3 Experimental for Chapter 3: Synthesis and Evaluation of Interactions of Glycine Derivatives of Medicinal Agents with Peptidylglycine α -Amidating Monooxygenase

8.3.1 Synthesis Work Described in Chapter 3

tert-Butyl-(4-(1-(3,5,5,8,8-pentamethyl-5,6,7,8-tetrahydronaphthalen-2-yl)vinyl)benzoyl)-glycinate (**3-8**)



3-8

Bexarotene (250 mg, 0.72 mmol), *tert*-butyl glycine hydrochloride (130 mg, 0.76 mmol, 1.06 eq) and BOP reagent (480 mg, 1.08 mmol, 1.50 eq) were combined and dissolved in DCM (10 mL). DIPEA (0.30 mL, 1.70 mmol, 2.36 eq) was added dropwise and the mixture was stirred for 24 h under nitrogen. The reaction mixture was concentrated under reduced pressure and subjected to silica gel flash column chromatography (EtOAc/n-hexane, 2:8, v/v). The appropriate fractions were combined and concentrated under reduced pressure to yield the compound **3-8** as a colourless amorphous solid (300 mg, 91%).

m.p.: 137.8-138.8 °C; $^1\text{H NMR}$ (300 MHz, CDCl_3): δ 7.73 (d, $J = 8.5$ Hz, 2H), 7.34 (d, $J = 8.5$ Hz, 2H), 7.12 (s, 1H), 7.07 (s, 1H), 6.61 (bt, $J = 4.9$ Hz, 1H), 5.79 (s, 1H), 5.30 (s, 1H), 4.13 (d, $J = 4.9$ Hz, 2H), 1.94 (s, 3H), 1.70 (s, 4H), 1.50 (s, 9H), 1.30 (s, 6H), 1.27 (s, 6H); $^{13}\text{C NMR}$ (75 MHz, CDCl_3): δ 169.2, 167.0, 149.0, 144.4, 144.3,

142.3, 138.0, 132.7, 132.6, 128.1, 128.0, 127.1, 126.7, 116.4, 82.5, 42.5, 35.2, 34.0, 33.9, 31.9, 28.1, 19.9; **MS (ESI) (+ve):** m/z 484.6 $[M+Na]^+$. **HRMS (ESI)** calcd. for $C_{30}H_{39}NO_3Na$ $[M+Na]^+$ m/z 484.2828, found m/z 484.2831 (**Figure 8.41**).

Elemental Composition Report

Page 1

Single Mass Analysis

Tolerance = 3.0 PPM / DBE: min = -1.5, max = 20.0

Element prediction: Off

Number of isotope peaks used for i-FIT = 3

Monoisotopic Mass, Even Electron Ions

140 formula(e) evaluated with 1 results within limits (all results (up to 1000) for each mass)

Elements Used:

C: 0-40 H: 0-50 N: 0-3 O: 0-3 ^{23}Na : 0-1

CG12/01/AJ

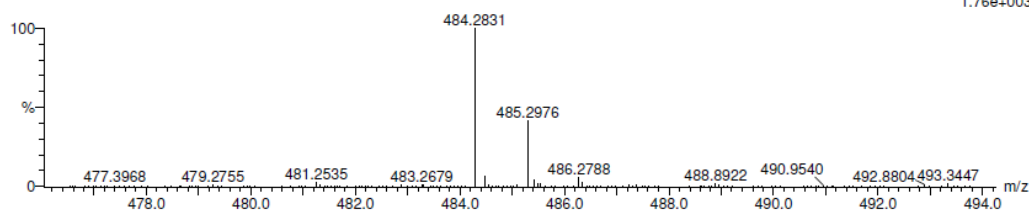
26562

0637 4 (0.172)

KE375

15-May-2013 14:52:33

1: TOF MS ES+
1.76e+003



Mass	Calc. Mass	mDa	PPM	DBE	i-FIT	Formula
484.2831	484.2828	0.3	0.6	11.5	10.3	$C_{30}H_{39}NO_3^{23}Na$

Figure 8.41 High resolution MS of compound **3-8**.

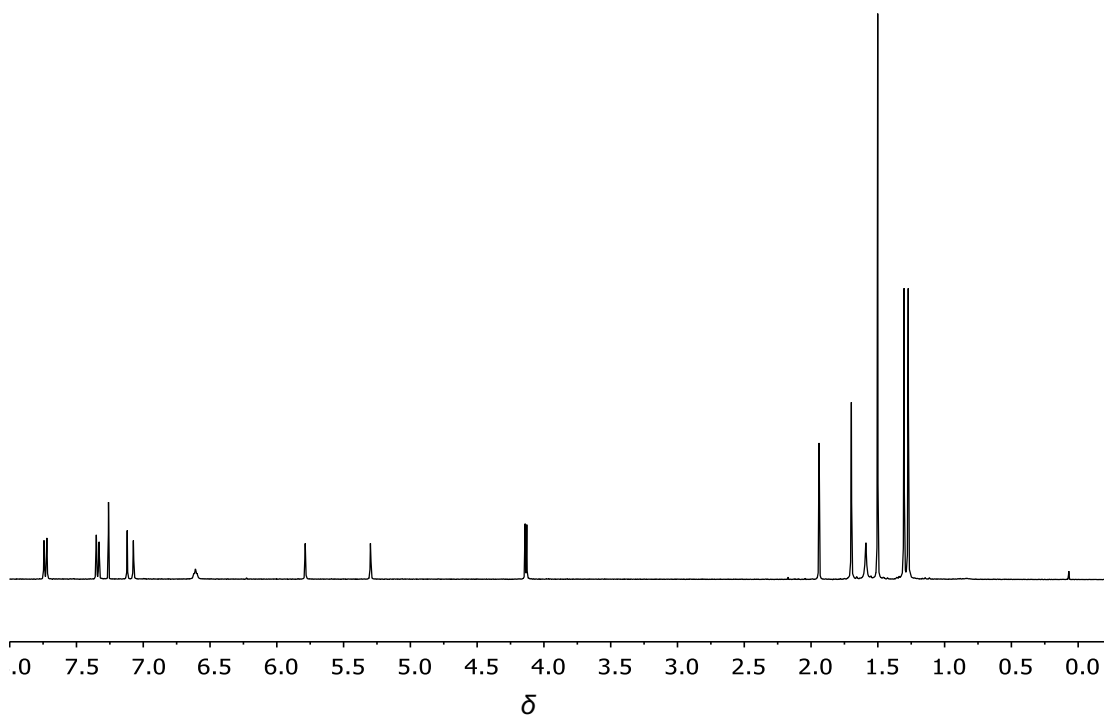
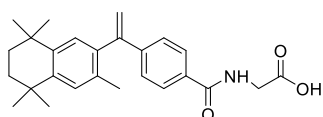


Figure 8.42 ^1H NMR of spectrum of compound **3-8**.

(4-(1-(3,5,5,8,8-pentamethyl-5,6,7,8-tetrahydronaphthalen-2-yl)vinyl)benzoyl)-glycine (3-4)



3-4

The glycine derivative **3-8** (100 mg, 0.22 mmol) was stirred in TFA (1 mL) for 2 h. Concentration under a nitrogen flow yielded the compound **3-4** as a colourless powder which was triturated from Et₂O to give a colourless solid (80 mg, 91%). A sample (approx. 3 mg) of the product precipitate was dissolved in 10% aqueous MeOH solution (50 μL) and analysed by HPLC using an Alltima C18 5 μ (22 \times 250 mm)

column at a flow rate of 8 mL/min with a UV-Vis detector. The analysis was carried out with a gradient maintained at 75:25 (MeCN: H₂O (0.1% TFA), v/v) for 5 min, followed by a linear gradient elution of 75:25 to 88:12 between 5-25 min and maintained at 75:25 for 5 min at 210 nm. The resulting HPLC chromatogram is reproduced in **Figure 8.43**, and showed that the resulting residue was pure, and the only dominant peak was at 22.30 min.

m.p.: 164.1-167.0 °C; **¹H NMR (300 MHz, CDCl₃):** δ7.73 (d, *J* = 8.2 Hz, 2H), 7.35 (d, *J* = 8.2 Hz 2H), 7.11 (s, 1H), 7.07 (s, 1H), 6.70 (bs, 1H), 5.79 (s, 1H), 5.31 (s, 1H), 4.27 (bs, 2H), 1.93 (s, 3H), 1.70 (s, 4H), 1.30 (s, 6H), 1.27 (s, 6H), 1.27 (s, 6H); **¹³C NMR (75 MHz, CDCl₃):** δ173.0, 168.1, 149.1, 145.1, 142.5, 138.1, 132.8, 132.0, 128.2, 127.4, 116.8, 35.3, 34.2, 34.0, 32.1, 20.1; **MS (ESI) (-ve):** *m/z* 404.5 [M-H]⁻. **HRMS (ESI) calcd.** for C₂₆H₃₀NO₃ [M-H]⁻ *m/z* 404.2226, found *m/z* 404.2225 (**Figure 8.44**).

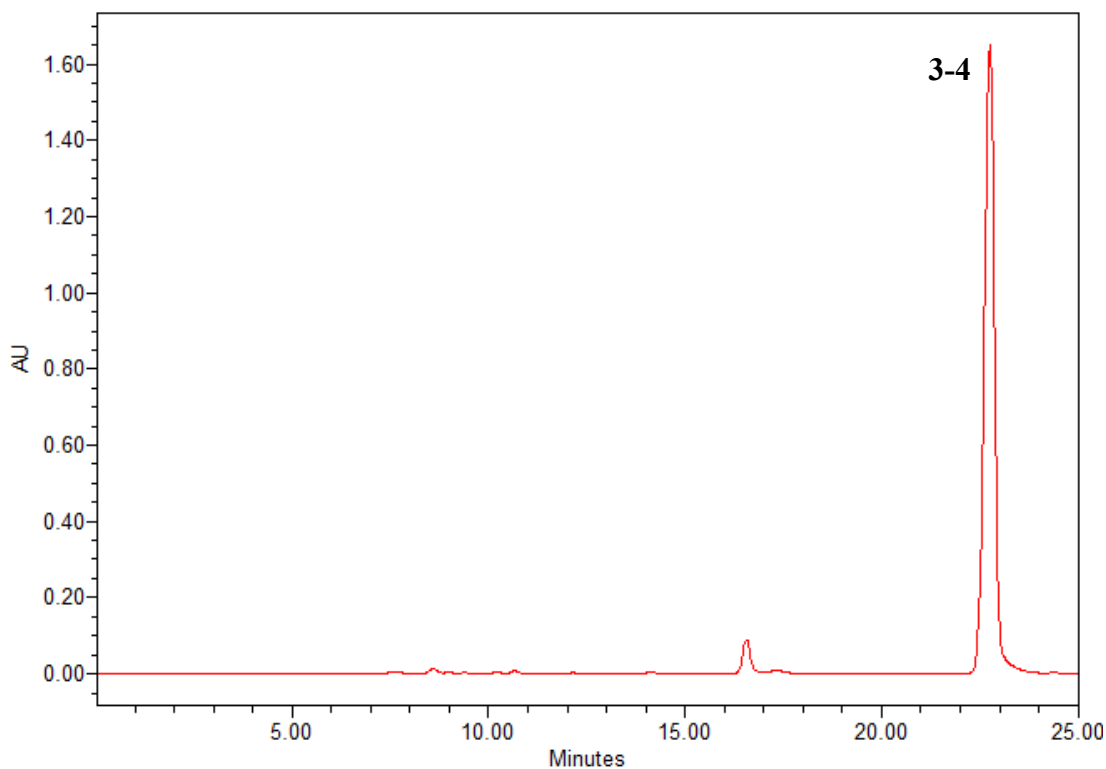


Figure 8.43 HPLC chromatogram of compound **3-4**.

Elemental Composition Report

Page 1

Single Mass Analysis

Tolerance = 3.0 PPM / DBE: min = -1.5, max = 20.0

Element prediction: Off

Number of isotope peaks used for i-FIT = 3

Monoisotopic Mass, Even Electron Ions

34 formula(e) evaluated with 1 results within limits (all results (up to 1000) for each mass)

Elements Used:

C: 0-50 H: 0-50 N: 0-1 O: 0-3

CG 13/AJ

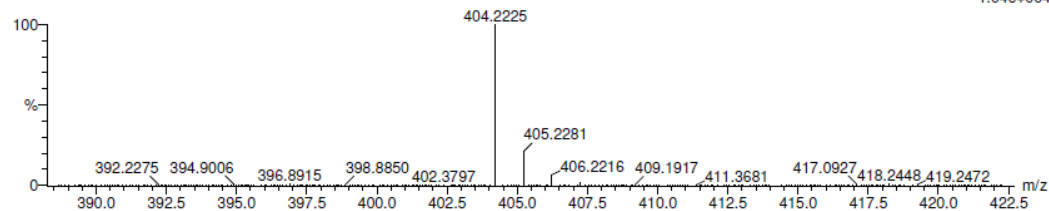
27534

0850 16 (0.699)

KE375

25-Jun-2013 17:12:46

1: TOF MS ES-
1.04e+004



Minimum:

Maximum: 5.0 3.0 -1.5

20.0

Mass	Calc. Mass	mDa	PPM	DBE	i-FIT	Formula
404.2225	404.2226	-0.1	-0.2	12.5	167.7	C ₂₆ H ₃₀ N O ₃

Figure 8.44 High resolution MS of compound **3-4**.

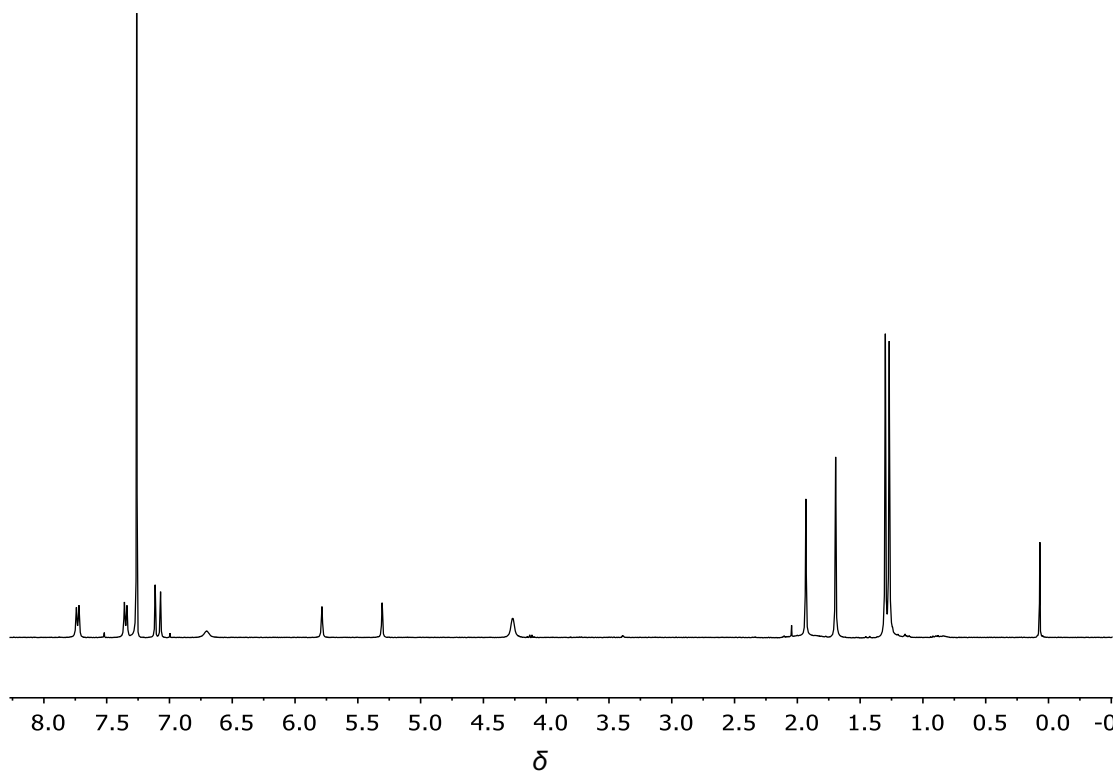
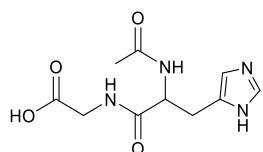


Figure 8.45 ^1H NMR of spectrum of compound **3-4**.

***N*-Ac-(*S*)-His(Bom)-Gly-COOH (**3-6**)**



3-6

To crude compound **2-2** (which was prepared in the exactly the same manner as described in **Section 8.2.1**) was added to Fmoc-(*S*)-His(Bom)-COOH (498 mg, 0.80 mmol, 2.00 eq), HOBt (108 mg, 0.80 mmol, 2.00 eq), HBTU (303 mg, 0.80 mmol, 2.00 eq), and DIPEA (280 μL , 1.60 mmol, 4.00 eq) in DMF (3.0 mL). The reaction mixture was agitated with a nitrogen flow at room temperature for 2 h, filtered in order to remove excess reagents, and then washed with DMF (3×5 mL). Fmoc deprotection

was then achieved by addition of piperidine in DMF (3.4 mL, 20%, v/v), agitation with a nitrogen flow at room temperature for 1 h, and washing with DMF (3 × 5 mL) to produce crude **3-10**. To compound **3-10** was added a mixture of excess Ac₂O (500 μL), piperidine (500 μL), and DMF (5 mL) and the mixture was then agitated with a nitrogen flow at room temperature for 30 min. After filtration, to the residue was added a mixture of TFA (3.2 mL), TIPS (0.1 mL) and H₂O (0.1 mL) and this was agitated manually at room temperature for 2 h. The reaction mixture was filtered and the resulting filtrate was transferred into cold Et₂O (80 mL) with Falcon tubes placed into a -20 °C freezer standing overnight for precipitation. After removing Et₂O by filtration, crude *N*-Ac-(*S*)-His(Bom)-Gly-COOH (**3-11**) was obtained as a white solid (130 mg). The peptide with the Bom protecting group was hydrogenated using MeOH (10 mL) as solvent and Pd/C (5 wt%, 26 mg) as catalyst under a hydrogen atmosphere by using a balloon. After the mixture was stirred at room temperature for 4 h, the catalyst was removed by filtration, and the solvent was evaporated to produce a white solid (58 mg). A sample (approx. 3 mg) of the precipitate was dissolved in 10% MeOH aqueous solution (50 μL) and subsequently analysed by preparative HPLC using an Alltima C18 5μ (22 × 250 mm) column, at a flow rate of 8 mL/min with a UV-Vis detector with peak detection at 210 nm. The analysis was carried out with an isocratic elution of 5:95 (MeOH: H₂O (0.1% TFA), v/v) for 15 min. The resulting HPLC chromatogram is reproduced in **Figure 8.46** and showed two dominant peaks. Samples corresponding to each of these were isolated through HPLC. Mass spectrometry of the peak at 12.30 min displayed ions at *m/z* 255.5, which corresponds to the [M+H]⁺ for dipeptide **3-6**; the peak at 10.50 min displayed ions at *m/z* 375.4, which corresponds to the [M+H]⁺ for the starting material **3-11**. Based on this analysis, preparative HPLC was used to

isolate **3-6**. The column fractions were concentrated *via* freeze drying to give compound **3-6** (9.9 mg, 37%) as a colourless powder.

m.p.: 159.1-163.0 °C; **¹H NMR (400 MHz, CDCl₃):** 8.57 (s, 1H), 7.26 (s, 1H), 4.49 (dd, *J* = 8.3, 5.0 Hz, 1H), 3.25 (dd, *J* = 15.3, 5.0 Hz, 1H), 3.08 (dd, *J* = 15.3, 8.3 Hz, 1H), 1.99 (s, 3H); **¹³C NMR (75 MHz, CDCl₃):** δ173.3, 173.0, 172.5, 134.9, 131.0, 118.6, 53.3, 41.8, 28.2, 22.5; **MS (ESI) (+ve):** *m/z* 255.5 [M+H]⁺. **HRMS (ESI) calcd.** for C₁₀H₁₅N₄O₄ [M+H]⁺ *m/z* 255.1093, found *m/z* 255.1093 (**Figure 8.47**).

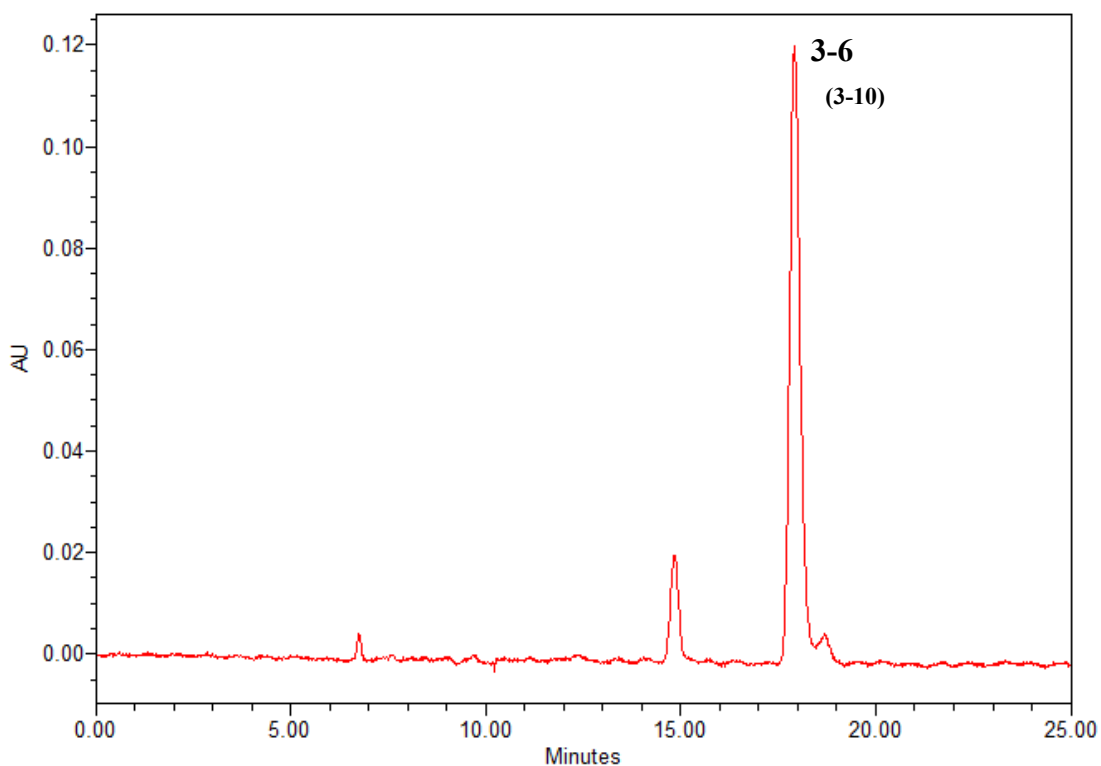


Figure 8.46 HPLC chromatogram of crude compound **3-6**.

Single Mass Analysis

Tolerance = 3.0 PPM / DBE: min = -1.5, max = 20.0

Element prediction: Off

Number of isotope peaks used for i-FIT = 3

Monoisotopic Mass, Even Electron Ions

4 formula(e) evaluated with 1 results within limits (all results (up to 1000) for each mass)

Elements Used:

C: 0-10 H: 0-16 N: 0-4 O: 4-4

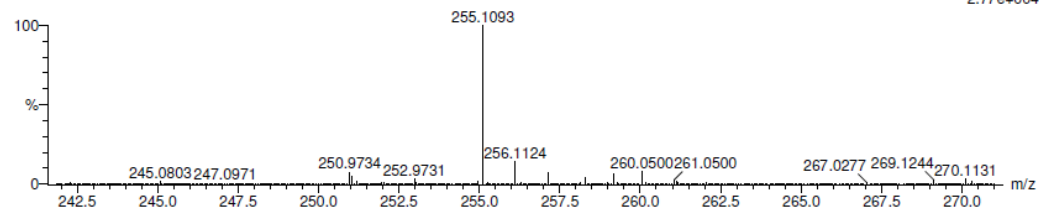
HG2-PERFECT/EO

29618

141071 (3.112) Cm (68:80)

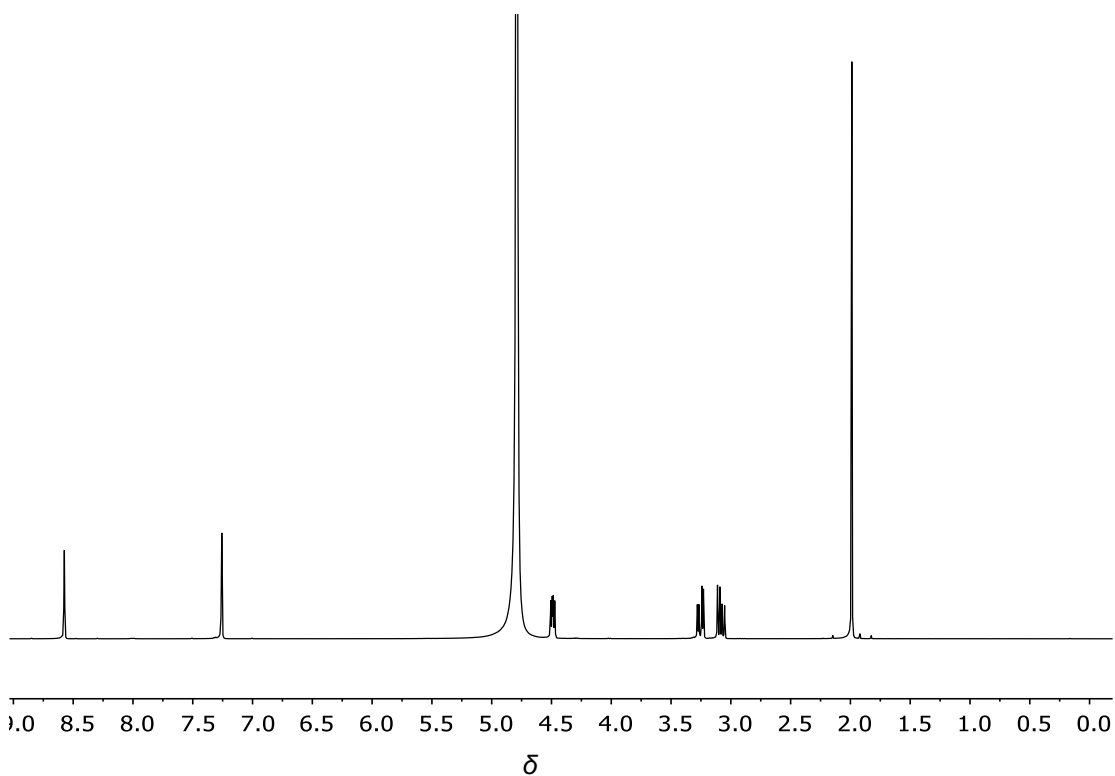
KE375

01-Nov-2013 10:14:06

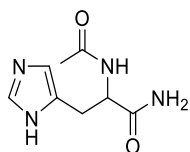
1: TOF MS ES+
2.77e+004

Minimum:				-1.5		
Maximum:		5.0	3.0	20.0		
Mass	Calc. Mass	mDa	PPM	DBE	i-FIT	Formula
255.1093	255.1093	0.0	0.0	5.5	n/a	C10 H15 N4 O4

Figure 8.47 High resolution MS of compound 3-6.

Figure 8.48 ¹H NMR of spectrum of compound 3-6.

N-Ac-(*S*)-His-NH₂ (**3-7**)



3-7

To a solution of *N*-Ac-(*S*)-histidine (200 mg, 0.99 mmol) in MeOH (5 mL) was added thionyl chloride (0.36 mL, 5.00 mmol, 5.00 eq), and the mixture was stirred at 0 °C for 30 min under nitrogen. Thereafter, the reaction mixture was concentrated and the resulting residue was added to water (10 mL), followed by the extraction of EtOAc (3 × 10 mL). The combined organic layers were washed with saturated NaHCO₃ (3 × 20 mL), brine (1 × 20 mL), dried MgSO₄, and concentrated to give the product **3-13** as a colourless oil (175 mg, 83%). Thereafter, the ester **3-13** was treated with concentrated ammonia solution (40 mL) and stirred for 30 min. The reaction mixture was then concentrated under reduced pressure and purified by HPLC. Analysis of compound **3-7** was carried out using a Luna 5μ C18 analytical column (4.60 × 250 mm) with an isocratic elution of 1:9 (MeOH: H₂O (0.1% TFA), v/v) for 15 min at 210 nm. As shown in **Figure 8.49**, there was one dominant peak at 10.00 min. Mass spectrometry of the peak displayed ions at *m/z* 197.3, which corresponds to the [M+H]⁺ for compound **3-7**. Based on this analysis, preparative HPLC was used to isolate compound **3-7**. The column fractions were concentrated *via* freeze drying to give compound **3-7** (80 mg, 41%) as a colourless powder.

¹H NMR (400 MHz, CDCl₃): 8.62 (s, 1H), 7.31 (s, 1H), 4.67 (dd, *J* = 8.8, 5.6 Hz, 1H), 3.29 (dd, *J* = 15.5, 5.6 Hz, 1H), 3.13 (dd, *J* = 15.5, 8.8 Hz, 1H), 1.99 (s, 3H); ¹³C

NMR (100 MHz, CDCl₃): δ 174.46, 174.12, 133.4, 128.6, 117.1, 52.3, 26.4, 21.7; **MS (ESI) (+ve):** m/z 197.3 [M+H]⁺. **HRMS (ESI) calcd.** for C₈H₁₃N₄O₂ [M+H]⁺ m/z 197.1039, found m/z 197.1040 (**Figure 8.50**).

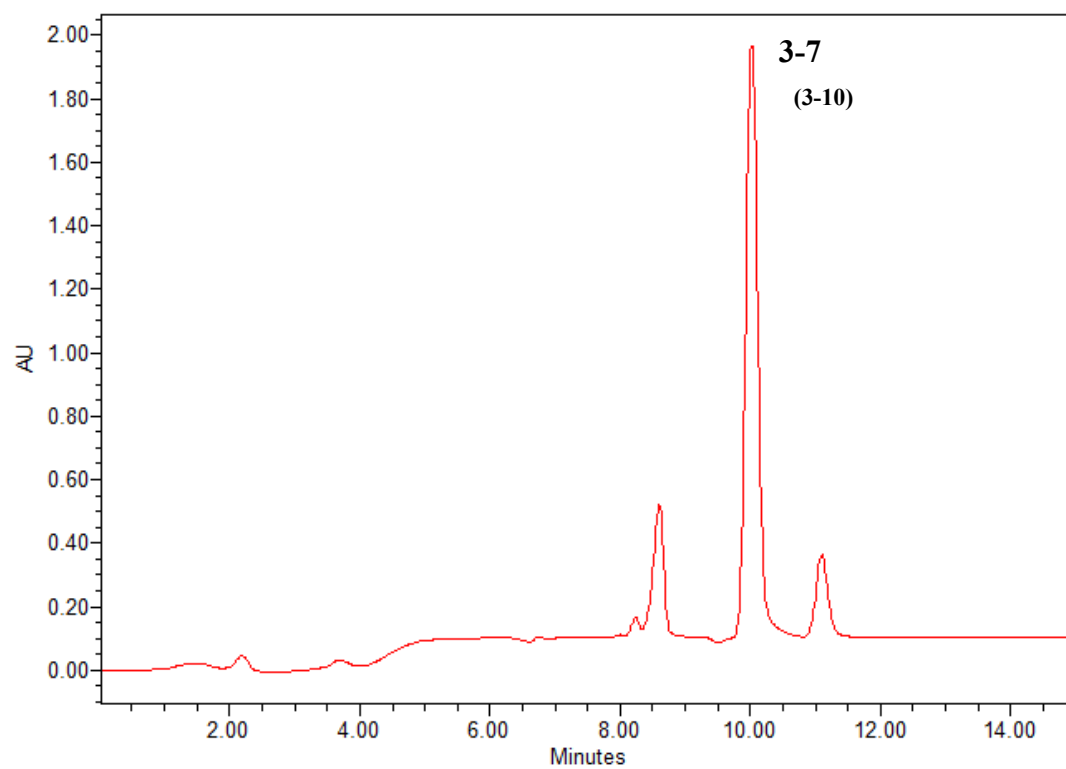


Figure 8.49 HPLC chromatogram of crude compound **3-7**.

Single Mass Analysis

Tolerance = 3.0 PPM / DBE: min = -1.5, max = 20.0

Element prediction: Off

Number of isotope peaks used for i-FIT = 3

Monoisotopic Mass, Odd and Even Electron Ions

150 formula(e) evaluated with 1 results within limits (all results (up to 1000) for each mass)

Elements Used:

C: 0-50 H: 0-70 N: 0-6 O: 0-9

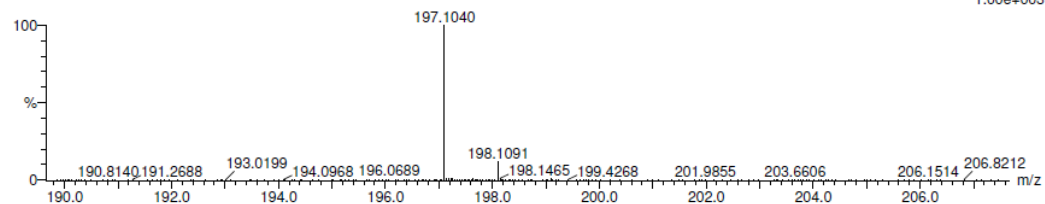
N-AC-HIS-NH2/EO

36838

0135 37 (1.647) Cm (36:42)

KE375

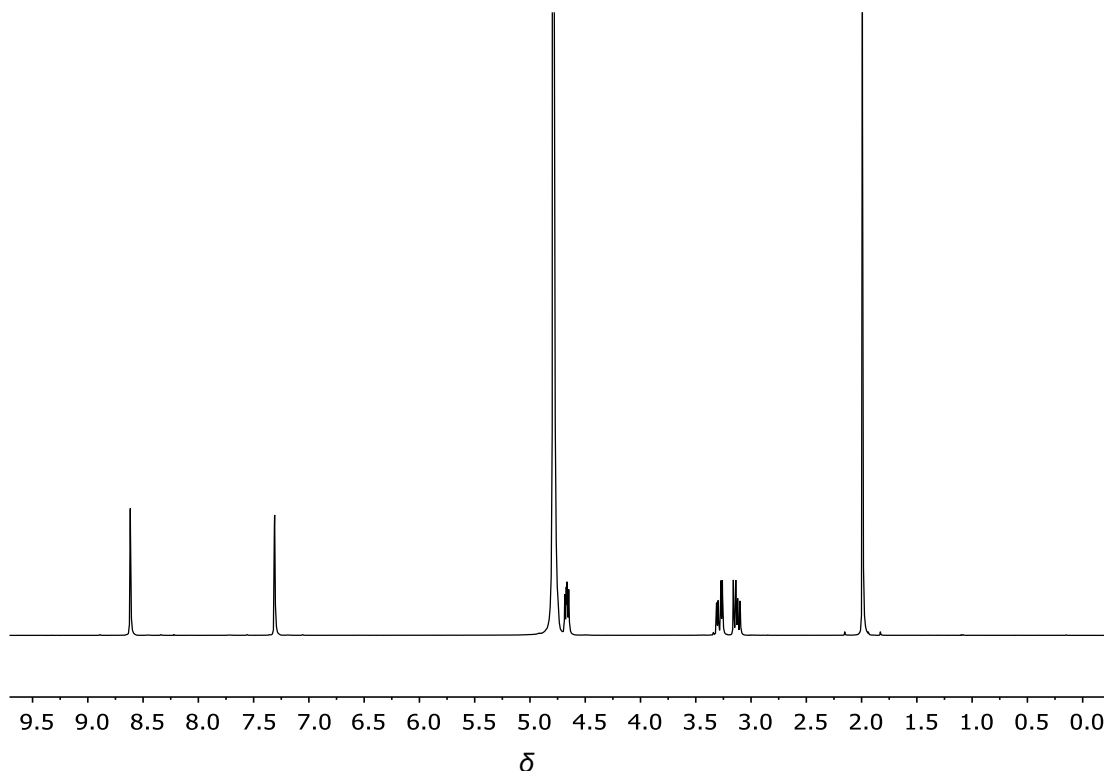
23-Jan-2015 12:04:16

1: TOF MS ES+
1.00e+003

Minimum: -1.5
Maximum: 20.0

Mass	Calc. Mass	mDa	PPM	DBE	i-FIT	Formula
197.1040	197.1039	0.1	0.5	4.5	n/a	C8 H13 N4 O2

Figure 8.50 High resolution MS of compound 3-7.

Figure 8.51 ¹H NMR of spectrum of compound 3-7.

8.3.2 Procedure for Determination of IC₅₀ of Prodrug Candidates with PAM

Assays were performed with 1.25 mM ascorbic acid, 10 μ M copper sulphate, 0.2 mg/mL bovine liver catalase, 1% EtOH, 1% DMSO, 50 μ M tripeptide substrate (*R*)-Tyr-(*S*)-Val-Gly-COOH and 600-0 μ M at 2X serial dilution of dipeptide **3-6** in 150 mM MES buffer at pH 5.8. Compound **3-4** was initially tested with 600-0 μ M at 2X dilution, followed by 4800-0 μ M at 2X dilution. Assays were initiated through the addition of concentrated medium PAM (5 μ L) to give a final volume of 100 μ L. The mixtures were incubated in a Lab Companion Model SI-600R open-air shaker at 37 °C for 2 h, with agitation at 80 rpm. At the end of the incubation, the reaction mixture was treated with 1 M NaOH (25 μ L) and incubated at 37 °C for 2 min, followed by neutralisation with 1 M HCl (25 μ L). The solutions were then passed through Amicon® Ultra YM-3 filters using a centrifuge for 15 min at 12000 rpm at room temperature, and the filtrates were then analysed by using the same HPLC method as described in **Section 8.2.4**. The competition assays were run at least in duplicate.

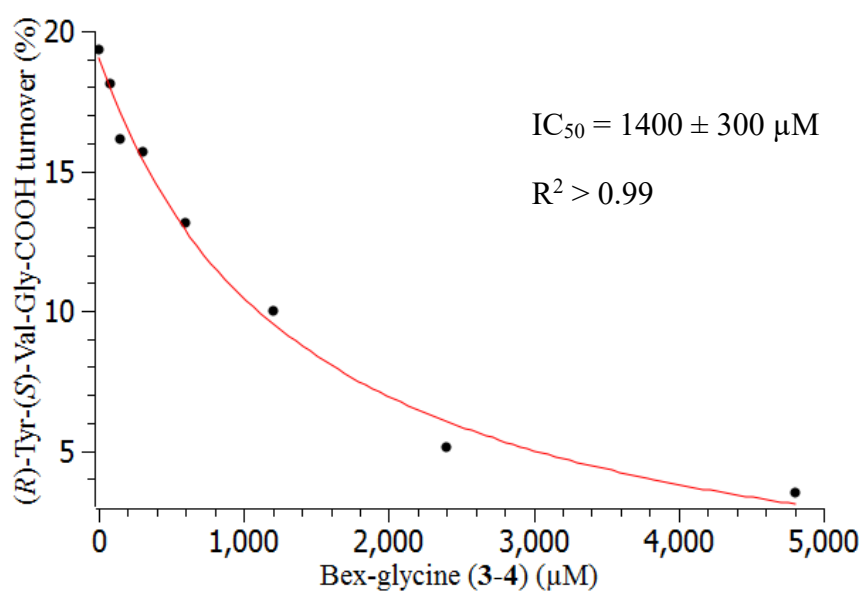
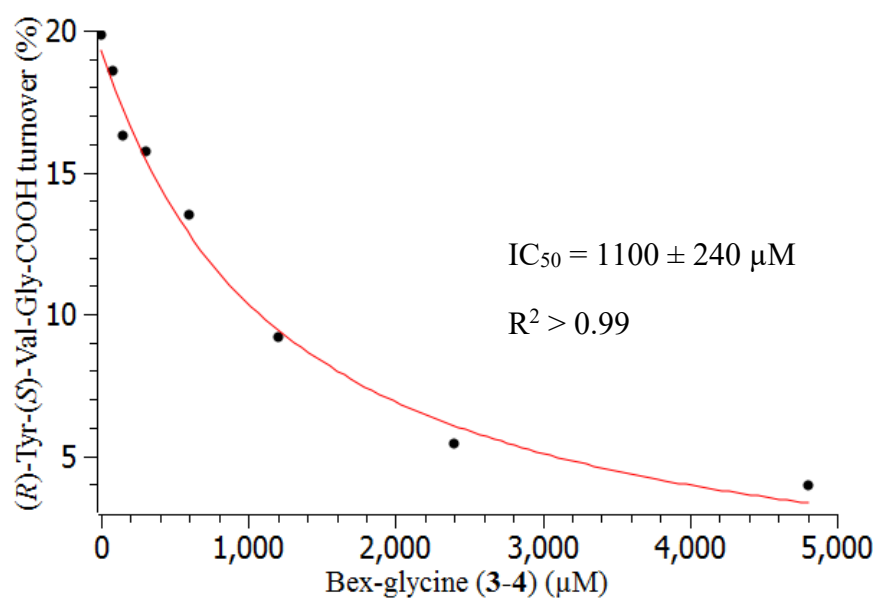


Figure 8.52 Determination of IC_{50} for Bex-glycine (3-4).

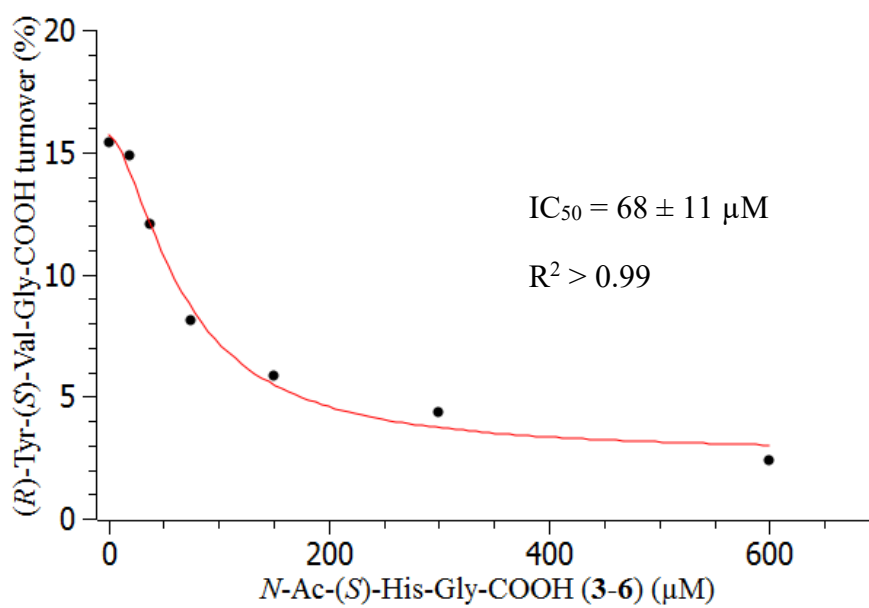
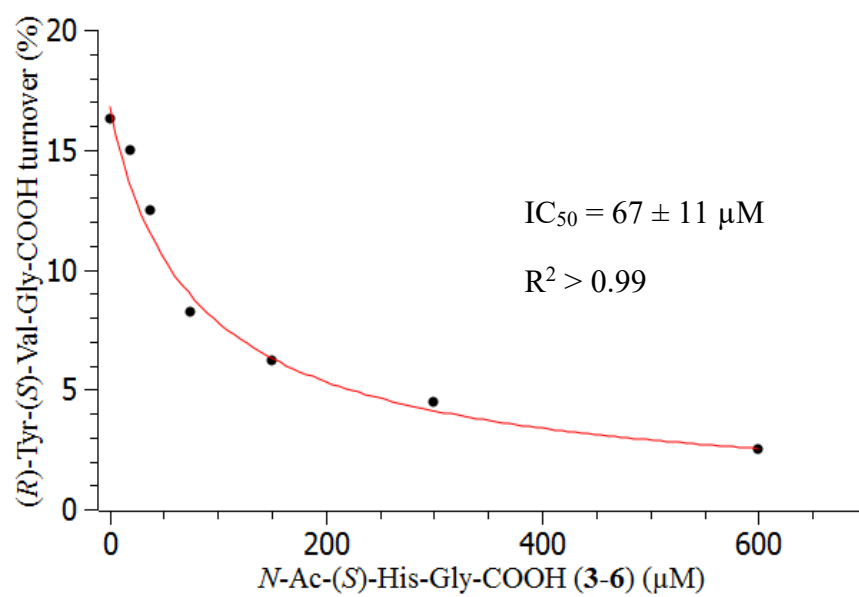


Figure 8.53 Determination of IC_{50} for N -Ac-Gly-(S)-His-Gly-COOH (3-6) (μ M)

8.3.3 Procedure for Cytotoxicity Evaluation of Bexarotene (3-1) and Bex-glycine (3-4)

Inhibition of growth proliferation was determined using CCK8 assays. At first, DMS53 cells were cultured, lifted as described before to give cell suspensions, a small amount of which were diluted with fresh medium and 0.4% trypan blue stain for cell counting with a BIO-RAD TC20TM automated cell counter. After cell counting, cell suspensions (5×10^3 cells mL⁻¹) were made by dilution with fresh medium and 100 μ L of the suspension was placed in a Nunclon 96-well plate and pre-incubated for 24 h in a Memmert incubator at 37 °C under a moist atmosphere of 5% CO₂/95% air. Following 24 h of incubation, 160-0 μ M at 2X serial dilution and 640 μ M of bexarotene (**3-1**) and compound **3-4** (10 μ L) was treated into the medium in the plate. The plate was incubated in the incubator for 72 h, followed by addition of CCK-8 solution (10 μ L) for each well and further incubation for 4 h. The absorbance of each well was then measured using a Microplate reader at 450 nm and the cell viability percentage and concentration were plotted and calculated to give LD₅₀ values using SciDAVis 0.2.4.

8.3.4 Procedure for Standard PAM Assay with *N*-Ac-(*S*)-His-Gly-COOH (3-6)

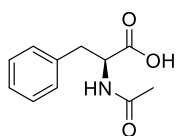
The assay was performed with 10 μ M CuSO₄, 1% DMSO, 1% EtOH, 75 μ M *N*-Ac-(*S*)-His-Gly-COOH (**3-6**), 1.25 mM ascorbic acid, and 0.2 mg/mL bovine liver catalase in 150 mM MES buffer at pH 5.8. Assay was initiated through the addition of 5 μ L medium PAM to give a final volume of 100 μ L. The mixture was incubated at 37 °C for 2 h, and the assay was quenched with 1 M NaOH (25 μ L), followed by being

neutralised with 1 M HCl (25 μ L). The resulting solution was passed through Amicon® Ultra YM-3 filters using a centrifuge for 15 min at 12000 rpm at room temperature. The filtrates were then analysed through a Primesep 100 column (4.6 \times 100 mm) by using analytical HPLC under an isocratic gradient of MeCN and H₂O (0.1% TFA) (5:95) for 15 min, which was monitored by UV-Vis spectroscopy at 220 nm.

8.4 Experimental for Chapter 4: Investigation of the Subunit Activity of Peptidylglycine α -Amidating Monooxygenase

8.4.1 Synthesis Work Described in Chapter 4

N-Ac-(*S*)-Phe-COOH (4-1)



4-1

(*S*)-Phenylalanine (6.60 g, 39.6 mmol) was suspended in aqueous NaHCO₃ solution (5% w/v, 100 mL) cooled to 0 °C. To this solution Ac₂O (5.1 mL, 47.5 mmol, 1.20 eq) was added dropwise over a period of 1 h. The mixture was stirred at room temperature for 2 h followed by acidification to pH 2-3 with concentrated HCl, then it was cooled over ice water. The resulting white precipitate was filtered, washed with water, and dried to give compound **4-1** (5.50 g, 67%) as a colourless powder.

m.p.: 172 °C; ^[222]¹H NMR (400 MHz, DMSO-d₆) 8.17 (m, 1H), 7.32-7.14 (m, 5H), 4.39 (dd, *J* = 9.5, 4.9 Hz, 1H), 3.03 (dd, *J* = 13.8, 4.9 Hz, 1H), 2.82 (dd, *J* = 13.8, 9.5 Hz, 1H), 1.77 (s, 3H); **MS (ESI) (-ve):** *m/z* 206.1 [M-H]⁻. **HRMS (ESI)** calcd. for C₁₁H₁₂NO₃ [M-H]⁻ *m/z* 206.0817, found *m/z* 206.0811 (**Figure 8.54**).

Single Mass Analysis

Tolerance = 5.0 PPM / DBE: min = -1.5, max = 20.0

Element prediction: Off

Number of isotope peaks used for i-FIT = 4

Monoisotopic Mass, Even Electron Ions

96 formula(e) evaluated with 1 results within limits (all results (up to 1000) for each mass)

Elements Used:

C: 0-50 H: 0-50 N: 0-5 O: 0-5

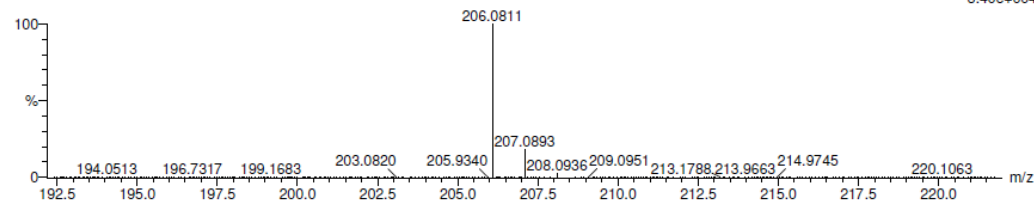
CG70/AJ

48123

1112 8 (0.347)

KE375

16-Aug-2016,14:46:05

1: TOF MS ES-
8.40e+004

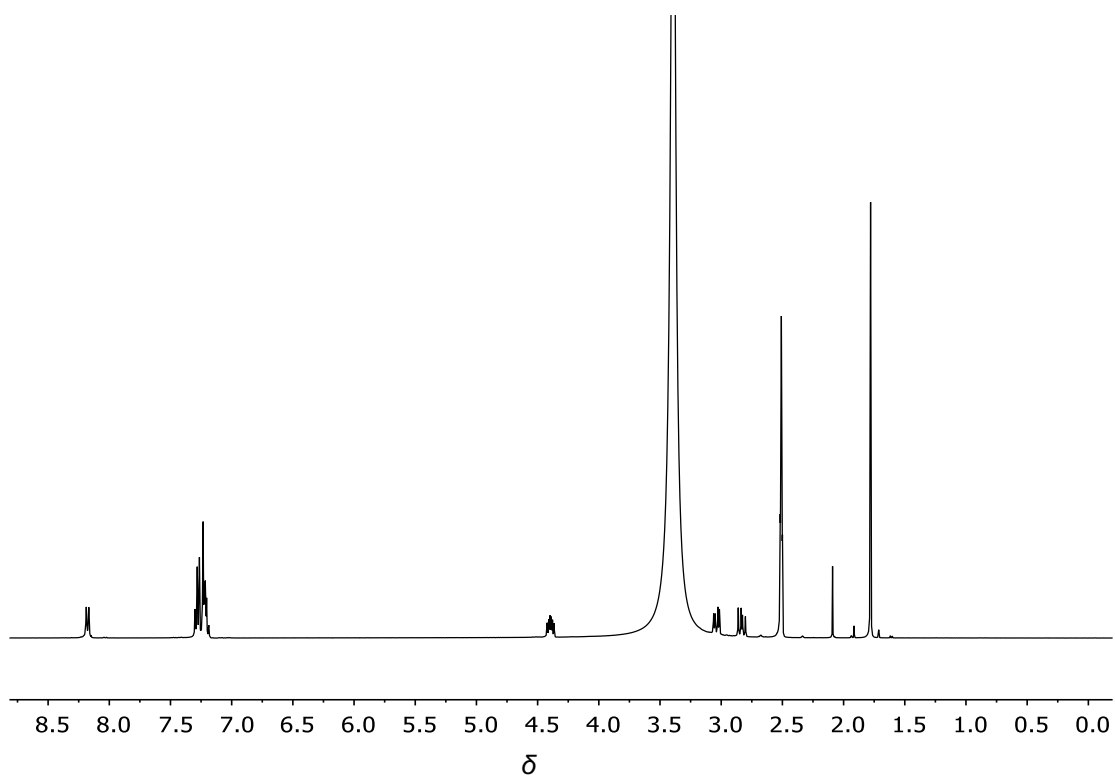
Minimum:

Maximum:

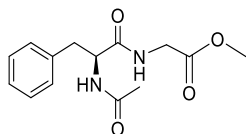
100.0 5.0 -1.5
20.0

Mass	Calc. Mass	mDa	PPM	DBE	i-FIT	Formula
206.0811	206.0817	-0.6	-2.9	6.5	841.7	C11 H12 N O3

Figure 8.54 High resolution MS of compound 4-1.

Figure 8.55 ¹H NMR of spectrum of compound 4-1.

(S)-N-Acetylphenylalanyl glycine methyl ester (4-2)



4-2

To a solution of *N*-Ac-(*S*)-Phe-COOH (**4-1**) (1.00 g, 4.78 mmol) in DCM (60 mL) was added BOP (2.18 g, 4.78 mmol, 1.00 eq) and DIPEA (3.36 mL, 19.11 mmol, 4.00 eq). The mixture was allowed to stir at room temperature under nitrogen for 30 min before the addition of glycine methyl ester hydrochloride (0.67 g, 5.26 mmol, 1.10 eq). Stirring of the reaction mixture was allowed to continue at room temperature under nitrogen for 16 h before it was diluted with EtOAc (150 mL). The organic layer was washed with 1 M HCl (3 x 30 mL), saturated NaHCO₃ solution (3 x 30 mL) and brine (1 x 40 mL), dried over MgSO₄, and concentrated *in vacuo* to give the title compound as a colourless solid (0.92 g, 69%).

¹H NMR (400 MHz, CDCl₃) δ 7.25 (m, 5H), 6.37 (m, 1H), 6.12 (m, 1H), 4.70 (m, 1H), 4.01 (dd, $J = 18.2, 5.5$ Hz, 1H), 3.90 (dd, $J = 18.2, 5.2$ Hz, 1H), 3.73 (s, 3H), 3.09 (d, $J = 7.2$ Hz, 1H), 3.07 (d, $J = 7.2$ Hz, 2H), 1.98 (s, 3H); **MS (ESI) (+ve):** m/z 301.1 [M+Na]⁺. **HRMS (ESI)** calcd. for C₁₄H₁₈N₂O₄Na [M+Na]⁺ m/z 301.1164, found m/z 301.1157 (**Figure 8.56**).

Single Mass Analysis

Tolerance = 5.0 PPM / DBE: min = -1.5, max = 15.0

Element prediction: Off

Number of isotope peaks used for i-FIT = 4

Monoisotopic Mass, Even Electron Ions

214 formula(e) evaluated with 1 results within limits (all results (up to 1000) for each mass)

Elements Used:

C: 0-50 H: 0-50 N: 0-10 O: 0-5 23Na: 1-1

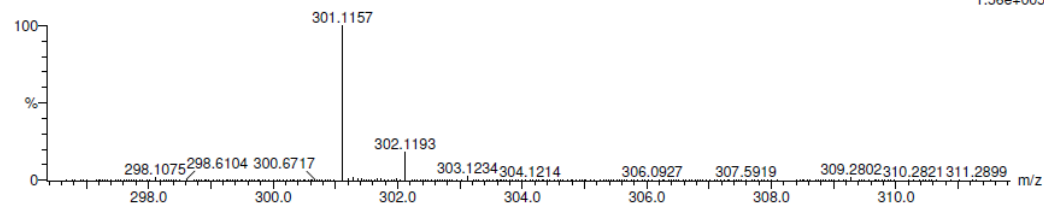
CG71

KE375

19-Aug-2016,13:10:35

48147

1139 10 (0.630) Cm (9:12)

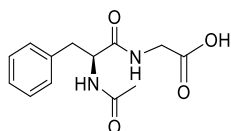
1: TOF MS ES+
1.56e+005

Minimum: -1.5
Maximum: 100.0 5.0 15.0

Mass	Calc. Mass	mDa	PPM	DBE	i-FIT	Formula
301.1157	301.1164	-0.7	-2.3	6.5	137.8	C14 H18 N2 O4 23Na

Figure 8.56 High resolution MS of compound 4-2.

(S)-N-Acetylphenylalanyl glycine (1-66)



1-66

To a solution of **4-2** (200 mg, 0.71 mmol) in THF (10 mL) and H₂O (10 mL) was added LiOH·H₂O (121 mg, 2.85 mmol, 4.00 eq), and the mixture was stirred at room temperature for 24 h, after which the mixture was extracted with DCM (3 × 20 mL) to remove any unreacted **4-2**. The mixture was acidified to pH 2 with 1 M HCl, and the aqueous layer was extracted with EtOAc (3 × 30 mL). The combined organic fractions were washed with brine (1 × 50 mL), dried over MgSO₄, and concentrated *in vacuo*,

followed by purification by preparative HPLC using an Alltima C18 5 μ (22 \times 250 mm) column (6 mL/min). The analysis was carried out with an isocratic elution of 60:40 (MeOH: H₂O (0.1% TFA), v/v) between 0-30 min. The resulting HPLC is reproduced in **Figure 8.57**, and showed two dominant peaks. Sample corresponding to the first peak was isolated through HPLC. Mass spectrometry of the peak at 14.50 min displayed ions at m/z 263.2, which corresponds to the [M-H]⁻ for compound **1-66**. Based on this analysis, preparative HPLC was used to isolate **1-66**. The column fractions were concentrated *via* freeze drying to give compound **1-66** (80 mg, 43%) as a colourless powder.

m.p.: 155.5-159.6 °C; **¹H NMR (400 MHz, CD₃OD):** δ 7.29-7.17 (m, 5H), 4.67 (dd, $J = 9.5, 5.2$ Hz, 1H), 3.90 (s, 2H), 3.20 (dd, $J = 14.0, 5.2$ Hz, 1H), 2.87 (dd, $J = 14.0, 9.5$ Hz, 1H), 1.89 (s, 3H); **¹³C NMR (100 MHz, CD₃OD):** δ 174.1, 173.2, 172.7, 138.6, 130.2, 129.4, 127.7, 55.9, 41.8, 38.8, 22.4; **MS (ESI) (-ve):** m/z 263.2 [M-H]⁻. **HRMS (ESI)** calcd. for C₁₃H₁₅N₂O₄ [M-H]⁻ m/z 263.1032, found m/z 263.1032 (**Figure 8.58**).

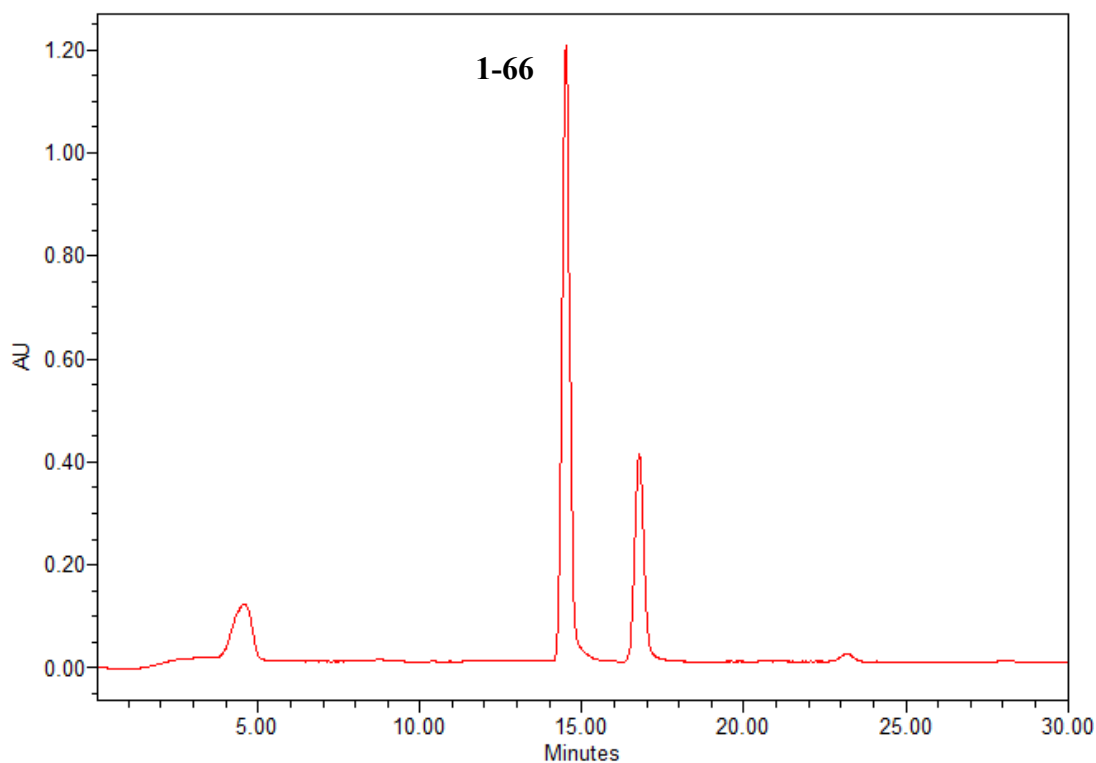


Figure 8.57 HPLC chromatogram of crude compound **1-66**.

Elemental Composition Report

Page 1

Single Mass Analysis

Tolerance = 3.0 PPM / DBE: min = -1.5, max = 10.0
 Element prediction: Off
 Number of isotope peaks used for i-FIT = 4

Monoisotopic Mass, Even Electron Ions
 198 formula(e) evaluated with 1 results within limits (all results (up to 1000) for each mass)

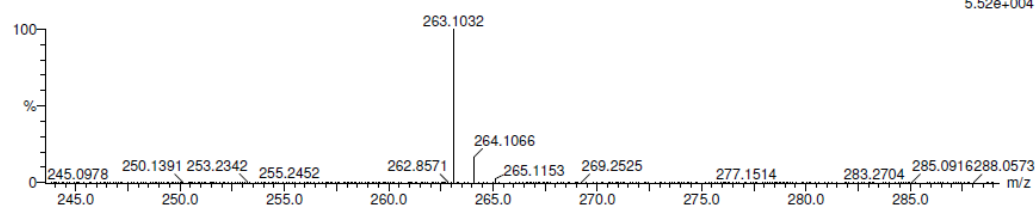
Elements Used:
 C: 0-50 H: 0-50 N: 0-5 O: 0-10

CG76/AJ
 48343
 1199 95 (4.170)

KE375

02-Sep-2016,09:29:55

1: TOF MS ES-
 5.52e-004



Minimum: -1.5
 Maximum: 100.0 3.0 10.0

Mass	Calc. Mass	mDa	PPM	DBE	i-FIT	Formula
263.1032	263.1032	0.0	0.0	7.5	40.7	C13 H15 N2 O4

Figure 8.58 High resolution MS of compound **1-66**.

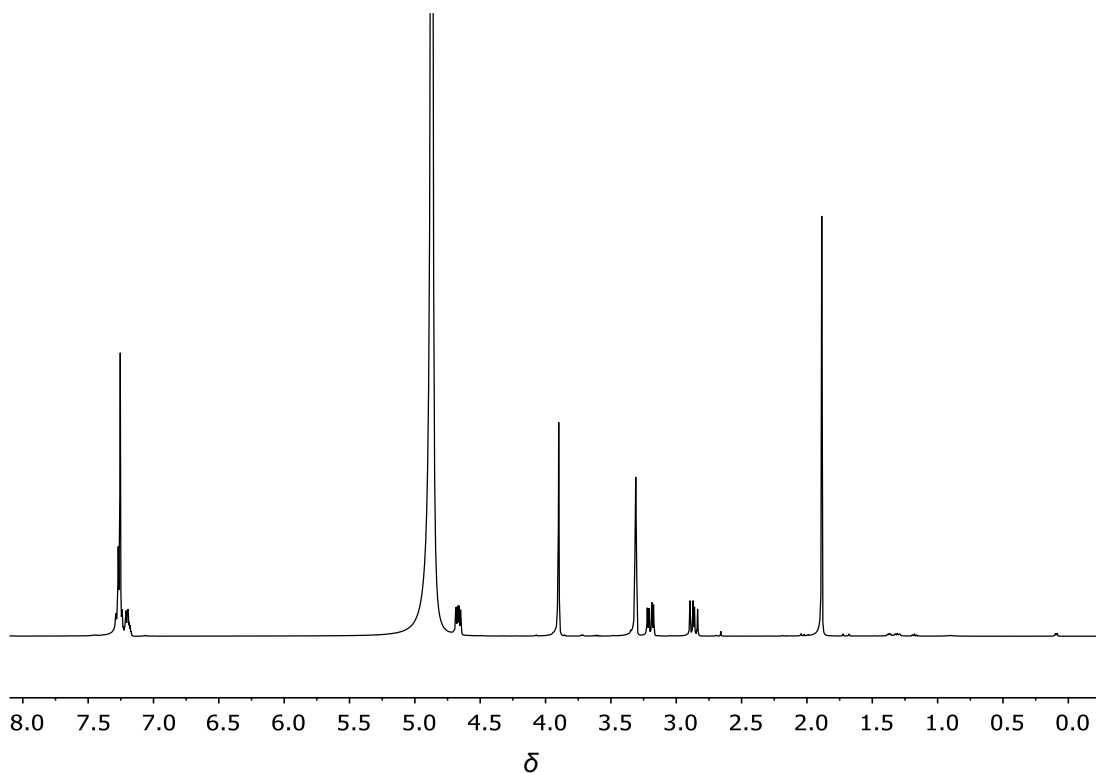
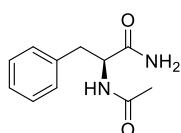


Figure 8.59 ^1H NMR of spectrum of compound **1-66**.

(S)-2-Acetamido-3-phenylpropanamide (4-3)



4-3

To a solution of *N*-acetyl-(*S*)-Phe-COOH (**4-1**) (0.20 g, 0.96 mmol) in MeOH (5 mL) was added thionyl chloride (0.35 mL, 4.78 mmol). The mixture was stirred at 0 °C for 30 min under nitrogen. Thereafter, the reaction mixture was concentrated and the resulting residue was poured into water (10 mL) and the solution was extracted with EtOAc (3 × 10 mL). The combined organic layers were washed with saturated

NaHCO₃ solution (3 × 10 mL), brine (3 × 10 mL), dried over MgSO₄, and concentrated to provide the intermediate as a white solid. Thereafter, the material was treated with concentrated ammonia solution (10 mL) and stirred for 30 min. The reaction mixture was then concentrated under reduced pressure and purified by preparative HPLC using an Alltima C18 5 μ (22 × 250 mm) column (6 mL/min). The analysis was carried out with a gradient elution of 40:60 (MeOH: H₂O (0.1% TFA), v/v) to 65:35 between 0-25 min, followed by maintenance at 40:60 for 10 min. The resulting HPLC is reproduced in **Figure 8.60**, and showed one dominant peak at 22.80 min. Sample corresponding to the main peak was isolated through HPLC. Mass spectrometry of this material displayed ions at *m/z* 229.1, which corresponds to the [M+Na]⁺ for compound **4-3**. Based on this analysis, preparative HPLC was used to isolate compound **4-3**. The column fractions were concentrated *via* freeze drying to give compound **4-3** (150 mg, 76%) as a colourless powder.

m.p.: 177.2-177.6 °C; **¹H NMR (400 MHz, CDCl₃):** δ 7.27 (m, 5H), 6.22 (m, 1H), 5.78 (s, 1H), 5.46 (s, 1H), 4.68 (m, 1H), 3.12 (dd, *J* = 13.8, 6.2 Hz, 1H), 3.03 (dd, *J* = 13.8, 7.9 Hz, 1H), 1.99 (s, 3H); **¹³C NMR (100 MHz, CDCl₃):** δ 173.2, 170.3, 136.5, 129.4, 128.9, 127.3, 54.3, 38.4, 23.3; **MS (ESI) (+ve):** *m/z* 229.1 [M+Na]⁺. **HRMS (ESI)** calcd. for C₁₁H₁₄N₂O₂Na [M+Na]⁺ *m/z* 229.0953, found *m/z* 229.0953 (**Figure 8.61**).

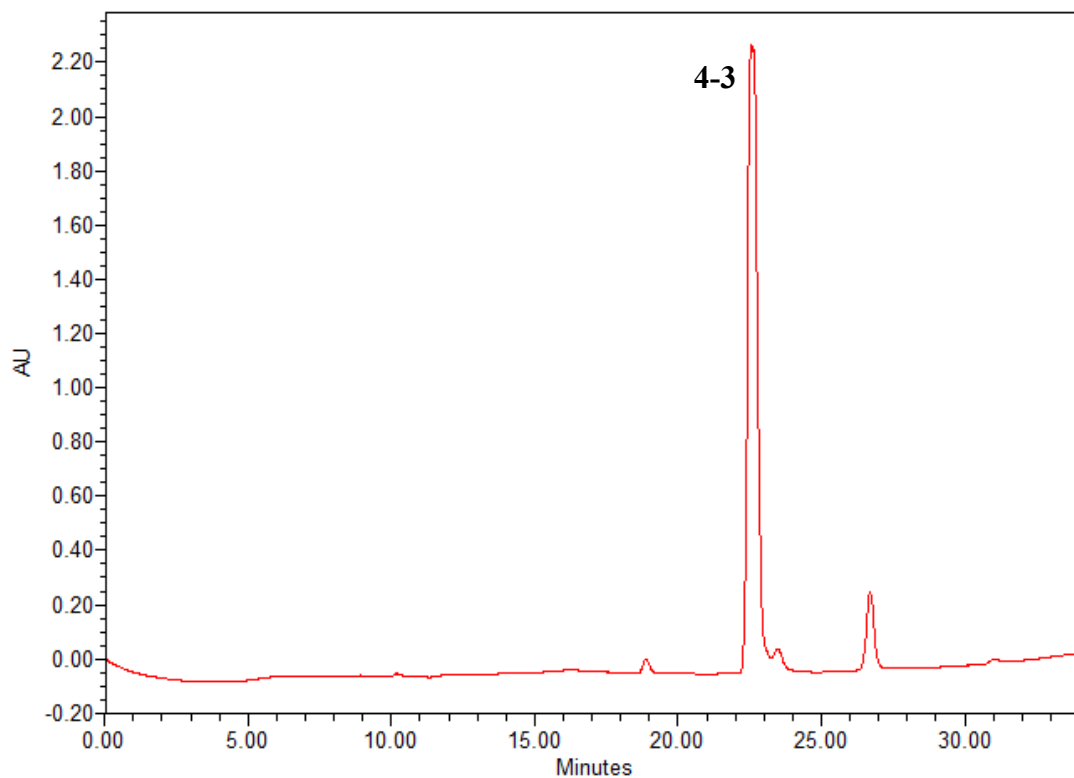


Figure 8.60 HPLC chromatogram of crude compound 4-3.

Elemental Composition Report

Page 1

Single Mass Analysis

Tolerance = 3.0 PPM / DBE: min = -1.5, max = 20.0
 Element prediction: Off
 Number of isotope peaks used for i-FIT = 4

Monoisotopic Mass, Even Electron Ions

205 formula(e) evaluated with 1 results within limits (all results (up to 1000) for each mass)

Elements Used:

C: 0-30 H: 0-50 N: 0-5 O: 0-5 ²³Na: 0-1

CG79/AJ

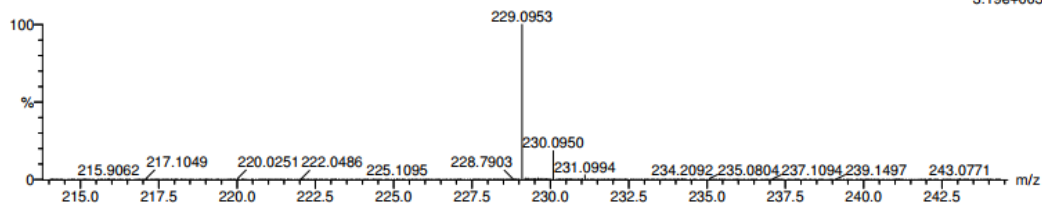
49284

1554 62 (3.310) Cm (60.63)

KE375

03-Nov-2016,14:41:10

1: TOF MS ES+
3.19e+003



Minimum:

Maximum:

100.0 3.0 -1.5
20.0

Mass	Calc. Mass	mDa	PPM	DBE	i-FIT	Formula
229.0953	229.0953	0.0	0.0	5.5	37.1	C11 H14 N2 O2 ²³ Na

Figure 8.61 High resolution MS of compound 4-3.

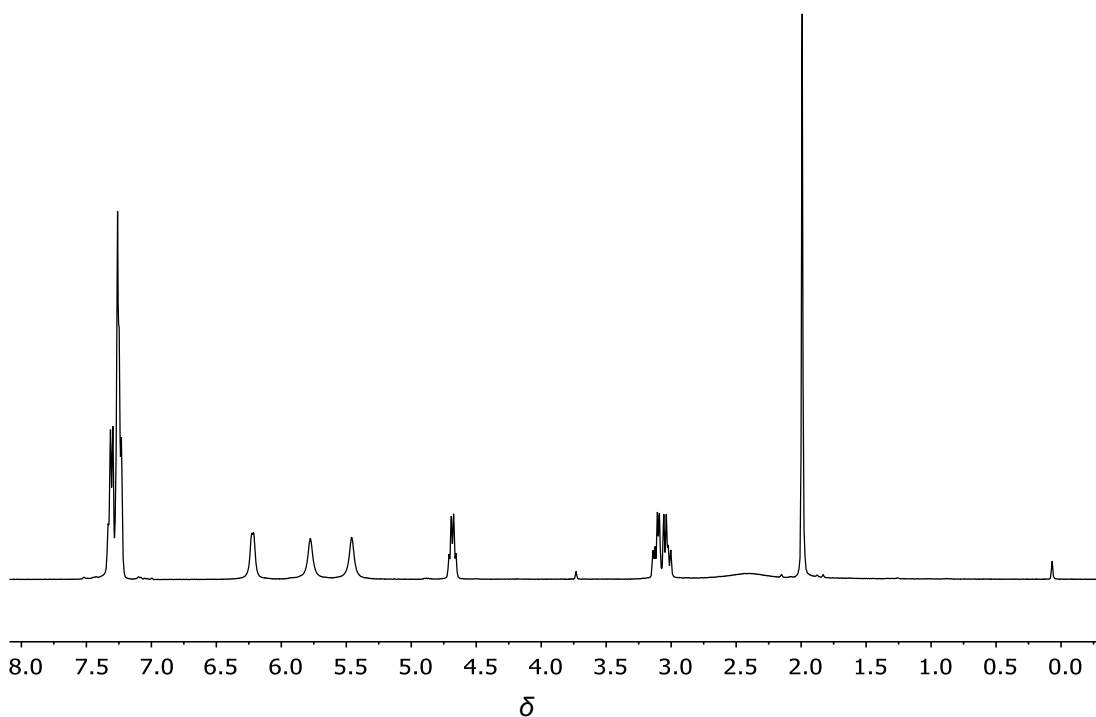


Figure 8.62 ^1H NMR of spectrum of compound **4-3**.

8.4.2 General Procedure for PAM assay using HPLC-MS

PAM assays were performed through the addition of 1.25 mM ascorbic acid, 10 μM copper sulphate, 0.2 mg/mL bovine liver catalase, 1% EtOH, 1% DMSO, 50 μM substrate (*R*)-Tyr-(*S*)-Val-Gly-COOH or *N*-Ac-(*S*)-Phe-Gly-COOH (**1-66**) in 150 mM MES buffer at pH 5.8. Assays were initiated through the addition of concentrated medium PAM (5 μL) to give a final volume of 100 μL . The mixtures were incubated in a Lab Companion Model SI-600R open-air shaker at 37 $^\circ\text{C}$ for 2 h, with agitation at 80 rpm. The solutions were then passed through Amicon[®] Ultra YM-3 filters using a centrifuge for 15 min at 12000 rpm at room temperature, and the filtrates (25 μL) were then analysed using a Waters Alliance 2695 HPLC with a Waters Atlantis C18 column (4.6 \times 150 mm) and flow splitter, followed by MS detection with a Waters ACQUITY

TQ detector. All the data were collected and processed with MassLynx 4.1 software. The solvent and gradient systems for analysis are illustrated in **Table 8.3** and **Table 8.4** below. All assays were run at least in duplicate.

Table 8.3 The gradient method for separation of (*R*)-Tyr-(*S*)-Val-Gly-COOH, HO-(*R*)-Tyr-(*S*)-Val-Gly-COOH, and (*R*)-Tyr-(*S*)-Val-NH₂.

Time (min)	Flow (mL/min)	Waters (0.1% Formic acid) (%)	MeCN (%)
0	0.5	95	5
0.5	0.5	95	5
7	0.5	75	25
10	0.5	75	25
10.5	0.5	95	5

Table 8.4 The gradient method for separation of *N*-Ac-(*S*)-Phe-Gly-COOH (**1-66**), OH-*N*-Ac-(*S*)-Phe-Gly-COOH, and *N*-Ac-(*S*)-Phe-NH₂ (**4-3**).

Time (min)	Flow (mL/min)	Waters (0.1% Formic acid) (%)	MeCN (0.1% Formic acid) (%)
0	1	97	3
4	1	85	15
9	1	80	20
10.5	1	80	20
11	1	97	3

8.4.3 Procedure for pH-Dependent PAM Assay

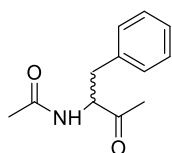
The pH-Dependent PAM Assays using (*R*)-Tyr-(*S*)-Val-Gly-COOH or *N*-Ac-(*S*)-Phe-Gly-COOH (**1-66**) were performed in the same manner as described in **Section 8.4.2**,

except that four more pH conditions of MES buffer were used, which were pH 5.5, 6.1, 6.4, and 6.7. All assays were run at least in duplicate.

8.5 Experimental for Chapter 5: Structure-Activity Relationship Study for Peptidyl- α -Hydroxyglycine α -Amidating Lyase Inhibition

8.5.1 Synthesis Work Described in Chapter 5

N-(3-Oxo-1-phenylbutan-2-yl)acetamide (5-1)



5-1

To a solution of (*S*)-Phe (1.00 g, 6.05 mmol) in pyridine (3.3 mL) was added Ac₂O (5.0 mL, 52.89 mmol, 8.74 eq), and the resulting mixture was heated to 100 °C for 5 h under nitrogen. Thereafter, the reaction mixture was cooled to room temperature and stirred further. The reaction mixture was then concentrated *in vacuo* and the residue taken up in EtOAc (2 × 20 mL), washed with saturated aqueous NaHCO₃ solution (3 × 20 mL), dried over MgSO₄, filtered and the filtrate concentrated *in vacuo*. The residue was crystallised from Et₂O and recrystallised from EtOAc to give long needle-shape colourless crystals (0.68 g, 55%).

m.p.: 90-93 °C; **¹H NMR (400 MHz, CDCl₃):** δ7.25 (m, 3H), 7.12 (m, 2H), 6.07 (s, 1H), 4.89 (dd, *J* = 6.9, 5.6 Hz, 1H), 3.16 (dd, *J* = 14.1, 6.9 Hz, 1H), 3.08 (dd, *J* = 14.1, 5.6 Hz, 1H), 2.15 (s, 3H), 1.98 (s, 3H); **MS (ESI) (+ve):** *m/z* 206.2 [M+H]⁺. **HRMS (ESI) calcd. for C₁₂H₁₆NO₂ [M+H]⁺ *m/z* 206.1181, found *m/z* 206.1181 (Figure 8.63).**

Elemental Composition Report

Page 1

Single Mass Analysis

Tolerance = 3.0 PPM / DBE: min = -1.5, max = 20.0

Element prediction: Off

Number of isotope peaks used for i-FIT = 4

Monoisotopic Mass, Even Electron Ions

96 formula(e) evaluated with 1 results within limits (all results (up to 1000) for each mass)

Elements Used:

C: 0-50 H: 0-50 N: 0-5 O: 0-5

CG01/AJ

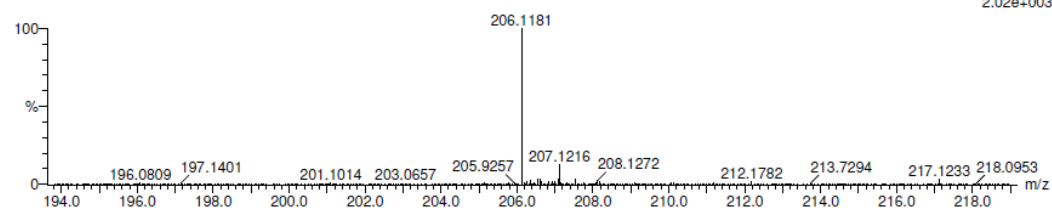
49069

1480 22 (1.174) Cm (18:28)

KE375

20-Oct-2016,9::6::3

1: TOF MS ES+
2.02e+003



Minimum: -1.5
Maximum: 100.0 3.0 20.0

Mass	Calc. Mass	mDa	PPM	DBE	i-FIT	Formula
206.1181	206.1181	0.0	0.0	5.5	6.5	C12 H16 N O2

Figure 8.63 High resolution MS of compound 5-1.

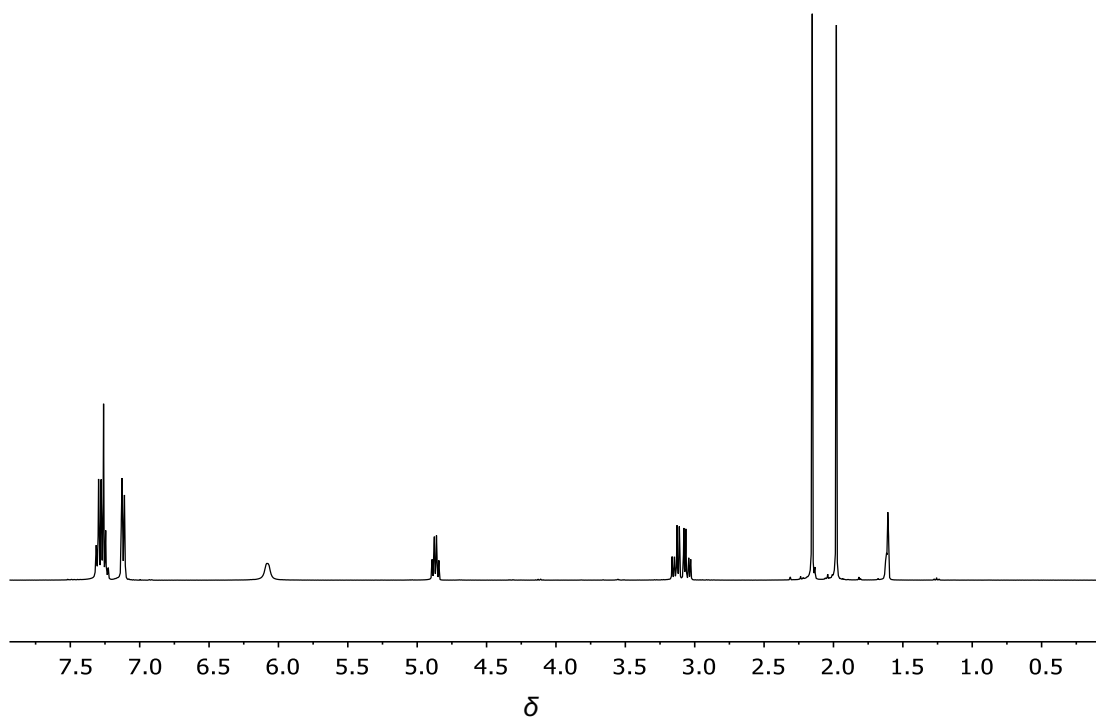
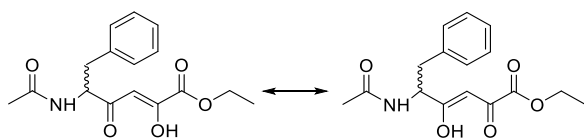


Figure 8.64 ^1H NMR of spectrum of compound **5-1**.

Ethyl 5-acetamido-2,4-dioxo-6-phenylhexanoate (5-4)



5-4

Na metal (90 mg, 3.90 mmol) was added to dry EtOH (5 mL) at room temperature under nitrogen. After the metal had dissolved, compound **5-1** (400 mg, 1.95 mmol, 0.50 eq) and diethyloxalate (0.53 mL, 3.90 mmol, 1.00 eq) were added and the reaction mixture stirred for 4 h. The mixture was then concentrated *in vacuo* and water (10 mL) was added to the residue. The aqueous layer was extracted with EtOAc (2 × 20 mL) and subsequently acidified by addition of concentrated HCl until the pH was below 3.

The resulting aqueous phase was extracted with DCM (3×20 mL) and the organic layer was dried over MgSO_4 and filtered. The residue was absorbed onto silica and purified through a plug of silica eluting with DCM followed by DCM: MeOH (95:5, v/v) to give a light yellow oil (520 mg). The ensuing residue was decoloured by decolourising carbon (3% w/w) and then subjected to silica gel flash column chromatography (EtOAc/n-hexane/MeOH, 1.5:8:0.5, v/v/v) to afford a colourless oil (280 mg, 47%).

^1H NMR (400 MHz, CDCl_3): δ 7.27 (m, 3H), 7.09 (m, 2H), 6.40 (s, 1H), 6.01 (m, 1H), 4.98 (m, 1H), 4.35 (q, $J = 7.1$ Hz, 2H), 3.19 (dd, $J = 14.0, 6.2$ Hz, 1H), 3.09 (dd, $J = 14.0, 5.5$ Hz, 1H), 2.00 (s, 3H), 1.37 (t, $J = 7.1$ Hz, 3H); **^{13}C NMR (100 MHz, CDCl_3):** δ 201.9, 169.9, 164.2, 161.7, 135.4, 129.5, 128.7, 127.5, 101.0, 62.9, 57.9, 37.9, 23.3, 14.2; **MS (ESI) (+ve):** m/z 306.2 $[\text{M}+\text{H}]^+$. **HRMS (ESI)** calcd. for $\text{C}_{16}\text{H}_{20}\text{NO}_5$ $[\text{M}+\text{H}]^+$ m/z 306.1341, found m/z 306.1339 (**Figure 8.65**).

Single Mass Analysis

Tolerance = 3.0 PPM / DBE: min = -1.5, max = 20.0

Element prediction: Off

Number of isotope peaks used for i-FIT = 4

Monoisotopic Mass, Even Electron Ions

71 formula(e) evaluated with 1 results within limits (all results (up to 1000) for each mass)

Elements Used:

C: 0-50 H: 0-50 N: 0-2 O: 0-5

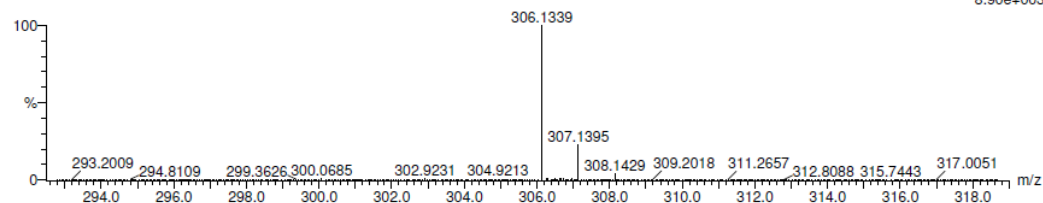
CG02/AJ

46232

0590 16 (0.852) Cm (15:18)

KE375

03-May-2016,16:16:58

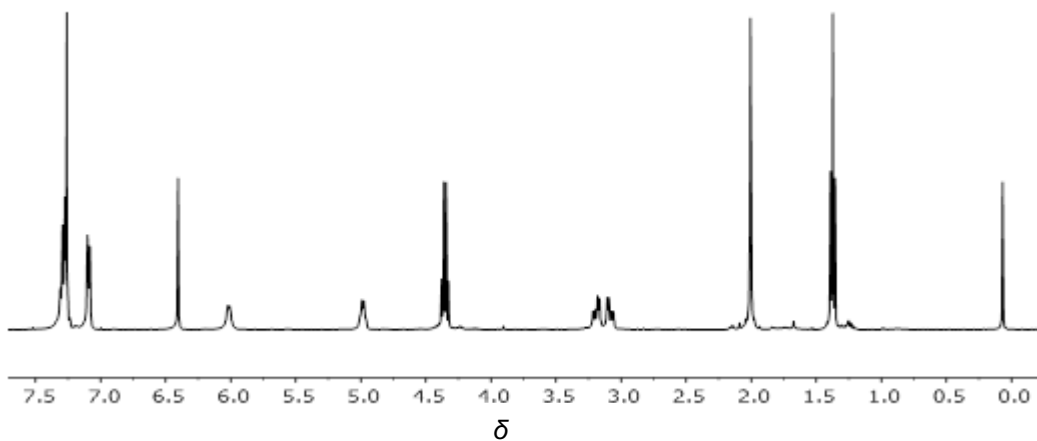
1: TOF MS ES+
8.90e+003

Minimum: -1.5

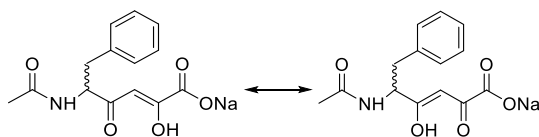
Maximum: 100.0 3.0 20.0

Mass	Calc. Mass	mDa	PPM	DBE	i-FIT	Formula
306.1339	306.1341	-0.2	-0.7	7.5	44.1	C16 H20 N O5

Figure 8.65 High resolution MS of compound 5-4.

Figure 8.66 ¹H NMR of spectrum of compound 5-4.

5-Acetamido-2,4-dioxo-6-phenylhexanoic acid (1-143) (sodium salt)



1-143

Lithium hydroxide monohydrate (30 mg, 0.72 mmol, 1.00 eq) was added to a solution of compound **5-4** (110 mg, 0.36 mmol, 0.50 eq) in THF/H₂O (6 mL, 5:1, v/v). The mixture was stirred at room temperature for 1 h under nitrogen. Thereafter, the reaction mixture was concentrated and added to water (10 mL). The aqueous solution was washed with EtOAc (3 × 20 mL) and acidified by the addition of concentrated HCl until the pH was below 3. The resulting aqueous solution was extracted with DCM (3 × 20 mL). The organic layers were combined, dried over MgSO₄, filtered and the filtrate concentrated *in vacuo* to give a yellow oil (72 mg). The resulting acid was dissolved in MeOH (5 mL) and converted to its sodium salt by addition of NaOH (10 mg, 0.26 mmol). The reaction mixture was stirred under nitrogen at room temperature for 2 h, filtered to remove insoluble precipitate, and concentrated *in vacuo*. Thereafter, cold Et₂O (2 mL) was added to precipitate a pale yellow solid (40 mg, 52%).

m.p.: decomposes. **¹H NMR (400 MHz, D₂O):** δ 7.36 (m, 5H), 3.21 (dd, *J* = 14.0, 4.6 Hz, 1H), 2.79 (dd, *J* = 14.0, 10.0 Hz, 1H), 1.82 (s, 3H). **MS (ESI) (-ve):** *m/z* 276.4 [M-H]⁻. **HRMS (ESI)** calcd. for C₁₄H₁₄NO₅ [M-H]⁻ *m/z* 276.0872, found *m/z* 276.0872 (Figure 8.67).

Single Mass Analysis

Tolerance = 3.0 PPM / DBE: min = -1.5, max = 20.0

Element prediction: Off

Number of isotope peaks used for i-FIT = 3

Monoisotopic Mass, Even Electron Ions

10 formula(e) evaluated with 1 results within limits (all results (up to 1000) for each mass)

Elements Used:

C: 0-14 H: 0-17 N: 0-1 O: 0-5

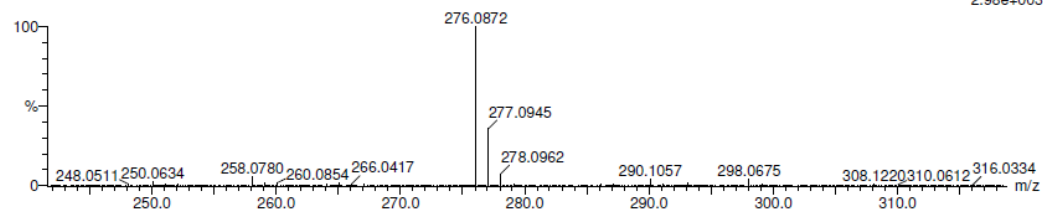
CG03/03/EO

2323662

0080 96 (4.206)

KE375

25-Jan-2013 10:25:08

1: TOF MS ES-
2.98e+003

Minimum:				-1.5		
Maximum:		5.0	3.0	20.0		
Mass	Calc. Mass	mDa	PPM	DBE	i-FIT	Formula
276.0872	276.0872	0.0	0.0	8.5	194.0	C14 H14 N O5

Figure 8.67 High resolution MS of compound 1-143.

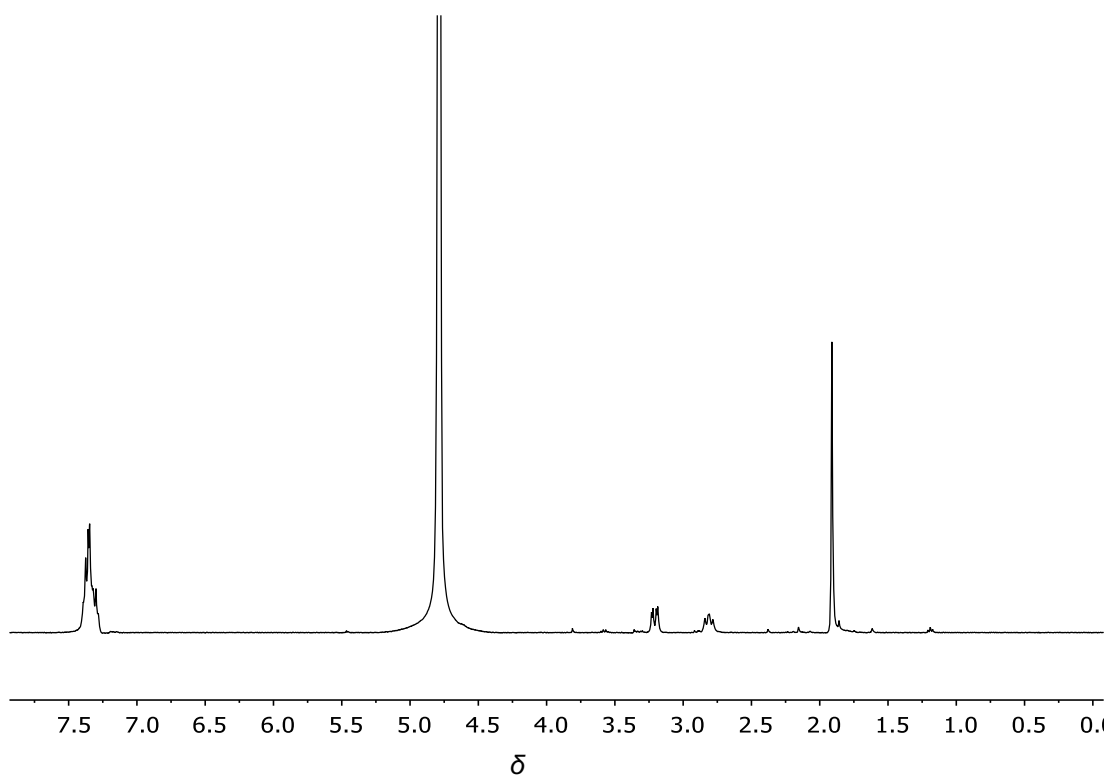
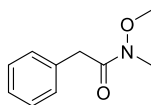


Figure 8.68 ¹H NMR of spectrum of compound 1-143.

***N*-Methoxy-*N*-methyl-2-phenylacetamide (5-5)**



5-5

To a solution of phenylacetic acid (2.00 g, 14.50 mmol) in DCM (25 mL) was added *N,O*-dimethylhydroxylamine hydrochloride (2.17 g, 21.80 mmol, 1.50 eq) and DMAP (2.72 g, 21.8 mmol, 1.50 eq) and the mixture was stirred overnight at room temperature. A saturated aqueous solution of NaCl was added and the mixture was extracted with DCM (2 × 20 mL). The combined organic layers were washed with 0.6 M HCl solution (20 mL) and saturated NaCl solution (30 mL), dried over MgSO₄ and the solvent was evaporated to afford a compound as a slightly yellow oil (2.40 g, 92%).

¹H NMR (400 MHz, CDCl₃): δ7.25 (m, 5H), 3.74 (s, 2H), 3.57 (s, 3H), 3.16 (s, 3H);

¹³C NMR (100 MHz, CDCl₃): δ172.6, 135.1, 129.4, 128.6, 126.9, 61.5, 39.6, 32.4;

MS (ESI) (+ve): *m/z* 180.1 [M+H]⁺. **HRMS (ESI)** calcd. for C₁₀H₁₄NO₂ [M+H]⁺ *m/z* 180.1025, found *m/z* 180.1026 (**Figure 8.69**).

Single Mass Analysis

Tolerance = 3.0 PPM / DBE: min = -1.5, max = 20.0

Element prediction: Off

Number of isotope peaks used for i-FIT = 4

Monoisotopic Mass, Even Electron Ions

161 formula(e) evaluated with 1 results within limits (all results (up to 1000) for each mass)

Elements Used:

C: 0-50 H: 0-50 N: 0-10 O: 0-10

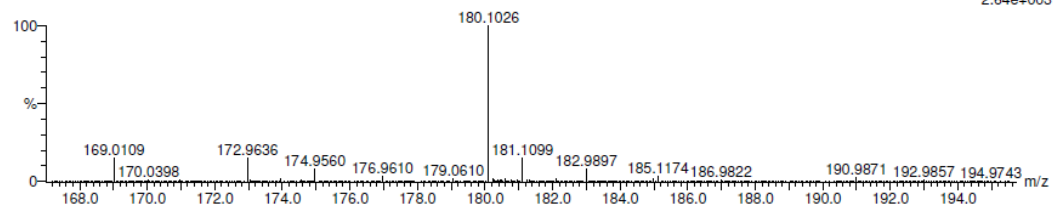
CG57/AJ

44896

0241 43 (2.314)

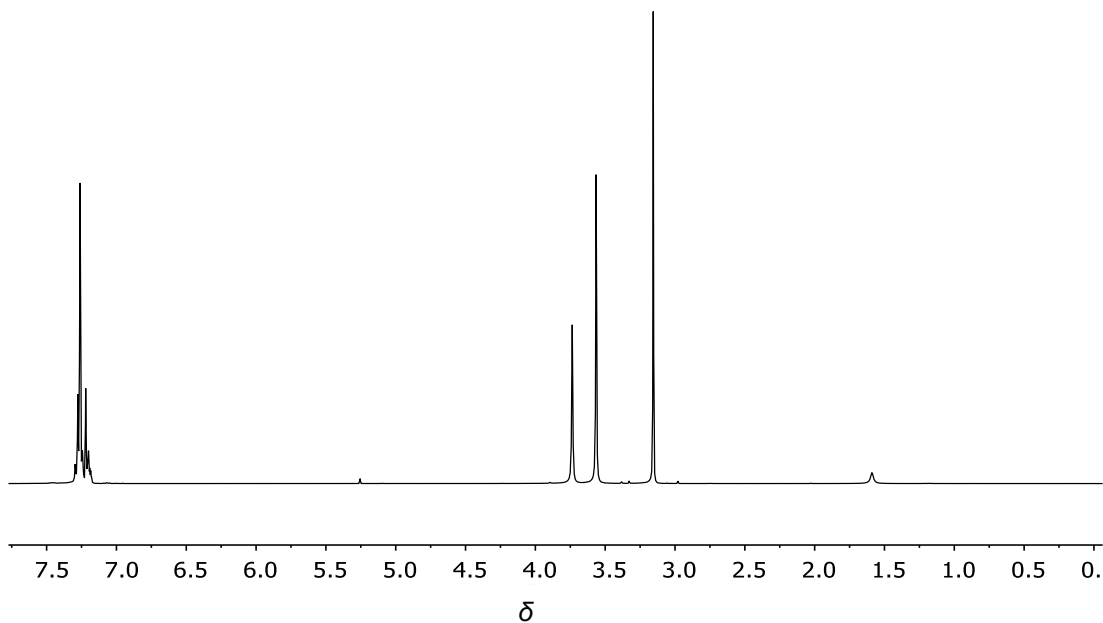
KE375

22-Feb-2016 10:54:11

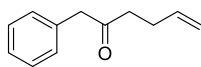
1: TOF MS ES+
2.64e+003

Mass	Calc. Mass	mDa	PPM	DBE	i-FIT	Formula
180.1026	180.1025	0.1	0.6	4.5	11.1	C10 H14 N O2

Figure 8.69 High resolution MS of compound 5-5.

Figure 8.70 ¹H NMR of spectrum of compound 5-5.

Ethyl 5-acetamido-1-phenylhex-5-en-2-one (5-6)



5-6

An oven-dried flask equipped with a reflux condenser and a magnetic stir bar was cooled under nitrogen and charged with freshly activated magnesium turnings (0.55 g, 22.32 mmol). Anhydrous Et₂O (10 mL) was added to the flask as well as a piece of iodine (approx. 2 mg). 4-Bromo-1-butene (1.17 mL, 11.16 mmol, 0.50 eq) was slowly added to the reaction mixture dropwise. Self-reflux occurred after warming the flask with a warm water bath (60 °C). After stirring for 30 min, the flask was cooled in an ice bath, after which compound **5-5** (1.00 g, 5.58 mmol, 0.25 eq) was added dropwise. The reaction mixture was stirred overnight at room temperature. Thereafter, a saturated solution of NH₄Cl (20 mL) was added at 0 °C. After warming to room temperature, the mixture was extracted with EtOAc (3 × 20 mL). The combined organic layers were washed with saturated NaCl solution (30 mL) and dried over MgSO₄. The organic layer was concentrated to afford a yellow oil (0.87 g, 89%) which was without further purification.

¹H NMR (400 MHz, CDCl₃): δ7.25 (m, 5H), 5.76 (ddt, *J* = 17.1, 10.3, 6.5 Hz, 1H), 5.01 (dd, *J* = 17.1, 1.7 Hz, 1H), 4.95 (dd, *J* = 10.3, 1.7 Hz, 1H), 3.69(s, 2H), 2.55 (t, *J* = 7.3 Hz, 2H), 2.30 (dt, *J* = 7.3, 6.5 Hz, 2H); **¹³C NMR (100 MHz, CDCl₃):** δ207.7, 137.1, 134.3, 129.6, 128.9, 127.2, 115.4, 50.4, 41.2, 27.8; **MS (EI) (+ve):**

m/z 174.1. HRMS (EI) calcd. For $C_{12}H_{14}O$ m/z 197.0942, found m/z 197.0937 (Figure 8.71).

Elemental Composition Report

Page 1

Single Mass Analysis

Tolerance = 3.0 PPM / DBE: min = -1.5, max = 20.0

Element prediction: Off

Number of isotope peaks used for i-FIT = 4

Monoisotopic Mass, Even Electron Ions

31 formula(e) evaluated with 1 results within limits (all results (up to 1000) for each mass)

Elements Used:

C: 0-50 H: 0-50 O: 0-5 ^{23}Na : 0-1

CG 58/AJ

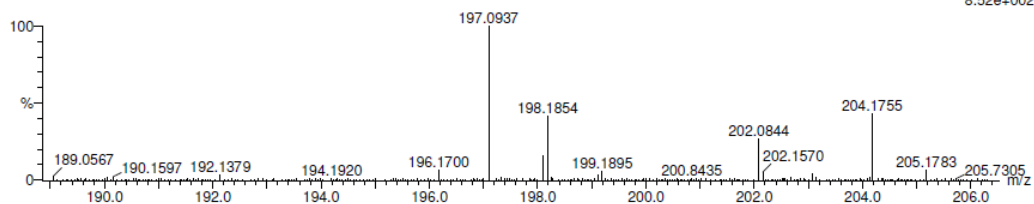
45297

0334 14 (0.745)

KE375

10-Mar-2016 12:44:45

1: TOF MS ES+
8.52e+002



Minimum: -1.5
Maximum: 100.0 3.0 20.0

Mass	Calc. Mass	mDa	PPM	DBE	i-FIT	Formula
197.0937	197.0942	-0.5	-2.5	5.5	n/a	C12 H14 O ^{23}Na

Figure 8.71 High resolution MS of compound 5-6.

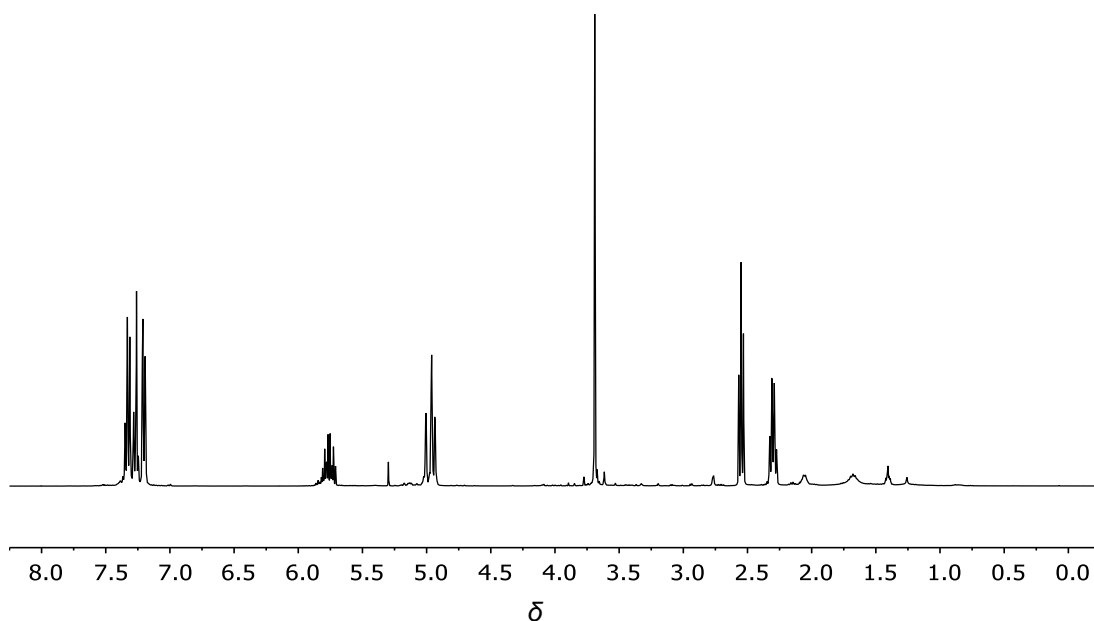
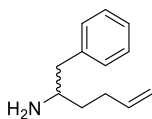


Figure 8.72 1H NMR of spectrum of compound 5-6.

1-Phenylhex-5-en-2-amine (5-7)



5-7

Compound **5-6** (0.60 g, 3.44 mmol) was dissolved in MeOH (2 mL) and then added to the solution of ammonium acetate (1.20 g, 15.49 mmol) and NaBH₃CN (0.39 g, 6.20 mmol) with activated molecular sieves 3Å. The resulting mixture was stirred at room temperature for 60 h. Afterwards the solution was transferred to a 100 mL-round-bottom flask and then quenched by dropwise addition of concentrated HCl (5 mL) until the pH was 1. The organic solvent was removed under reduced pressure, and the residue diluted with water (15 mL). The aqueous layer was washed with Et₂O (2 × 25 mL) and treated by addition of KOH solution until the pH was 12. It was then extracted with Et₂O (3 × 30 mL). The combined organic layers were dried over MgSO₄, filtered, and the solvent was removed in vacuum to afford a slightly yellow oil (0.33 g, 55%).

¹H NMR (400 MHz, CDCl₃): δ 7.30 (m, 5H), 5.82 (ddt, $J = 17.0, 10.3, 6.5$ Hz 1H), 5.10 (dd, $J = 10.3, 1.7$ Hz, 1H), 5.02 (dd, $J = 17.0, 1.7$ Hz, 1H), 3.60 (bs, 2H), 3.22 (dd, $J = 7.6, 5.8$ Hz, 1H), 2.91 (dd, $J = 13.6, 5.8$ Hz, 1H), 2.78 (dd, $J = 13.6, 7.6$ Hz 1H), 2.25 (m, 2H), 1.67 (m, 2H); **¹³C NMR (100 MHz, CDCl₃):** δ 138.2, 137.8, 129.7, 129.5, 128.5, 126.8, 115.5, 52.7, 42.7, 34.7, 30.3; **MS (ESI) (+ve):** m/z 176.2 [M+H]⁺. **HRMS (ESI)** calcd. for C₁₂H₁₈N [M+H]⁺ m/z 176.1439, found m/z 176.1441 (**Figure 8.73**).

Single Mass Analysis

Tolerance = 3.0 PPM / DBE: min = -1.5, max = 20.0

Element prediction: Off

Number of isotope peaks used for i-FIT = 4

Monoisotopic Mass, Even Electron Ions

17 formula(e) evaluated with 1 results within limits (all results (up to 1000) for each mass)

Elements Used:

C: 0-50 H: 0-50 N: 0-5

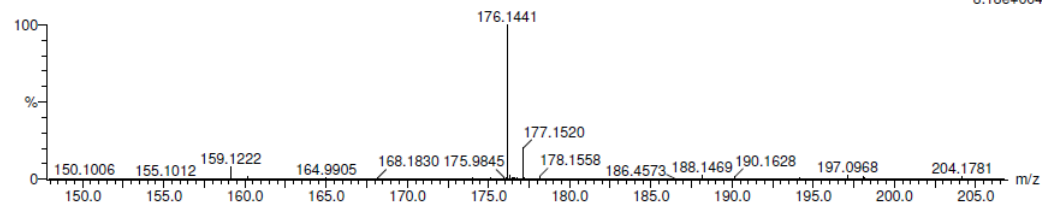
CG 59/AJ

45298

0335 8 (0.424) Cm (2:16)

KE375

10-Mar-2016 13:19:07

1: TOF MS ES+
8.18e+004

Minimum: -1.5
Maximum: 100.0 3.0 20.0

Mass	Calc. Mass	mDa	PPM	DBE	i-FIT	Formula
176.1441	176.1439	0.2	1.1	4.5	n/a	C12 H18 N

Figure 8.73 High resolution MS of compound 5-7.

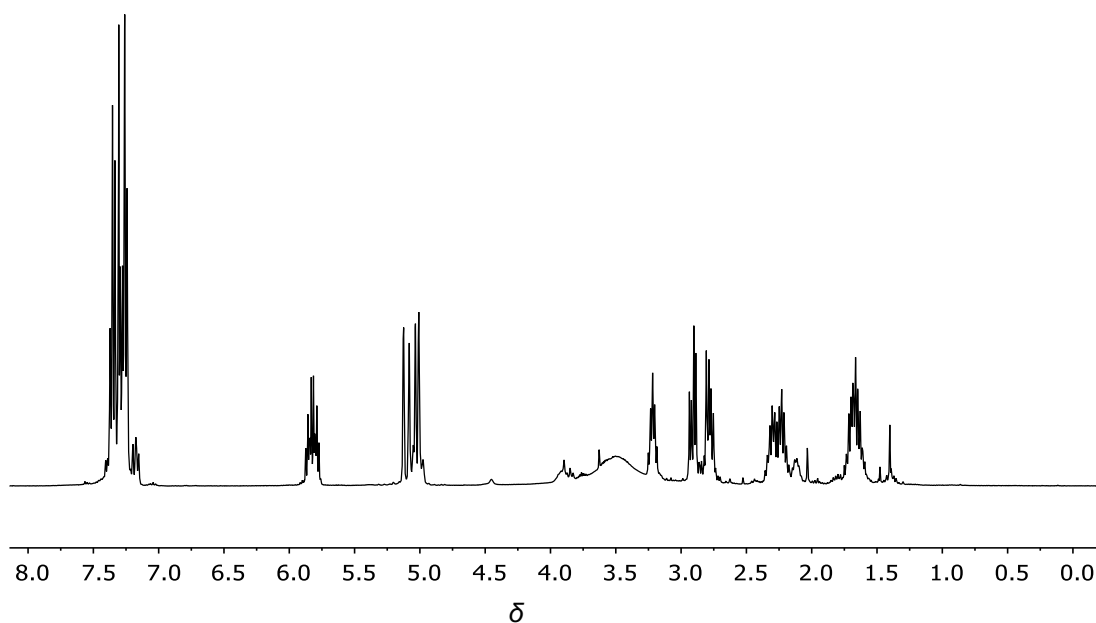
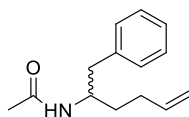


Figure 8.74 ¹H NMR of spectrum of compound 5-7.

N-(1-Phenylhex-5-en-2-yl)acetamide (**5-8**)



5-8

Compound **5-7** (330 mg, 1.88 mmol) was dissolved in anhydrous DCM (15 mL) in a round-bottom flask under nitrogen. The solution was cooled to 0 °C under stirring. Et₃N (1.31 mL, 9.41 mmol, 5.00 eq) was added *via* a syringe followed by dropwise addition of Ac₂O (0.53 mL, 5.65 mmol, 3.00 eq). The reaction mixture was then warmed up to room temperature and kept stirring overnight. The reaction mixture was washed with 0.12 M HCl solution (3 × 30 mL) and saturated NaHCO₃ (3 × 30 mL). The organic layer was dried over MgSO₄ and concentrated under reduced pressure and the ensuing residue obtained was subjected to silica gel flash column chromatography (EtOAc/n-hexane, 1:1, v/v) to afford a white solid (0.31 g, 76%).

m.p.: 77.5-78.1 °C; **¹H NMR (400 MHz, CDCl₃):** δ7.25 (m, 5H), 5.77 (ddt, *J* = 17.0, 10.2, 6.6 Hz, 1H), 5.37 (s, 1H), 5.00 (dd, *J* = 17.0, 1.27 Hz, 1H), 4.90 (dd, *J* = 10.2, 1.27 Hz, 1H), 4.20 (m, 1H), 2.82 (dd, *J* = 13.8, 6.4 Hz, 1H), 2.78 (dd, *J* = 13.8, 6.5 Hz, 1H), 2.10 (m, 2H), 1.94 (s, 3H), 1.62 (m, 1H), 1.44 (m, 1H); **¹³C NMR (100 MHz, CDCl₃):** δ171.2, 137.8, 137.7, 129.5, 128.6, 126.7, 115.4, 51.3, 40.8, 33.2, 30.5, 22.5; **MS (ESI) (+ve):** *m/z* 240.2 [M+Na]⁺. **HRMS (ESI)** calcd. for C₁₄H₂₀NO [M+H]⁺ *m/z* 218.1545, found *m/z* 218.1546 (**Figure 8.75**).

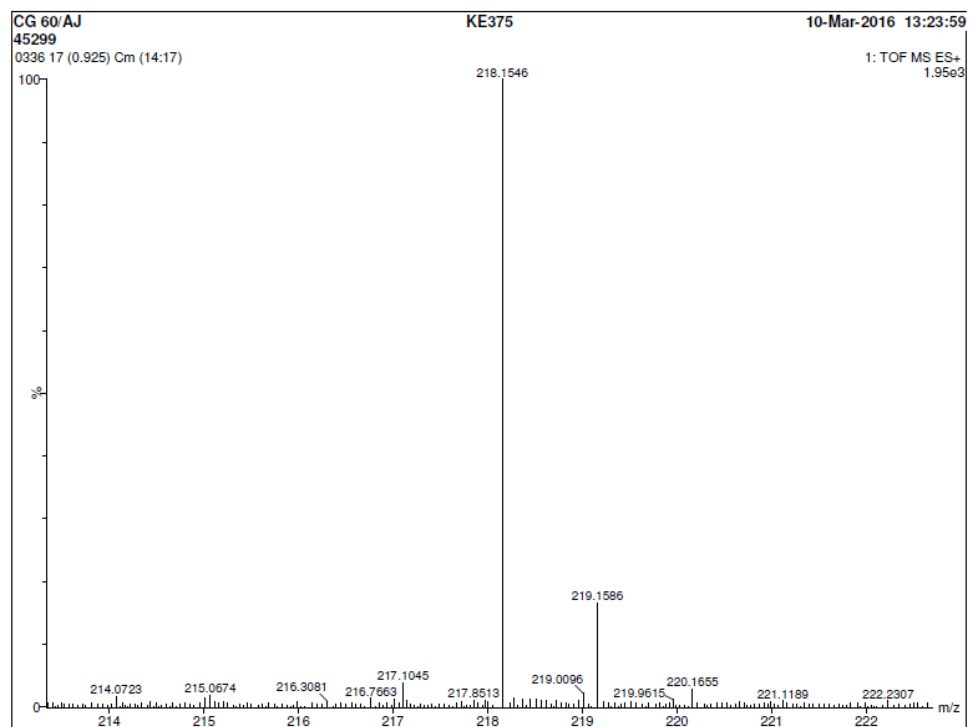


Figure 8.75 High resolution MS of compound **5-8**.

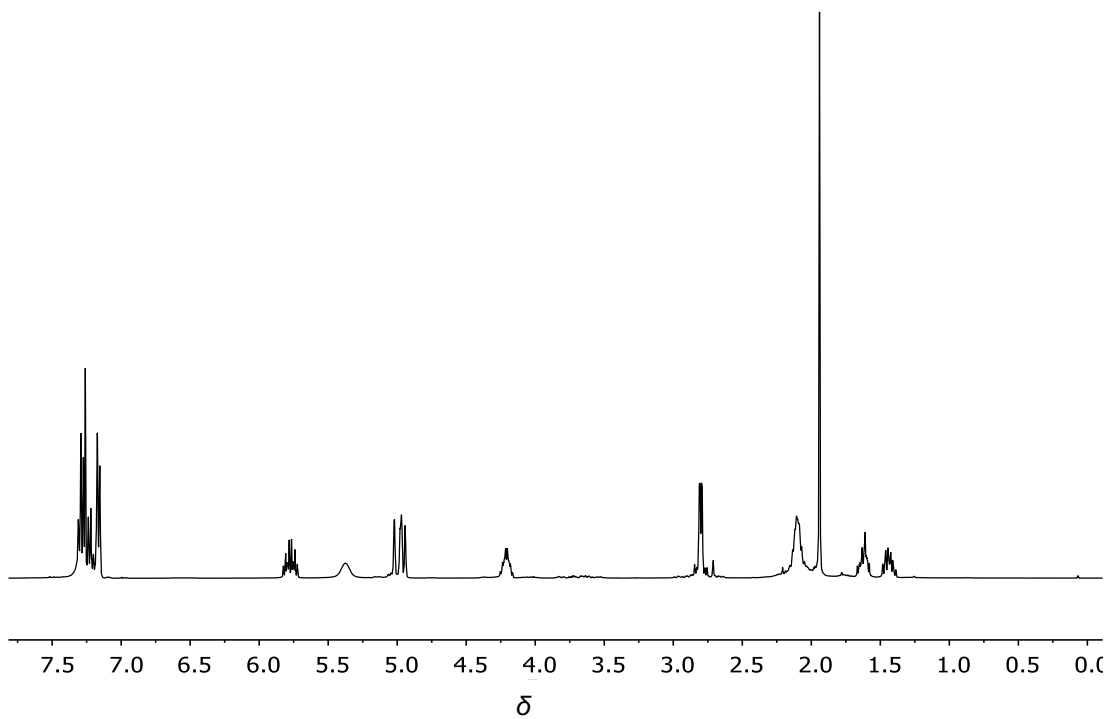
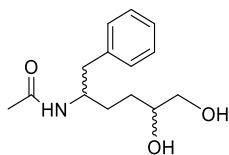


Figure 8.76 ^1H NMR of spectrum of compound **5-8**.

***N*-(5,6-Dihydroxy-1-phenylhexan-2-yl)acetamide (5-9)**



5-9

The 25 mL-two-neck round-bottom flask was equipped with compound **5-8** (220 mg, 1.01 mmol) and NMO (150 mg, 1.22 mmol, 1.21 eq), followed by addition of acetone (9 mL), H₂O (1 mL), and OsO₄ (4% w/w in H₂O, 160 μL, 0.025 mmol, 0.25 eq). The reaction mixture was stirred under nitrogen for 5 h. Thereafter, saturated Na₂S₂O₅ solution (3 mL) was added to quench OsO₄, and brine (25 mL) was then added. After extraction with EtOAc (3 × 20 mL), the combined organic phase was dried over MgSO₄ and the ensuing residue was subjected to silica gel flash column chromatography (DCM/MeOH, 9:1, v/v) to afford a colourless oil (220 mg, 88%).

¹H NMR (400 MHz, CD₃OD): (mixture of two diastereomers) δ7.23 (m, 10H), 4.08 (m, 2H), 3.60 (m, 2H), 3.47 (m, 4H), 2.83 (dd, *J* = 13.6, 6.4 Hz, 1H), 2.82 (dd, *J* = 13.6, 6.4 Hz, 1H), 2.77 (dd, *J* = 13.6, 7.6 Hz, 1H), 2.76 (dd, *J* = 13.6, 7.6 Hz, 1H), 1.88 (s, 3H), 1.87 (s, 3H), 1.77 (m, 8H); **¹³C NMR (100 MHz, CD₃OD):** (mixture of two diastereomers) δ172.8, 140.0, 130.4, 129.3, 128.2, 127.3, 127.2, 73.3, 72.8, 67.4, 67.3, 52.5, 52.0, 42.3, 42.2, 31.6, 31.4, 31.1, 30.8, 22.6; **MS (ESI) (+ve):** *m/z* 252.2 [M+H]⁺. **HRMS (ESI)** calcd. for C₁₄H₂₂NO₃ [M+H]⁺ *m/z* 252.1600, found *m/z* 252.1602 (Figure 8.77).

Single Mass Analysis

Tolerance = 3.0 PPM / DBE: min = -1.5, max = 20.0

Element prediction: Off

Number of isotope peaks used for i-FIT = 4

Monoisotopic Mass, Even Electron Ions

118 formula(e) evaluated with 1 results within limits (all results (up to 1000) for each mass)

Elements Used:

C: 0-50 H: 0-50 N: 0-5 O: 0-5

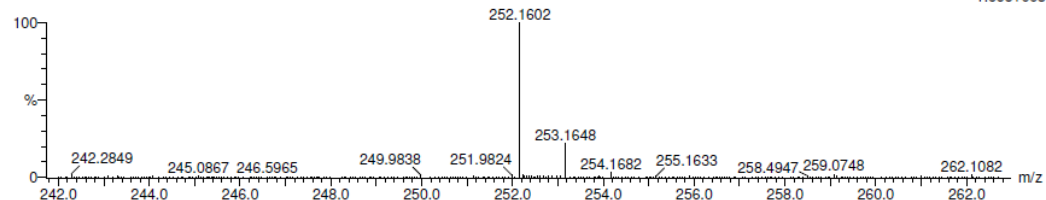
CG061/AJ

45296

0333 15 (0.817)

KE375

10-Mar-2016 12:37:32

1: TOF MS ES+
1.66e+003

Minimum:

Maximum: 100.0 3.0 -1.5

Mass	Calc. Mass	mDa	PPM	DBE	i-FIT	Formula
252.1602	252.1600	0.2	0.8	4.5	15.2	C14 H22 N O3

Figure 8.77 High resolution MS of compound 5-9.

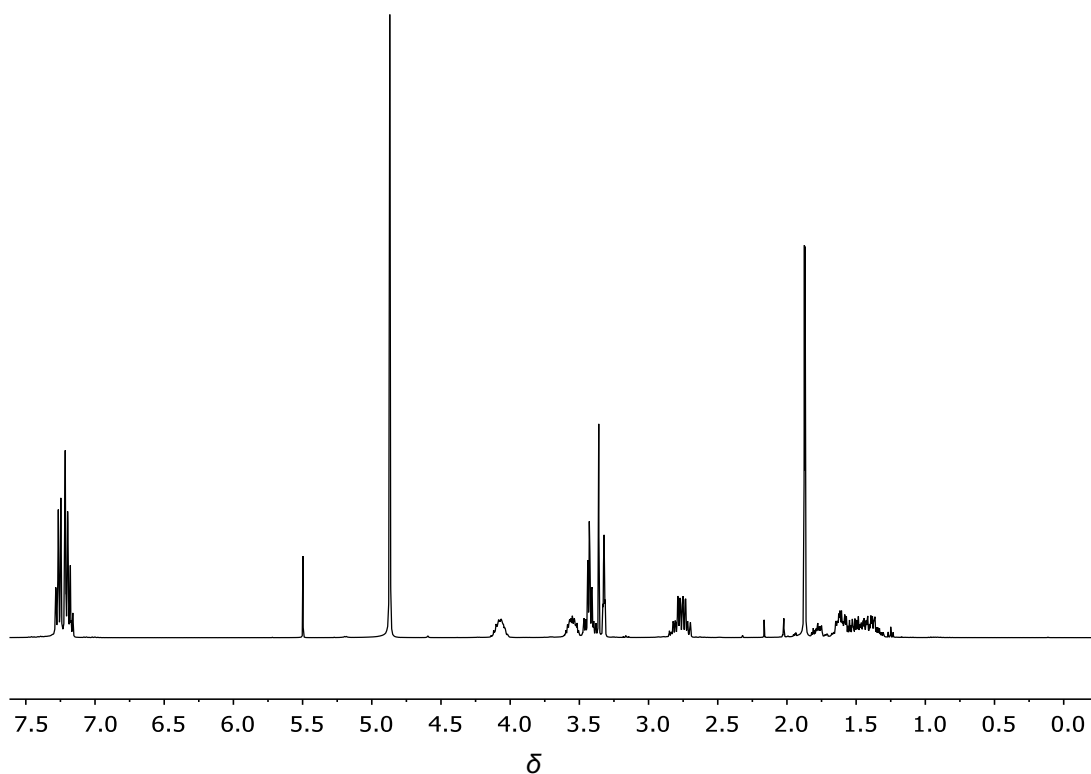
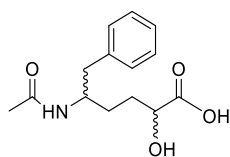


Figure 8.78 ^1H NMR of spectrum of compound 5-9 (The peak at δ 5.49 is attributed to DCM).

5-Acetamido-2-hydroxy-6-phenylhexanoic acid (5-2)



5-2

Diol **5-9** (18 mg, 0.073 mmol) was dissolved in EtOAc (0.66 mL), followed by addition of TEMPO (1.20 mg, 0.0074 mmol, 0.10 eq) in 1 M sodium phosphate buffer (0.47 mL, pH = 6.8) at room temperature. Then NaClO₂ (80%, 50 mg, 0.44 mmol, 6.00 eq) and NaClO solution (0.60 M, 6.2 μ L, 0.0037 mmol, 0.05 eq) were added simultaneously in one minute. The mixture was stirred at 50 °C for 24 h. Thereafter, the reaction was quenched with 1 M sodium phosphate buffer (pH = 2.1), followed by the extraction with EtOAc (3 \times 10 mL). The combined organic layers were dried over MgSO₄ and concentrated under reduced pressure. The ensuing residue was subjected to silica gel flash column chromatography (MeOH/DCM, 1:9, v/v and MeOH/THF/AcOH, 1:9:0.1, v/v/v) to afford a colourless oil (7 mg, 37%).

¹H NMR (400 MHz, D₂O): (mixture of two diastereomers) δ 7.31 (m, 10H), 4.21 (m, 4H), 4.03 (m, 4H), 2.96 (dd, J = 13.4, 4.8 Hz 1H), 2.95 (dd, J = 13.4, 4.8 Hz, 1H), 2.68 (dd, J = 13.4, 9.4 Hz, 1H), 2.67 (dd, J = 13.4, 9.4 Hz, 1H), 1.87 (s, 6H), 1.69 (m, 8H); **¹³C NMR (175 MHz, D₂O):** (mixture of two diastereomers) δ 178.6, 174.2, 139.4, 130.2, 129.2, 127.2, 70.9, 70.5, 51.8, 51.5, 41.2, 41.0, 30.9, 30.7, 30.1, 30.0, 22.5; **MS (ESI) (-ve):** m/z 264.3 [M-H]⁻. **HRMS (ESI)** calcd. for C₁₄H₁₈NO₄ [M-H]⁻ m/z 264.1236, found m/z 264.1235 (**Figure 8.79**).

Single Mass Analysis

Tolerance = 3.0 PPM / DBE: min = -1.5, max = 10.0

Element prediction: Off

Number of isotope peaks used for i-FIT = 4

Monoisotopic Mass, Even Electron Ions

122 formula(e) evaluated with 1 results within limits (all results (up to 1000) for each mass)

Elements Used:

C: 0-50 H: 0-50 N: 0-5 O: 0-5

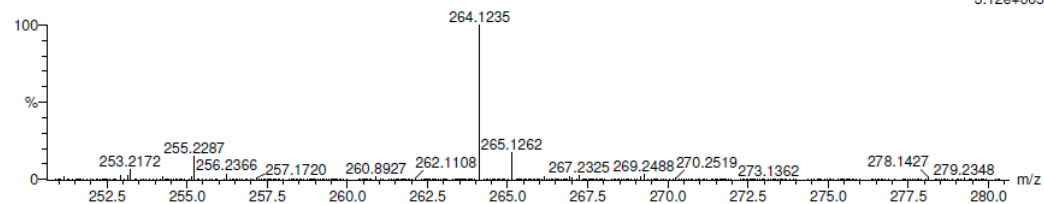
CG63/AJ

45713

0451 31 (1.363) Cm (31.34)

KE375

01-Apr-2016,10:10:32

1: TOF MS ES-
3.12e+005

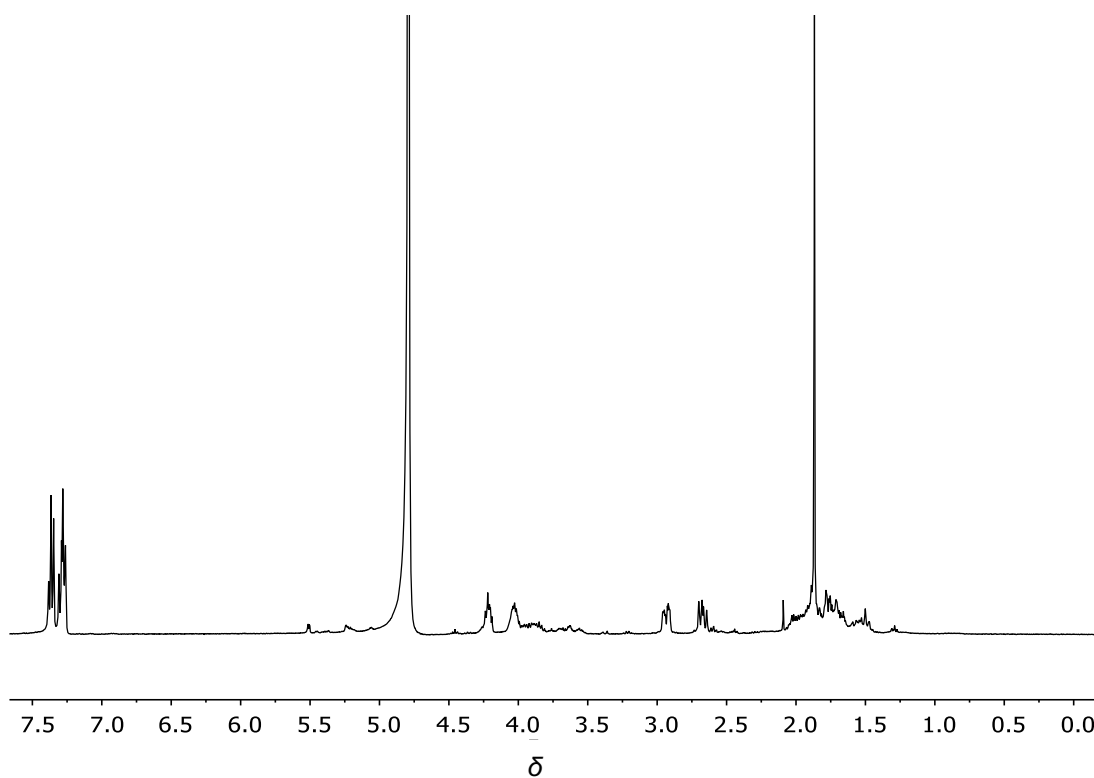
Minimum:

Maximum: 100.0 3.0 -1.5

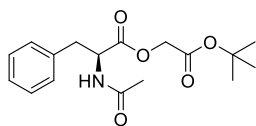
Mass Calc. Mass mDa PPM DBE i-FIT Formula

Mass	Calc. Mass	mDa	PPM	DBE	i-FIT	Formula
264.1235	264.1236	-0.1	-0.4	6.5	165.5	C14 H18 N O4

Figure 8.79 High resolution MS of compound 5-2.

Figure 8.80 ¹H NMR of spectrum of compound 5-2.

***tert*-Butyl-*O* α -((*S*)-*N*-acetylphenylalanyl)-glycolate (5-10)**



5-10

To a solution of compound **4-1** (1.00 g, 4.78 mmol) in acetone (100 mL) was added potassium carbonate (1.32 g, 9.56 mmol, 2.00 eq) and *tert*-butyl bromoacetate (0.72 mL, 4.78 mmol, 1.00 eq). The mixture was heated at reflux overnight under nitrogen, and evaporated under reduced pressure. The crude oil was partitioned between *n*-hexane (100 mL) and water (100 mL). The organic fraction was dried over MgSO₄, filtered, and evaporated under reduced pressure to give the title compound (1.35 g, 88%) as a colourless oil.

¹H NMR (400 MHz, CDCl₃): δ 7.24 (m, 5H), 5.81 (d, J = 7.8 Hz, 1H), 4.97 (dt, J = 7.8, 6.1 Hz, 1H), 4.62 (d, J = 15.6 Hz, 1H), 4.50 (d, J = 15.6 Hz, 1H), 3.28 (dd, J = 14.1, 5.7 Hz, 1H), 3.12 (dd, J = 14.1, 6.5 Hz, 1H), 1.96 (s, 3H), 1.49 (s, 9H); **MS (ESI) (+ve):** m/z 344.2 [M+Na]⁺. **HRMS (ESI)** calcd. for C₁₇H₂₃NO₅Na [M+Na]⁺ m/z 344.1474, found m/z 344.1471 (**Figure 8.81**).

Single Mass Analysis

Tolerance = 4.0 PPM / DBE: min = -1.5, max = 15.0

Element prediction: Off

Number of isotope peaks used for i-FIT = 4

Monoisotopic Mass, Even Electron Ions

250 formula(e) evaluated with 1 results within limits (all results (up to 1000) for each mass)

Elements Used:

C: 0-50 H: 0-50 N: 0-10 O: 0-5 ²³Na: 1-1

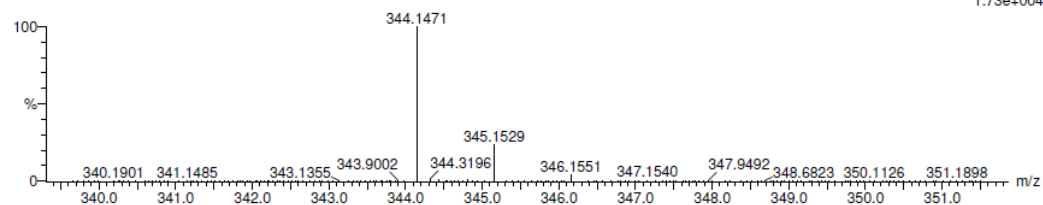
KE375

19-Aug-2016,13:15:29

CG72

48148

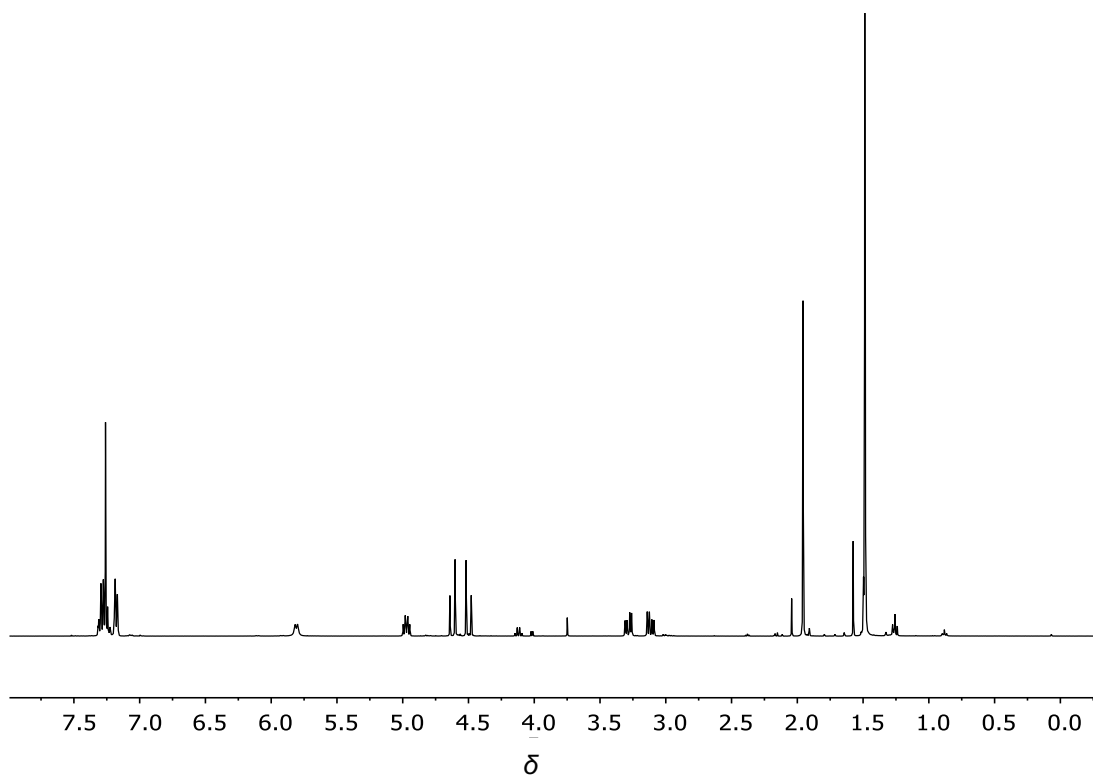
1140 20 (1.165) Cm (20:21)

1: TOF MS ES+
1.73e+004

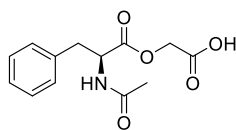
Minimum: -1.5
Maximum: 100.0 4.0 15.0

Mass	Calc. Mass	mDa	PPM	DBE	i-FIT	Formula
344.1471	344.1474	-0.3	-0.9	6.5	55.5	C17 H23 N O5 ²³ Na

Figure 8.81 High resolution MS of compound 5-10.

Figure 8.82 ¹H NMR of spectrum of compound 5-10.

***O*α-((*S*)-*N*-Acetylphenylalanyl)-glycolic acid (1-57)**



1-57

A solution of compound **5-10** (200 mg, 0.62 mmol) in neat TFA (2 mL) was stirred at room temperature under nitrogen for 30 min, before evaporation of solvent under reduced pressure. Et₂O was added and the mixture was concentrated under reduced pressure to give the title compound (140 mg, 86%) as an oil. The purity was checked by preparative HPLC using the same method as described for compound **4-3**. The resulting HPLC is reproduced in **Figure 8.83**, and showed one dominant peak at 27.90 min. Sample corresponding to the peak was isolated through HPLC. Mass spectrometry of the peak at 27.90 min displayed ions at *m/z* 264.1, which corresponds to the [M-H]⁻ for compound **1-57**.

¹H NMR (400 MHz, CDCl₃): δ7.23 (m, 5H), 6.15 (d, *J* = 7.7 Hz, 1H), 4.96 (m, 1H), 4.73 (d, *J* = 16.2 Hz, 1H), 4.68 (d, *J* = 16.2 Hz, 1H), 3.25 (dd, *J* = 14.1, 5.8 Hz, 1H), 3.11 (dd, *J* = 14.1, 6.7 Hz, 1H), 1.99 (s, 3H); **¹³C NMR (100 MHz, CDCl₃):** δ171.5, 171.1, 170.5, 135.5, 129.4, 128.9, 127.5, 61.1, 53.4, 37.4, 22.9; **MS (ESI) (+ve):** *m/z* 264.1 [M-H]⁻. **HRMS (ESI)** calcd. for C₁₃H₁₄NO₅ [M-H]⁻ *m/z* 264.0872, found *m/z* 264.0873 (**Figure 8.84**).

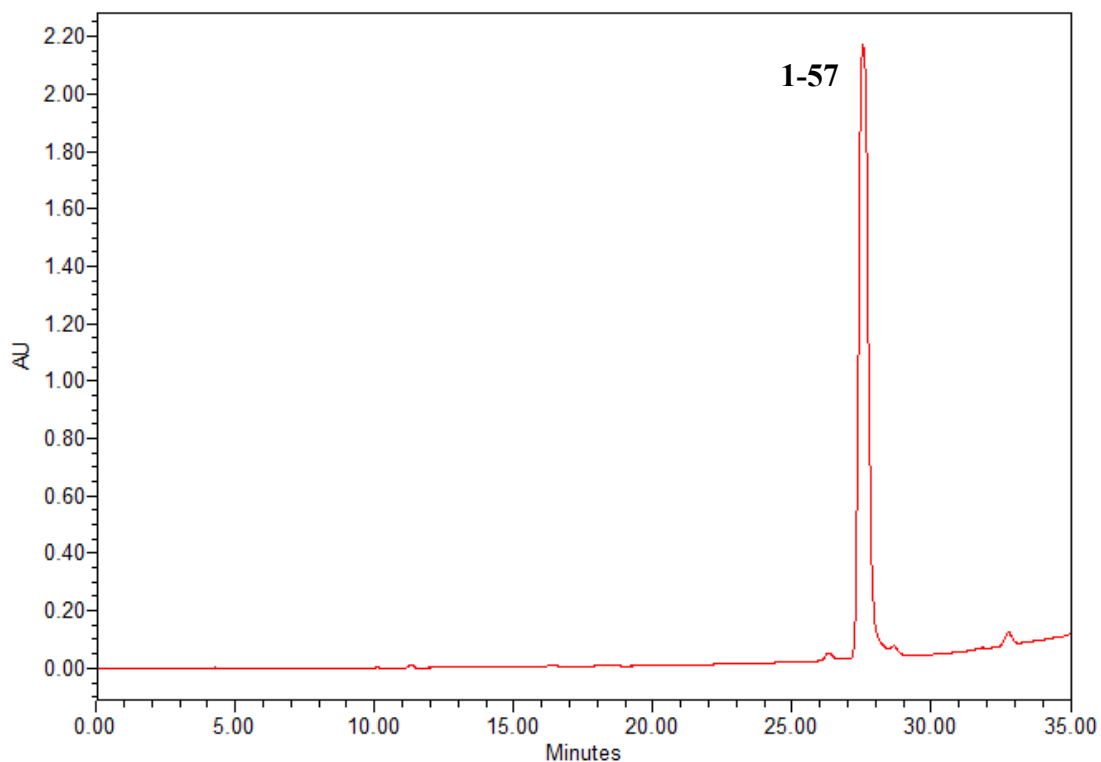


Figure 8.83 HPLC chromatogram of compound **1-57**.

Elemental Composition Report

Page 1

Single Mass Analysis

Tolerance = 3.0 PPM / DBE: min = -1.5, max = 10.0
 Element prediction: Off
 Number of isotope peaks used for i-FIT = 4

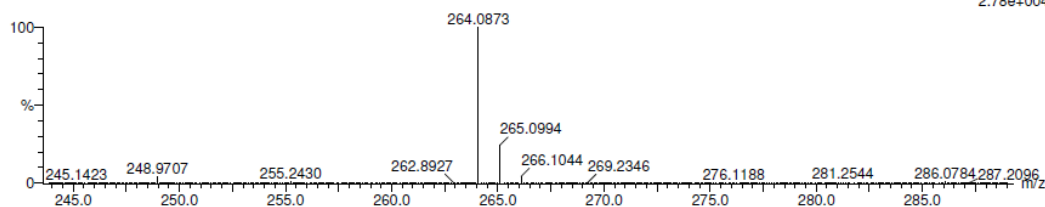
Monoisotopic Mass, Even Electron Ions
 195 formula(e) evaluated with 1 results within limits (all results (up to 1000) for each mass)

Elements Used:
 C: 0-50 H: 0-50 N: 0-5 O: 0-10
 CG75/AJ
 48342
 1198 75 (3.293) Cm (74.76)

KE375

02-Sep-2016,09:22:58

1: TOF MS ES-
 2.78e+004



Mass	Calc. Mass	mDa	PPM	DBE	i-FIT	Formula
264.0873	264.0872	0.1	0.4	7.5	578.6	C13 H14 N O5

Figure 8.84 High resolution MS of compound **1-57**.

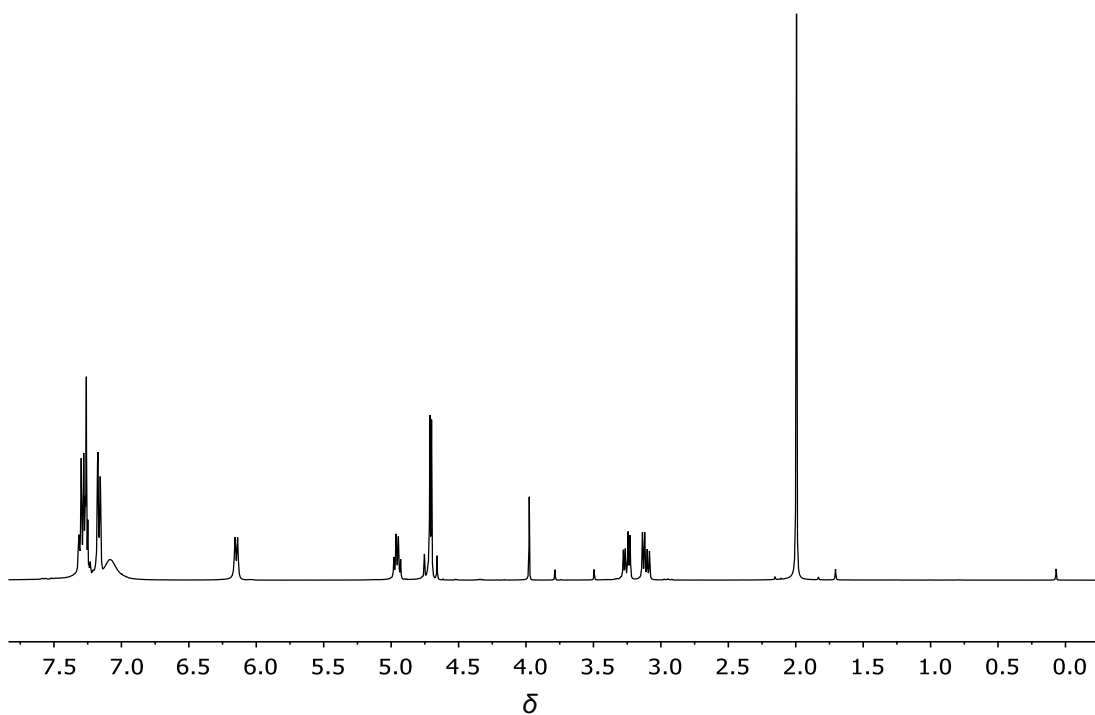
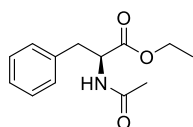


Figure 8.85 ^1H NMR of spectrum of compound **1-57**.

Ethyl *N*-acetyl-(*S*)-phenylalaninate (5-11**)**



5-11

To a solution of **4-1** (3.00 g, 14.30 mmol) in EtOH (72 mL) was added concentrated HCl (0.3 mL); the reaction mixture was refluxed overnight and then concentrated under reduced pressure. The residual solid was dissolved in EtOAc (10 mL), washed with saturated NaHCO_3 solution (2×20 mL) and H_2O (1×10 mL). The organic phase was dried over MgSO_4 and concentrated under reduced pressure to give compound **5-11** (2.77 g, 82%) as a white solid.

¹H NMR (400 MHz, CDCl₃): δ 7.27 (m, 3H), 7.10 (m, 2H), 5.91 (bd, $J = 7.8$ Hz, 1H), 4.87 (dd, $J = 7.8, 5.8, 4.8$ Hz, 1H), 4.17 (q, $J = 7.2$ Hz, 2H), 3.15 (dd, $J = 12.7, 4.8$ Hz, 1H), 3.15 (dd, $J = 12.7, 5.8$ Hz, 1H), 1.99 (s, 3H), 1.25 (t, $J = 7.2$ Hz, 3H); **MS (ESI) (+ve):** m/z 258.2 [M+Na]⁺. **HRMS (ESI)** calcd. for C₁₃H₁₇NO₃Na [M+Na]⁺ m/z 258.1106, found m/z 258.1113 (**Figure 8.86**).

Elemental Composition Report

Page 1

Single Mass Analysis

Tolerance = 4.0 PPM / DBE: min = -1.5, max = 15.0
 Element prediction: Off
 Number of isotope peaks used for i-FIT = 4

Monoisotopic Mass, Even Electron Ions

187 formula(e) evaluated with 1 results within limits (all results (up to 1000) for each mass)

Elements Used:

C: 0-50 H: 0-50 N: 0-10 O: 0-5 ²³Na: 1-1

CG73

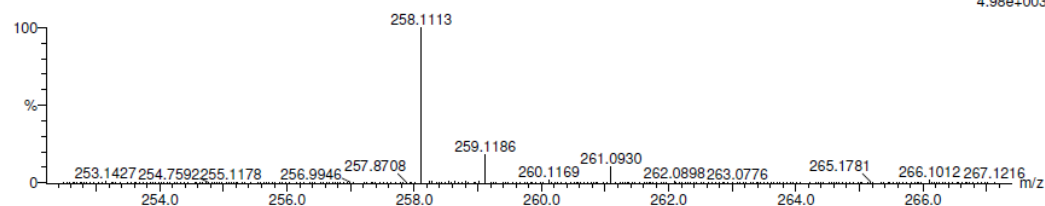
KE375

19-Aug-2016,13:20:18

48149

1: TOF MS ES+
4.98e+003

114116 (0.951) Cm (16:17)



Mass	Calc. Mass	mDa	PPM	DBE	i-FIT	Formula
258.1113	258.1106	0.7	2.7	5.5	n/a	C13 H17 N O3 ²³ Na

Figure 8.86 High resolution MS of compound 5-11.

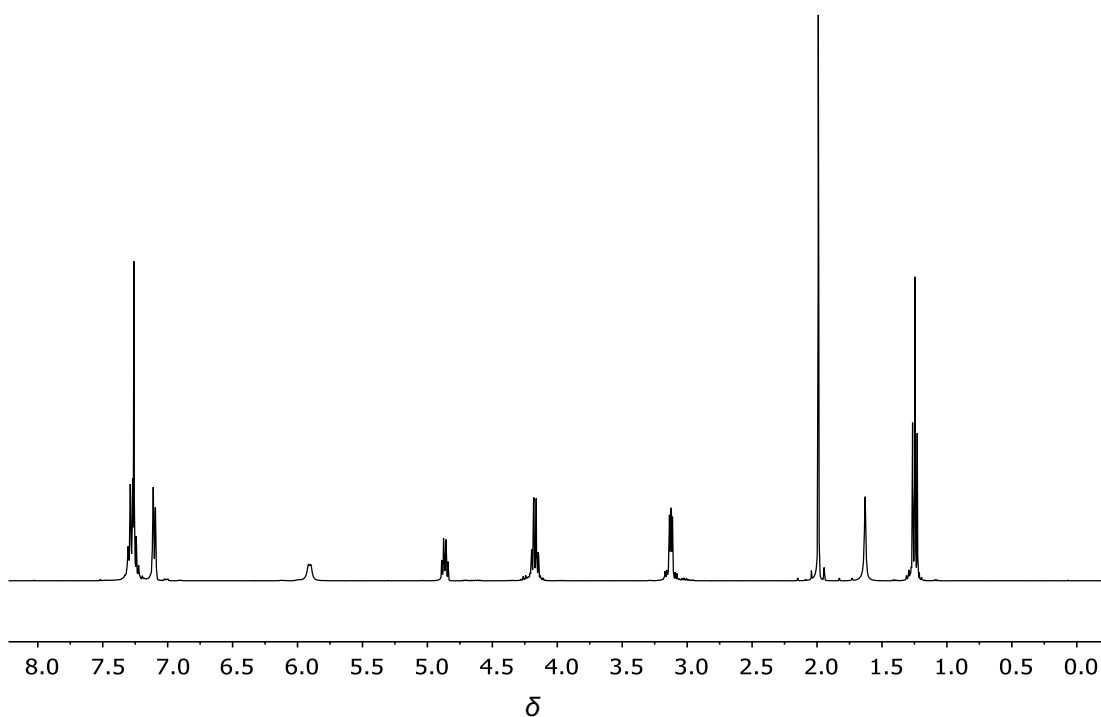
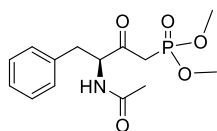


Figure 8.87 ^1H NMR of spectrum of compound **5-11**.

Dimethyl (*S*)-(3-acetamido-2-oxo-4-phenylbutyl)-phosphonate (5-12**)**



5-12

n-Butyl-lithium (5.56 mL, 8.50 mmol) was slowly added, under nitrogen, to a solution of dimethyl methylphosphonate (0.95 mL, 8.50 mmol, 1.00 eq) in anhydrous THF (20 mL) kept at $-78\text{ }^{\circ}\text{C}$. The reaction mixture was stirred at $-78\text{ }^{\circ}\text{C}$ for 30 min, during which a white precipitate was formed, followed by the addition of compound **5-11** (1.00 g, 4.25 mmol, 0.50 eq) in THF (1 mL). The mixture was slowly brought to room temperature, stirred overnight, monitored by TLC with eluting solvent EtOAc, and

quenched by the addition of H₂O (5 mL), followed by the extraction with Et₂O (3 × 10 mL). The aqueous layer was acidified by the addition of concentrated HCl and extracted with DCM (3 × 10 mL); the extracts were dried over MgSO₄, filtered, and concentrated under reduced pressure. The crude product **5-12** was subjected to silica gel flash column chromatography with the eluting solvent DCM/MeOH (20:1, v/v), to give a colourless oil (669 mg, 50%).

¹H NMR (400 MHz, CDCl₃): δ7.23 (m, 5H), 6.44 (d, *J* = 7.8 Hz, 1H), 4.90 (m, 1H), 3.75 (m, 6H), 3.23 (m, 2H), 3.02 (m, 2H), 1.98 (s, 3H); MS (ESI) (+ve): *m/z* 336.1 [M+Na]⁺. HRMS (ESI) calcd. for C₁₄H₂₀NO₅NaP [M+Na]⁺ *m/z* 336.0977, found *m/z* 336.0991 (Figure 8.88).

Elemental Composition Report

Page 1

Single Mass Analysis

Tolerance = 10.0 PPM / DBE: min = -1.5, max = 30.0

Element prediction: Off

Number of isotope peaks used for i-FIT = 4

Monoisotopic Mass, Even Electron Ions

90 formula(e) evaluated with 1 results within limits (all results (up to 1000) for each mass)

Elements Used:

C: 0-50 H: 0-50 N: 0-3 O: 0-5 23Na: 1-1 P: 1-1

CG74

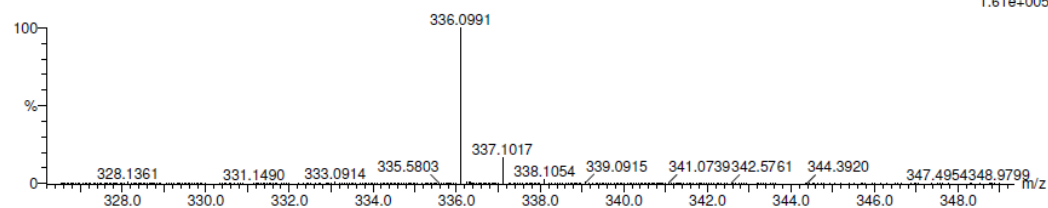
KE375

23-Aug-2016, 15:04:23

48222

1147 10 (0.631) Cm (9:13)

1: TOF MS ES+
1.61e+005



Mass	Calc. Mass	mDa	PPM	DBE	i-FIT	Formula
336.0991	336.0977	1.4	4.2	5.5	192.9	C14 H20 N O5 23Na P

Figure 8.88 High resolution MS of compound **5-12**.

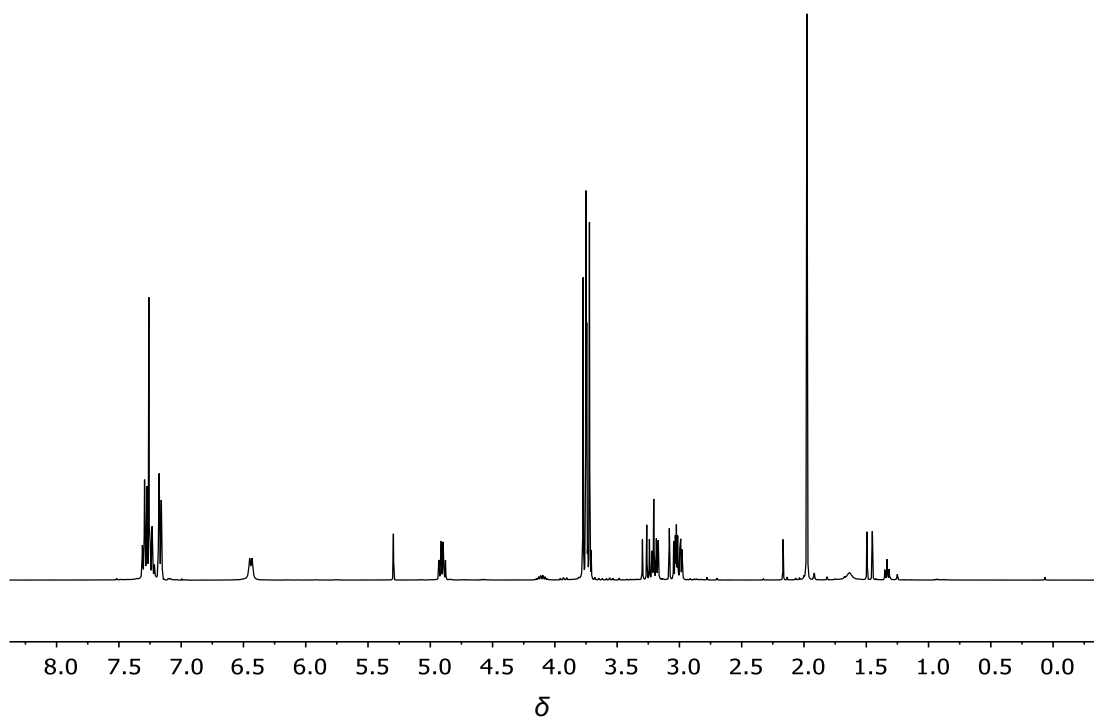
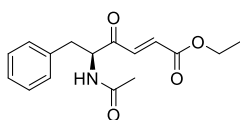


Figure 8.89 ^1H NMR of spectrum of compound **5-12**.

Ethyl (*S,E*)-5-acetamido-4-oxo-6-phenylhex-2-enoate (5-13**)**



5-13

To a 50 mL-round-bottom flask equipped with a magnetic stirring bar was added commercial ethyl glyoxalate solution (50% w/w in toluene, 10 mL). The solution was warmed to 50 °C at 35 mbar to remove most of toluene *in vacuo*. Afterwards, the flask was attached to distillation apparatus and warmed to 90 °C (observed 62 °C) to get rid of the rest of toluene. Then the pressure was reduced to 200 mbar and the oil bath was

slowly warmed to 115 °C to depolymerise and collect ethyl glyoxalate. To a mixture of compound **5-12** (373 mg, 1.19 mmol) and ethyl glyoxalate (freshly distilled) (147 mg, 1.43 mmol, 1.20 eq) was added potassium carbonate (329 mg, 2.38 mmol, 2.00 eq) in water (20 mL). The reaction mixture was stirred at 0 °C for 30 min, producing suspended white solid. After dried under freeze dryer, the solid was recrystallised from hot hexane to yield pure compound **5-13** (190 mg, 55%) as white needle-shape crystals.

m.p.: 117.0-119.6 °C; **¹H NMR (400 MHz, CDCl₃):** δ7.26 (m, 3H), 7.13 (d, *J* = 15.8 Hz, 1H), 7.06 (m, 2H), 6.77 (d, *J* = 15.8 Hz, 1H), 6.06 (d, *J* = 7.2 Hz, 1H), 5.13 (ddd, *J* = 7.2, 6.7, 5.6 Hz, 1H), 4.27 (q, *J* = 7.1 Hz, 1H), 3.21 (dd, *J* = 14.1, 6.7 Hz, 1H), 3.09 (dd, *J* = 14.1, 5.6 Hz, 1H), 2.00 (s, 3H), 1.33 (t, *J* = 7.1 Hz, 3H); **¹³C NMR (100 MHz, CDCl₃):** δ197.0, 169.8, 165.1, 136.3, 135.3, 132.9, 129.5, 128.9, 127.5, 61.7, 58.6, 37.2, 23.3, 14.3; **MS (ESI) (+ve):** *m/z* 312.1 [M+Na]⁺. **HRMS (ESI) calcd.** for C₁₆H₁₉NO₄Na [M+Na]⁺ *m/z* 312.1212, found *m/z* 312.1213 (**Figure 8.90**).

Single Mass Analysis

Tolerance = 3.0 PPM / DBE: min = -1.5, max = 20.0

Element prediction: Off

Number of isotope peaks used for i-FIT = 4

Monoisotopic Mass, Even Electron Ions

315 formula(e) evaluated with 1 results within limits (all results (up to 1000) for each mass)

Elements Used:

C: 0-50 H: 0-50 N: 0-5 O: 0-6 23Na: 0-1

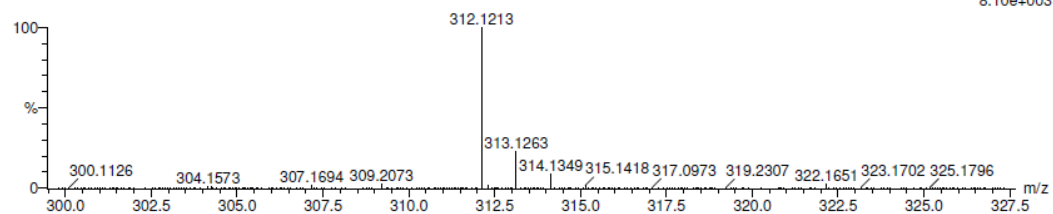
CG77/AJ

48652

1289 16 (0.851)

KE375

21-Sep-2016,10:03:49

1: TOF MS ES+
8.10e+003

Minimum:

Maximum:

100.0

3.0

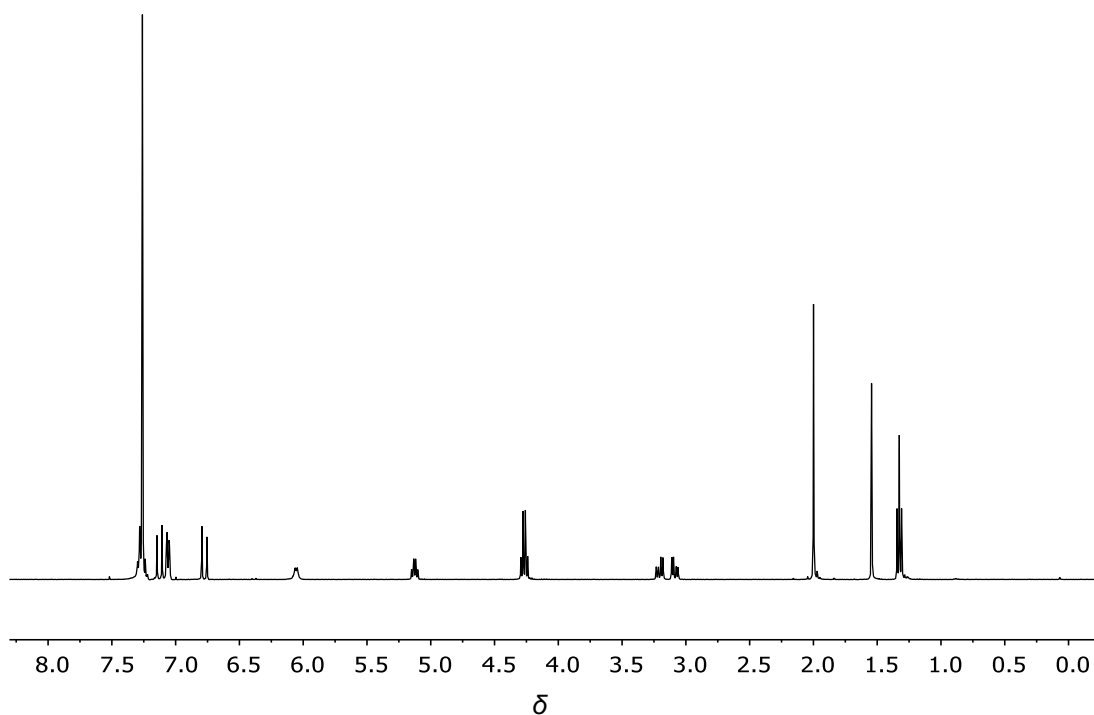
-1.5

20.0

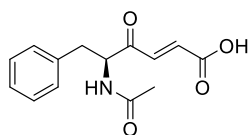
Mass	Calc. Mass	mDa	PPM	DBE	i-FIT	Formula
------	------------	-----	-----	-----	-------	---------

312.1213	312.1212	0.1	0.3	7.5	234.5	C16 H19 N O4 23Na
----------	----------	-----	-----	-----	-------	-------------------

Figure 8.90 High resolution MS of compound 5-13.

Figure 8.91 ¹H NMR of spectrum of compound 5-13.

4-Oxo-5-acetamido-6-phenyl-hex-2-enoic acid (1-39)



1-39

To a solution of compound **5-13** (37 mg, 0.13 mmol) in MeOH (2 mL) was added 0.1 M phosphate buffer (20 mL, pH 7.0) and pig liver esterase (370 units, 22 mg). The reaction mixture was shaken vigorously in the incubator at 30 °C for 18 h and washed with Et₂O (2 × 20 mL). The aqueous layer was acidified by the addition of concentrated HCl (approx. pH 3, turned cloudy) and extracted with DCM (3 × 20 mL, emulsion). The combined organic extracts were dried over MgSO₄, concentrated under reduced pressure and finally purified by preparative HPLC using an Alltima C18 5μ (22 × 250 mm) column (6 mL/min). The analysis was carried out with a linear gradient elution of 50:50 (MeOH: H₂O (0.1% TFA), v/v) to 70:30 between 0-30 min, followed by maintenance of 50:50 between 30-35 min. The resulting HPLC is reproduced in **Figure 8.92**, and showed one dominant peak at 24.50 min. Sample corresponding to the peak was isolated through HPLC. Mass spectrometry of the peak at 24.50 min displayed ions at *m/z* 260.2, which corresponds to the [M-H]⁻ for compound **1-39**. Based on this analysis, preparative HPLC was used to isolate compound **1-39**. The column fractions were concentrated *via* freeze drying to give compound **1-39** (16 mg, 48%) as a colourless powder.

m.p.: decomposes; **¹H NMR (400 MHz, DMSO-d₆):** δ8.41 (d, *J* = 7.4 Hz, 1H), 7.23 (m, 5H), 7.09 (d, *J* = 15.8 Hz, 1H), 6.58 (d, *J* = 15.8 Hz, 1H), 4.71 (ddd, *J* = 9.5, 7.4, 5.2 Hz, 1H), 3.05 (dd, *J* = 13.9, 5.2 Hz, 1H), 2.78 (dd, *J* = 13.9, 9.5 Hz, 1H), 1.79 (s, 3H); **¹³C NMR (100 MHz, DMSO-d₆):** δ197.8, 169.5, 166.4, 137.5, 136.4, 132.1, 129.2, 128.2, 126.4, 58.5, 34.9, 22.2; **MS (ESI) (+ve):** *m/z* 260.2 [M-H]⁻. **HRMS (ESI) calcd. for C₁₄H₁₄NO₄ [M-H]⁻ *m/z* 260.0923, found *m/z* 260.0923 (Figure 8.93).**

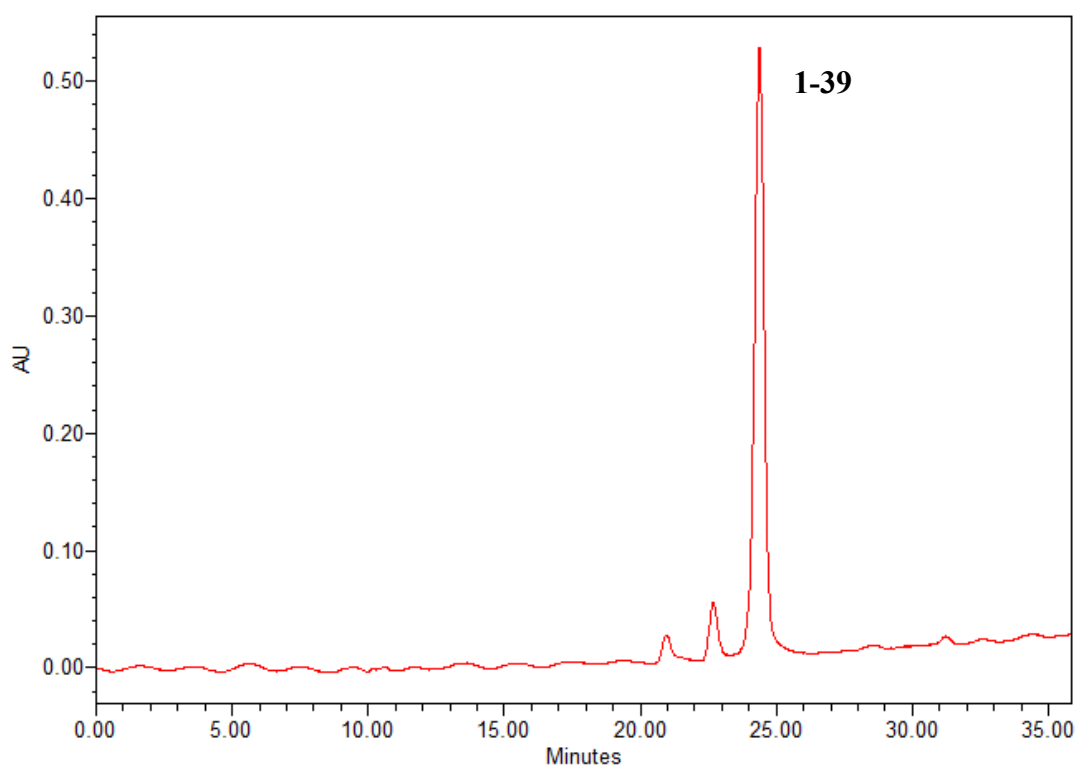


Figure 8.92 HPLC chromatogram of compound **1-39**.

Single Mass Analysis

Tolerance = 3.0 PPM / DBE: min = -1.5, max = 20.0

Element prediction: Off

Number of isotope peaks used for i-FIT = 4

Monoisotopic Mass, Even Electron Ions

338 formula(e) evaluated with 1 results within limits (all results (up to 1000) for each mass)

Elements Used:

C: 0-80 H: 0-110 N: 0-10 O: 0-32

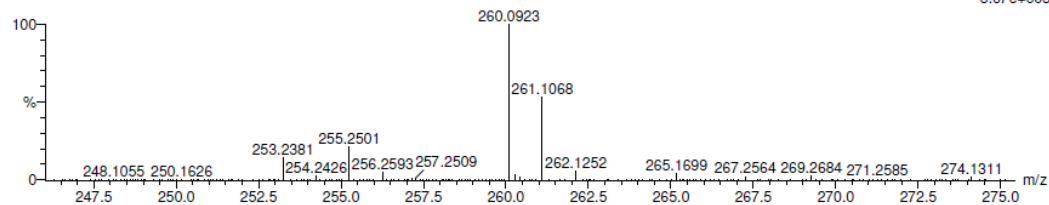
CG78/AJ

48739

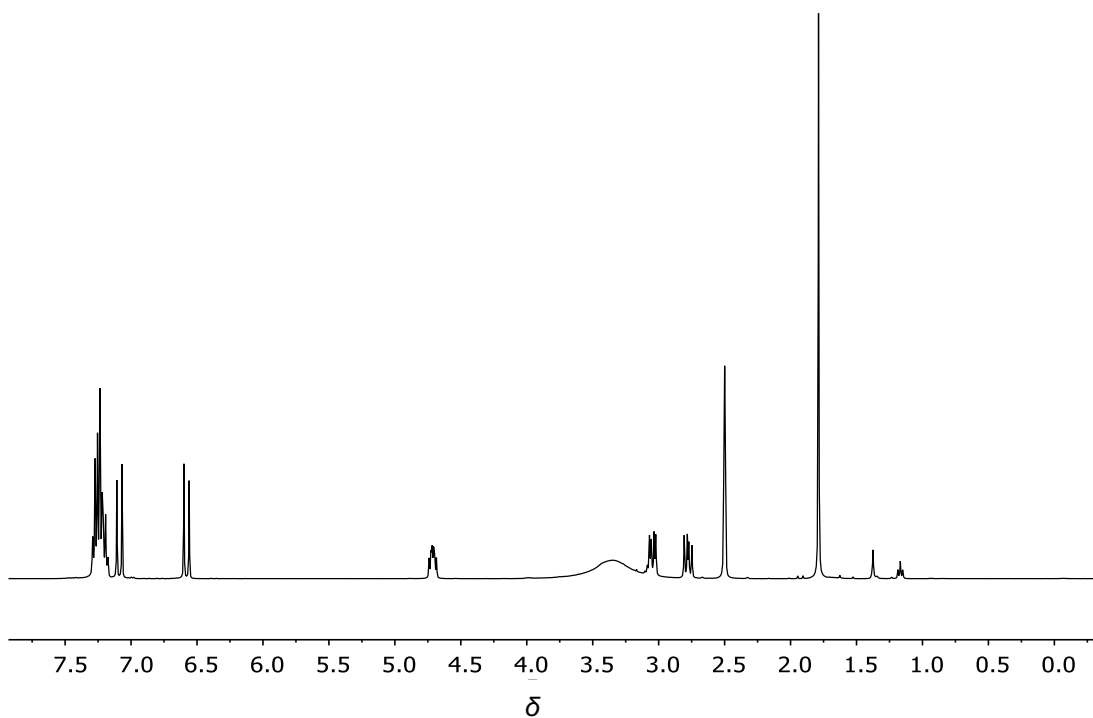
1339 6 (0.279)

KE375

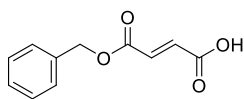
28-Sep-2016,11:15:36

1: TOF MS ES-
8.67e+003

Minimum:				-1.5		
Maximum:		100.0	3.0	20.0		
Mass	Calc. Mass	mDa	PPM	DBE	i-FIT	Formula
260.0923	260.0923	0.0	0.0	8.5	n/a	C14 H14 N O4

Figure 8.93 High resolution MS of compound **1-39**.**Figure 8.94** ^1H NMR of spectrum of compound **1-39**.

(E)-4-(Benzyloxy)-4-oxobut-2-enoic acid (5-3)



5-3

Fumaric acid (1.00 g, 8.62 mmol) and benzyl alcohol (890 μ L, 8.62 mmol, 1.00 eq) were dissolved in anhydrous DMF (10 mL). NMM (0.97 mL, 8.62 mmol, 1.00 eq) was added at 0 $^{\circ}$ C followed by EDC (1.65 g, 8.62 mmol, 1.00 eq) after 30 min. The reaction was stirred for 16 h at room temperature. Thereafter, the reaction mixture was concentrated *in vacuo* and dissolved in EtOAc (10 mL), followed by extraction with saturated aqueous NaHCO₃ solution (3 \times 40 mL). The combined aqueous layer was then acidified with concentrated HCl to pH 2. The product was extracted with EtOAc (2 \times 20 mL), and the organic phase was washed with H₂O (2 \times 20 mL) and dried over MgSO₄. The ensuing residue was subjected to silica gel flash column chromatography (EtOAc/n-hexane/AcOH, 5:4.9:0.1, v/v/v) to afford a white solid (0.89 g, 50%).

m.p.: 113.5-114.7 $^{\circ}$ C; **¹H NMR (400 MHz, CDCl₃):** δ 7.38 (m, 5H), 6.98 (d, J = 15.8 Hz, 1H), 6.88 (d, J = 15.8 Hz, 1H) 5.25 (s, 2H); **¹³C NMR (100 MHz, CDCl₃):** δ 169.2, 164.6, 135.6, 135.2, 132.9, 128.8, 128.7, 128.6, 67.5; **MS (ESI) (+ve):** m/z 229.1 [M+Na]⁺. **HRMS (ESI)** calcd. for C₁₁H₁₀O₄Na [M+Na]⁺ m/z 229.0477, found m/z 229.0482 (**Figure 8.95**).

Single Mass Analysis

Tolerance = 3.0 PPM / DBE: min = -1.5, max = 20.0

Element prediction: Off

Number of isotope peaks used for i-FIT = 3

Monoisotopic Mass, Odd and Even Electron Ions

23 formula(e) evaluated with 1 results within limits (all results (up to 1000) for each mass)

Elements Used:

C: 0-50 H: 0-50 O: 0-8 23Na: 1-1

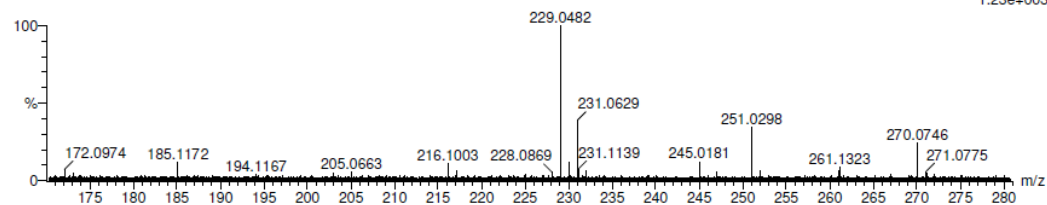
CG35/EO

KE375

15-Jul-2015 11:33:35

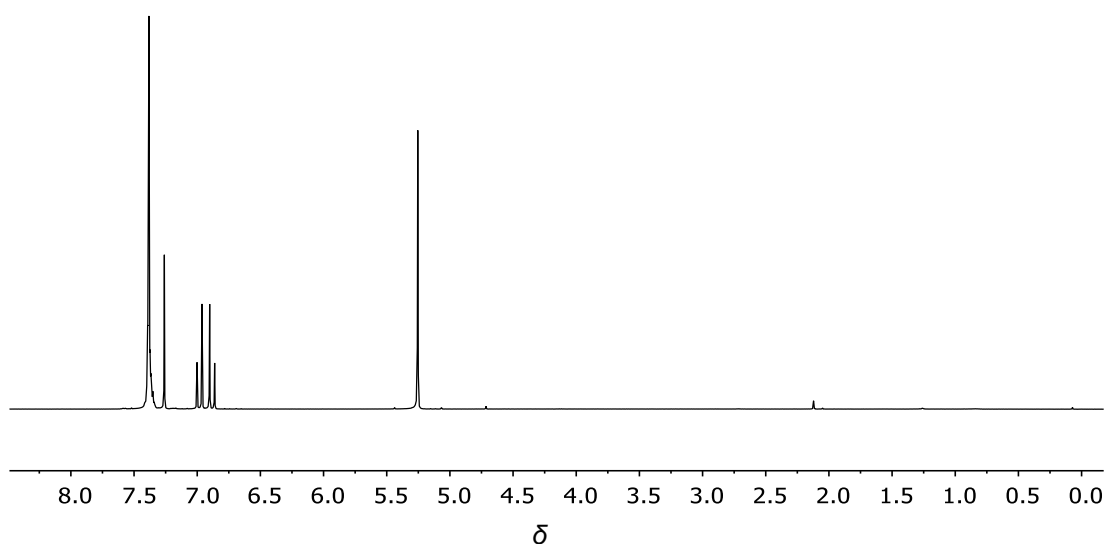
40699

1362 120 (5.257) Cm (35:133)

1: TOF MS ES+
1.23e+003

Minimum:									
Maximum:	5.0	3.0	-1.5						
Mass	Calc. Mass	mDa	PPM	DBE	i-FIT	Formula			
229.0482	229.0477	0.5	2.2	6.5	224.6	C11	H10	O4	23Na

Figure 8.95 High resolution MS of compound 5-3.

Figure 8.96 ¹H NMR of spectrum of compound 5-3.

8.5.2 Procedure for PAM Inhibition Assay

Assays were performed with 1.25 mM ascorbic acid, 10 μ M copper sulphate, 0.2 mg/mL bovine liver catalase, 1% EtOH, 1% DMSO, 50 μ M tripeptide substrate (*R*)-Tyr-(*S*)-Val-Gly-COOH and 0.4-0 μ M (for PAL inhibition assay) and 100-0 μ M (for PHM inhibition assay) at 2X serial dilution of compound **1-143** in 150 mM MES buffer at pH 5.8. For the concentration selection of other compound candidates, compounds **5-1** and **5-2** were tested with 400-0 μ M at 10X serial dilution; compound **1-57** was tested with 100-0 μ M (for PAL inhibition assay) and 2000-0 μ M (for PHM inhibition assay) at 2X serial dilution; compound **1-39** was tested with 100-0 μ M at 2X serial dilution; compound **5-3** was tested with 150-0 μ M at 2X serial dilution; compound **1-17** was tested with 20-0 μ M at 2X serial dilution and 100 μ M. Assays were initiated through the addition of concentrated PAM (5 μ L) to give a final volume of 100 μ L. The mixtures were incubated in a Lab Companion Model SI-600R open-air shaker at 37 °C for 2 h, with agitation at 80 rpm. The solutions were then passed through Amicon[®] Ultra YM-3 filters using a centrifuge for 15 min at 12000 rpm at room temperature. All prepared samples were analysed using HPLC-MS system except that the samples of compound **5-3** were analysed using HPLC with a fluorescence detector, of which the solvent system and column conditions were exactly same as described in **Section 8.2.4**. In the trace reproduced by HPLC with a fluorescence detector, the peak of hydroxylated tripeptide appears at 18.63 min. The data for all assessment that not shown in Chapter 5 are illustrated below in **Figure 8.97 – Figure 8.101**.

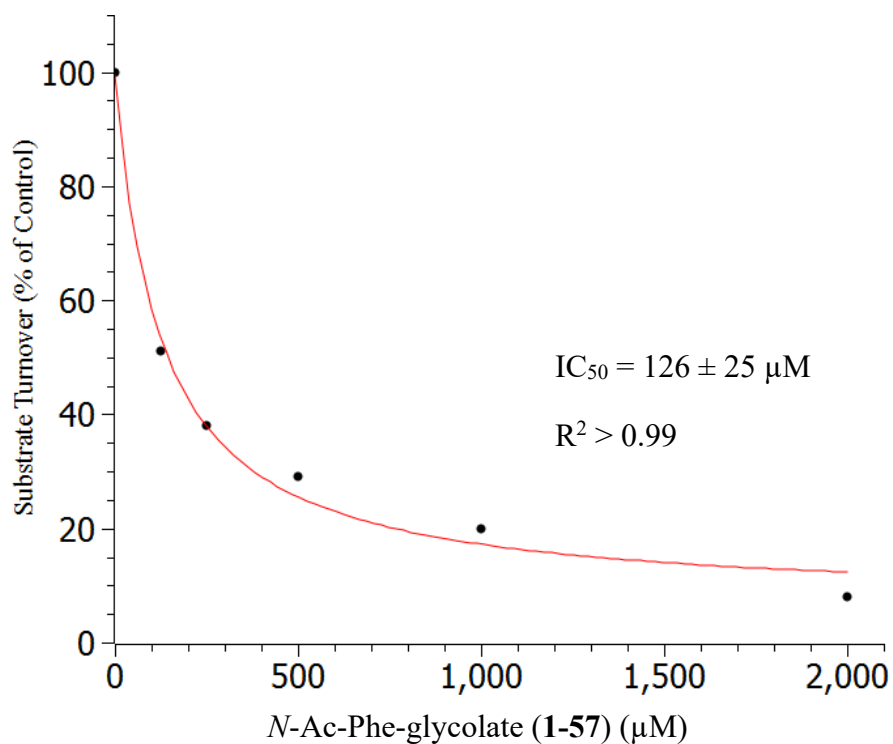
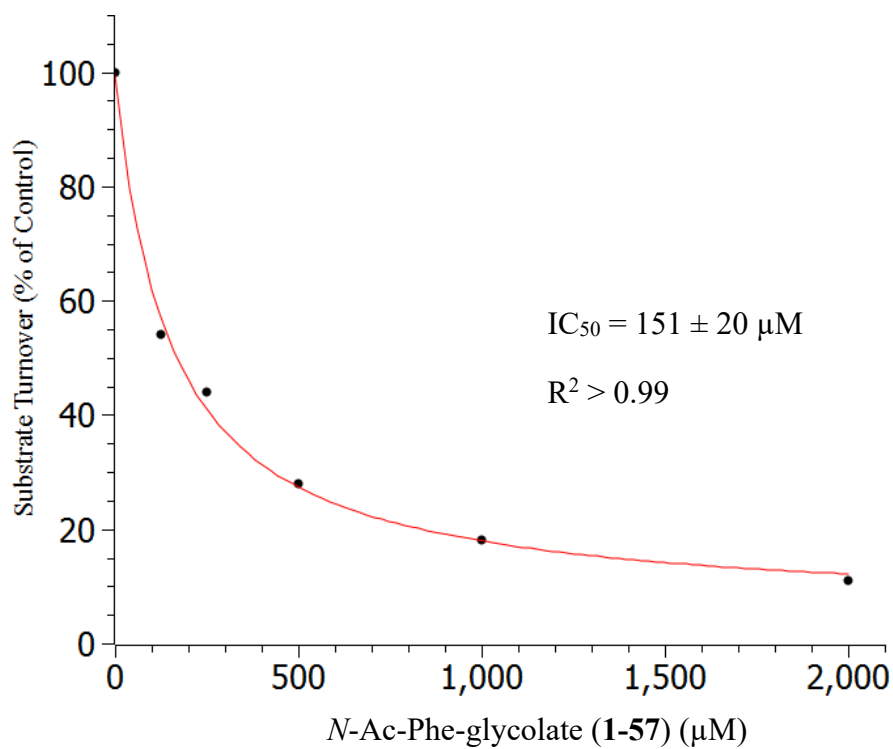


Figure 8.97 Determination of IC_{50} against PHM for *N*-Ac-Phe-glycolate (**1-57**) (μM)

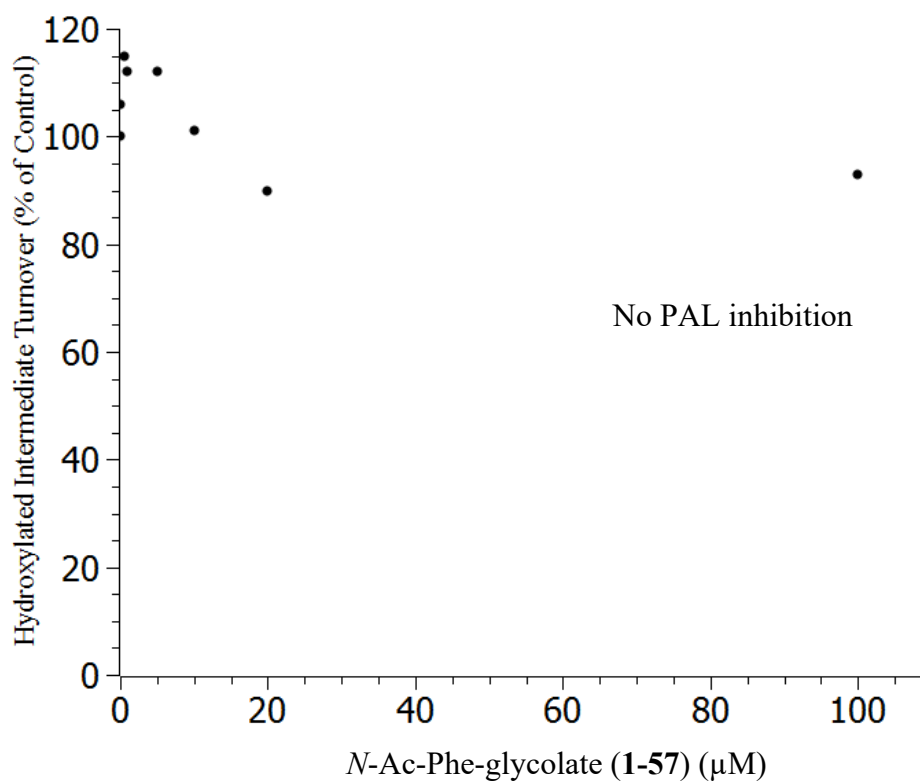
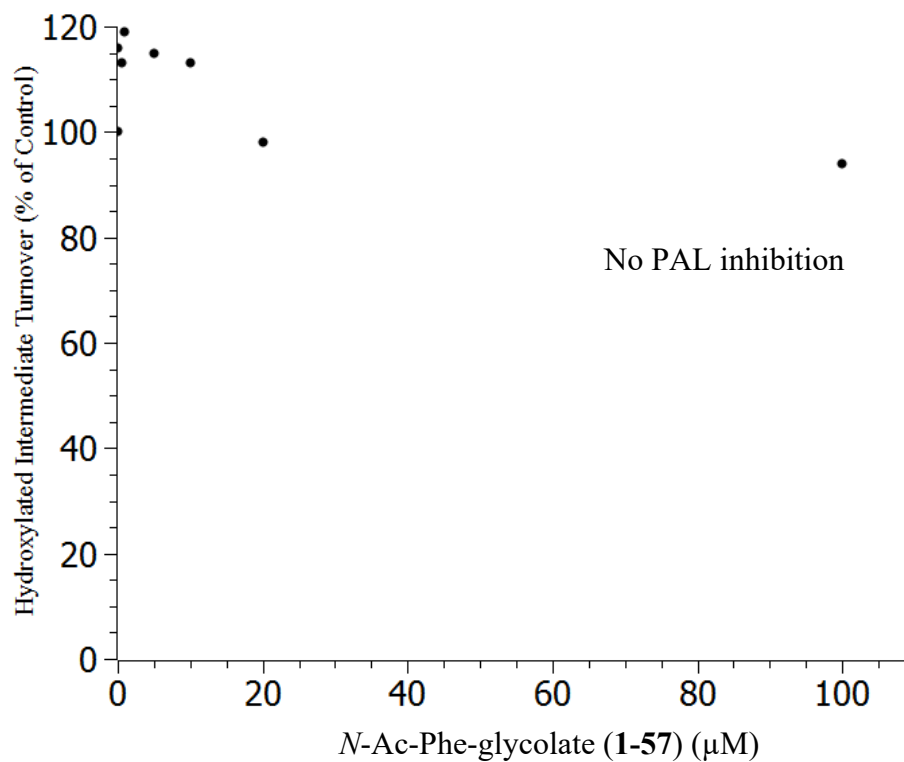


Figure 8.98 Data of PAL inhibition using *N*-Ac-Phe-glycolate (1-57) (μM)

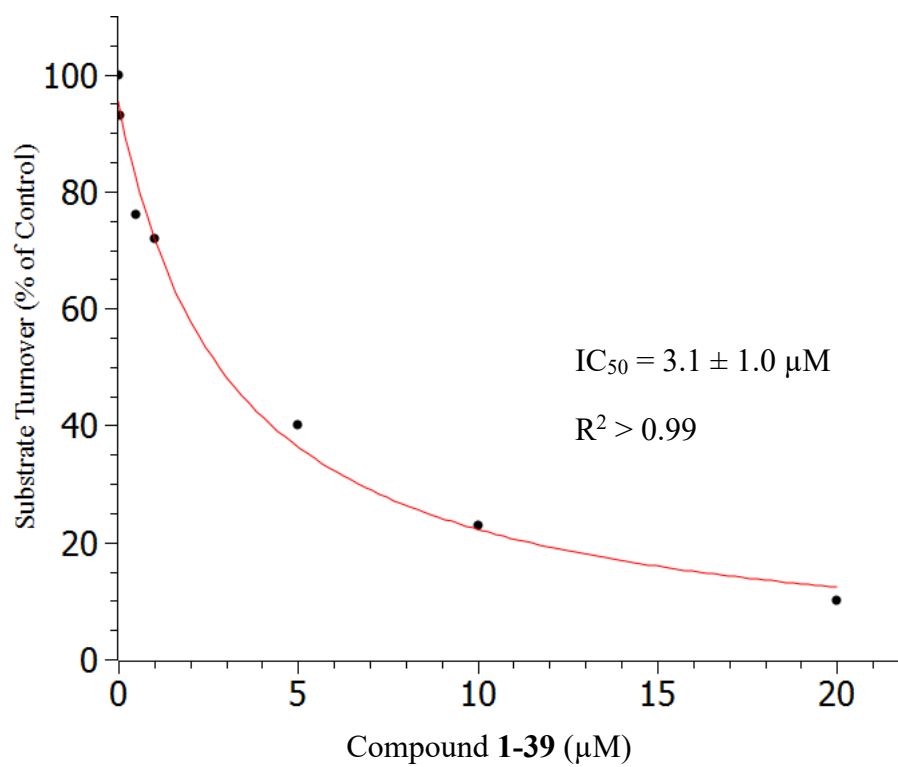
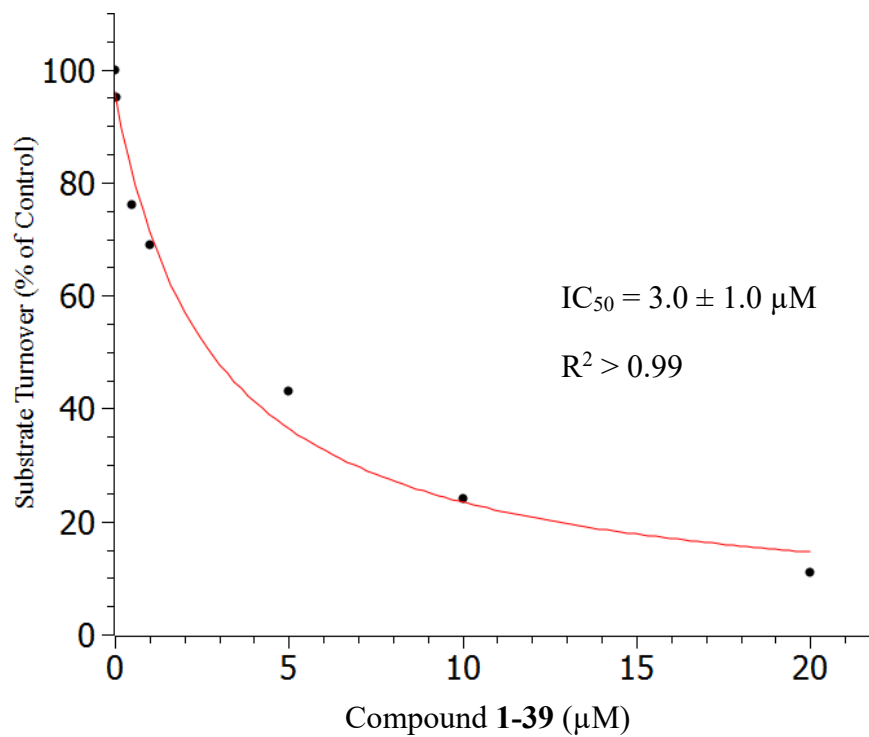


Figure 8.99 Determination of IC_{50} against PHM for compound 1-39 (μM)

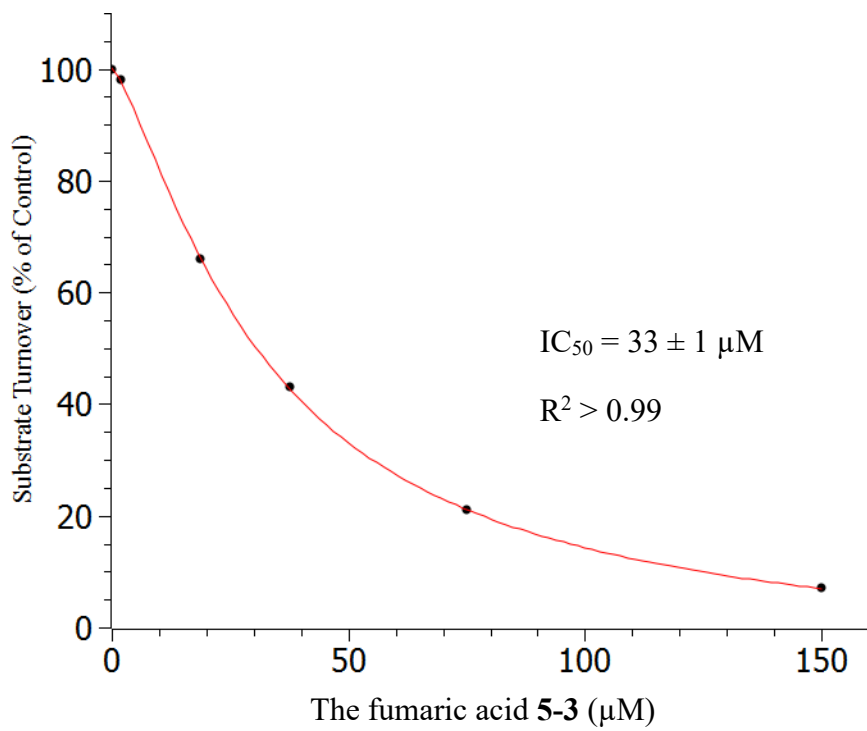
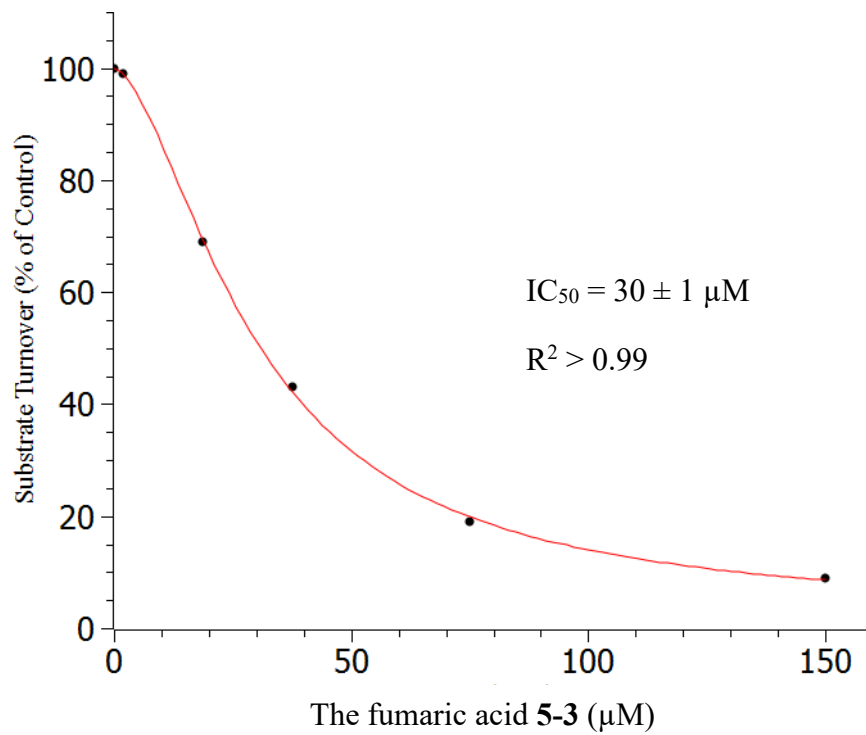


Figure 8.100 Determination of IC_{50} against PHM for the fumaric acid 5-3 (μM)

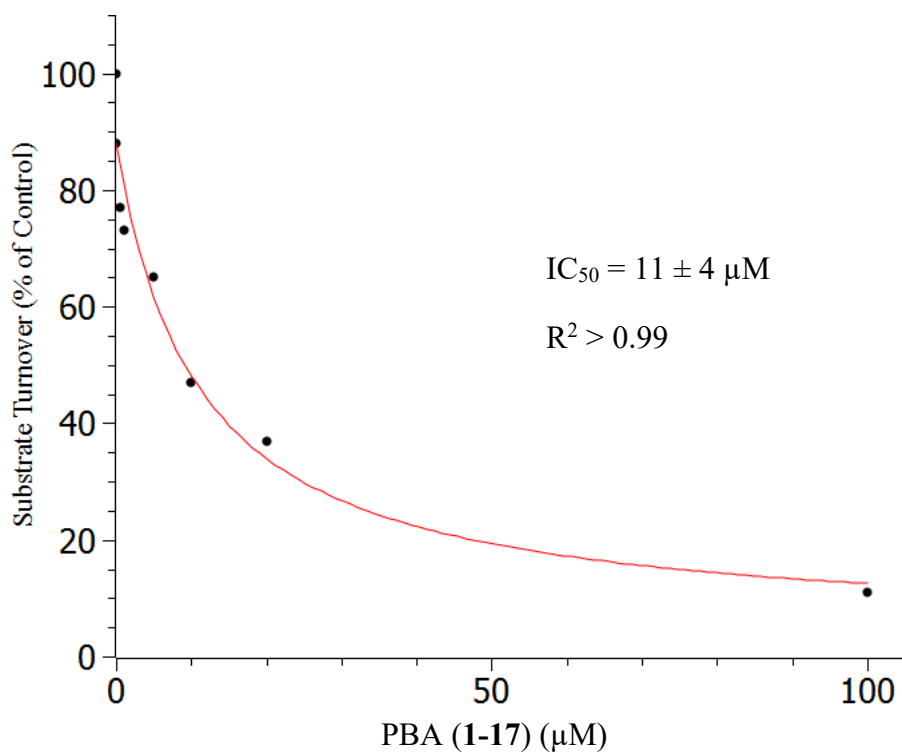
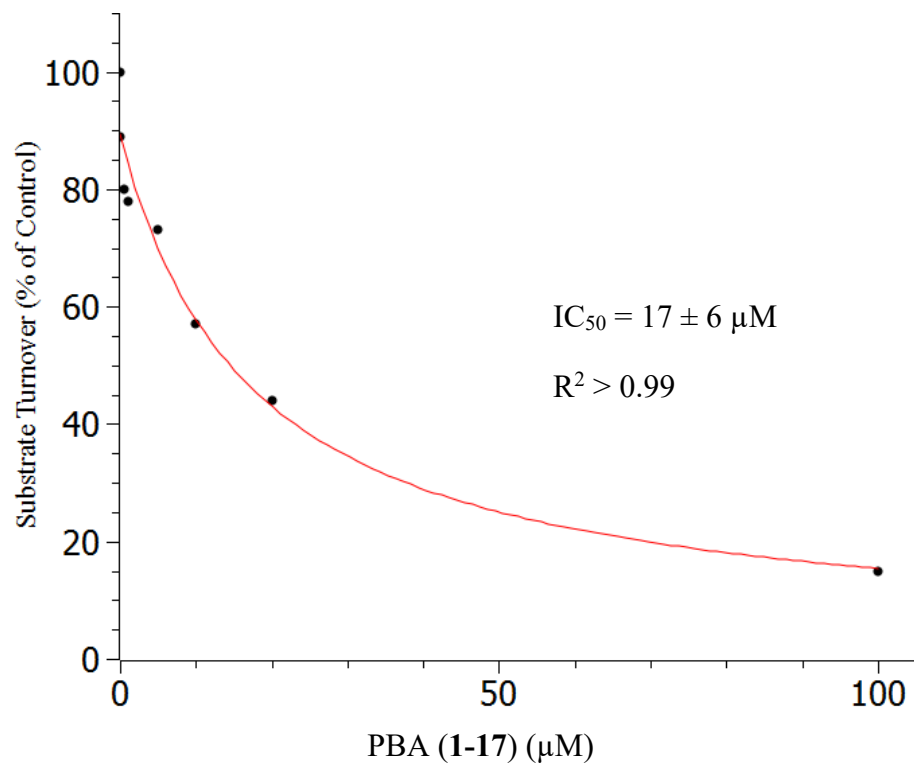


Figure 8.101 Determination of IC_{50} against PHM for PBA (1-17) (μM)

8.5.3 Procedure for pH-Dependent PAL Inhibition Assay Using *N*-Ac-Phe-pyruvate (1-143)

The pH-dependent PAL Assays using *N*-Ac-Phe-pyruvate (1-143) were performed in the same manner as described in **Section 8.5.2**, except that four more pH conditions of MES buffer were used, which were pH 5.5, 6.1, 6.4 and 6.7. All assays were run at least in duplicate. Data related to pH 5.5, 6.1, 6.4 and 6.7 were shown below (**Figure 8.102 – Figure 8.105**).

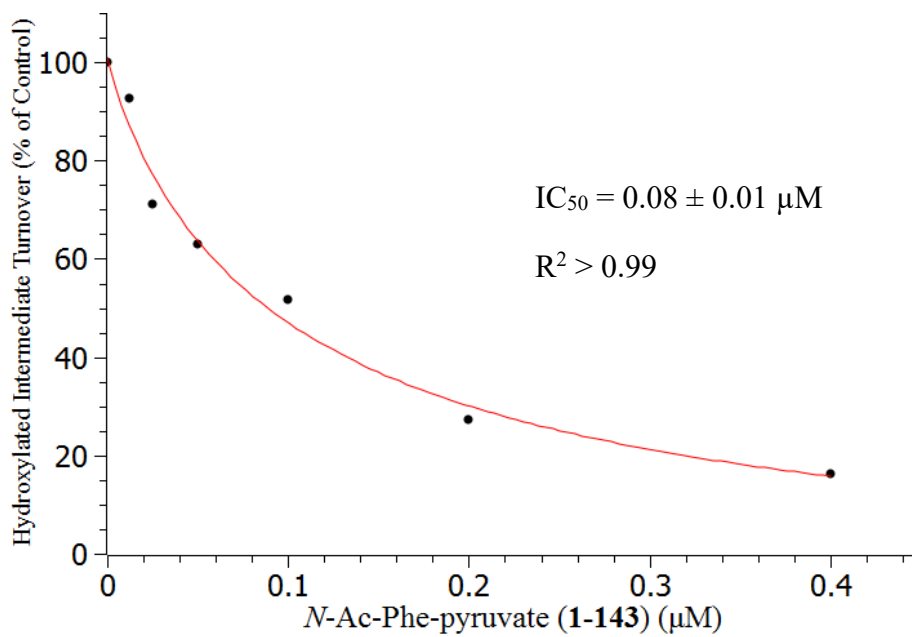
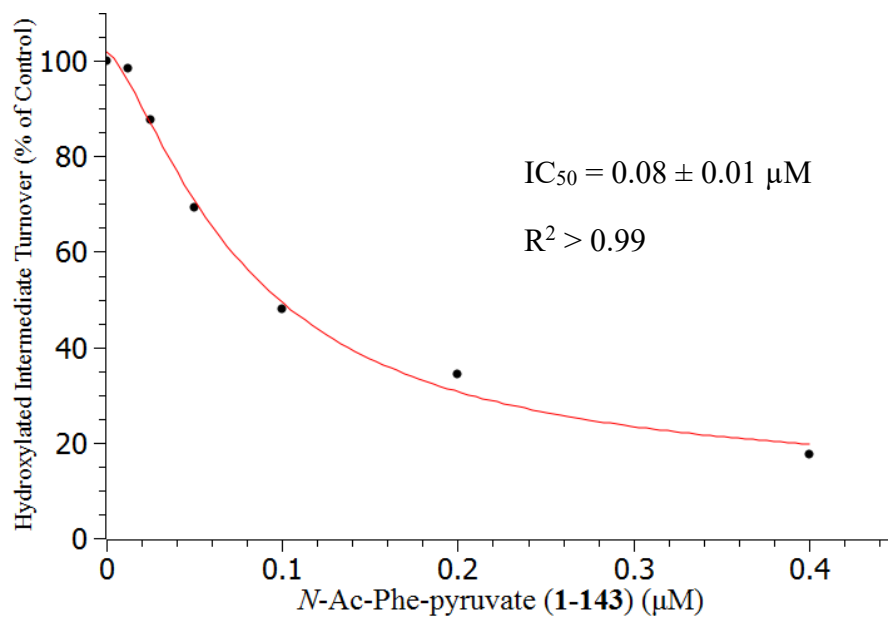


Figure 8.102 Determination of IC_{50} against PAL for *N*-Ac-Phe-pyruvate (1-143) (µM) at pH 5.5

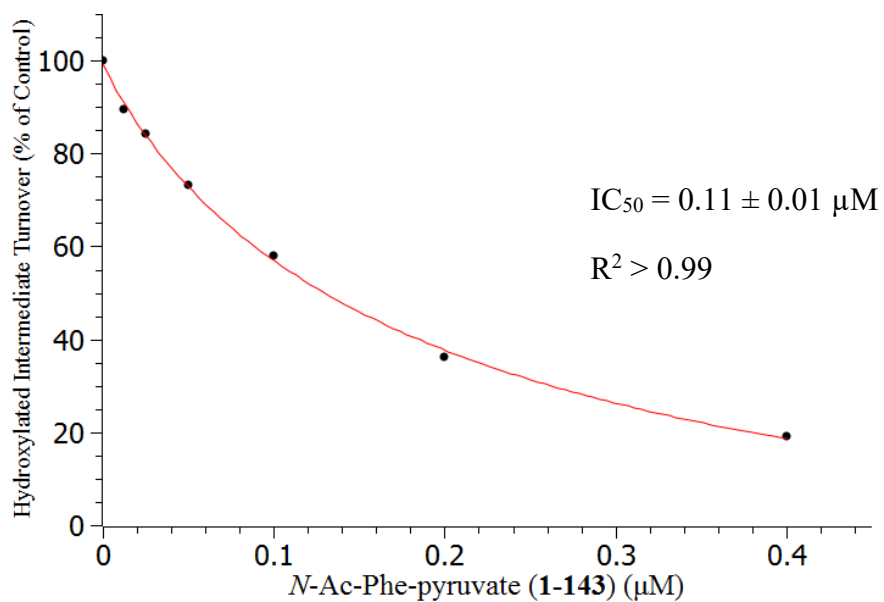
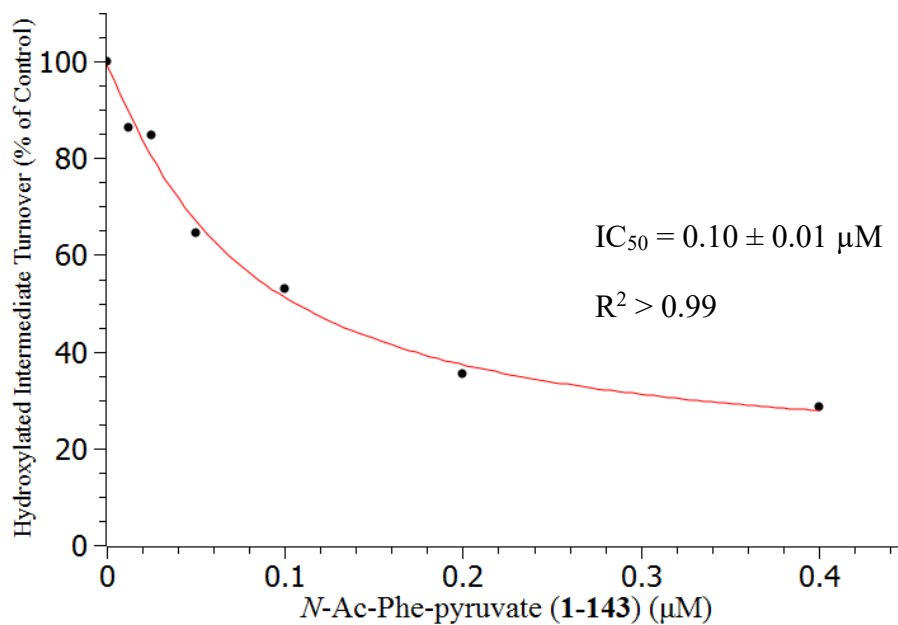


Figure 8.103 Determination of IC_{50} against PAL for *N*-Ac-Phe-pyruvate (1-143) (μM) at pH 6.1

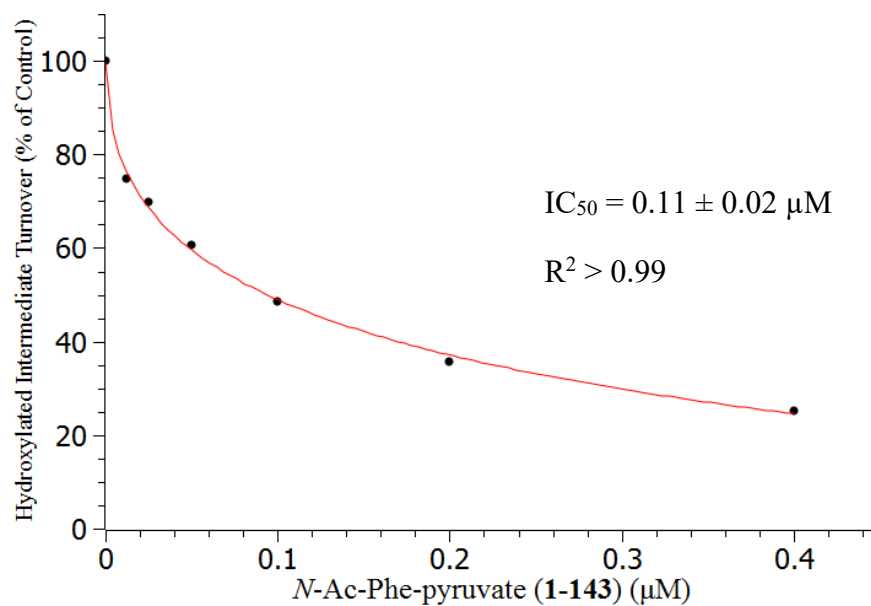
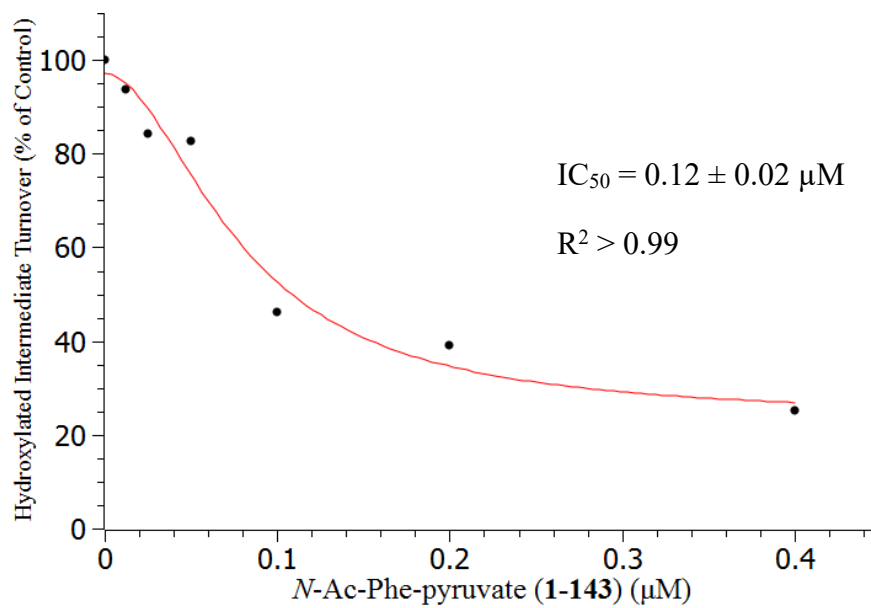


Figure 8.104 Determination of IC_{50} against PAL for *N*-Ac-Phe-pyruvate (**1-143**) (μM) at pH 6.4

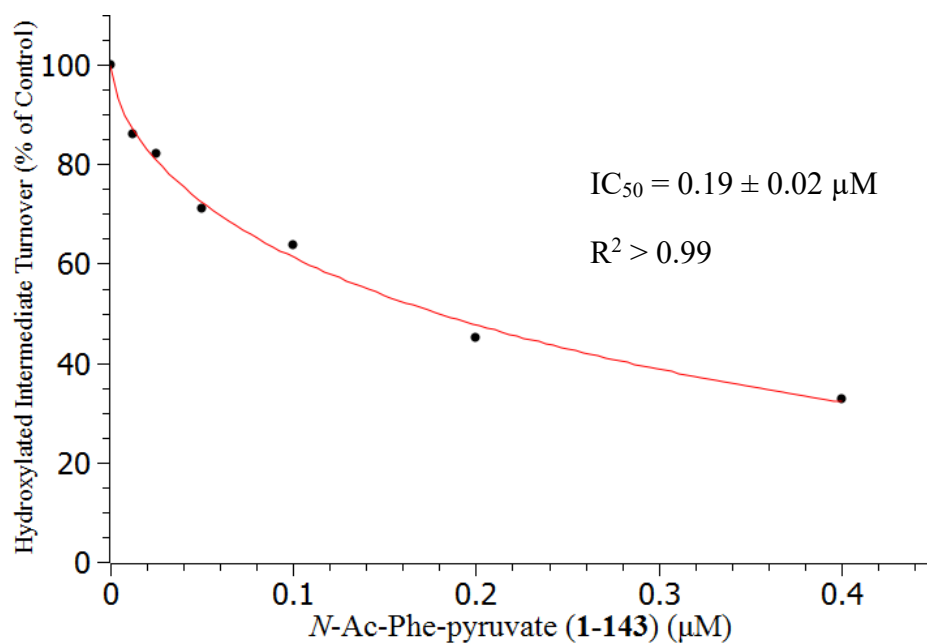
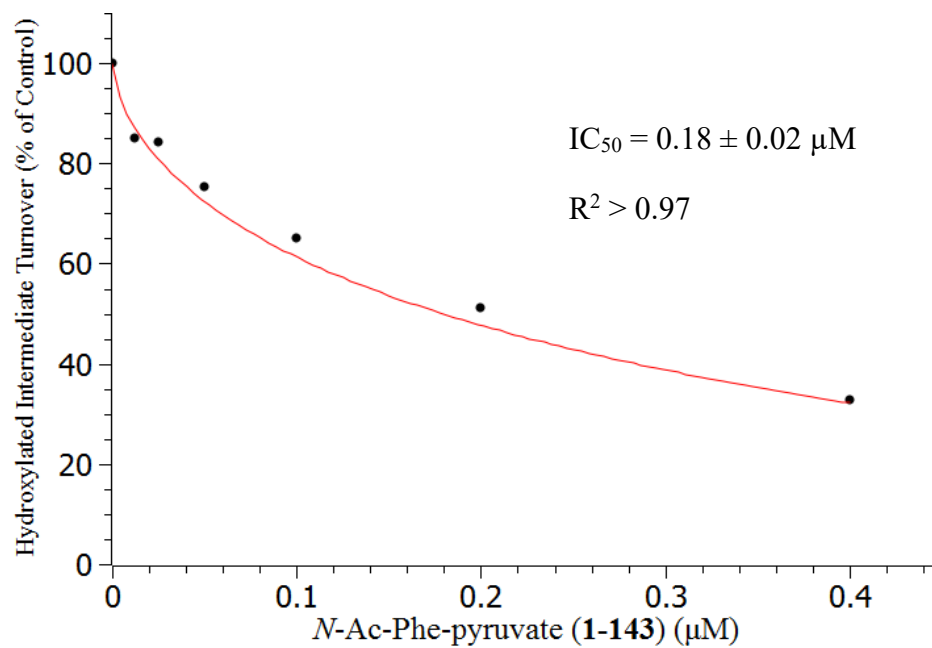


Figure 8.105 Determination of IC_{50} against PAL for *N*-Ac-Phe-pyruvate (1-143) (μM) at pH 6.7

Appendix

Ascorbate-concentration-dependent isolated PAM assay was performed by using substrate tripeptide (*R*)-Tyr-(*S*)-Val-Gly-COOH. Except concentrations of ascorbate, other assay conditions are similar to that described in **Section 8.4.2**. The substrate turnover were analysed by using HPLC with a fluorescence detector as described in **Section 8.2.4**. **Figure A1** shows that when the concentration of ascorbate is below 0.31 mM, the substrate turnover is below two percent. The increasing of concentration from 0.31 mM to 2.5 mM increases the substrate turnover. The continuously increasing concentrations of ascorbate then decrease substrate turnover.

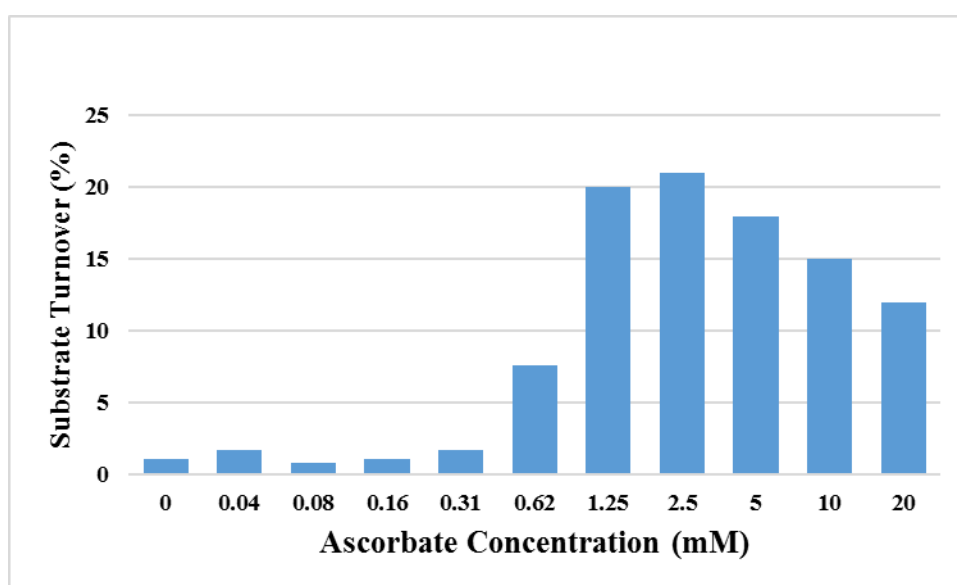


Figure A1 Substrate turnover in ascorbate concentration-dependent assay.

In PAM activity, the product from the oxidation of ascorbate in PAM has been confirmed as semidehydroascorbate (SD), which requires semidehydroascorbate reductase (SDR), a type of NADH oxidase, to reduce back to ascorbate to form a recycling of ascorbate.^[99] The NADH oxidase activity is a major source of superoxide anion and is inhibited by peroxynitrite (ONOO⁻).^[223] Based on this, our hypothesis is that if SDR is inhibited by addition of ONOO⁻ the level of ascorbate participating in PAM activity is expected to decrease and thus decrease the level of amidated product. Considering the complexity of the environment of the medium of DMS53 cells, it is convenient to get a quick answer on whether doping ONOO⁻ in the whole cell assay could accumulate the level of CTG and decrease the level of CT. Due to the short biological half-life of ONOO⁻ (can be < 0.1 s), chronic exposure to micromolar ONOO⁻ was simulated by treatment of 3-morpholinosydnonimine hydrochloride (SIN-1) with repetitive pulses of ONOO⁻ in the micromolar range.^[223-224] The whole cell assay with SIN-1 was performed by adding 0, 1mM, and 2 mM SIN-1 every 12 h for 24 h after DMS53 cells growing to about 80 % density. The medium samples were collected and injected onto HPLC with fluorescence detection. The number of cells was counted in the same way as the whole cell PAL inhibition assay did. The HPLC traces were shown in **Figure A2** below.

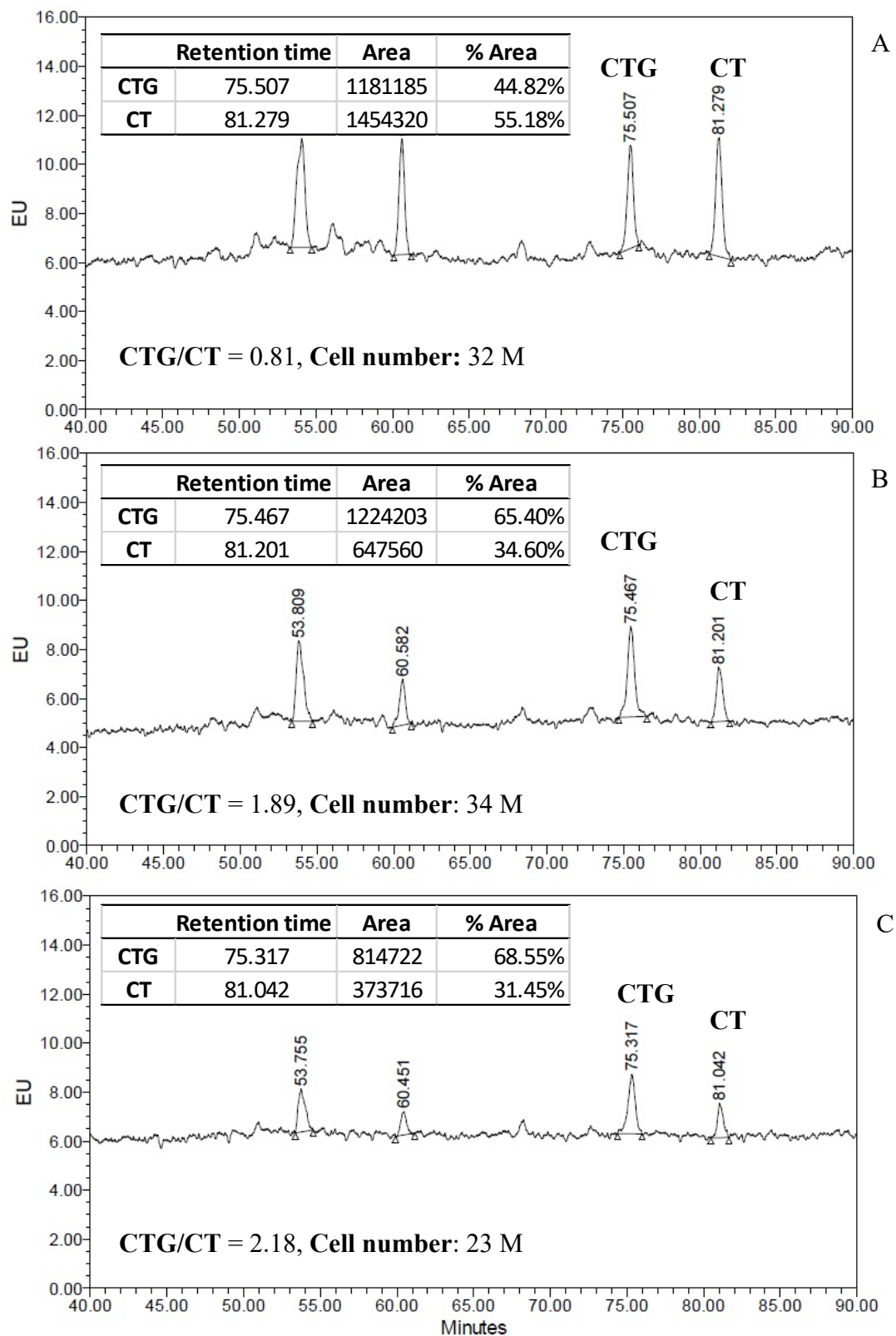


Figure A2 HPLC trace of (A) DMS53 medium sample; (B) DMS53 medium sample with 1 mM SIN-1; (C) DMS53 medium sample with 2 mM SIN-1.

Compared with the level of CTG and CT in the blank sample (**Figure A2A**), the level of CTG in 1mM SIN-1 sample slightly increases while the CT level decreases significantly (**Figure A2B**), where CTG/CT value in **Figure A2A** was 0.81 while the value in **Figure A2B** increased to 1.89. This indicates that SIN-1 inhibits PHM activity, which is consistent with our hypothesis. When the concentration of SIN-1 is 2 mM, CTG/CT value is similar to that in 1 mM sample, but CTG and CT levels dropped about 33% and 50%, respectively. It is likely that SIN-1 with 2 mM shows cytotoxic against DMS53 cells, which is consistent with the fact that counted cell number decreases by around 33%.

Bibliography

1. K. E. L. McColl; D. Gillen; E. El-Omar, *Best Practice & Research Clinical Gastroenterology* **2000**, *14*, 13-26.
2. J. Silva, *Annals of Internal Medicine* **2003**, *139*, 205-213.
3. A. M. Wren; C. J. Small; H. L. Ward; K. G. Murphy; C. L. Dakin; S. Taheri; A. R. Kennedy; G. H. Roberts; D. G. A. Morgan; M. A. Ghatei; S. R. Bloom, *Endocrinology* **2000**, *141*, 4325-4328.
4. S. L. Clark; K. R. Simpson; G. E. Knox; T. J. Garite, *American Journal of Obstetrics and Gynecology* **2009**, *200*, 35.e1-35.e6.
5. T. M. O'Connor; J. O'Connell; D. I. O'Brien; T. Goode; C. P. Bredin; F. Shanahan, *Journal of Cellular Physiology* **2004**, *201*, 167-180.
6. E. Frank; R. Landgraf, *European Journal of Pharmacology* **2008**, *583*, 226-242.
7. K.-H. Kim; B. L. Seong, *Biotechnology and Bioprocess Engineering* **2001**, *6*, 244-251.
8. B. A. Eipper, *Annual Review of Physiology* **1988**, *50*, 333-344.
9. J. Vikman; B. Ahrén, *Diabetes, Obesity and Metabolism* **2009**, *11*, 197-201.
10. J. H. Boyd; C. L. Holmes; Y. Wang; H. Roberts; K. R. Walley, *Resuscitation* **2008**, *79*, 325-331.
11. M. M. Lim; L. J. Young, *Neuroscience* **2004**, *125*, 35-45.
12. R. A. Liddle, *American Journal of Physiology - Gastrointestinal and Liver Physiology* **1995**, *269*, G319-G327.
13. G. Shillabeer; J. S. Davison, *American Journal of Physiology - Regulatory, Integrative and Comparative Physiology* **1987**, *252*, R353-R360.
14. P. Zwanzger; K. Domschke; J. Bradwejn, *Depression and Anxiety* **2012**, *29*, 762-774.
15. J. Bradwejn, *Journal of Psychiatry and Neuroscience* **1993**, *18*, 178-188.
16. M. D. Erion; J. Tan; M. Wong; A. Y. Jeng, *Journal of Medicinal Chemistry* **1994**, *37*, 4430-4437.
17. M. Salido; J. Vilches; A. López; G. M. Roomans, *Cancer* **2002**, *94*, 368-377.
18. S. Schifter, *Peptides* **1997**, *18*, 307-317.
19. K. Kitamura; K. Kangawa; M. Kawamoto; Y. Ichiki; S. Nakamura; H. Matsuo; T. Eto, *Biochemical and Biophysical Research Communications* **1993**, *192*, 553-560.
20. K. Takahashi; K. Kikuchi; Y. Maruyama; T. Urabe; K. Nakajima; H. Sasano; Y. Imai; O. Murakami; K. Totsune, *Peptides* **2006**, *27*, 1383-1389.
21. J. H. Walsh; H. T. Debas; M. I. Grossman, *Journal of Clinical Investigation* **1974**, *54*, 477-485.
22. M. Zaidi; A. M. Inzerillo; B. S. Moonga; P. J. R. Bevis; C. L. H. Huang, *Bone* **2002**, *30*, 655-663.
23. M. R. Edbrooke; D. Parker; J. H. McVey; J. H. Riley; G. D. Sorenson; O. S. Pettengill; R. K. Craig, *The EMBO Journal* **1985**, *4*, 715-724.
24. S. J. Wimalawansa; H. R. Morris; A. Etienne; I. Blench; M. Panico; I. MacIntyre, *Biochemical and Biophysical Research Communications* **1990**, *167*, 993-1000.
25. J. Shively; J. R. Reeve; V. E. Eysselein; C. Ben-Avram; S. R. Vigna; J. H. Walsh, *American Journal of Physiology* **1987**, *252*, G272-5.

26. D. Koulischer; L. Moroder; M. Deschodt-Lanckman, *Regulatory Peptides* **1982**, *4*, 127-139.
27. D. Vishnuvardhan; M. C. Beinfeld, *Biochemistry* **2000**, *39*, 13825-13830.
28. R. S. Izzo; W. R. Brugge; M. Praissman, *Regulatory Peptides* **1984**, *9*, 21-34.
29. J. R. Reeve; V. Eysselein; J. H. Walsh; C. M. Ben-Avram; J. E. Shively, *Journal of Biological Chemistry* **1986**, *261*, 16392-16397.
30. S. W. Sutton; D. P. Behan; S. L. Lahrichi; R. Kaiser; A. Corrigan; P. Lowry; E. Potter; M. H. Perrin; J. Rivier; W. W. Vale, *Endocrinology* **1995**, *136*, 1097-1102.
31. N. M. Page; N. J. Bell; S. M. Gardiner; I. T. Manyonda; K. J. Brayley; P. G. Strange; P. J. Lowry, *Proceedings of the National Academy of Sciences* **2003**, *100*, 6245-6250.
32. D. F. Orr; T. Chen; A. H. Johnsen; R. Chalk; K. D. Buchanan; J. M. Sloan; P. Rao; C. Shaw, *Proteomics* **2002**, *2*, 1586-1600.
33. M. Carrasco; A. Hernanz; M. De La Fuente, *Regulatory Peptides* **1997**, *70*, 135-142.
34. C. P. Hansen; F. Stadil; J. F. Rehfeld, *American Journal of Physiology - Gastrointestinal and Liver Physiology* **2000**, *279*, G903-G909.
35. C. P. Hansen; F. Stadil; J. F. Rehfeld, *American Journal of Physiology - Gastrointestinal and Liver Physiology* **1995**, *269*, G600-G605.
36. J. F. Rehfeld; A. H. Johnsen, *European Journal of Biochemistry* **1994**, *223*, 765-773.
37. A. M. Lebacq-Verheyden; P. G. Kasprzyk; M. G. Raum; K. Van Wyke Coelingh; J. A. Lebacq; J. F. Battey, *Molecular and Cellular Biology* **1988**, *8*, 3129-3135.
38. C. Orskov; M. Bersani; A. H. Johnsen; P. Højrup; J. J. Holst, *Journal of Biological Chemistry* **1989**, *264*, 12826-12829.
39. L. Tan; P. Rousseau, *Biochemical and Biophysical Research Communications* **1982**, *109*, 1061-1071.
40. R. B. White; J. A. Eisen; T. L. Kasten; R. D. Fernald, *Proceedings of the National Academy of Sciences* **1998**, *95*, 305-309.
41. J. Roh; C. L. Chang; A. Bhalla; C. Klein; S. Y. T. Hsu, *Journal of Biological Chemistry* **2004**, *279*, 7264-7274.
42. N. Itoh; K.-i. Obata; N. Yanaihara; H. Okamoto, *Nature* **1983**, *304*, 547-549.
43. T. Sanke; G. I. Bell; C. Sample; A. H. Rubenstein; D. F. Steiner, *Journal of Biological Chemistry* **1988**, *263*, 17243-6.
44. T. Ohtaki; Y. Shintani; S. Honda; H. Matsumoto; A. Hori; K. Kanehashi; Y. Terao; S. Kumano; Y. Takatsu; Y. Masuda; Y. Ishibashi; T. Watanabe; M. Asada; T. Yamada; M. Suenaga; C. Kitada; S. Usuki; T. Kurokawa; H. Onda; O. Nishimura; M. Fujino, *Nature* **2001**, *411*, 613-617.
45. M. Kotani; M. Detheux; A. Vandenbogaerde; D. Communi; J.-M. Vanderwinden; E. Le Poul; S. Brézillon; R. Tyldesley; N. Suarez-Huerta; F. Vandeput; C. Blanpain; S. N. Schiffmann; G. Vassart; M. Parmentier, *Journal of Biological Chemistry* **2001**, *276*, 34631-34636.
46. A. Bertolini; R. Tacchi; A. V. Vergoni, *Pharmacological Research* **2009**, *59*, 13-47.
47. M. Fenger; A. H. Johnsen, *Biochemical Journal* **1988**, *250*, 781-788.
48. E. Theodorsson-Norheim; M. Andersson; H. JÖRnvall; I. Norheim; K. ÖBerg; G. Jacobsson, *European Journal of Biochemistry* **1987**, *166*, 693-698.
49. N. M. Page; R. J. Woods; S. M. Gardiner; K. Lomthaisong; R. T. Gladwell; D. J. Butlin; I. T. Manyonda; P. J. Lowry, *Nature* **2000**, *405*, 797-800.

50. I. M. Krane; S. L. Naylor; D. Helin-Davis; W. W. Chin; E. R. Spindel, *Journal of Biological Chemistry* **1988**, *263*, 13317-13323.
51. H. Ohki-Hamazaki, *Progress in Neurobiology* **2000**, *62*, 297-312.
52. K. Mori; M. Miyazato; T. Ida; N. Murakami; R. Serino; Y. Ueta; M. Kojima; K. Kangawa, *The EMBO journal* **2005**, *24*, 325-335.
53. C. Austin; G. Lo; K. A. Nandha; L. Meleagros; S. R. Bloom, *Journal of Molecular Endocrinology* **1995**, *14*, 157-169.
54. M. J. Bannon; M. S. Poosch; D. M. Haverstick; M. Anita; I. C. H. Xue; K. Shibata; L. J. Dragovic, *Molecular Brain Research* **1992**, *12*, 225-231.
55. A. M. Attademo; T. A. R. Rondini; B. C. Rodrigues; J. C. Bittencourt; M. E. Celis; C. F. Elias, *Neuroendocrinology* **2006**, *83*, 313-324.
56. M. Jászberényi; Z. Bagosi; B. Thurzó; I. Földesi; G. Szabó; G. Telegdy, *Hormones and Behavior* **2009**, *56*, 24-34.
57. S. Catarsi; K. Babinski; P. Séguéla, *Neuropharmacology* **2001**, *41*, 592-600.
58. H.-Y. T. Yang; M. J. Iadarola, *Peptides* **2006**, *27*, 943-952.
59. L. Moulédous; C. Mollereau; J.-M. Zajac, *BioFactors* **2010**, *36*, 423-429.
60. S. A. Monks; G. Karagianis; G. J. Howlett; R. S. Norton, *Journal of Biomolecular NMR* **1996**, *8*, 379-390.
61. C. D. Minth; P. C. Andrews; J. E. Dixon, *Journal of Biological Chemistry* **1986**, *261*, 11974-9.
62. M. Grönberg; A. V. Tsolakis; L. Magnusson; E. T. Janson; J. Saras, *J Histochem Cytochem* **2008**, *56*, 793-801.
63. H.-Y. Kim; E. Hong; J.-I. Kim; W. Lee, *J Biochem Mol Biol* **2004**, *37*, 565-573.
64. J. H. Lee; E. Bang; K. J. Chae; J. Y. Kim; D. W. Lee; W. Lee, *European Journal of Biochemistry* **1999**, *266*, 831-839.
65. S. Bord; D. C. Ireland; P. Moffatt; G. P. Thomas; J. E. Compston, *Journal of Histochemistry & Cytochemistry* **2005**, *53*, 1181-1187.
66. K. Sekiya; M. A. Ghatei; N. Minamino; D. Bretherton-Watt; H. Matsuo; S. R. Bloom, *FEBS Lett* **1988**, *228*, 153-156.
67. K. A. D'Amour; A. G. Bang; S. Eliazar; O. G. Kelly; A. D. Agulnick; N. G. Smart; M. A. Moorman; E. Kroon; M. K. Carpenter; E. E. Baetge, *Nature Biotechnology* **2006**, *24*, 1392-1401.
68. K. Tatemoto; I. Nakano; G. Makk; P. Angwin; M. Mann; J. Schilling; V. L. W. Go, *Biochemical and Biophysical Research Communications* **1988**, *157*, 713-717.
69. L. Degen; S. Oesch; M. Casanova; S. Graf; S. Ketterer; J. Drewe; C. Beglinger, *Gastroenterology* **2005**, *129*, 1430-1436.
70. V. Wray; C. Kakoschke; K. Nokihara; S. Naruse, *Biochemistry* **1993**, *32*, 5832-5841.
71. V. K. Batra; M. Mathur; S. A. Mir; R. Kapoor; M. A. Kumar, *Regulatory Peptides* **1990**, *30*, 77-87.
72. A. F. M. Altelaar; I. M. Taban; L. A. McDonnell; P. D. E. M. Verhaert; R. P. J. de Lange; R. A. H. Adan; W. J. Mooi; R. M. A. Heeren; S. R. Piersma, *International Journal of Mass Spectrometry* **2007**, *260*, 203-211.
73. S. Lucyk; H. Taha; H. Yamamoto; M. Miskolzie; G. Kotovych, *Biopolymers* **2006**, *81*, 295-308.
74. S. Hinuma; Y. Habata; R. Fujii; Kawamata Yuji; M. Hosoya; S. Fukusumi; C. Kitada; Y. Masuo; T. Asano; H. Matsumoto; M. Sekiguchi; T. Kurokawa; O. Nishimura; H. Onda; M. Fujino, *Nature* **1998**, *393*, 272-276.

75. Y. Ibata; N. Iijima; Y. Kataoka; K. Kakihara; M. Tanaka; M. Hosoya; S. Hinuma, *Neuroscience Research* **2000**, *38*, 223-230.
76. H. A. Yoshio Takei, Kazuyoshi Tsutsui, *Handbook of Hormones 1st Edition Comparative Endocrinology for Basic and Clinical Research*. Academic Press: **2015**; p 6.
77. M. Shichiri; S. Ishimaru; T. Ota; T. Nishikawa; T. Isogai; Y. Hirata, *Nat Med* **2003**, *9*, 1166-1172.
78. L. Y. Korman; D. N. Carney; M. L. Citron; T. W. Moody, *Cancer Research* **1986**, *46*, 1214.
79. R. Guillemain; P. Brazeau; P. Bohlen; F. Esch; N. Ling; W. B. Wehrenberg, *Science* **1982**, *218*, 585.
80. J. L. Walewski; F. Ge; H. Lobdell; N. Levin; G. J. Schwartz; J. Vasselli; A. Pomp; G. Dakin; P. D. Berk, *Obesity (Silver Spring, Md.)* **2014**, *22*, 1643-1652.
81. E. Gáspár; C. Hardenbicker; E. Bodó; B. Wenzel; Y. Ramot; W. Funk; A. Kromminga; R. Paus, *The FASEB Journal* **2010**, *24*, 393-403.
82. C. J. Donaldson; S. W. Sutton; M. H. Perrin; A. Z. Corrigan; K. A. Lewis; J. E. Rivier; J. M. Vaughan; W. W. Vale, *Endocrinology* **1996**, *137*, 2167-2170.
83. C. Li; P. Chen; J. Vaughan; K.-F. Lee; W. Vale, *Proceedings of the National Academy of Sciences* **2007**, *104*, 4206-4211.
84. I. Gozes; M. Bodner; Y. Shani; M. Fridkin, *Peptides* **1986**, *7*, Supplement 1, 1-6.
85. B. A. Eipper; S. L. Milgram; E. Jean Husten; H.-Y. Yun; R. E. Mains, *Protein Science* **1993**, *2*, 489-497.
86. C. D. Oldham; C. Li; P. R. Girard; R. M. Nerem; S. W. May, *Biochemical and Biophysical Research Communications* **1992**, *184*, 323-329.
87. A. A. Ogonowski; S. W. May; A. B. Moore; L. T. Barrett; C. L. O'Bryant; S. H. Pollock, *Journal of Pharmacology and Experimental Therapeutics* **1997**, *280*, 846-853.
88. R. S. Klein; L. D. Fricker, *Brain Research* **1992**, *569*, 300-310.
89. K. M. Braas; D. A. Stoffers; B. A. Eipper; V. May, *Molecular Endocrinology* **1989**, *3*, 1387-1398.
90. P. J. O'Donnell; W. J. Driscoll; N. Bäck; E. Muth; G. P. Mueller, *Journal of Molecular and Cellular Cardiology* **2003**, *35*, 915-922.
91. S. T. Prigge; A. S. Kolhekar; B. A. Eipper; R. E. Mains; L. M. Amzel, *Science* **1997**, *278*, 1300-1305.
92. P. Chen; E. I. Solomon, *Journal of the American Chemical Society* **2004**, *126*, 4991-5000.
93. A. Crespo; M. A. Martí; A. E. Roitberg; L. M. Amzel; D. A. Estrin, *Journal of the American Chemical Society* **2006**, *128*, 12817-12828.
94. W. A. Francisco; D. J. Merkler; N. J. Blackburn; J. P. Klinman, *Biochemistry* **1998**, *37*, 8244-8252.
95. S. T. Prigge; B. A. Eipper; R. E. Mains; L. M. Amzel, *Science* **2004**, *304*, 864-867.
96. B. A. Eipper; A. S. W. Quon; R. E. Mains; J. S. Boswell; N. J. Blackburn, *Biochemistry* **1995**, *34*, 2857-2865.
97. R. Kulathila; K. A. Merkler; D. J. Merkler, *Natural Product Reports* **1999**, *16*, 145-154.
98. J. C. Freeman; J. J. Villafranca; D. J. Merkler, *Journal of the American Chemical Society* **1993**, *115*, 4923-4924.

99. D. J. Merkler; R. Kulathila; A. P. Consalvo; S. D. Young; D. E. Ash, *Biochemistry* **1992**, *31*, 7282-7288.
100. E. Abad; J. B. Rommel; J. Kästner, *Journal of Biological Chemistry* **2014**, *289*, 13726-13738.
101. A. F. Bradbury; J. Mistry; B. A. Roos; D. G. Smyth, *European Journal of Biochemistry* **1990**, *189*, 363-368.
102. A. G. Katopodis; S. W. May, *Biochemistry* **1990**, *29*, 4541-4548.
103. P. Chen; E. I. Solomon, *Proceedings of the National Academy of Sciences* **2004**, *101*, 13105-13110.
104. F. Cao; C. J. Easton, *Australian Journal of Chemistry* **2013**, *66*, 297.
105. E. E. Chufan; M. De; B. A. Eipper; R. E. Mains; L. M. Amzel, *Structure* **2009**, *17*, 965-973.
106. M. De; J. Bell; N. J. Blackburn; R. E. Mains; B. A. Eipper, *Journal of Biological Chemistry* **2006**, *281*, 20873-20882.
107. A. S. Kolhekar; J. Bell; E. N. Shiozaki; L. Jin; H. T. Keutmann; T. A. Hand; R. E. Mains; B. A. Eipper, *Biochemistry* **2002**, *41*, 12384-12394.
108. B. A. Eipper; R. E. Mains; C. C. Glembotski, *Proceedings of the National Academy of Sciences* **1983**, *80*, 5144-5148.
109. P. D. Simpson; B. A. Eipper; M. J. Katz; L. Gandara; P. Wappner; R. Fischer; E. J. Hodson; P. J. Ratcliffe; N. Masson, *Journal of Biological Chemistry* **2015**, *290*, 24891-24901.
110. S. T. Prigge; R. E. Mains; B. A. Eipper; L. M. Amzel, *Cellular and Molecular Life Sciences* **2000**, *57*, 1236-1259.
111. K. Carlson; S. C. Pomerantz; O. Vafa; M. Naso; W. Strohl; R. E. Mains; B. A. Eipper, *BMC biotechnology* **2015**, *15*, 95.
112. R. E. Mains; L. P. Park; B. A. Eipper, *Journal of Biological Chemistry* **1986**, *261*, 11938-41.
113. C. C. Glembotski, *Annals of the New York Academy of Sciences* **1987**, *498*, 54-62.
114. B. A. Eipper; R. E. Mains, *The American Journal of Clinical Nutrition* **1991**, *54*, 1153S-1156S.
115. A. F. Bradbury; D. G. Smyth, *Biochemical and Biophysical Research Communications* **1983**, *112*, 372-377.
116. M. Bersani; A. H. Johnsen; P. Højrup; B. E. Dunning; J. J. Andreasen; J. J. Holst, *FEBS Lett* **1991**, *283*, 189-194.
117. C. J. Dickinson; D. Daugherty; Y. J. Guo; B. Stadler; S. Finniss; T. Yamada, *Journal of Biological Chemistry* **1993**, *268*, 15929-34.
118. P. P. Tamburini; S. D. Young; B. N. Jones; R. A. Palmesino; A. P. Consalvo, *Int J Pept Protein Res* **1990**, *35*, 153-156.
119. D. Ping; C. E. Mounier; S. W. May, *Journal of Biological Chemistry* **1995**, *270*, 29250-29255.
120. K. M. Morris; F. Cao; H. Onagi; T. M. Altamore; A. B. Gamble; C. J. Easton, *Bioorganic & Medicinal Chemistry Letters* **2012**, *22*, 7015-7018.
121. A. F. Bradbury; D. G. Smyth, *European Journal of Biochemistry* **1987**, *169*, 579-584.
122. J. M. Siegfried; Y. H. Han; M. A. DeMichele; J. D. Hunt; A. L. Gaither; F. Cuttitta, *Journal of Biological Chemistry* **1994**, *269*, 8596-8603.
123. G. V. Shah; S. Thomas; A. Muralidharan; Y. Liu; P. L. Hermonat; J. Williams; J. Chaudhary, *Endocrine-Related Cancer* **2008**, *15*, 953-964.

124. N. R. McIntyre; E. W. Lowe; M. R. Battistini; J. W. Leahy; D. J. Merkler, *Journal of Enzyme Inhibition and Medicinal Chemistry* **2015**, *0*, 1-12.
125. G. P. Mueller; W. J. Driscoll; B. A. Eipper, *Journal of Pharmacology and Experimental Therapeutics* **1999**, *290*, 1331-1336.
126. C. E. Mounier; J. Shi; S. R. Sirimanne; B.-H. Chen; A. B. Moore; M. M. Gill-Woznichak; D. Ping; S. W. May, *Journal of Biological Chemistry* **1997**, *272*, 5016-5023.
127. D. J. Merkler; A. S. Asser; L. E. Baumgart; N. Carballo; S. E. Carpenter; G. H. Chew; C. C. Cosner; J. Dusi; L. C. Galloway; A. B. Lowe; E. W. Lowe Jr; L. King Iii; R. D. Kendig; P. C. Kline; R. Malka; K. A. Merkler; N. R. McIntyre; M. Romero; B. J. Wilcox; T. C. Owen, *Bioorganic & Medicinal Chemistry* **2008**, *16*, 10061-10074.
128. E. Langella; S. Pierre; W. Ghattas; M. Giorgi; M. Réglier; M. Saviano; L. Esposito; R. Hardré, *ChemMedChem* **2010**, *5*, 1568-1576.
129. J. A. Sunman; M. S. Foster; S. L. Folse; S. W. May; D. F. Matesic, *Molecular Carcinogenesis* **2004**, *41*, 231-246.
130. N. Iwai; A. Martínez; M.-J. Miller; M. Vos; J. L. Mulshine; A. M. Treston, *Lung Cancer* **1999**, *23*, 209-222.
131. M. S. Foster; C. D. Oldham; S. W. May, *Tetrahedron: Asymmetry* **2011**, *22*, 283-293.
132. D. Ping; A. G. Katopodis; S. W. May, *Journal of the American Chemical Society* **1992**, *114*, 3998-4000.
133. F. Cao; A. B. Gamble; H.-K. Kim; H. Onagi; M. J. Gresser; J. Kerr; C. J. Easton, *MedChemComm* **2011**, *2*, 760-763.
134. C. H. Rhodes; C. Honsinger, *Annals of the New York Academy of Sciences* **1993**, *689*, 663-666.
135. B. J. W. Barratt; C. J. Easton; D. J. Henry; I. H. W. Li; L. Radom; J. S. Simpson, *Journal of the American Chemical Society* **2004**, *126*, 13306-13311.
136. P. Casara; A. Ganzhorn; C. Philippo; M. C. Chanal; C. Danzin, *Bioorganic & Medicinal Chemistry Letters* **1996**, *6*, 393-396.
137. M. Klinge; H. Cheng; T. M. Zabriskie; J. C. Vederas, *Journal of the Chemical Society, Chemical Communications* **1994**, 1379-1380.
138. J. A. Trendel; N. Ellis; J. G. Sarver; W. A. Klis; M. Dhananjeyan; C. A. Bykowski; M. D. Reese; P. W. Erhardt, *Journal of Biomolecular Screening* **2008**, *13*, 804-809.
139. M. D. Andrews; K. A. O'Callaghan; J. C. Vederas, *Tetrahedron* **1997**, *53*, 8295-8306.
140. J. Feng; J. Shi; S. R. Sirimanne; C. E. Mounier-Lee; S. W. May, *Biochem J* **2000**, *350 Pt 2*, 521-530.
141. N. R. McIntyre; E. W. Lowe; G. H. Chew; T. C. Owen; D. J. Merkler, *FEBS Lett* **2006**, *580*, 521-532.
142. T. M. Zabriskie; H. Cheng; J. C. Vederas, *Journal of the American Chemical Society* **1992**, *114*, 2270-2272.
143. S. A. Mueller; W. J. Driscoll; G. P. Mueller, *Pharmacology* **1999**, *58*, 270-280.
144. A. Y. Jeng; R. A. Fujimoto; M. Chou; J. Tan; M. D. Erion, *Journal of Biological Chemistry* **1997**, *272*, 14666-14671.
145. G. D. Sorenson; O. S. Pettengill; T. Brinck-Johnsen; C. C. Cate; L. H. Maurer, *Cancer* **1981**, *47*, 1289-1296.
146. K. Caron. PhD Thesis, Australian National University, Canberra, 2015.
147. R. B. Merrifield, *Journal of the American Chemical Society* **1963**, *85*, 2149-2154.

148. M. Veronika; E.-H. Sylvia; G. B.-S. Annette, *Beilstein J Org Chem* **2014**, *10*, 1197-1212.
149. F. Albericio, *Current Opinion in Chemical Biology* **2004**, *8*, 211-221.
150. A. El-Faham; F. Albericio, *Chemical Reviews* **2011**, *111*, 6557-6602.
151. M. Amblard; J.-A. Fehrentz; J. Martinez; G. Subra, *Molecular Biotechnology* **2006**, *33*, 239-254.
152. J. Ramachandran; C. H. Li, *The Journal of Organic Chemistry* **1962**, *27*, 4006-4009.
153. H. Yajima; K. Akaji; K. Mitani; N. Fujii; S. Funakoshi; H. Adachi; M. Oishi; Y. Akazawa, *International journal of peptide and protein research* **1979**, *14*, 169-176.
154. L. A. Carpino; H. Shroff; S. A. Triolo; E.-S. M. E. Mansour; H. Wenschuh; F. Albericio, *Tetrahedron Letters* **1993**, *34*, 7829-7832.
155. Y. Shimonishi; S. Sakakibara; S. Akabori, *Bulletin of the Chemical Society of Japan* **1962**, *35*, 1966-1970.
156. S. Funakoshi; H. Tamamura; N. Fujii; K. Yoshizawa; H. Yajima; K. Miyasaka; A. Funakoshi; M. Ohta; Y. Inagaki; L. A. Carpino, *Journal of the Chemical Society, Chemical Communications* **1988**, 1588-1590.
157. P. Sieber; B. Riniker, *Tetrahedron Letters* **1991**, *32*, 739-742.
158. AAPTEC, Practical Synthesis Guide to Solid Phase Peptide Chemistry. [https://www.peptide.com/custdocs/aapptec%20synthesis%20guide%2020%20\(2\).pdf?osCsid=nimursvr8lvbpg3k77m9eusrf5](https://www.peptide.com/custdocs/aapptec%20synthesis%20guide%2020%20(2).pdf?osCsid=nimursvr8lvbpg3k77m9eusrf5)
159. G. C. Windridge; E. C. Jorgensen, *Journal of the American Chemical Society* **1971**, *93*, 6318-6319.
160. M. Beyermann; P. Henklein; A. Klose; R. Sohr; M. Bienert, *Int J Pept Protein Res* **1991**, *37*, 252-256.
161. J. Hachmann; M. Lebl, *Peptide Science* **2006**, *84*, 340-347.
162. R. Knorr; A. Trzeciak; W. Bannwarth; D. Gillessen, *Tetrahedron Letters* **1989**, *30*, 1927-1930.
163. R. D. Dimarchi; J. P. Tam; R. B. Merrifield, *International Journal of Peptide and Protein Research* **1982**, *19*, 270-279.
164. H. Yajima; S. Futaki; A. Otaka; T. Yamashita; S. Funakoshi; K. Bessho; N. Fujii; K. Akaji, *Chemical & Pharmaceutical Bulletin* **1986**, *34*, 4356-4361.
165. M. Mergler; F. Dick; B. Sax; P. Weiler; T. Vorherr, *Journal of Peptide Science* **2003**, *9*, 36-46.
166. C. O'Connor, *Quarterly Reviews, Chemical Society* **1970**, *24*, 553-564.
167. P. P. Tamburini; S. D. Young; B. N. Jones; R. A. Palmesino; A. P. Consalvo, *Int J Pept Protein Res* **1990**, *35*, 153-156.
168. A. F. Bradbury; M. D. A. Finnie; D. G. Smyth, *Nature* **1982**, *298*, 686-688.
169. G. S. Wand; R. L. Ney; S. Baylin; B. Eipper; R. E. Mains, *Metabolism* **1985**, *34*, 1044-1052.
170. M. Roumy; J.-M. Zajac, *European Journal of Pharmacology* **1998**, *345*, 1-11.
171. J. H. Jhamandas; F. Simonin; J.-J. Bourguignon; K. H. Harris, *American Journal of Physiology - Regulatory, Integrative and Comparative Physiology* **2007**, *292*, R1872-R1880.
172. B. Vadokas; F. E. Lüdtkke; G. Lepsien; K. Golenhofen; K. Mandrek, *Neurogastroenterology & Motility* **1997**, *9*, 265-270.
173. A. Ferrand; T. C. Wang, *Cancer Letters* **2006**, *238*, 15-29.
174. O. Chaudhri; C. Small; S. Bloom, *Philosophical Transactions of the Royal Society B: Biological Sciences* **2006**, *361*, 1187-1209.

175. S. D. Brain; T. J. Williams; J. R. Tippins; H. R. Morris; I. MacIntyre, *Nature* **1985**, *313*, 54-56.
176. J. McCulloch; R. Uddman; T. A. Kingman; L. Edvinsson, *Proceedings of the National Academy of Sciences* **1986**, *83*, 5731-5735.
177. M. Soloff; M. Alexandrova; M. Fernstrom, *Science* **1979**, *204*, 1313-1315.
178. A. M. Treston; J. L. Mulshine; F. Cuttitta, *Journal of the National Cancer Institute. Monographs* **1992**, 169-175.
179. J. L. Mulshine; A. M. Treston; P. H. Brown; M. J. Birrer; G. L. Shaw, *CHEST* **1993**, *103*, 4S-11S.
180. L. Saldise; A. Martínez; L. M. Montuenga; A. Treston; D. R. Springall; J. M. Polak; J. J. Vázquez, *J Histochem Cytochem* **1996**, *44*, 3-12.
181. A. Ali; T. Burns; J. Lucrezi; S. May; G. Green; D. Matesic, *Investigational New Drugs* **2015**, *33*, 827-834.
182. M. F. Boehm; L. Zhang; B. A. Badea; S. K. White; D. E. Mais; E. Berger; C. M. Suto; M. E. Goldman; R. A. Heyman, *Journal of medicinal chemistry* **1994**, *37*, 2930-2941.
183. A. Fanjul; M. I. Dawson; P. D. Hobbs; L. Jong; J. F. Cameron; E. Harlev; G. Graupner; X. P. Lu; M. Pfahl, *Nature* **1994**, *372*, 107-11.
184. L. Altucci; A. Rossin; O. Hirsch; A. Nebbioso; D. Vitoux; E. Wilhelm; F. Guidez; M. De Simone; E. M. Schiavone; D. Grimwade; A. Zelent; H. de Thé; H. Gronemeyer, *Cancer Research* **2005**, *65*, 8754-8765.
185. S.-F. Wong, *Annals of Pharmacotherapy* **2001**, *35*, 1056-1065.
186. L. Qu; X. Tang, *Cancer Chemotherapy and Pharmacology* **2010**, *65*, 201-205.
187. O. Hurst. Monitoring and Modulation of Peptidylglycine alpha-Amidating Monooxygenase Activity. Honours Thesis, Australian National University, Canberra, 2012.
188. B. H. Lok; E. E. Gardner; V. E. Schneeberger; A. Ni; P. Desmeules; N. Rekhman; E. de Stanchina; B. A. Teicher; N. Riaz; S. N. Powell; J. T. Poirier; C. M. Rudin, *Clinical Cancer Research* **2017**, *23*, 523-535.
189. M. C. Pietanza; K. Kadota; K. Huberman; C. S. Sima; J. J. Fiore; D. K. Sumner; W. D. Travis; A. Heguy; M. S. Ginsberg; A. I. Holodny; T. A. Chan; N. A. Rizvi; C. G. Azzoli; G. J. Riely; M. G. Kris; L. M. Krug, *Clinical Cancer Research* **2012**, *18*, 1138-1145.
190. Y. Liu; H. Wang; J. Wei; R. Zhou; Z. Chen; H. Liang, *Journal of Chemical Research* **2012**, *36*, 520-522.
191. R. Gašparac; C. R. Martin; E. Stupnišek - Lisac; Z. Mandic, *Journal of The Electrochemical Society* **2000**, *147*, 991-998.
192. E. A. Perez; F. M. Hack; L. M. Webber; T.-C. Chou, *Cancer Chemotherapy and Pharmacology* **1993**, *33*, 245-250.
193. M. Ishiyama; Y. Miyazono; K. Sasamoto; Y. Ohkura; K. Ueno, *Talanta* **1997**, *44*, 1299-1305.
194. H. Tominaga; M. Ishiyama; F. Ohseto; K. Sasamoto; T. Hamamoto; K. Suzuki; M. Watanabe, *Analytical Communications* **1999**, *36*, 47-50.
195. Y. Hsiao; L. S. Hegedus, *The Journal of Organic Chemistry* **1997**, *62*, 3586-3591.
196. H. Bundgaard; A. H. Kahns, *Peptides* **1991**, *12*, 745-748.
197. A. A. Christman; P. W. Foster; M. B. Esterer, *Journal of Biological Chemistry* **1944**, *155*, 161-171.
198. G.-J. de Klerk; J. Hanecakova; J. Jásik, *Plant Cell, Tissue and Organ Culture* **2008**, *95*, 285.

199. G. L. Buchanan, *Chemical Society Reviews* **1988**, *17*, 91-109.
200. N. L. Allinger; G. L. Wang; B. B. Dewhurst, *The Journal of Organic Chemistry* **1974**, *39*, 1730-1735.
201. R. C. Wende; A. Seitz; D. Niedek; S. M. M. Schuler; C. Hofmann; J. Becker; P. R. Schreiner, *Angewandte Chemie International Edition* **2016**, *55*, 2719-2723.
202. K. C. Nicolaou; A. A. Estrada; M. Zak; S. H. Lee; B. S. Safina, *Angewandte Chemie* **2005**, *117*, 1402-1406.
203. P. García-Domínguez; M. Weiss; I. Lepore; R. Álvarez; L. Altucci; H. Gronemeyer; Á. R. de Lera, *ChemMedChem* **2012**, *7*, 2101-2112.
204. A. K. Ghosh; C. D. Martyr; C.-X. Xu, *Organic Letters* **2012**, *14*, 2002-2005.
205. H. Ma; D. Li; W. Yu, *Organic Letters* **2016**, *18*, 868-871.
206. G. A. Molander; R. Figueroa, *Organic Letters* **2006**, *8*, 75-78.
207. K. Furukawa; M. Shibuya; Y. Yamamoto, *Organic Letters* **2015**, *17*, 2282-2285.
208. D. S. Karanewsky; M. F. Malley; J. Z. Gougoutas, *The Journal of Organic Chemistry* **1991**, *56*, 3744-3747.
209. W. R. Roush; M. Murphy, *The Journal of Organic Chemistry* **1992**, *57*, 6622-6629.
210. S. K. Thompson; C. H. Heathcock, *The Journal of Organic Chemistry* **1990**, *55*, 3386-3388.
211. Ö. D. Ekici; Z. Z. Li; A. J. Campbell; K. E. James; J. L. Asgian; J. Mikolajczyk; G. S. Salvesen; R. Ganesan; S. Jelakovic; M. G. Grütter; J. C. Powers, *Journal of Medicinal Chemistry* **2006**, *49*, 5728-5749.
212. J. L. Burdett; M. T. Rogers, *Journal of the American Chemical Society* **1964**, *86*, 2105-2109.
213. J. W. Bunting; J. P. Kanter; R. Nelander; Z. Wu, *Canadian Journal of Chemistry* **1995**, *73*, 1305-1311.
214. P. Yin; D. Bousquet-Moore; S. P. Annangudi; B. R. Southey; R. E. Mains; B. A. Eipper; J. V. Sweedler, *PLoS ONE* **2011**, *6*, e28679.
215. D. H. Copp; B. Cheney, *Nature* **1962**, *193*, 381-382.
216. A. M. Inzerillo; M. Zaidi; C. L. H. Huang, Calcitonin: Physiological Actions and Clinical Applications. In *Journal of Pediatric Endocrinology and Metabolism*, 2004; Vol. 17, p 931.
217. R. Schneider; J. Waldmann; Z. Swaid; A. Ramaswamy; V. Fendrich; D. K. Bartsch; K. Schlosser, *Pancreas* **2011**, *40*, 213-221.
218. C. J. Hillyard; R. C. Coombes; P. B. Greenberg; L. S. Galante; I. MacIntyre, *Clinical Endocrinology* **1976**, *5*, 1-8.
219. M. Kováčová; M. Filková; M. Potočárová; S. Kiňová; U. Pajvani, *Endocrine Practice* **2014**, *20*, e140-e144.
220. H. Kwon; W. G. Kim; Y. M. Choi; E. K. Jang; M. J. Jeon; D. E. Song; J. H. Baek; J.-S. Ryu; S. J. Hong; T. Y. Kim; W. B. Kim; Y. K. Shong, *Clinical Endocrinology* **2015**, *82*, 598-603.
221. F. Cao; A. B. Gamble; H. Onagi; J. Howes; J. E. Hennessy; C. Gu; J. A. M. Morgan; C. J. Easton, *Analytical Chemistry* **2017**, *89*, 6992-6999.
222. V. Du Vigneaud; O. J. Irish, *Journal of Biological Chemistry* **1938**, *122*, 349-370.
223. F. J. Martin-Romero, **2004**.
224. A. K. Samhan-Arias; M. A. Garcia-Bereguain; C. Gutierrez-Merino, *Biochemical and Biophysical Research Communications* **2009**, *388*, 718-722.

